ABSTRACT

Title of dissertation: AMIDINATE BASED CATALYSTS FOR THE STEREOSPECIFIC AND LIVING ZIEGLER-NATTA POLYMERIZATION OF α-OLEFINS

Richard J. Keaton, Doctor of Philosophy, 2003

Dissertation directed by: Professor Lawrence R. Sita
Department of Chemistry and Biochemistry

The living Ziegler-Natta polymerization of α-olefins has been accomplished with a series of precatalysts based on cyclopentadienyl and pentamethylcyclopentadienyl zirconium amidinates (Cp and Cp*ZA's, respectively) upon activation by a borate cocatalyst at –10 °C in chlorobenzene. For the latter, the symmetry of the precatalyst determines the polymer microstructure: C_1-symmetry gives isotactic polymer, while C_s-symmetry gives nearly atactic material. The living behavior has been proven through kinetic analyses, narrow molecular weight distribution polymers, formation of telechelic polymers, and synthesis of well defined block copolymers. Aside from simple straight chain α-olefins, non-conjugated dienes and vinylcyclohexane have also been polymerized in a living fashion with this series of precatalysts.

Characterization of several catalytically active derivatives through solution NMR studies and single crystal X-ray analyses were successful. In the solid state, the initiator appears as a Zr-Me cation that is involved in a doubly methyl bridged dimeric structure. The presence of ether is sufficient to break up the dimer affording a monomeric species. Also, substantially increasing the steric hindrance of the amidinate ligand yields a monomeric structure.

The Zr-Me cations undergo rapid methyl group exchange as evidenced through a crossover experiment between C_1- and C_s-symmetric initiators. Similarly, the methyl cations can engage in methyl-polymer group exchange, thus providing a new method toward stereoblock copolymer production. Insertion of cyclopentene is also successful into the Zr-Me bond, though further propagation steps do not occur. The product of initiation is the previously unobserved cis-1,2-product, which upon warming quantitatively isomerizes to the cis-1,3-product. The former features a β-hydrogen agostic interaction with a low $^1J_{CH}$ value of 87.7 Hz. Upon isomerization, two β-agostic hydrogens are present, with $^1J_{CH}$ values of 97.5 and 107.2 Hz.

Oligomeric polymers were prepared from low ratios of monomer to initiator. Extensive NMR studies showed a 9 : 1 selectivity for the enantiofacial selectivity of the initiation step and perfect stereospecificity thereafter. Quenching the polymerization after extremely long times, or performing the polymerization at higher temperatures, afforded evidence that β-hydride elimination was a rare, yet active, path, and that chain-walking occurs along the alkyl chain of the last inserted monomer unit.

AMIDINATE BASED CATALYSTS FOR THE STEREOSPECIFIC AND LIVING ZIEGLER-NATTA POLYMERIZATION OF α-OLEFINS

by

Richard J. Keaton

Dissertation submitted to the Faculty of the Graduate School of
the University of Maryland, College Park in partial fulfillment
of the requirements for the degree of
Doctor of Philosophy
2003

Advisory Committee:

Professor Lawrence R. Sita, Chair
Professor Jeffery T. Davis
Professor Brian W. Eichhorn
Assistant Professor Lyle Isaacs
Associate Professor Peter Kofinas

ACKNOWLEDGEMENTS

I would like to extend my gratitude to my advisor, Dr. Lawrence R. Sita, for giving me the opportunity to work in his research lab. It is not possible for me to imagine a better graduate experience than that which I enjoyed. His support, exuberance, and guidance made all this possible, and I thank him greatly.

Also, I would like to thank the entire Sita group, past and present, for providing a great environment in which to work. In particular, it is necessary to point out Dr. Kumudini Jayaratne, Yonghui (Felix) Zhang, and Matthew Harney. These particular individuals provided continuous excitement and mirth in the lab that made every day better than the last. Their friendship is invaluable.

Finally, I would never have gotten to this point of my life without the unwavering support and encouragement provided by my family. Without them, I should have foundered long ago. This dissertation is a direct testimony of their fortitude and belief in me.

TABLE OF CONTENTS

LIST OF TABLES

LIST OF FIGURES

LIST OF SCHEMES

LIST OF ABBREVIATIONS

AFM	atomic force microscopy
Ar	aryl
^{i}Bu	*iso*-butyl
^{n}Bu	n-butyl
^{t}Bu	*tert*-butyl
CGC	constrained geometry catalyst
Cp	cyclopentadienyl (η^5-C_5H_5)
Cp*	pentamethylcyclopentadienyl (η^5-C_5Me_5)
CpZA	cyclopentadienylzirconium amidinate
Cp*ZA	pentamethylcyclopentadienylzirconium amidinate
Cy	cyclohexyl
EBI	ethylenebis(indenyl)
eq	equivalents
Et	ethyl
GC	gas chromatography
GPC	gel permeation chromatography
MAO	methylaluminoxane
Me	methyl
Mes	mesityl
MeOH	methanol
M_n	number average molecular weight
M_w	weight average molecular weight
nOe	nuclear Overhauser effect
NMR	nuclear magnetic resonance
P	polymer chain
PDI	polydispersity index
PE	polyethylene
PH	poly(1-hexene)
Ph	phenyl
PhCl	chlorobenzene
PMCP	poly(methylenecyclopentane)
^{i}Pr	isopropyl
^{n}Pr	n-propyl
PP	polypropylene
PVCH	poly(vinylcyclohexane)
R	any alkyl group
RT	room temperature
THF	tetrahydrofuran
TMM	trimethylenemethane
TMS	trimethylsilyl
VCH	vinylcyclohexane

Chapter 1

Introduction to Ziegler-Natta Polymerization

1.1. Background and Discovery

Today, polymers are ubiquitous in society, having found utility in nearly every walk of life. Whether for work or pleasure, synthetic polymers have established themselves as quite the workhorse when other materials could not be suitably employed. Minor alterations in chemical composition, backbone stereochemistry, or molecular weights of a polymer can noticeably affect its properties, broadening the potential applications of a particular polymer. Catalyst development, then, presents a key step to additional operations which may be found for polymers, with new polymeric characteristics being obtained which vary with the selection of the catalyst system.

The field of transition metal coordination polymerization was opened wide through the seminal works of Ziegler and Natta.[1] The work of Ziegler culminated in the discovery of heterogeneous mixtures of a transition metal halide (i.e., VCl_3, $TiCl_4$, etc.) and a main group metal alkyl (i.e. $AlEt_3$) that could polymerize ethylene into low molecular weight, linear polyethylene (PE).[2] Using similar polymerization systems, Natta was able to produce crystalline polyolefins for the first time, such as polypropylene (PP), poly(1-butene), and polystyrene (PS), containing long segments of monomer units bearing asymmetric carbon atoms of the same stereochemical configuration, which they termed “isotactic”.[3] Of note, however, are the following observations: 1) not all possible combinations of metal alkyl plus transition metal halide produced an active polymerization system (aluminum alkyls were preferred over those of zinc, magnesium, and lithium, while the best metal halides were those of Ti, V, Cr, Co, and Ni), and 2)

catalysts active for polymerization of α-olefins were also active for ethylene, while the reverse was discovered not always to be true.

Previous to these investigations, stereoregular, crystalline polyolefins could not be synthesized using conventional polymerization methods. The cationic polymerization of propylene provided a highly viscous, liquid polymer which showed evidence for branches in the polymer backbone greater than Me (Et and ^{n}Pr branches).[4] Oligomeric, atactic PP was retrieved from radically initiated polymerizations.[5] Low density, or highly branched, PE could be produced through high pressure radical procedures.[6]

With Ziegler-Natta type catalysts capable of polymerizing α-olefins in a stereoregular manner, a remarkable new door in polymerization catalysis had been opened. A wide variety of potential monomers could be polymerized under much less stringent conditions as compared to cationic, anionic, and free radical systems, making this method of extreme industrial interest and spawning many academic pursuits. Indeed, with the metal alkyl structure, transition metal halide structure, and experimental procedure all influencing the resulting polymer, this sensitivity provided a platform upon which further catalyst design could rest, for ascertaining mechanisms behind these susceptible factors would supply insight into how best to control stereoregularity.

1.2. Metallocenes.

Early Ziegler-Natta polymerization catalyst systems based on Ti were heterogeneous mixtures. In order to gain a handle on the mechanisms active during polymerization or any intermediates present, a homogeneous catalyst system needed to be elaborated in order to allow for sufficient modes of spectroscopy to aid in characterization. Other advantages in favor of homogeneous systems are the ease of separation of the catalyst from the polymer upon quenching, more uniform type of active

centers, numerically more active centers compared to only the active surface of a heterogeneous system, and a more consistent molecular weight distribution since all active sites should be similar.

A soluble catalyst for the polymerization of ethylene, but not for propylene or other α-olefins, was discovered in the late 1950's.[7,8] A highly linear PE with a narrower molecular weight distribution than it's heterogeneous predecessors was achieved using bis(cyclopentadienyl)titanium dichloride (Cp_2TiCl_2, where Cp = η^5-C_5H_5) with alkylaluminum compounds (e.g. $AlEt_2Cl$). Several early reports shed considerable light on what the active catalyst in solution may be.[9] It was postulated that the aluminum species first alkylates the titanium precatalyst through a ligand exchange as shown in Scheme 1. The monoalkylated titanocene chloride subsequently forms a Lewis acid-base adduct with the aluminum, which serves to place a partially positive charge on the Ti center. The aluminum anion is tetracoordinate, so an olefin complex with it is unlikely. The nucleophilic alkene would then bind to electron deficient Ti. Complexation would decrease the charge on the metal, allowing for the olefin to insert into the weakened Ti-alkyl bond.

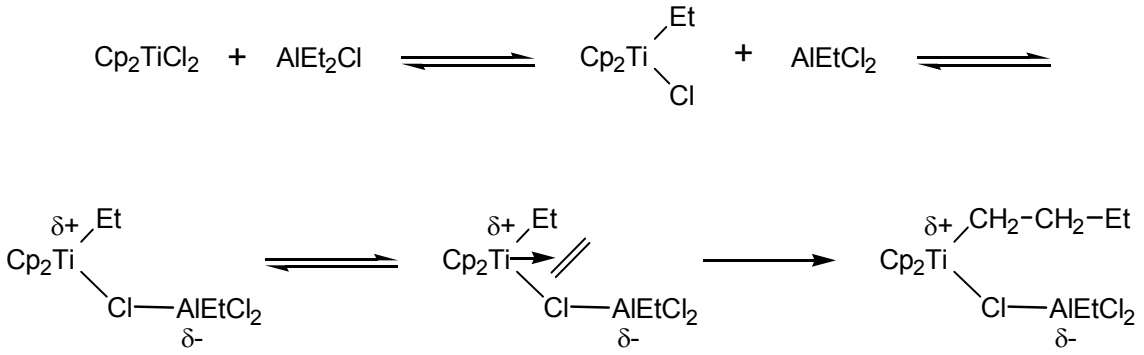

Scheme 1. Mechanism producing the proposed active catalyst for the Cp_2TiCl_2 / $AlEt_2Cl$ system.

Support for this mechanism was provided by a crystal structure determination of a Ziegler-Natta insertion product. Eisch and coworkers noted that the interaction of Cp_2TiCl_2 with an equimolar amount of $AlMeCl_2$ yielded a system that was capable of performing a single insertion of the ethylene mimic, trimethylsilylphenylacetylene, as depicted in Scheme 2.[10] This product was quite informative, for it argued strongly for many different aspects of the polymerization system. First, insertion of the alkyne occurs between a titanium-carbon bond in a regiospecific and cis-specific manner. Second, this product must have been reached through the intermediacy of $Cp_2TiCH_3^+$, thus establishing the set of equilibrium shown in Scheme 1, except that instead of insertion into the chloro-bridged adduct, the Lewis acidic Al center fully abstracts the final Cl from Ti forming two distinct solvent separated ion pairs. In fact, the tetrachloroaluminate anion has no close contacts with the Ti center in the crystal structure, suggesting that distinct cationic Ti species can exist while ion-paired with $AlCl_4^-$. Further establishment of the cationic nature of the Ti atom was given by the observations that this reaction was totally shut down in the presence of Lewis bases and that the rate of insertion of the acetylene was heightened by more polar solvents.

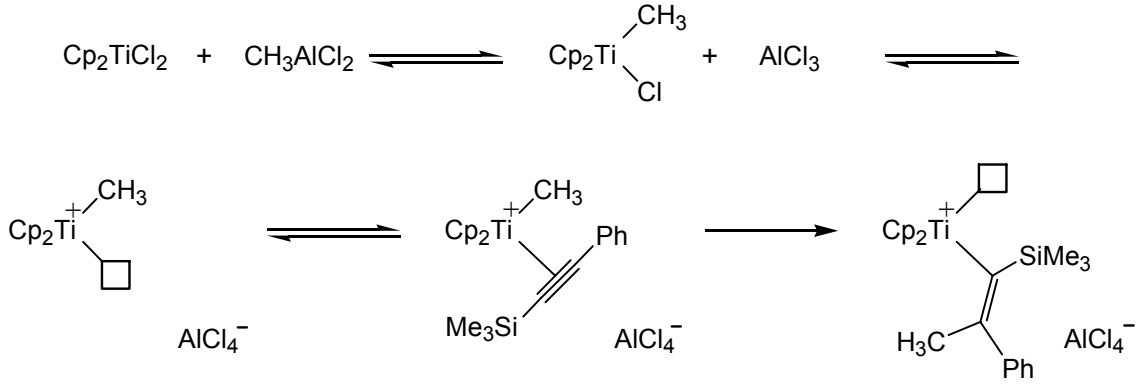

Scheme 2. Mechanism for production of a discrete coordinatively unsaturated metal cation and interception via insertion of trimethylsilylphenylacetylene.

The findings from the structure obtained following initial insertion in a Ziegler-Natta catalyst system were consistent with the favored mechanism for olefin incorporation into a growing polymer chain. Several potential mechanisms to explain the insertion of olefins have been proposed over the years, but the accepted mechanistic scheme is that proposed by Cossee and Arlman.[11-13] As detailed in Scheme 3, monomer coordination to the cationic metal (A) binds the olefin face-on with its double bond parallel to the metal-carbon bond, followed by polymer chain migratory insertion of the polymer chain to the π-coordinated olefin (B). This chain elongation

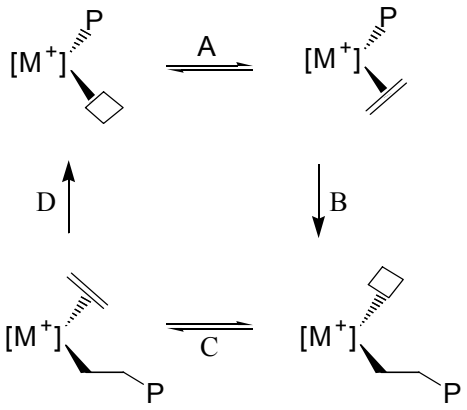

Scheme 3. Cossee-Arlman mechanism for olefin insertion. P denotes a polymer chain of arbitrary length.

goes through a metallocyclobutane transition state with the olefin insertion occurring with 1,2-cis-addition across the double bond. The migratory insertion step provides a new vacant site for a new molecule of monomer to bind (C), and this subsequently inserts providing the original vacant site (D). Although improved versions of this mechanism have been offered that implicate α-hydrogen agostic interactions in either both the ground state and transition state or only the latter,[14] they do not stray from the idea that monomer insertion is a two-step process requiring coordination to an active

metal center having a site of unsaturation, followed by alkyl chain migratory insertion with a cis-opening of the double bond.

Activated metallocenes were unable to polymerize prochiral olefins, such as propylene, 1-butene, etc., using standard alkyl aluminum cocatalysts. This severely limited their utility in the field of olefin polymerization. While their performance for ethylene was moderate, higher olefins were simply inactive. Further development would be necessary to overcome this deficit.

1.3. New Cocatalysts.

It was not until the late 1970's / early 1980's that any significant headway was made in terms of enhancing the performance of metallocene catalysts. With an electrophilic metal center, Lewis bases should deactivate Ziegler-Natta catalysts. Contrary to this was the recognition that a small amount of water surprisingly enhanced the rate of ethylene polymerization for the $Cp_2Ti(Et)(Cl)$ / $AlEtCl_2$ system.[15] Subsequent studies with the otherwise inactive combination of Cp_2ZrMe_2 and $AlMe_3$ led the authors to propose that the water was interacting with the Al species, creating a stronger Lewis acid cocatalyst, which could more efficiently activate the Zr precatalyst and boost the activity seen for ethylene polymerization.[16] The suspected product of partial hydrolysis of $AlMe_3$ was thought to be an oligomeric methylaluminoxane (MAO) of approximate composition $(\text{-Al(Me)-O-})_n$ where n ~ 5-20. Rather than preparing MAO *in situ*, Kaminsky illustrated the controlled synthesis of MAO, which when used in tandem with Cp_2ZrMe_2 proved to be exceptionally active for production of polyethylene at 70 °C, exhibiting a gap between consecutive insertion steps of only 0.3 ms.[17]

Shortly thereafter, Sinn and Kaminsky noticed that MAO-activated metallocene-based catalysts were in fact adept at polymerizing propylene and higher olefins.[18,19] This stands in stark contrast to previous studies of similar homogeneous metallocenes

which, when activated by aluminum alkyls, failed to polymerize α-olefins. Unlike their heterogeneous predecessors, these homogeneous Cp_2MX_2 / MAO systems did not produce stereoregular polymers, yielding only atactic oils. However, this research effort into more potent cocatalysts revitalized research into Ziegler-Natta catalysis, for metallocenes were now poised to be suitable heterogeneous model structures.

Despite its success as an exceptionally potent Lewis acid cocatalyst, the exact structure and composition of MAO is still shrouded in mystery. Many one-, two-, and three-dimensional structures have been proposed for this oligomeric species. The most widely accepted mode of Cp_2MCl_2 activation by MAO is similar to that of alkyl aluminum species described in Scheme 2: ligand exchange to alkylate the metal followed by abstraction of the remaining halide (or methyl group if sufficiently high MAO concentrations are used) from the *in situ* prepared $Cp_2M(Me)(X)$ (or Cp_2MMe_2), yielding Cp_2MMe^+ and a weakly coordinating MAO^- anion. This reaction appears to be quite rapid and reversible, as evidenced through $^{13}CH_3$ scrambling in the $Cp_2Zr(^{13}CH_3)_2$ / MAO system.[20] Other studies support the concept of cation formation, Cp_2ZrMe^+, which is stabilized by coordinative contact with the MAO^- anion that can be displaced to allow for olefin binding, a presumed prerequisite for the polymerization mechanism.[21-23]

The success of MAO as a potent cocatalyst is undeniable, but it is not without problematic issues. With its structure still uncertain, using MAO as a model for catalytically active systems is not fruitful since not all steps leading to such a point are well understood. In some cases, extremely high Al : Zr ratios, as high as 10,000 : 1, are necessary to achieve good polymerization activity and relatively stable kinetic profiles. Removing such large amounts of cocatalyst from the produced polymer also poses a major problem. Invariably, MAO is always contaminated by residual $AlMe_3$ which can compete in unfavorable side reactions (see Section 1.5.). These factors are not conducive toward characterization of the catalytically active species. As such, new

cocatalysts were necessary to permit more acceptable attempts at modeling the cationic Ziegler-Natta active sites.

A novel breakthrough in this respect was reported by Marks when his group utilized the strongly Lewis acidic perfluorinated borane, $B(C_6F_5)_3$, in combination with Group IV metallocene dialkyls for high activity olefin polymerization.[24] Remarkably, they were able to obtain a crystal structure of the zirconocene catalyst, [1,2-$(CH_3)_2C_5H_3$]$ZrCH_3^+$ (**i**), stabilized by close contacts with the $CH_3B(C_6F_5)_3^-$ anion.[25] This is the first report of a crystallographically characterized Ziegler-Natta polymerization system that proved to be active for both ethylene and propylene. Natta had obtained crystals that contained Ti and Al that were most likely decomposition products as they were inactive for polymerization.[26] In Marks' structure, the borane is viewed as abstracting a CH_3 group from Zr to generate the cation. The Zr center is still in close contact with the removed C atom since it serves as a bridging methyl group featuring a bond distance only 0.3 Å longer than the remaining terminal Zr-CH_3 group. Of interest, the bond angles about the B atom are virtually tetrahedral, the B-CH_3 length is typical of B-C single bonds, and the hydrogen atoms of the bridging methyl group are pointed away from B and toward Zr with no evidence for Zr···H(C) agostic interactions.

Although the analysis of the crystal structure gave detailed information about the static structure of the ion pairing, the inherent dynamics of the system would be evident in solution. Unlike the rapid equilibria that haunted solution structural characterization for MAO systems, borane systems are stable and readily identifiable in appropriate solvents. At ambient temperatures and below, the ^1H NMR spectrum of **i** are similar with no detectable line broadening, hinting that any exchange processes are significantly slow at these temperatures and that the symmetry deduced from the single crystal X-ray analysis remains in solution.[27,28] In such systems at elevated temperatures, two

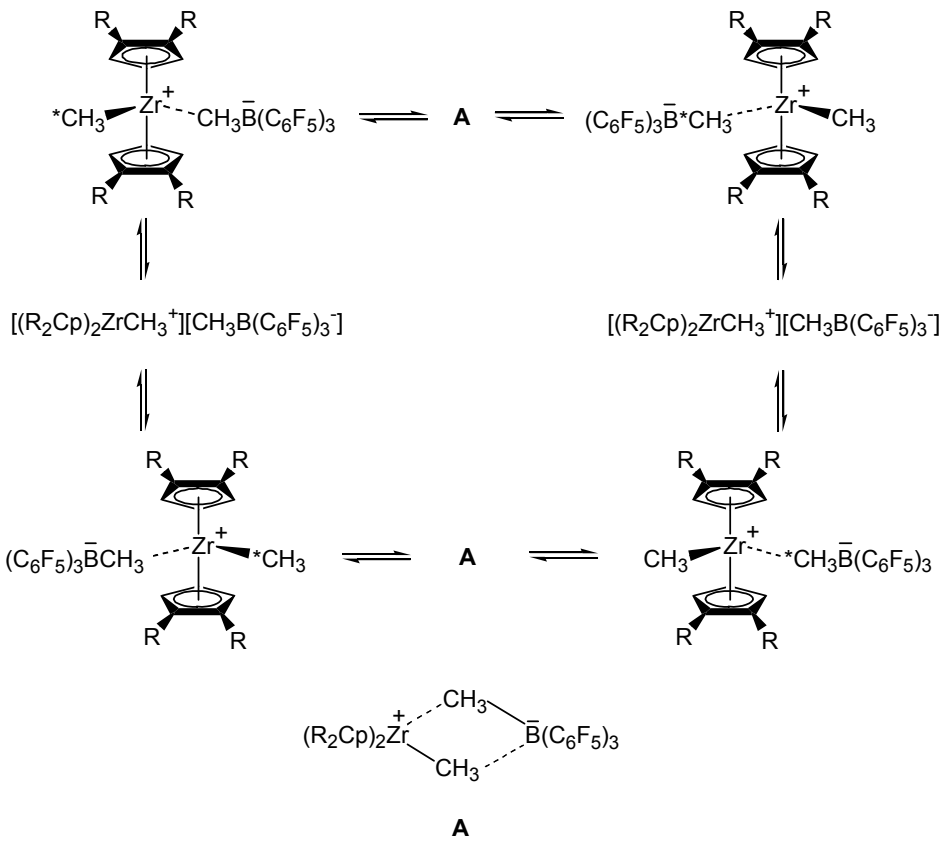

Scheme 4. Dynamic processes in solution for $Cp_2M(CH_3)_2$ / $B(C_6F_5)_3$ systems.

dynamic processes appear to be active, as depicted in Scheme 4. The mechanisms, both found to be unimolecular, were described as a methyl group exchange and an ion pair reorganization. The first is described as a Zr-Me / B-Me methyl exchange and is proposed to have a concerted transition state as shown in **A**. The second is a cation-anion dissociation / reorganization process which serves to transfer the $CH_3B(C_6F_5)_3^-$ anion from one side of the complex to the other. The activation barrier for the two methods is lowest for ion pair reorganization, since it requires breaking of the weakest "bond" in the adduct, the Zr···CH_3-B interaction. This barrier is substantially reduced upon switching to more polar solvents (from toluene to chlorobenzene) while the barrier to methyl group exchange remains unchanged, and this is interpreted as a stabilization of the solvent separated ion pair during the reorganization process.

Though borane-activated metallocenes can induce polymerization of olefins, the fact that the counterion interacted so strongly with the metal cation meant that this contact had to be easily broken to permit olefin coordination. The more strongly the anion coordinated to the cation, the harder it would be to displace, and lower catalytic activity would result. Removing / minimizing any such association would generate cations that were more bare and more electrophilic, aspects favoring olefin coordination.

Toward this end, complete abstraction of the methyl group was envisioned. Reacting metallocene dimethyls with the perfluorinated borates, $[Ph_3C][B(C_6F_5)_4]$ or $[PhNHMe_2][B(C_6F_5)_4]$, proves very effective for monodemethylation, through either methide abstraction or facile protonolysis, respectively.[24,29] The resulting metallocene cations are full-fledged cations, not "cation-like" as borane activated systems, without a bridging methyl group linkage to the borate, and they exhibit superior olefin polymerization activity. Low rates for propylene polymerization were discovered for Cp_2ZrMe^+ together with the tetraphenylborate, $B(C_6H_5)_4^-$, and this is associated with strong interactions between the two through π-arene coordination.[24,30] However, incorporation of F atoms on the phenyl rings suppresses π-coordination, making the anion even more weakly coordinating, and thus the system was more active. These fluorinated phenyl rings reduce the proficiency with which the B-C_{ipso} bond may be broken, which has been shown to be a termination pathway during polymerization.[31,32] A crystal structure of a Th adduct showed two F atoms in close contact with the metal, though they were outside typical distances indicative of any stabilization, producing a well-defined cation.[24]

In spite of the $B(C_6F_5)_4^-$-based activators proven efficacy for highly potent olefin polymerization, poor solubility in hydrocarbon solvents and difficulty in obtaining crystalline materials has hindered some of the characterizations attempted with this

anion. Further development of cocatalyst design will undoubtedly offer additional options for activation of transition-metal complexes toward more efficient, soluble, and stable polymerization catalysts.[33,34]

With a binding pocket defined upon removal of a σ-bonded halide or alkyl group, the next step of the insertion mechanism requires the coordination of a monomer. For prochiral olefins, this binding has been found to orient the pendant substituent of the monomer in an anti-manner with respect to the polymer chain. This is more clearly shown in Scheme 5. When insertion occurs in a 1,2-fashion, the face selectivity is such

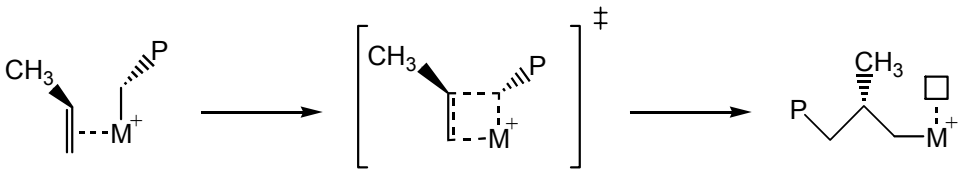

Scheme 5. Primary coordination of an olefin with its CH_3 group anti to the CH_2-P bond.

that the pendant R substituent of the olefin is anti to the growing polymer chain in the metallocyclobutane intermediate to avoid nonbonding steric interactions. This also illustrates the point that in the site control mechanism, the ligand framework enforces a particular environment where the polymer chain can occupy which affects the orientation of the β-carbon of the polymer chain. This subsequently influences monomer face selectivity, such that the face which can most effectively avoid steric congestion is selected.

Monomer insertion is quite facile, and cationic metal-alkyl species having coordinated free olefins have often only been studied computationally. An insertion barrier of only ca. 0.5 kcal / mol was calculated for ethylene with Cp_2ZrEt^+ providing a highly stabilized γ-agostic $Cp_2Zr^nBu^+$ in an overall exothermic reaction (ca. ΔH = -8.9

kcal / mol).[35] With effectively no barrier to insertion, it would appear that observation of metal cations with coordinated free alkene, if possible, would only be so at extremely low temperatures. By contrast, late transition metal alkyl / ethylene complexes can be observed at low temperatures via NMR.[36]

One method through which this difficulty was circumvented for early transition metals was via attachment of an olefinic moiety to part of the ligand framework. Represented in Figure 1 are examples of species in which studies were performed using tethered alkenes. Investigations using these complexes revealed that olefin coordination and decomplexation are quite facile processes. Cationic Group IV and neutral Group III complexes are d^0 species and cannot contribute to d-π^* backbonding which would be adventitious toward observing alkene bound species without the need for the chelate. Through ^{1}H NMR and X-ray structural studies, it was deduced that a build-up of positive charge within alkene bound Zr complexes was occurring on the internal vinyl carbon of the alkene.[37-39] Effectively, this is a polarization of the alkene π-bond delocalizing some of the positive charge off of the metal, making it less electrophilic.

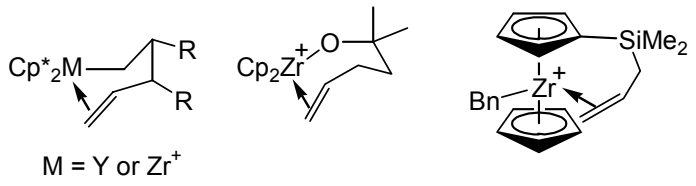

Figure 1. Examples of models for olefin coordination via tethered double bonds.

Further development has afforded nonchelated alkene and alkyne complexes. Jordan has described a bis-Cp alkoxy system which suggests that ethylene and propylene have similar binding energies as well as equal proclivity toward

displacement.[40] In this system, bound ethylene did not appear to be displaced by free ethylene, rather that the solvent, CD_2Cl_2, served to replace the monomer through an associative mechanism. They also noticed that ethylene coordination was influenced by addition of C_6H_5Cl to CD_2Cl_2 solutions of the cation, presumably due to the production of the $Zr^+(O^tBu)(ClPh)$ adduct, analogues of which they have been able to obtain evidence for through crystallographic characterization. Addition of excess borate anion did not have any effects on the coordination kinetics, suggesting that anion displacement was not a factor.

The studies by Jordan with alkoxy instead of alkyl ligands is not entirely accurate since this should serve to decrease the Lewis acidity of the Zr. Because of this, the monomer is likely to bind to the metal more weakly for Zr^+-OR systems as compared to Zr^+-R. Also, migratory insertion rates would not be attainable since chain migration would insert into a Zr-O bond. A more compelling case was made by the group of Casey in which they employed neutral Y-based species at low temperatures to observe a nonchelated metal-alkene complex.[41] With these species being isoelectronic with cationic metallocenes while utilizing only carbon based ligands, they provide a more suitable model since both coordination and insertion of monomer can be obtained.

Previous work with chelated Y-alkene species afforded an enthalpy for monomer binding of -4.6 kcal mol^{-1}.[42] At -150 °C, they were able to observe chemical shift differences in the ^1H NMR spectrum for the bound propylene molecule that mimicked those seen in the chelated Y-alkene species shown in Figure 1. Through a 1D nOe experiment, evidence for propylene coordination was further demonstrated via proximity of the vinyl hydrogen, C*H*(CH_3), to the Cp* rings. Through kinetic evaluations, a value of ΔH° = -4.5 kcal mol^{-1} was found, which is quite indistinguishable from the value for the model chelate. Also found was a higher free energy for coordinated propylene insertion

into the yttrium-alkyl bond as compared to the free energy for decomplexation from the metal (cf., 11.5 kcal mol^{-1} vs 5.1 kcal mol^{-1}). This establishes more facile monomer dissociation than chain migratory insertion.

1.4. Metallocene Advancement: Stereoregular Polyolefins.

Heterogeneous metallocene mixtures have a variety of different sites available on the surface of the crystal, providing multiple sites from which arise different polymer microstructures, polymer molecular weights, and polymerization kinetics. Homogeneous activated metallocenes are considered to be single-site polymerization catalysts, in which one type of site is capable of polymerizing a coordinated monomer. Early work with the simplest metallocenes did not offer much hope for stereospecific polymerization of prochiral olefins. However, with the potential to modify the metallocene framework available through simple synthetic preparations, an empirical approach could be taken toward development of stereospecific polymerization catalysts.

First, a point needs to be made in terms of defining the stereoregularity of a polymer. Polymer microstructure is described in terms of the relative configuration of the asymmetric carbon atoms of two consecutive insertion events. For two successive insertions, the pendant alkyl chains can either occupy the same side of the polymer chain or opposites. Such a sequence would lead to what are termed *meso* (*m*) and *racemic* (or *rac*, *r*) dyads, respectively, as displayed in Figure 2. Purely isotactic chains would necessarily give all *m* dyads and syndiotactic chains would give *r* dyads. For stereoregular polyolefins which have many consecutive *m* dyads, a wider breadth is considered, typically encompassing the pentad level of analysis for five consecutive monomer units. Since monomer insertions do not occur with perfect stereochemical fidelity, pentads also aid in the identification of insertion stereoerrors, in which the incorrect face of the olefin is inserted into the growing chain. All ten potential pentads

are also shown in Figure 2. Within the pentad scheme, a stereoerror during isospecific polymerization gives rise to the *mmmr* pentad. Similarly, a stereoerror during syndiospecific polymerization yields the *rrrm* pentad. How the next insertion step relates

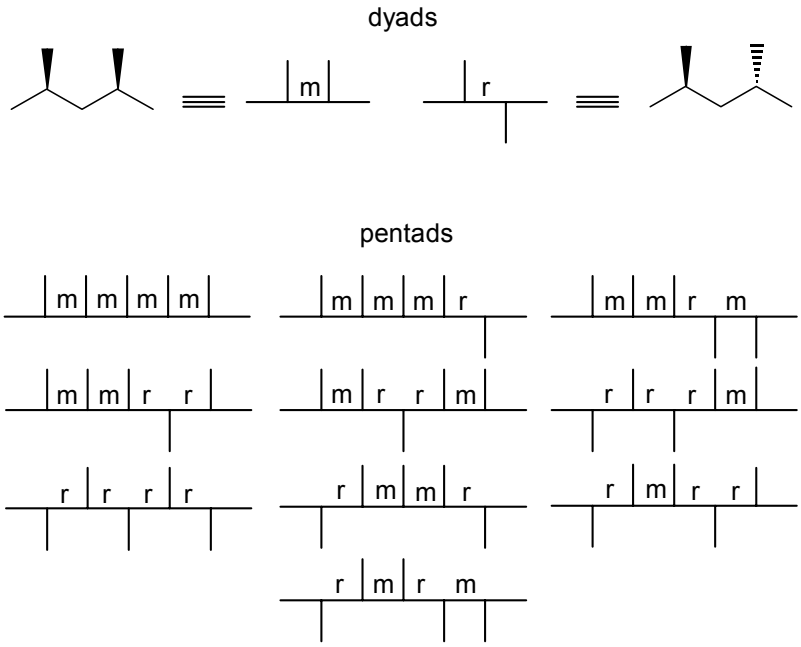

Figure 2. Microstructure relationships of polyolefin sat the dyad and pentad levels.

to the previous one depends on the type of mechanism that is active for enantioface selectivity during the polymerization.

There are two possible modes of enantioface selectivity during olefin insertion. The first relays chiral information of the reaction site to the incoming olefin. Based on the ligand framework about the transition metal, a preferential orientation of the olefin face can be induced, and this is referred to as enantiomorphic site control, or simply site control. In actuality, the chirality of the catalytic complex determines the orientation of the polymer group, specifically the β-carbon, which relays steric information to the incoming olefin.[43] This was proposed via ab initio calculations[44] and substantiated

through work which showed that for a given ligand framework, propylene insertion into a Zr-Et bond occurred with high face selectivity, whereas insertion into a Zr-Me bond occurred with equal selectivity for both the re and si monomer faces.[45,46]

The second mechanism obtains its chiral induction from the last inserted monomer unit, referred to as chain-end control. Stereochemical information about the polymer chain is lost and only the previously inserted monomer unit impacts subsequent insertions. During polymerization under chain end control, a mistake into an isotactic chain is propagated, such that a misinsertion is followed by another and results in the *mmrm* pentad. Similar behavior in a syndiotactic polymerization under chain end control will produce the *rrmr* pentad. Upon misinsertion in the site control mechanism, the mistake is immediately rectified to put the chain back into regularity. This means that for isotactic polymer, an opposite insertion is followed by a correct insertion, leading to the *mmrr* pentad. Two consecutive insertions of the incorrect olefin face during this mechanism, producing the *mmrm* pentad, are quite improbable. Site control also dictates that for syndiospecific polymerization, the *rrmm* pentad is created. It can be seen that the chain end control mechanism features isolated stereoerrors, whereas site control corrects itself before continuing.

Four possibilities exist for monomer incorporation into a metal-polymer bond for prochiral olefins. These different modes are depicted in Scheme 6. First, the olefin can coordinate to the metal such that the head, or the CH(R), end is closest to the polymer chain. This is the most common form of coordination, for it leads to a primary, or 1,2-insertion of the monomer and a primary center bound to the metal. If the tail, or CH_2, portion of the olefin is closest to the polymer chain, this is termed a secondary, or 2,1-coordination and insertion provides a secondary C center next to the metal, Zr-CH(R)-P. The arrangement of the head and tail portions of the olefin determines the regiochemistry of an insertion step.

primary or 1,2-insertion secondary or 2,1-insertion

Scheme 6. Regiochemistry of prochiral monomer insertion.

Secondly, the olefin face selectivity governs the chirality of the asymmetric carbon atom about to be generated and this determines the stereoselectivity of a polymerization. Inspection of the olefin-metal "bond" and the relative orientation of the alkyl substituent factors into face selectivity. Viewing down the alkene-metal bond of the alkene with the substituted end up and the metal in back, an R group on the top right side is defined as the *re* face, while the left side is determined as the *si* face. Since every α-olefin insertion creates a new stereogenic center, consecutive insertion of the same face provides an isotactic polymer since the mechanism involves cis-opening of the double bond.

Polymer microstructure was not discussed earlier for only colorless, sticky oils had previously been obtained from MAO / Cp_2MX_2-cocatalyst systems, where M = Ti, Zr, or Hf, and X = Cl or Me. The first stereoregular polyolefin from a metallocene catalyst was detailed in 1984. Ewen reported the combination of Cp_2TiPh_2 and MAO at –45 °C produced a partially isotactic PP with a modest *mmmm* pentad content of 52%.[47] Analysis of the ^{13}C NMR of this polymer featured stereochemical errors attributable to a chain-end control mechanism (both *mmmr* and *mmrm* in a 1 : 1 ratio).[48,49] Employing an *ansa*-bridged catalyst previously prepared by Brintzinger,[50] Ewen also expounded in the same paper that employing a mixture of MAO-activated *rac*- and *meso*-ethylene-bis(indenyl)$TiCl_2$ (EBI$TiCl_2$) yielded a mixture of isotactic and atactic PP having similar molecular weights (see Figure 3). Whereas he speculated that the isotactic polymer

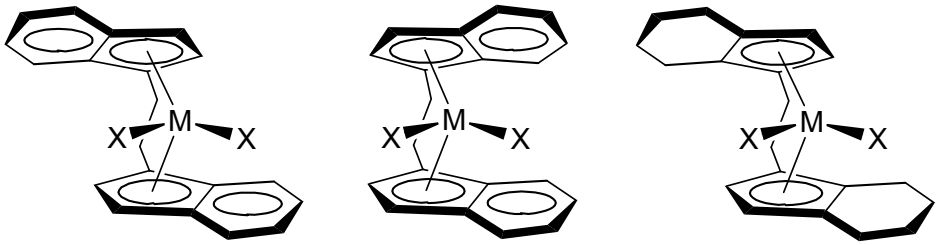

rac-EBIMX_2 *meso*-EBIMX_2 *rac*-EBTHIMX_2

Figure 3. Bridged metallocene precatalysts for olefin polymerization.

arose from polymerization using the *rac* isomer, Kaminsky and Brintzinger confirmed this assumption with the chiral metallocene isomer of a structurally related zirconium analogue, *rac*-ethylene-bis-(4,5,6,7-tetrahydroindenyl)$ZrCl_2$ (EBTHI$ZrCl_2$).[51] The isotactic polymer so obtained conformed to a microstructure indicative of an enantiomorphic site control mechanism (*mmmr* = *mmrr* = 2 *mrrm*).[48,49] Ensuing investigations of Hf analogues revealed nearly identical activities and stereoselectivities as compared with Zr, though the hafnium system produced polymers of higher molecular weights.[52] These studies corroborate the trends that Ti(IV) is most active presumably due to the weaker Ti-C σ-bond strength and that Zr and Hf are active at higher temperatures thanks to more stable M(IV) oxidation states.

The chiral metallocenes sparked a resurgence of interest into Ziegler-Natta polymerization. Despite their inferior performance when compared to heterogeneous systems, covalently tethered, conformationally rigid metallocenes contained the advantageous feature of rational modifications of the bridging linker and the Cp ring which could produce a multitude of derivatives from which details of polymerization studies would provide great insight into the effects structural factors play during monomer insertion. More importantly, this lead to the discovery of a link between the symmetry of the precatalyst and the resultant polymer microstructure.[53]

With a basis for how monomer insertion occurs (from π-face selectivity, chain migratory insertion, cis-addition across the double bond, etc.), the microstructure of polyolefins are now more predictable. Under the two-site migratory insertion methodology of the site control mechanism, the symmetry of the respective olefin coordination sites to eachother determines the face selectivity and thus polymer microstructure. Employing steric factors to ascertain polymer tacticity within metallocene systems is now referred to as Ewen's symmetry rules.[53] This concept is demonstrated in Figure 4. The simplest metallocenes (i.e. Cp_2ZrMe_2) have olefin binding sites related by C_{2v}-symmetry. As such, either face of an incoming olefin will bind to the metal with equal energy and thus the same probability of insertion. This lack of enantiofacial selectivity leads to an atactic polymer microstructure. With a chiral metallocene like *rac*-EBIMX_2, the two sites are correlated by C_2-symmetry and are homotopic. Both are enantioselective sites, binding the same olefin face for each insertion step, producing an isotactic polymer. Two possible cases exist for the relationship of sites related through C_s-symmetry: atactic or syndiotactic polymer. For the former, an example of which was mentioned previously with *meso*-EBITiCl_2, the two sites are not interchangeable (diastereotopic), but each respective site binds either enantioface of the olefin with the same energy. For the latter, the binding sites are related by a mirror plane that bisects the metal and ligand framework. Their enantiofacial selectivity will be opposite yielding a syndiotactic polymer. Polymers

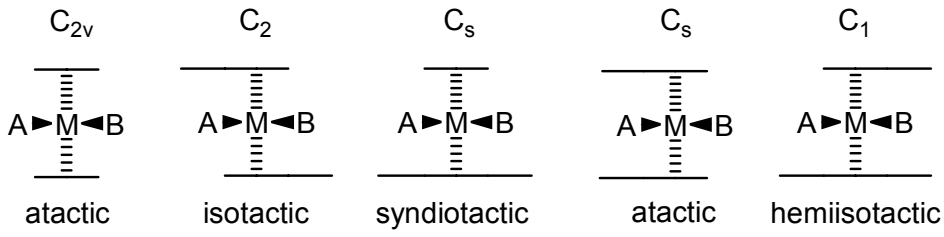

Figure 4. Symmetry of active sites determines polymer microstructure.

from C_1-symmetric systems are highly variable and can cover the entire range of possible microstructures. One case will be discussed in greater detail later (see Chapter 8.1.).

1.5. Metallocenes: Additional Elementary Steps.

It should by no means be assumed that all insertion steps will be regiospecific or stereospecific, that all polymer chains will grow to astronomical molecular weights, or that all polymer chains will have the same number of monomer units. There are many side reactions that occur during the polymerization pathway which haunt metallocenes.[54] Most of these are reactions in which the growing polymer chain is released from the metal center resulting in a termination event. This does not, however, necessarily reflect a termination of the catalyst, for the metal species thus created can typically create a new polymer chain through consequent monomer insertions.

The most common chain termination event is a β-hydride elimination from the polymer chain to the metal center. This is depicted in Scheme 7. After a cis-1,2-insertion of, in this case, a propylene monomer, a β-hydrogen transfer to the metal occurs producing a cationic metal-hydride in a π-complex with the product of elimination, a 1,1-disubstituted alkene. The release of this alkene opens a vacant coordination site upon which another molecule of propylene can bind to the metal. This species can then

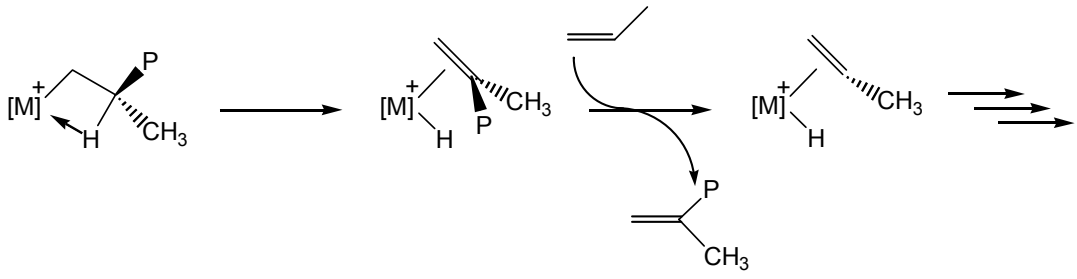

Scheme 7. Mechanism for β-hydride elimination during propylene polymerization.

readily undergo insertion to initiate another polymer chain from the same metal center. Unlike the eliminated polymer which first underwent a monomer insertion into a M-CH_3 bond to produce an isobutyl end group, this newly formed chain will have a diagnostic n-propyl end group upon insertion. It has been found, however, that within the chiral ligand set *rac*-EBTHIM$^+$R, insertion into a M$^+$-H bond occurs with opposite enantiofacial selectivity compared to the M$^+$-polymeryl bond with the same ligands.[55]

A second chain termination event involves β-hydride transfer to monomer, depicted in Scheme 8. This process is the preferred chain release pathway for

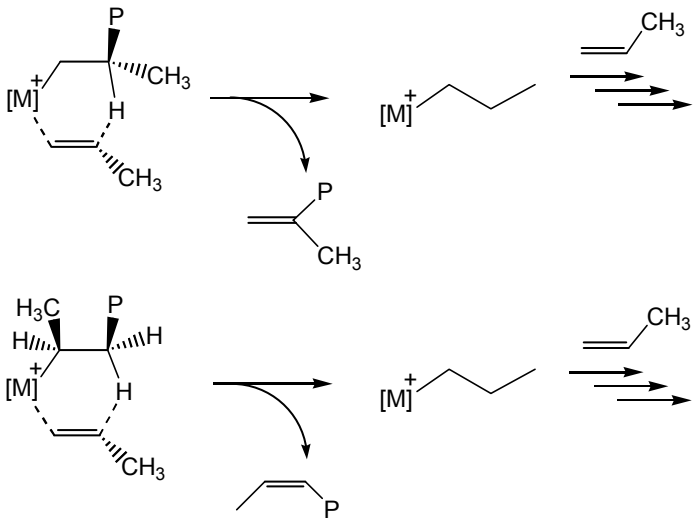

Scheme 8. Two modes of β-hydride transfer to monomer: (top) after primary insertion, and (bottom) after secondary insertion.

heterogeneous propylene polymerization systems.[56,57] Termination via β-hydride transfer to monomer can occur after either a primary or a secondary insertion, yielding different organic products. Since the rate of a primary insertion on a secondary growing chain, (M-CH(CH_3)-CH_2-P), is slower than insertion on a primary growing chain (M-CH_2-CH(CH_3)-P), the rates of side reactions can become relevant when during consecutive

primary insertions they were negligible. The transfer after a 2,1-insertion has the potential to occur from either the β-methylene of the chain producing an internal, cis-alkene, or the β-CH_3 yielding an external alkene. Upon performing the experiments, only the internal alkene has been observed for this bimolecular process.[58,59]

Also relevant during olefin polymerization, especially when the metal has cyclopentadienyl rings that are highly substituted,[60-62] is β-methyl transfer to the metal, reforming a metal-methyl cation and liberating an allyl terminated olefin (Scheme 9). This pathway produces PP capped with an isobutyl group on one end and an allyl group on the other. From a molecular modeling perspective, using the simplified system $Cl_2Zr(^nPr)^+$, the π-complex from β-methyl transfer, $Cl_2ZrCH_3(ethylene)^+$, was much more stable compared to the product of β-hydride transfer, $Cl_2ZrH(propylene)^+$.[63] Added to

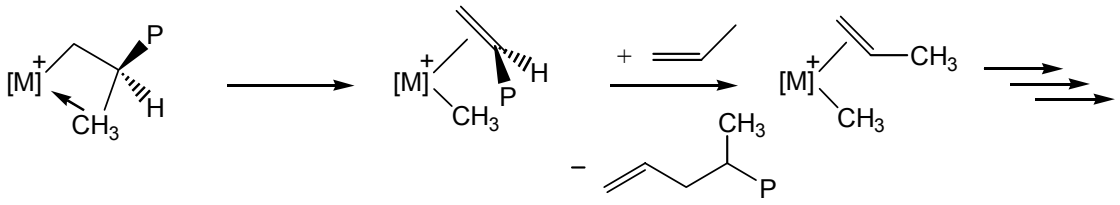

Scheme 9. Mechanism for β-methyl transfer to the metal.

this, upon dissociation of the olefin, the resulting methyl cation was significantly more stable (~ 18 kcal / mol) than the Zr^+-H cation, presumably due to the methyl groups capability to engage in α-agostic interactions.

In polymerizations employing MAO as the cocatalyst, especially in high Al : Zr ratios, a chain transfer to aluminum has been seen. This is believed to be attributable to residual $AlMe_3$ present in MAO. In Scheme 10, chain transfer produces a new M-CH_3 bond which can undergo further chain elongation. Hydrolysis produces a polymer with isobutyl groups on both ends of the chain. The previous chain termination mechanisms

provided unsaturated polymers. The rate of this reaction is slow such that it is commonly seen only in systems with a low level of productivity.[64,65]

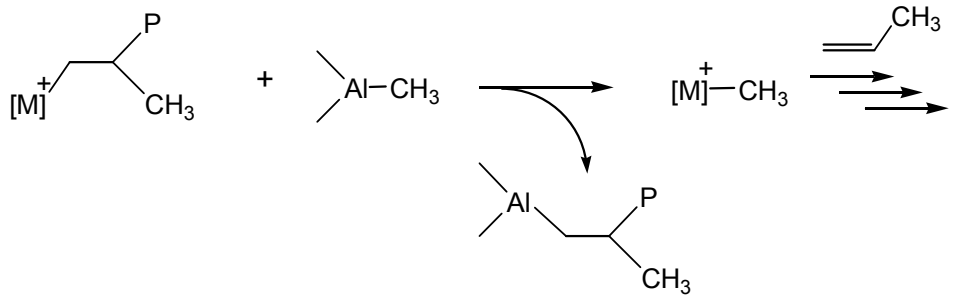

Scheme 10. Chain transfer to an aluminum cocatalyst as a termination event.

Finally, a common practice for molecular weight control during propylene polymerization is chain release via a transfer reagent, which is most typically molecular hydrogen. With fast rates of propagation, high molecular weight polymers are easily realized, but controlling the molecular weight aids in processing of the isolated polymer. The presumed mechanism for this hydrogenolysis is through direct insertion of H_2 into the metal-polymer bond.[66-68] Productivity of catalysts in the presence of H_2 is regularly higher than when H_2 is absent. This is rationalized through analysis of polymer end groups. A larger number of n-butyl end groups are present in PP prepared under H_2 pressure, and this is coupled with a decrease in the number of regioerrors in the polymer produced. With the rate of monomer insertion after a 2,1-misinsertion being slower, the rate of hydrogenolysis now becomes competitive, such that these mistakes are cleaved, producing the linear ^{n}Bu end group, and the resulting M-H species can reinitiate polymerization, producing the ^{n}Pr end group.[69,70] Insertion into M-H bonds is more facile than secondary centers, such that the metal center is thrust back into catalytic activity instead of lying “dormant” as a secondary growing chain.

One last side reaction that affects the polymer microstructure of C_2-symmetric *ansa*-bridged metallocenes is the chain-end epimerization of a primary inserted monomer. At low propylene pressures, a dramatic reduction in isotacticity was detected for *rac*-EBIZrCl$_2$ and *rac*-EBTHIZrCl$_2$, becoming virtually atactic under "catalyst starvation" conditions.[71] The enantiomorphic site control mechanism of propagation dictates facial preference from steric interactions relayed from the chiral metal environment such that the last inserted monomer unit plays no role in determining the chirality of the next generated asymmetric carbon center. Instead, this apparent stereoerror is explained as a result of epimerization of the primary growing chain.

The generally accepted mechanism for epimerization is presented in Scheme 11. Upon primary insertion, a β-hydride elimination occurs providing the cationic alkene bound hydrido species. An in-plane alkene rotation followed by a 2,1-insertion into the Zr-H bond generates a tertiary center. Another elimination is followed by alkene rotation and 1,2-insertion to regenerate the product of a primary insertion, except now with

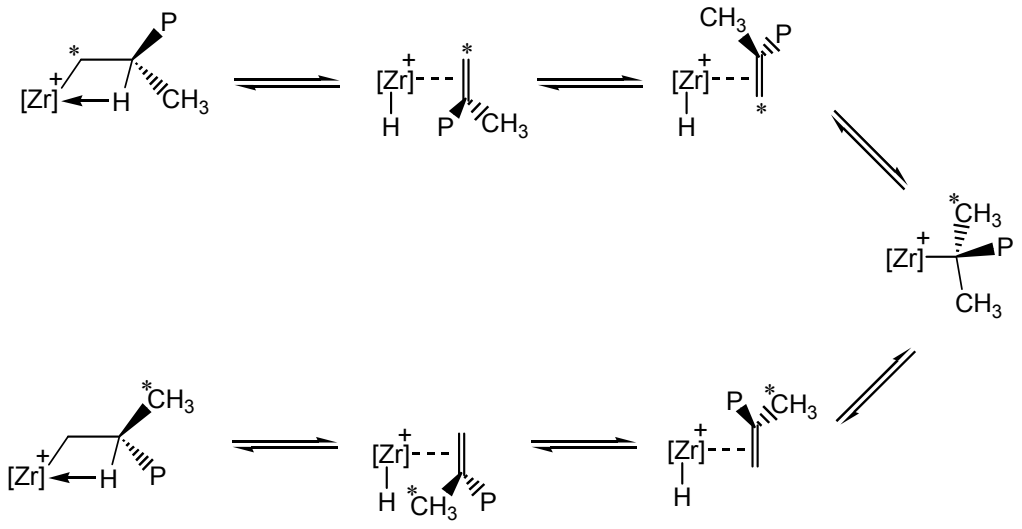

Scheme 11. Mechanism for chain-end epimerization via β-hydride elimination, alkene rotation, and reinsertion.

opposite handedness at the asymmetric center. Along the sequence of steps, detachment of the eliminated polymer chain is not necessary, for if that were the case it would be unlikely that this series of steps would proceed, for even at low propylene concentrations, excess monomer is present which could easily displace the *gem*-disubstituted olefin. This mechanism has been supported by several elaborate ^{2}H and ^{13}C labeling experiments.[72-74] These determined that the methylene group (labeled with an *) bound to Zr is transformed into the methyl group of opposite chirality through this mechanism.

Other mechanisms that have been proposed include intermediacy of an η^3-allyl / dihydrogen metal species after β-hydride elimination,[75] and direct intramolecular hydrogen transfer from the γ-methyl group to the α-methylene carbon with concomitant Zr-C(γ) formation and Zr-C(α) cleavage.[76] Without going into a lengthy discussion, the latter is unlikely due to high energy barriers to hydrogen transfer, and the former should allow for formation of labeled species that are absent in ^{13}C NMR spectra of doubly labeled propylene.

1.6. Late Transition Metals.

Early transition metal complexes are highly oxophilic, and thus are quite sensitive to any trace amounts of air or moisture present. This also makes them susceptible to poisoning from functionalized, polar monomers. While polar monomers such as acrylates can be copolymerized with ethylene using metallocenes in special circumstances,[77-79] late transition metals are typically utilized for this application. A wealth of information does not exist for homopolymerization of olefins using late transition metal catalysts due to an inherent loss of polymerization activity compared to early metal catalysts. Also, a competition exists between the rates of β-hydride

elimination and monomer incorporation such that only low molecular weight oligomers are produced.[36]

This dogma was reformed when Brookhart reported a series of Ni(II) and Pd(II) α-diimine catalysts capable of polymerizing ethylene and α-olefins to high molecular weight materials.[80-82] Activation of dimethyl complexes with $[H(Et_2O)_2][B(3,5\text{-}(CF_3)_2C_6H_3]$ provided the ether stabilized metal-methyl cations which were competent for polymerization of ethylene and α-olefins (Scheme 11). To bypass isolation of the ether adduct, polymerizations were also performed with MAO activated nickel dihalide complexes. The most interesting feature of polymerization with these late transition metal catalysts is seen in the polymer microstructure. Polyethylene produced from these systems range in microstructure from linear to highly branched. Higher pressures were found to decrease the number of branches, as was decreasing the steric bulk of

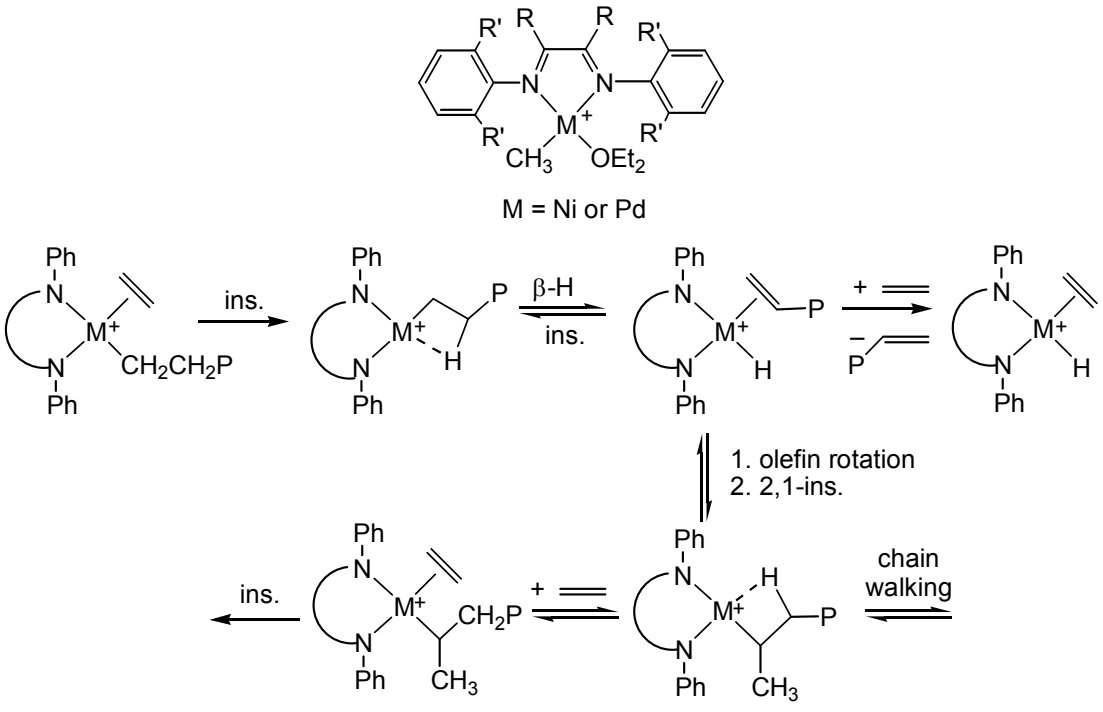

Scheme 12. Mechanism for chain-walking in ethylene polymerization with α-diimine catalysts of Ni and Pd.

groups on the 2,6-disubstituted phenyl ring from ^{i}Pr to Me. The most sterically hindered systems have the highest polymerization activity, as do Ni systems over those of Pd.[83] Details of ethylene polymerization were established through numerous NMR experiments at low temperature using the ether adducts. At –80 °C, the resting state of the catalyst is the alkyl cation with a coordinated molecule of ethylene, and exchange of bound ethylene with free ethylene was dependent upon ethylene concentration. The authors have also observed initial insertion products for propylene favoring a 2,1-insertion mode for α-olefins. Observed rate constants for migratory insertion and ethylene exchange are consistent with a faster ethylene decomplexation / recoordination than chain growth.

The rate determining step is chain migratory insertion from the resting state, which for ethylene is the olefin bound metal–alkyl cation and for α-olefins is the β-agostic hydrogen species.[83] Chain growth is then independent of ethylene concentration, while being first order in propylene. Following insertion, a β-agostic alkyl complex is formed that can be broken up via monomer coordination for further polymerization, or that can eliminate to provide a Pd-H with a bound alkene (Scheme 12). This terminated polymer chain can be displaced by ethylene to continue polymerization. Similar to chain epimerization seen with metallocenes, a rotation of the olefin adduct occurs followed by 2,1-insertion to yield a secondary center bound to the metal. This can then be trapped by monomer to grow a longer chain with a methyl branch. Lowering ethylene pressure allows a series of β-hydride eliminations, rotations, and readditions before ethylene coordination and insertion, generating even longer branches and amorphous polymers. The ability to observe ^{s}Bu branches requires the intermediacy of a tertiary alkyl bound to the metal, of which they have evidence in the form of a Pd(^{t}Bu) cation.[84] This mode of branch formation is called chain walking and it

is quite useful since a single feedstock monomer, which in this case typically provides highly crystalline polymers, can be polymerized to create an amorphous material similar to that seen in ethylene / α-olefin copolymerizations. Analogous polymers can be created from only ethylene by utilization of mixtures of multiple catalysts, an oligomerization catalyst to produce α-olefins *in situ* for incorporation with a polymerization catalyst.[85]

For α-olefin polymerization, the number of branches observed along the polymer backbone is less than should be expected for consecutive 1,2-insertions, and stretches of linear segments are apparent.[80,81] For instance, PP of any tacticity should contain 333 branches per 1000 carbons, and PH (poly(1-hexene)) should display 167 branches per 1000 carbons. This behavior for Ni and Pd systems was rationalized via a similar chain walking methodology as proposed for ethylene polymerization. As shown in Scheme 13, insertions can occur in either a 1,2- or 2,1-fashion to produce primary or secondary carbons, respectively, attached to the metal. Chain walking at this point along the pendant alkyl group of the last inserted monomer unit locates the metal center bound to a series of consecutive methylenes, resembling a segment of linear PE. The isomerization after a 2,1-insertion creates a lone methyl branch followed by methylenes

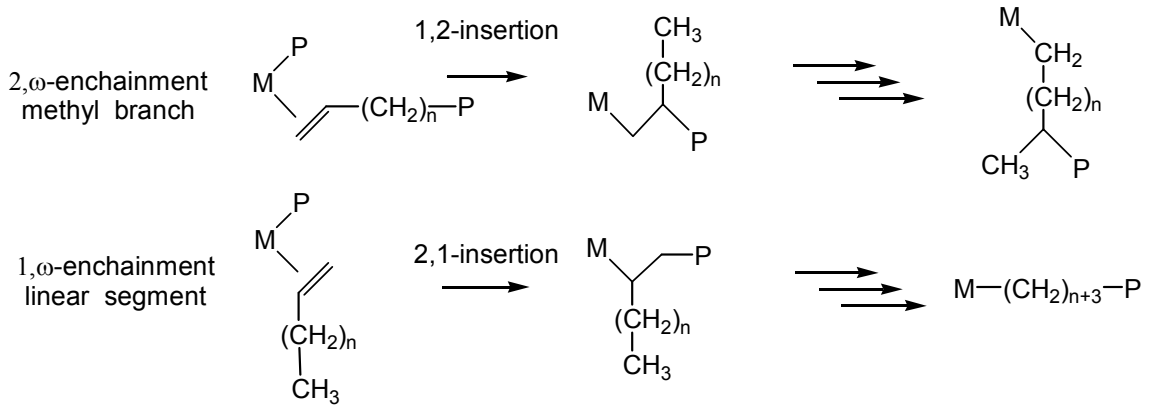

Scheme 13. Pathways leading to linear segments in α-olefin polymerization.

equivalent to the number of carbon atoms of the alkyl group. Intermediate branch lengths are typically not present since α-olefins cannot insert into secondary centers, which are products of metal migration along the pendant chain.[36]

1.7. Living Polymerizations.

In the realm of Ziegler-Natta polymerizations, few systems have been developed that have the ability to polymerize terminal olefins in a living fashion (i.e. devoid of irreversible termination or chain transfer). Such systems are highly desirable for the production of monodisperse polymers having well defined structures and tunable molecular weights. Of equal importance, these have the capacity to provide end group functionalized polymers through selection of appropriate terminating reagents and diblock copolymers through sequential monomer introduction. Since the first discoveries by Ziegler and Natta[2,3], numerous research groups have elucidated a wide range of potential available through selection of different metals and modification of ligand frameworks. This has led to homogeneous systems that can more easily be studied to elucidate the structure, reactivity, and mechanisms of polymerization. Due to their slow development, only recently have living Ziegler-Natta polymerization methods been in the spotlight.

The concept of living polymerizations was first described by Szwarc.[86,87] During the anionic polymerization of styrene, he found that the green THF solution of the naphthalene anion would turn immediately red upon introduction of styrene. Accompanying this would be an increase in the viscosity of the solution over time as the monomer was consumed. Addition of more monomer once the first had been exhausted caused an even greater increase in the solution viscosity due to continued polymer chain growth from the added styrene. If, after the first set of styrene was polymerized, isoprene was next added instead of styrene, again the viscosity would increase, but

after inducing termination with Et_3SiH no homopolymers of styrene or isoprene could be isolated. Thus, Szwarc was able to form a diblock copolymer (i.e. …A-A-A-B-B-B…, a polymer in which a sequence of one monomer unit is covalently linked to another) through the living polymerization of styrene and isoprene.

Since this discovery, a number of catalyst systems for all modes of polymerization have been reported to portray living polymerization, and the terminology has become quite loose. A set of common rules to outline the capabilities of a living polymerization catalyst system was introduced by Quirk.[88] Simply put, the guidelines were as follows:

1. polymerizations proceed until 100% monomer consumption, and readdition of monomer continues the polymerization;
2. number average molecular weight (M_n) of the polymer is a linear function of conversion;
3. the number of polymer molecules, and thus the number of catalytically active centers, remains constant throughout the polymerization;
4. the polymer molecular weight can be tuned through reaction stoichiometry, related to the degree of polymerization, DP = $[M]_o$ / $[I]_o$, where $[M]_o$ is the initial monomer concentration and $[I]_o$ is the initial initiator concentration;
5. narrow molecular weight distribution polymers must be produced, as evidenced by a narrow polydispersity index, PDI = M_w / M_n ~ 1, where M_w is the weight average molecular weight;
6. block copolymers can be prepared through sequential monomer addition;
7. chain end functionalized polymers can be prepared in quantitative yield.

No one criterion by itself defines a living system. Block copolymers can be prepared through consecutive monomer addition, although the polydispersity is quite broad. As

such, it is typically necessary to meet many of the above requirements before suggesting a system is living. With this collection of guidelines, it was now possible to fully gauge a catalysts capabilities toward propagation fidelity. With living polymerizations preferring monomer insertion as opposed to other side reactions, another handle was gained over polymerization methods.

Doi described one of the first living coordination polymerization systems for propylene using a homogeneous vanadium catalyst, $V[(acac)_3]$.[89] Activation was slow with $AlEt_2Cl$ as cocatalyst at the lowest temperatures, requiring hours to produce a constant number of polymer molecules. As mentioned previously, a constant concentration of propagating species was defined as a criterion of a living polymerization. Despite this, narrow molecular weight distributions of polypropylene were obtained (PDI ~ 1.25). However, when going to higher temperatures, larger polydispersities were noticed due to irreversible deactivation of the metal center concomitant with chain-transfer to Al.

McConville discovered a Ti based system that showed living behavior for higher olefin polymerization upon activation by $B(C_6F_5)_3$ (Scheme 14).[90] In early studies, chain transfer to aluminum was proposed to be terminating polymerizations involving MAO as the cocatalyst based on slightly broadened polydispersities (determined from gel permeation chromatography, GPC) and a lack of olefinic end groups in both the ^1H and ^{13}C NMR of the resulting polymers, which would have implicated β-hydrogen elimination as the terminating culprit. However, switching to the borane had the beneficial impact of narrowing the molecular weight distribution (PDI < 1.1). They also noted that in the absence of monomer, a catalytically inactive product was formed from perfluorophenyl group abstraction from the cocatalyst (Scheme 13).[31]

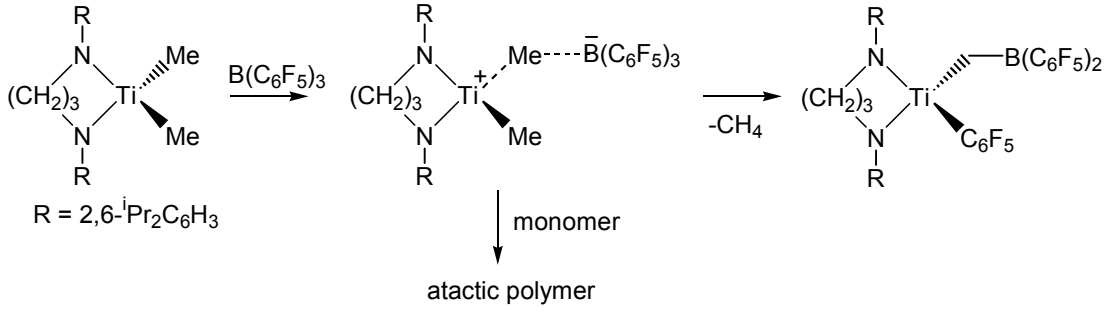

Scheme 14. Chelating diamide catalyst in the absence and presence of monomer.

Living polymerization of olefins by α-diimine catalysts has been proven by Brookhart and coworkers.[81] For the nickel compound shown in Scheme 15, activation with MAO at 23 °C in toluene yields polypropylene with M_w / M_n values as high as 1.8

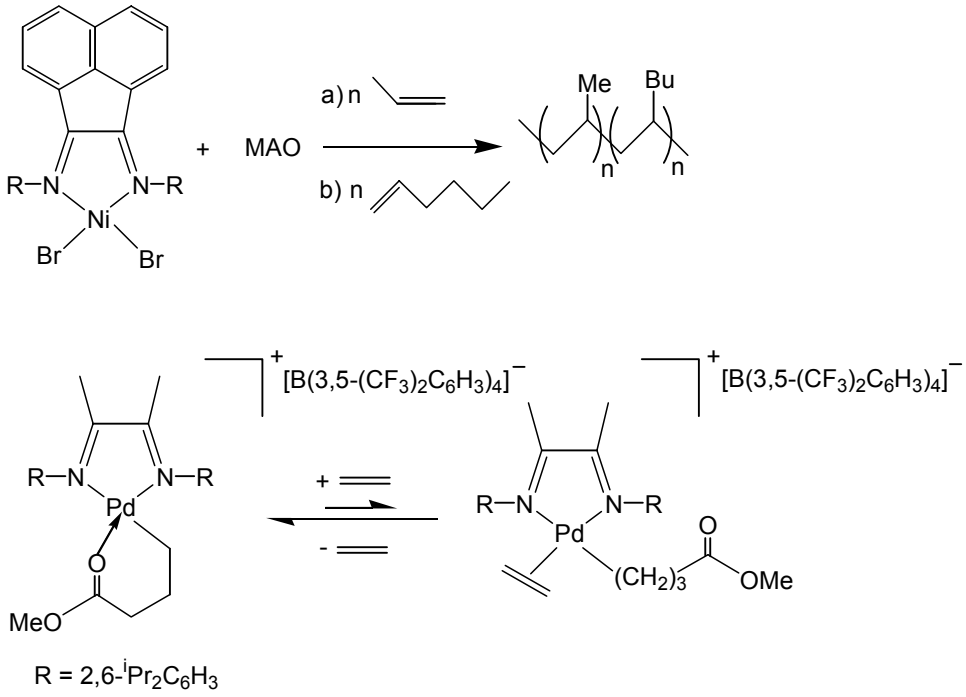

Scheme 15. Living α-diimine systems of late transition metals.

which demonstrate that some chain transfer reactions are present. However, these detrimental side reactions can be circumvented by lowering the temperature to –10 °C

and monomer concentration to around 1M, as evidenced by PDI of 1.13 for polypropylene (M_n=161 000). Further proof of the living nature of the species was detailed by a kinetic plot of M_n as a function of time, which proved to be linear. Finally, Brookhart was able to synthesize diblock copolymers of narrow block length by sequentially polymerizing propylene and 1-hexene, displaying a shift to a shorter retention time for GPC curves of the diblock compared to the homopolymer.

Also shown in Scheme 15 is the Pd chelate complex which Brookhart also has shown to be living for ethylene polymerization.[91] At low monomer pressures (1 atm), a low molecular weight tail was evident in the GPC curves of the resultant polymers, which is a factor not favoring true living behavior. The authors argued that an equilibrium existed between the chelate and the ethylene bound adduct, with the former being favored at low monomer concentrations and the latter being the precursor to initiation by migratory insertion. The chelate will dominate at low ethylene pressures, such that the rate of initiation will be slower in comparison to the ethylene bound species and all chains will not grow at the same rate leading to the broader PDI that they observe. Matyjaszewski has discussed this dilemma previously.[92]

Scheme 16 shows a series of tridentate zirconium complexes that have been developed by Schrock. Once activated by a borate cocatalyst, Schrock showed that the derivative with a diamido / ether linkage was a competent catalyst not only for ethylene but also for 1-hexene.[93] A linear plot of M_n vs time was found at 0 °C to provide

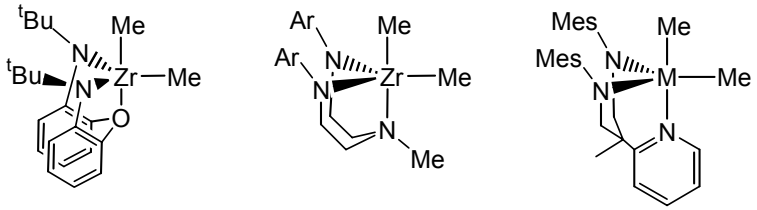

Scheme 16. Schrock's three tridentate catalysts for living polymerization of 1-hexene.

evidence of a living system, along with narrow polydispersities (PDI < 1.14). As with the polymerization systems mentioned previous to this, the polymer thus obtained is atactic according to ^{13}C NMR. The ^{t}Bu group was necessary to maintain catalytic activity, for complexes containing aryl groups with methyl substituents only serve to oligomerize 1-hexene.[36] No mention was made in regard to block copolymer formation with this system.

Schrock also introduced two additional nitrogen based tridentate complexes for living olefin polymerization.[94-96] While these will be discussed in greater detail later, a brief synopsis of the findings should be made. Both were capable of producing PH of extremely narrow molecular weight distributions (PDI $\leq$ 1.08), although choice of ligand environment was critical. For the ethylene separated [N_3], broad polydispersities were obtained when the phenyl group of the cationic complex employed was mesityl due to C-H bond activation of an ortho-CH_3 group.[97] Switching to 2,6-dichlorophenyl avoided this decomposition pathway, and at 0 °C narrow polydispersity PH was generated.

For the pyridine-containing [N_3], NMR evidence suggested that heptenes were being generated during 1-hexene polymerization when R = Me, presumably from 2,1-insertion.[95] Upon β-hydride elimination, a catalytically inactive species is formed, allowing those propagating species already formed to be the only actively growing centers in solution. With R = ^{i}Bu, no heptenes were found via NMR, although the cationic species was found to decompose in the absence of monomer. Nevertheless, narrow polydispersity PH's were formed while the molecular weights were found to be higher than the expected ratio $[M]_o$ / $[I]_o$.

The first living and stereospecific polymerization of α-olefins via Ziegler-Natta polymerization was provided by Shiono.[98] This group utilized a constrained geometry

catalyst (CGC, Scheme 17) at low temperature in conjunction with a boron cocatalyst for the living polymerization of propylene. When activated by $[Ph_3C][B(C_6F_5)_4]$ at –50 °C, a graph of polymer yield vs time is linear initially, but at longer times the yield no longer followed a linear behavior due to an unidentified deactivation process. However, when the borane $B(C_6F_5)_3$ was used over the same reaction time, the yield was linear with time throughout, and the molecular weight distributions remained lower. Upon warming to 0 °C, this polymerization was plagued by nonlinearity as well, indicating that the deactivation processes are amplified at higher temperatures. Homopolymers of both propylene and 1-hexene prepared from this system were syndiotactic-rich and the polypropylene pentad distribution matched up with the chain-end controlled syndiospecific polymerization mechanism.

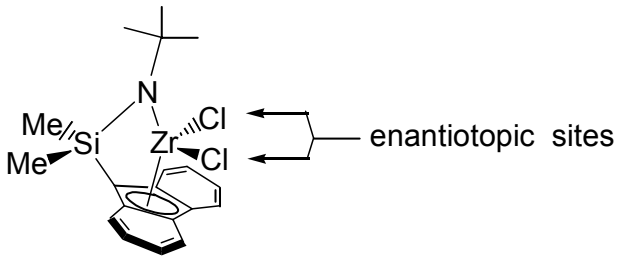

Scheme 17. A CGC that produces syndiotactic polymer at low temperatures.

Fukui and Soga explored the possibility of biscyclopentadienyl metallocenes being utilized as living Ziegler-Natta systems at low temperatures.[99] With Cp_2ZrCl_2 at –78 °C, and Cp_2HfCl_2 at –50 °C, the living polymerization of propylene can be accomplished according to linear plots of both polymer yield and M_n vs time when activated by $B(C_6F_5)_3$. The investigators also studied rac-EBIZrMe_2 / $B(C_6F_5)_3$ under similar conditions. Broad polydispersities were obtained even at this low temperature ($M_w / M_n > 2$) with large increases in the number of polymer chains present. However,

the polymer was highly stereoregular according to ^{13}C NMR, without the production of olefinic resonances thus showing that β-hydride elimination is not a prevalent pathway at this temperature. The polymer is of sufficiently low molecular weight (M_n ~ 4000), that the isobutyl end groups can be seen, which show that the polymerization proceeded via 1,2-enchainment.

Kol and coworkers have recently prepared a C_2-symmetric non-metallocene (Scheme 17) since a previously prepared C_s-symmetric derivative of this catalyst, which was able to produce narrow polydispersity block copolymers, provided only atactic poly(1-hexene).[100,101] Upon activation with $B(C_6F_5)_3$, a modest yield of PH is obtained

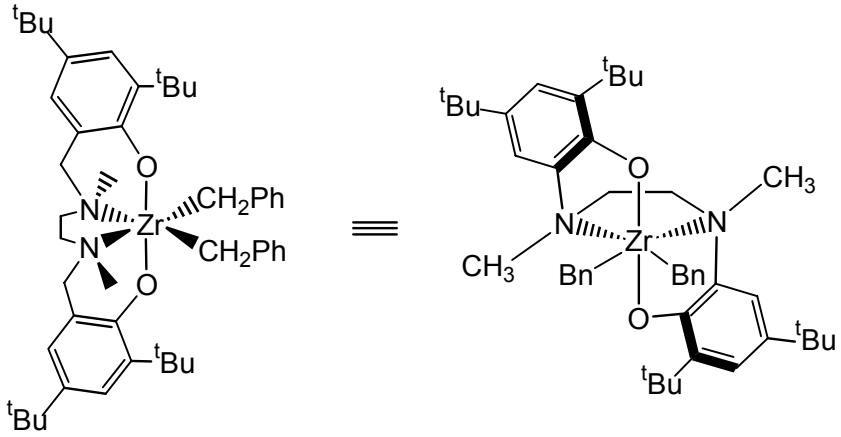

Scheme 18. C_2-symmetric di(alkoxo) complex for isospecific living polymerization of 1-hexene.

from the reaction run in neat monomer. The molecular weight of the polymer grows linearly with the amount of monomer consumption, a good indication that the system is living. Substitution with Me groups for the four ^{t}Bu groups provides, upon activation, a higher activity for the polymerization of 1-hexene, and a higher molecular weight, but a noticeably larger polydispersity, PDI ~ 1.6. Also this substitution drastically alters the

polymer microstructure, going from 95% isotactic to fully atactic. Judging by these facts, the bulk of the ^{t}Bu groups aids in stereodifferentiation of prochiral faces of the incoming olefin and sufficiently retards any terminating events.

A syndiospecific polymerization catalyst was developed by Mitsui and Coates, and it has additional attractive features that the catalyst by Kol lacked. This breed of living catalyst is based on bis(salicylaldiminato)titanium complexes which were found to polymerize propylene in a syndiospecific manner when activated with MAO (Scheme 19).[102,103] Pentafluorophenyl groups on the titanium bound N atoms were utilized with

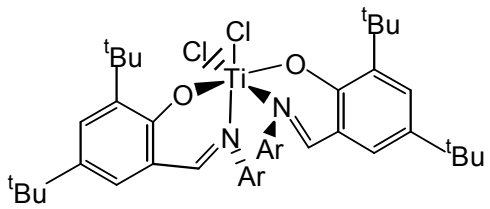

Scheme 19. Titanium catalyst for living syndiospecific polymerization.

the thought that further removal of electron density from the metal would provide a more electrophilic cation and a more active catalyst.[104] Aside from heightened activity, this catalyst provides low PDI, no β-hydrogen or β-Me elimination, no chain transfer, a linear plot of M_n vs yield, no olefinic end groups, and a calculated monomer to initiator ratio that reflects the molecular weight of the polymers, evidence that each active site produced a single chain during the reaction.[105] Of note, block copolymer formation with ethylene and propylene can be achieved with low PDI (1.12).

Living systems are of great interest for a variety of reasons: tuning of molecular weights, end group functionalization, block copolymer formation, etc. Determining the features that would provide a living system requires further elucidation, though N-based

ligands have thus far proven to be highly superior to metallocenes for establishing living behavior. The catalysts listed above have developed from a myriad of predecessors, which started with cyclopentadienyl ligands, to confer some level of control over polymerization.[106] Additional handles over stereospecificity and novel methods to retard terminating events will push living systems toward still greater heights.

1.8. References.

(1) Pino, P.; Mulhaupt, R. *Angew. Chem., Int. Ed. Engl.* **1980**, *19*, 857.

(2) Ziegler, K. *Angew. Chem.* **1952**, *64*, 323.

(3) Natta, G.; Pino, P.; Corradini, P.; Danusso, F.; Mazzanti, G.; Moraglio, G. *J. Am. Chem. Soc.* **1955**, *77*, 1708.

(4) Ketley, A. D.; Harvey, M. C. *J. Org. Chem.* **1961**, *26*, 4649.

(5) Samoilov, S. M. *J. Macromol. Sci.; Rev. Macromol. Chem.* **1981**, *C20*, 333.

(6) Doak, K. W. *Encycl. Polym. Sci. Eng.* **1986**, *6*, 386.

(7) Natta, G.; Pino, P.; Mazzanti, G.; Giannini, U. *J. Am. Chem. Soc.* **1957**, *79*, 2975.

(8) Breslow, D. S.; Newburg, N. R. *J. Am. Chem. Soc.* **1959**, *81*, 81.

(9) Brintzinger, H. H.; Fischer, D.; Mulhaupt, R.; Rieger, B.; Waymouth, R. M. *Angew. Chem., Int. Ed. Engl.* **1995**, *34*, 1143.

(10) Eisch, J. J.; Piotrowski, A. M.; Brownstein, S. K.; Gabe, E. J.; Lee, F. L. *J. Am. Chem. Soc.* **1985**, *107*, 7219.

(11) Cossee, P. *J. Catal.* **1964**, *3*, 80.

(12) Arlman, E. J. *J. Catal.* **1964**, *3*, 89.

(13) Arlman, E. J.; Cossee, P. *J. Catal.* **1964**, *3*, 99.

(14) Resconi, L.; Cavallo, L.; Fait, A.; Piemontesi, F. *Chem. Rev.* **2000**, *100*, 1253.

(15) Reichert, K. H.; Meyer, K. R. *Makromol. Chem.* **1973**, *169*, 163.

(16) Andreson, A.; Cordes, H. G.; Herwig, H.; Kaminsky, W.; Merk, A.; Mottweiler, R.; Pein, J.; Sinn, H.; Vollmer, H. J. *Angew. Chem., Int. Ed. Engl.* **1976**, *15*, 630.

(17) Sinn, H.; Kaminsky, W.; Vollmer, H. J.; Woldt, R. *Angew. Chem., Int. Ed. Engl.* **1980**, *19*, 390.

(18) Herwig, J.; Kaminsky, W. *Polym. Bull.* **1983**, *1983*.

(19) Kaminsky, W.; Miri, M.; Sinn, H.; Woldt, R. *Makromol. Chem. Rapid Commun.* **1983**, *4*, 417.

(20) Khrushch, N. E.; Dyachkovskii, F. S.; Marin, V. P.; Bravaya, N. M. *Kinetics and Catalysis* **1997**, *38*, 350.

(21) Gassman, P. G.; Callstrom, M. R. *J. Am. Chem. Soc.* **1987**, *109*, 7875.

(22) Sishta, C.; Hathorn, R. M.; Marks, T. J. *J. Am. Chem. Soc.* **1992**, *114*, 1112.

(23) Harlan, C. J.; Mason, M. R.; Barron, A. R. *J. Am. Chem. Soc.* **1994**, *13*, 2957.

(24) Yang, X. M.; Stern, C. L.; Marks, T. J. *Organometallics* **1991**, *10*, 840.

(25) Yang, X. M.; Stern, C. L.; Marks, T. J. *J. Am. Chem. Soc.* **1991**, *113*, 3623.

(26) Natta, G.; Corradini, P.; Bassi, I. W. *J. Am. Chem. Soc.* **1958**, *80*, 755.

(27) Yang, X. M.; Stern, C. L.; Marks, T. J. *J. Am. Chem. Soc.* **1994**, *116*, 10015.

(28) Siedle, A. R.; Newmark, R. A. *J. Organomet. Chem.* **1995**, *497*, 119.

(29) Chien, J. C. W.; Tsai, W.-M.; Rausch, M. D. *J. Am. Chem. Soc.* **1991**, *113*, 8570.

(30) Hlatky, G. G.; Eckman, R. R.; Turner, H. W. *Organometallics* **1992**, *11*, 1413.

(31) Scollard, J. D.; McConville, D. H.; Rettig, S. J. *Organometallics* **1997**, *16*, 1810.

(32) Thorn, M. G.; Vilardo, J. S.; Fanwick, P. E.; Rothwell, I. P. *Chem. Commun.* **1998**, 2427.

(33) Piers, W. E.; Chivers, T. *Chem. Soc. Rev.* **1997**, *26*, 345.

(34) Chen, E. Y. X.; Marks, T. J. *Chem. Rev.* **2000**, *100*, 1391.

(35) Woo, T. K.; Fan, L.; Ziegler, T. *Organometallics* **1994**, *13*, 2252.

(36) Ittel, S. D.; Johnson, L. K.; Brookhart, M. *Chem. Rev.* **2000**, *100*, 1169.

(37) Wu, Z.; Jordan, R. F.; Petersen, J. L. *J. Am. Chem. Soc.* **1995**, *117*, 5867.

(38) Casey, C. P.; Hallenbeck, S. L.; Wright, L. M.; Landis, C. R. *J. Am. Chem. Soc.* **1997**, *119*, 9680.

(39) Carpentier, J.-F.; Wu, Z.; Lee, C. W.; Stromberg, S.; Christopher, J. N.; Jordan, R. F. *J. Am. Chem. Soc.* **2000**, *122*, 7750.

(40) Stoebenau III, E. J.; Jordan, R. F. *J. Am. Chem. Soc.* **2003**, *125*, 3222.

(41) Casey, C. P.; Lee, T. Y.; Tunge, J. A.; Carpenetti, D. W. *J. Am. Chem. Soc.* **2001**, *123*, 10762.

(42) Casey, C. P.; Klein, J. F.; Fagan, M. A. *J. Am. Chem. Soc.* **2000**, *122*, 4320.

(43) Corradini, P.; Guerra, G. *Prog. Polym. Sci.* **1991**, *16*, 239.

(44) Yoshida, T.; Koga, N.; Morokuma, K. *Organometallics* **1996**, *15*, 766.

(45) Longo, P.; Grassi, A.; Pellecchia, C.; Zambelli, A. *Macromolecules* **1987**, *20*, 1015.

(46) Sacchi, M. C.; Barsties, E.; Tritto, I.; Locatelli, P.; Brintzinger, H. H.; Stehling, U. *Macromolecules* **1997**, *30*, 3955.

(47) Ewen, J. A. *J. Am. Chem. Soc.* **1984**, *106*, 6355.

(48) Resconi, L.; Abis, L.; Franciscono, G. *Macromolecules* **1992**, *25*, 6814.

(49) Hagihara, H.; Shiono, T.; Ikeda, T. *Macromol. Chem. Phys.* **1998**, *199*, 2439.

(50) Wild, F. R. W. P.; Zsolnai, L.; Huttner, G.; Brintzinger, H. H. *J. Organomet. Chem.* **1982**, *232*, 233.

(51) Kaminsky, W.; Kulper, K.; Brintzinger, H. H. *Angew. Chem., Int. Ed. Engl.* **1985**, *24*, 507.

(52) Ewen, J. A.; Haspeslach, L.; Atwood, J. L.; Zhang, H. *J. Am. Chem. Soc.* **1987**, *109*, 6544.

(53) Ewen, J. A. *J. Mol. Catal. A: Chem.* **1998**, *128*, 103.

(54) Resconi, L.; Camurati, I.; Sudmeijer, O. *Top. Catal.* **1999**, *7*, 145.

(55) Waymouth, R. M.; Pino, P. *J. Am. Chem. Soc.* **1990**, *112*, 4911.

(56) Kashiwa, N.; Yoshitake, J. *Polym. Bull.* **1984**, *11*, 479.

(57) Cavallo, L.; Guerra, G.; Corradini, P. *J. Am. Chem. Soc.* **1998**, *120*, 2428.

(58) Resconi, L.; Piemontesi, F.; Camurati, I.; Balboni, D.; Sironi, A.; Moret, M.; Rychlicki, H.; Zeigler, R. *Organometallics* **1996**, *15*, 5046.

(59) Schneider, M. J.; Mulhaupt, R. *Makromol. Chem. Phys.* **1997**, *198*, 1121.

(60) Resconi, L.; Piemontesi, F.; Franciscono, G.; Abis, L.; Fiorani, T. *J. Am. Chem. Soc.* **1992**, *114*, 1025.

(61) Hajela, S.; Bercaw, J. E. *Organometallics* **1994**, *13*, 1147.

(62) Guo, Z.; Swenson, D.; Jordan, R. F. *Organometallics* **1994**, *13*, 1424.

(63) Sini, G.; Macgregor, S. A.; Eisenstein, O.; Teuben, J. H. *Organometallics* **1994**, *13*, 1049.

(64) Chien, J. C. W.; Razavi, A. *J. Polym. Sci., A: Polym. Chem.* **1988**, *26*, 2369.

(65) Resconi, L.; Bossi, S.; Abis, L. *Macromolecules* **1990**, *23*, 4489.

(66) Gell, K. I.; Schwartz, J. *J. Am. Chem. Soc.* **1978**, *100*, 3246.

(67) McAlister, D. R.; Erwin, D. K.; Bercaw, J. E. *J. Am. Chem. Soc.* **1978**, *100*, 5966.

(68) Sperry, C. K.; Bazan, G. C.; Cotter, W. D. *J. Am. Chem. Soc.* **1999**, *121*, 1513.

(69) Tsutsui, T.; Kashiwa, N.; Mizuno, A. *Makromol. Chem. Rapid Commun.* **1990**, *11*, 565.

(70) Jungling, S.; Mulhaupt, R.; Stehling, U.; Brintzinger, H. H.; Fisher, D.; Langhauser, F. *J. Polym. Sci., A: Polym. Chem.* **1995**, *33*, 1305.

(71) Resconi, L.; Fait, A.; Piemontesi, F.; Colonnesi, M.; Rychlicki, H.; Zeigler, R. *Macromolecules* **1995**, *28*, 6667.

(72) Leclerc, M. K.; Brintzinger, H. H. *J. Am. Chem. Soc.* **1995**, *117*, 1651.

(73) Leclerc, M. K.; Brintzinger, H. H. *J. Am. Chem. Soc.* **1996**, *118*, 9024.

(74) Yoder, J. C.; Bercaw, J. E. *J. Am. Chem. Soc.* **2002**, *124*, 2548.

(75) Resconi, L. *J. Molec. Catal. A: Chem.* **1999**, *146*, 167.

(76) Lohrenz, J. C. W.; Buhl, M.; Weber, M.; Thiel, W. *J. Organomet. Chem.* **1999**, *592*, 11.

(77) Chung, T. C. *Macromolecules* **1988**, *21*, 865.

(78) Kesti, M. R.; Coates, G. W.; Waymouth, R. *J. Am. Chem. Soc.* **1992**, *114*, 9679.

(79) Wilen, C. E.; Luttikhedde, H.; Hjertberg, T.; Nasman, J. H. *Macromolecules* **1996**, *28*, 8569.

(80) Johnson, L. K.; Killian, C. M.; Brookhart, M. *J. Am. Chem. Soc.* **1995**, *117*, 6414.

(81) Killian, C. M.; Tempel, D. J.; Johnson, L. K.; Brookhart, M. *J. Am. Chem. Soc.* **1996**, *118*, 11664.

(82) Gates, D. P.; Svejda, S. K.; Onate, E.; Killian, C. M.; Johnson, L. K.; White, P. S.; Brookhart, M. *Macromolecules* **2000**, *33*, 2320.

(83) Svejda, S. A.; Johnson, L. K.; Brookhart, M. *J. Am. Chem. Soc.* **1999**, *121*, 10634.

(84) Shultz, L. H.; Tempel, D. J.; Brookhart, M. *J. Am. Chem. Soc.* **2001**, *123*, 11539.

(85) Komon, Z. J. A.; Diamond, G. M.; Leclerc, M. K.; Murphy, V.; Okazaki, M.; Bazan, G. C. *J. Am. Chem. Soc.* **2002**, *124*, 15280.

(86) Szwarc, M. *Nature* **1956**, *178*, 1168.

(87) Szwarc, M.; Levy, M.; Milkovich, R. *J. Am. Chem. Soc.* **1956**, *78*, 2656.

(88) Quirk, R. P.; Lee, B. *Polym. Int.* **1992**, *27*, 359.

(89) Doi, Y.; Suzuki, S.; Soga, K. *Macromolecules* **1986**, *19*, 2896.

(90) Scollard, J. D.; McConville, D. H. *J. Am. Chem. Soc.* **1996**, *118*, 10008.

(91) Gottfried, A. C.; Brookhart, M. *Macromolecules* **2001**, *34*, 1140.

(92) Matyjaszewski, K. *J. Phys. Org. Chem.* **1995**, *8*, 197.

(93) Baumann, R.; Davis, W. M.; Schrock, R. R. *J. Am. Chem. Soc.* **1997**, *119*, 3830.

(94) Liang, L. C.; Schrock, R. R.; Davis, W. M.; McConville, D. H. *J. Am. Chem. Soc.* **1999**, *121*, 5797.

(95) Mehrkhodavandi, P.; Bonitatebus, P. J.; Schrock, R. R. *J. Am. Chem. Soc.* **2000**, *122*, 7841.

(96) Mehrkhodavandi, P.; Schrock, R. R. *J. Am. Chem. Soc.* **2001**, *123*, 10746.

(97) Schrock, R. R.; Bonitatebus, P. J.; Schrodi, Y. *Organometallics* **2001**, *20*, 1056.

(98) Hagihara, H.; Shiono, T.; Ikeda, T. *Macromolecules* **1998**, *31*, 3184.

(99) Fukui, Y.; Murata, M.; Soga, K. *Macromol. Rapid Commun.* **1999**, *20*, 637.

(100) Tshuva, E. Y.; Goldberg, I.; Kol, M.; Weitman, H.; Goldschmidt, Z. *Chem. Commun.* **2000**, 379.

(101) Tshuva, E. Y.; Goldberg, I.; Kol, M. *J. Am. Chem. Soc.* **2000**, *122*, 10706.

(102) Matsui, S.; Tohi, Y.; Mitani, M.; Saito, J.; Makio, H.; Tanaka, H.; Nitabaru, M.; Nakano, T.; Fujita, T. *Chem. Lett.* **1999**, 1065.

(103) Tian, J.; Coates, G. W. *Angew. Chem., Int. Ed. Engl.* **2000**, *112*, 3772.

(104) Tian, J.; Hustad, P. D.; Coates, G. W. *J. Am. Chem. Soc.* **2001**, *123*, 5134.

(105) Hustad, P. D.; Tian, J.; Coates, G. W. *J. Am. Chem. Soc.* **2002**, *124*, 3614.

(106) Coates, G. W.; Hustad, P. D.; Reinartz, S. *Angew. Chem., Int. Ed. Engl.* **2002**, *41*, 2237.

Chapter 2

Preparation of Amidinate Precatalysts

2.1. Introduction.

The Ziegler-Natta polymerization of α-olefins remains an alluring academic and industrial interest thanks to the continued success and development of highly active, stereospecific, and living catalyst systems. Research in this area has long been dominated by bis-cyclopentadienyl (bis-Cp) Group IV complexes, known as metallocenes, viewed as homogeneous analogues of the initial heterogeneous catalysts utilized by Ziegler and Natta for ethylene and propylene polymerization. While early strides in this arena revolved around structurally simplistic titanocene dichloride, which when activated provided atactic polymers from prochiral olefins, exploration into the diversification of the bis-Cp motif lead to the highly successful ansa-bridged metallocenes for stereospecific olefin polymerization. These single-site polymerization catalysts have warranted such notoriety that they have been extensively reviewed.[1-6]

Advances in ligand frameworks deviating from the bis-Cp moiety have only recently received significant interest due to the latter's success. One of the earliest non-metallocene species explored was the half-sandwich amides of Ti and Zr, also referred to as the constrained geometry catalysts (CGC's), which have been developed for commercial exploitation.[7] The Ni α-diimine systems first introduced by Brookhart also showed that catalysts with ancillary ligands bearing heteroatoms contained the potential to expand the horizon beyond metallocenes.[8] Continued investigation of oxygen- and nitrogen-based ligands has contributed significantly to the range of structural geometries

and ligation environments about the central metal, which serve to affect the steric and electronic properties of the compound.[9,10]

One ligand set of interest has been the amidinate, $[N(R^1)C(R^2)N(R^3)]^{1-}$, a monoanionic, 4 electron donor which can be viewed as a hetero-atom containing allylic species. It has remained a popular ligand due to the wide variety of f-block element, transition metal, and main group metal complexes available, since the steric and electronic properties of this ligand are readily tailored by controlled manipulation of the substituents, R^1, R^2, and R^3.[11,12] For Group IV metal-containing complexes, the bulk of previous work has focused on benzamidinates, where R^2 is a phenyl derivative, although other R^2 substituents have also been reported, pertinent here are formamidinates (R^2 = H), *tert*-butylamidinates (R^2 = ^{t}Bu), and acetamidinates (R^2 = methyl). Many mono- (**1**), bis- (**2**), and tris-amidinate (**3**) complexes have been prepared which have shown activity toward the catalytic isomerization of olefins, as well as olefin polymerization when activated by methylaluminoxane (MAO). Literature reports on the synthesis of Group IV amidinate complexes chiefly involve one of two routes: 1) salt elimination between MCl_4 and an alkali-metal amidinate, or 2) metathesis between MCl_4 and an N-silylated amidine. While in both cases, the NCN-containing starting material must be prepared in a previous step, they both provide compounds of the formula $[N(R^1)C(R^2)N(R^3)]_nMCl_{4-n}$, although for n > 1, route 1 is typically employed. These compounds can also be alkylated in another step involving the appropriate ratio of alkyl lithium or alkyl Grignard reagent.

Extension of the utility of amidinate ligands led to the mixed-ligand systems using an amidinate in tandem with a Cp moiety.[13-16] With the amidinate drawing comparisons to a Cp ligand,[17-19] these complexes were intriguing since the resulting compounds would inherently be more electron deficient (cf., Cp is a 6-electron donor while amidinates are 4-electron donors), yet still potentially retaining many of the advantages

of its bis-Cp relatives. Early reports of these complexes exploited a salt elimination route similar to the one mentioned earlier, as depicted in Scheme 20. The metal trihalides, (η^5-C_5R_5)MX_3 [R = H or Me, M = Ti, Zr, or Hf and X = F or Cl], react with one

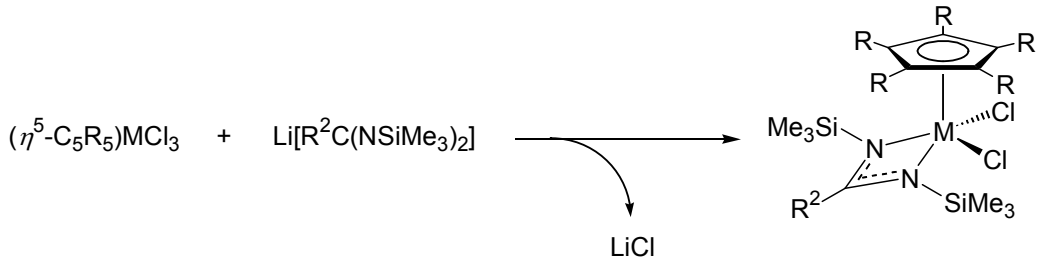

Scheme 20. Salt elimination route to provide first mixed ligand Group IV complexes.

equivalent of lithium amidinate to afford the penta-coordinate complexes, (η^5-C_5R_5)[$R^2C(NSiMe_3)_2$]MX_2 (**4**), as air-sensitive crystals. These heteroallylic species can be subsequently alkylated by employing MeLi, $MgMe_2$, KCH_2Ph, etc.

The aforementioned benzamidinate complexes have been limited to the N,N'-bis(trimethylsilyl) ligands, $R^1 = R^3 = SiMe_3$. One significant disadvantage to this class of compounds is the hydrolytic instability of the N-Si bond, of which each compound has several, providing compounds that are difficult to characterize and to handle.[20] A remedy for this is the inclusion of alkyl groups on the two nitrogen atoms. Making use of lithium amidinates derived from the reaction of R^2Li and an N-alkylated carbodiimide ($R^1N=C=NR^3$), the amidinates **1**-**4** can be prepared through appropriate stoichiometry. Indeed, these complexes display markedly greater stability than their N-$SiMe_3$ counterparts, being stable in air for days as crystalline solids.

Our interest in the monoamidinate mono-Cp mixed ligand system stems from the high degree of tunability inherent in its structure shown at right. With a large number of Cp-based ligands that can be

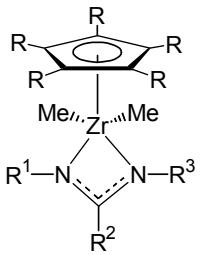

readily prepared, from the slim Cp to the large fluorenyl, it is possible to open up or shut down access to much of the "top" of the zirconium atom. For the amidinate functionality, three positions are now present that may be manipulated, the two nitrogen substituents, R^1 and R^3, and the central carbon substituent, R^2. With such a large level of manipulation possible, determining the best possible combination of factors for polymerization is an achievable goal through structure / property relationships, so long as the synthetic steps to realize the multitude of possibilities is minimal.

One method for preparation of transition metal amidinates that has received little attention has been the insertion of carbodiimides into metal-alkyl bonds. The first evidence for this reaction was published nearly 30 years ago with an insertion occurring between Me_nMCl_{5-n} (M = Ta or Nb and n = 1-3) and a disubstituted, symmetrical carbodiimide, though the yields were very low.[21] In a study of CO_2-like molecules, Floriani was able to spectroscopically observe insertion into the Zr-Me bond of dimethylzirconocene, Cp_2ZrMe_2, with p-tolylcarbodiimide in only 45% yield after long reaction times under forcing conditions.[22,23] However, insertion into main group metal alkyl bonds appears to be much more facile, occurring at RT for $AlMe_3$.[24,25]

In spite of the lack of success seen previously with carbodiimide insertion reactions with transition metal complexes, this methodology has been shown to be an effective route to mixed ligand systems of Ti.[26-28] The following chapter will discuss achievements made upon application of this methodology toward Zr compounds, as well as more traditional approaches toward producing derivatives having different R^2 groups, and comparisons of their respective solid state characteristics and solution behaviors.

2.2. Pentamethylcyclopentadienyl Zirconium Amidinates (Cp*ZA's).

2.2.1. Synthesis. As mentioned previously, carbodiimide insertion into transition metal-alkyl bonds has not met great success. However, from our lab, symmetric ($R^1 = R^3$) and unsymmetric ($R^1 \neq R^3$) carbodiimides are known to undergo insertion into titanium-methyl bonds of (η^5-C_5R_5)$TiMe_3$ (R = H or Me) to afford dimethylmonocyclopentadienyl titanium acetamidinates.[26-28] Similarly, by employing

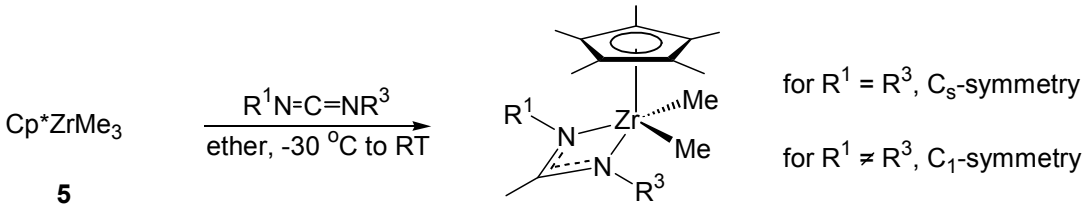

	R^1	R^3
6a	^{t}Bu	Et
6b	^{t}Bu	Cy
6c	^{t}Bu	2,6-^{i}Pr$_2$Ph
6d	Cy	Cy
6e	^{i}Pr	^{i}Pr

Scheme 21. Preparation of compounds **6a**-**e** through carbodiimide insertion.

Cp^*ZrMe_3 (**5**),[29] the synthesis of a series of pentamethylcyclopentadienylzirconium acetamidinate (Cp*ZA) derivatives of $Cp^*ZrMe_2[R^1NC(CH_3)NR^3]$ **6** can be accomplished in good yields according to Scheme 21.[30] While yields from this reaction were high, starting material **5**, prepared from Cp^*ZrCl_3 and 3 eq. MeLi, is known to be thermally unstable upon isolation which can cause problems with handling. To remove this as a potential problem, **5** was utilized *in situ* in a one-pot, two step synthesis detailed in Scheme 22. To prevent any excess MeLi from performing undesirable side reactions, Me_3SiCl is added to quench the methylating reagent prior to the addition of the carbodiimide. This sequence is ideal since it precludes the isolation of **5** and capitalizes

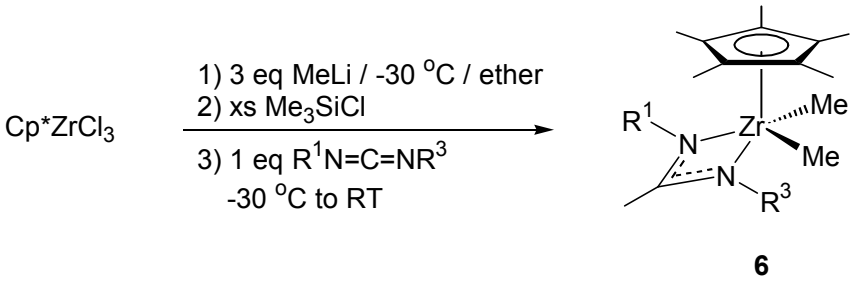

6

Scheme 22. One-pot direct synthesis of zirconium amidinates **6a**-**e** via **5** prepared *in situ*.

on the fact that all materials are commercially available. With the ease with which **6a**-**e** can be prepared, the range of Cp*ZA's that can be realized is solely dependent on the spectrum of carbodiimides available. Fortunately, a facile pathway to a series of carbodiimides has already been elucidated, allowing a highly tunable environment about **6** (see Figure 5).[31] For instance, insertion of a symmetric carbodiimide into a zirconium-methyl bond results in a complex with C_s-symmetry (meso compound) in which the mirror plane bisects the two homotopic methyl groups. For asymmetric carbodiimides, the organometallic product no longer has any symmetry elements. With the molecule having C_1-symmetry, the methyl groups are no longer equivalent, thus being diastereotopic. Compounds of this genre are generated as mixtures of inseparable enantiomers, varying in the relative orientation of the R^1 and R^3 groups to the metal.

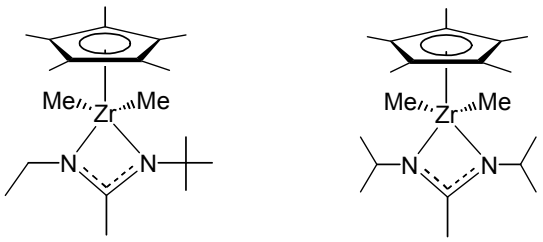

6a (C_1) **6e** (C_s)

Figure 5. Symmetry considerations for zirconium amidinate complexes.

While insertion into zirconium-methyl bonds is quite facile for Cp*ZA's, other researchers have investigated insertion reactions into other Zr-X bonds. Carbodiimides have also been shown to insert into the Zr-H and Zr-Ph bonds of $Cp_2ZrH(Cl)$ and Cp_2ZrPh_2, respectively, with a crystal structure being obtained for the former.[23] This reaction was not, however, applicable to insertion into the Zr-CH_2Ph bond, even in refluxing toluene. While these reactions are useful, they are not germane toward the one-step production of dimethyl precatalysts.

2.2.2. Other Synthetic Methods. As mentioned in the Introduction, the most prevalent method for production of amidinate complexes is the salt elimination route between a metal halide and an alkali-metal amidinate. For the amidinate species

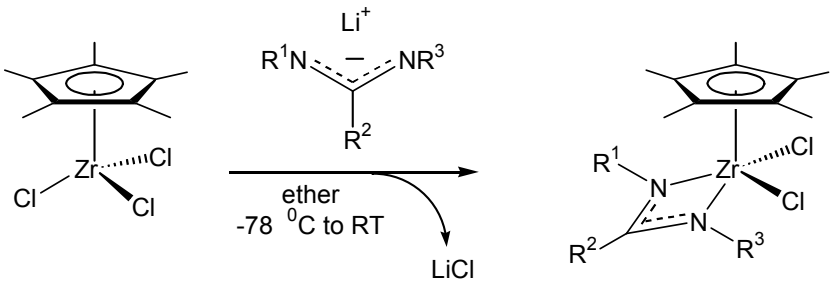

7 (R^2 = H), **8** (R^2 = CH_3), **9** (R^2 = ^{t}Bu), **10** (R^2 = Ph)

Scheme 23. Preparation of dichloro species **7**-**10** via lithium amidinates.

discussed herein, their synthesis was conducted as depicted in Scheme 23. As shown, several variants of R^2 were prepared through this method in excellent yields. Upon filtration of the LiCl, crude materials were quite clean and were fractionally crystallized from any minor byproducts. In order to obtain dimethyl precatalysts, compounds **7**-**10** were methylated using two equivalents (eq.) of MeLi to provide the alkylated derivatives **11**, **6**, **12**, and **13**, respectively. For alkylation, MeMgBr could not be used as an

alkylating agent of **7**-**10** since double alkylation was not seen even in the presence of a ten-fold excess of the Grignard. While this method is effective for the production of **6**, overall yields, with respect to Cp^*ZrCl_3, are higher from the carbodiimide insertion route.

Also referred to earlier was the metathesis method between a transition metal halide and an N-silylated amidine.[11,12] This was attempted for the preparation of the series of formamidines **7** as depicted in Scheme 24. Employing the N-silylformamidines **14**,[32] the formamidinates **7** could be prepared in toluene with few byproducts as a crude material. In ether, at either RT or reflux, no reaction was observed as only starting materials were recovered. However, attempts at recrystallization of **7** were thwarted through cocrystallization of the minor side products of the reaction and the coproduced Et_3SiCl.

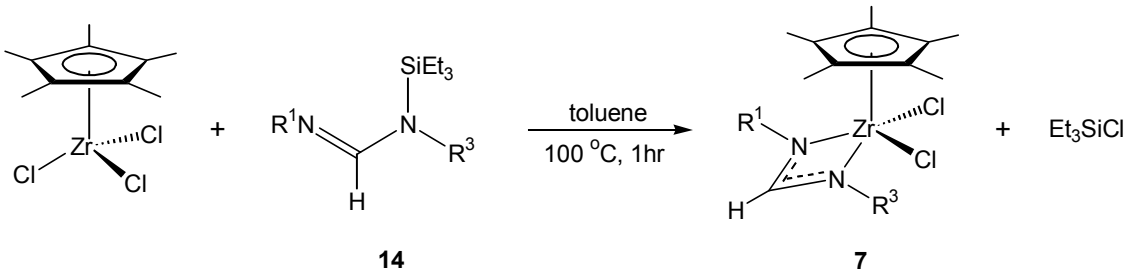

14 **7**

Scheme 24. Production of formamidines **11** from metathesis route.

2.3. Solid State Structural Characterization of Precatalysts.

Upon recrystallization of the crude reaction mixtures, single crystals were obtained that allowed for structural analysis of the Cp*ZA's from X-ray diffraction studies. Several of these have been reproduced in Figure 6 which provides examples of the assortment of R^1 and R^3 groups that are possible. All Cp*ZA's are monomeric in the solid state and exist in four-legged piano stool conformations, the two Me groups and the two amidinate nitrogens serving as the legs. While amidinates are known to serve

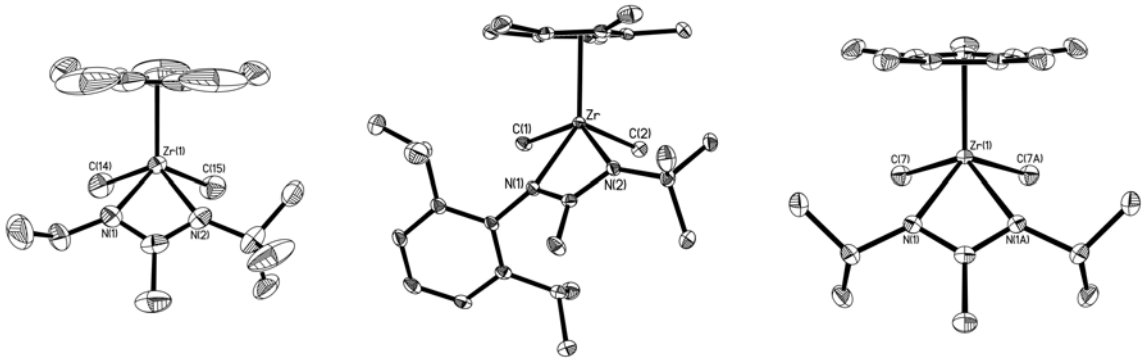

6a **6c** **6e**

Figure 6. Selected solid state structures for Cp*ZA's of **6** having varying acetamidinate nitrogen substituents, R^1 and R^3. Hydrogen atoms have been omitted for the sake of clarity.

as bimetallic monodentate bridging ligands,[33,34] they act in a bidentate fashion for these amidinate compounds. Overall, there exist no unusual bond lengths, bond angles, or coordination geometries within this series of compounds as compared with other Group IV amidinate complexes. A brief comparison of trends, or lack thereof, is presented. It should be noted here that no molecular structures of dimethyl Cp*ZA's have been presented in the literature.

For the amidinate metallacycles within **6**, the Zr-N bond lengths fall within expected ranges, although the Zr-N(1) distance tends to be shorter than Zr-N(2) for the dissymmetric **6a** and **6c** (cf., 2.251(3) vs 2.265(2) Å for **6a** and 2.2469(18) vs 2.3249(17) Å for **6c**). Also of note, the delocalization of the charge throughout the NCN fragment is apparent. In a static sense, the chelating mode for an amidinate should be through a covalent bond from an amine and a dative bond from an imine as in Scheme 25. However, the N(1)-C(CH_3) and N(2)-C(CH_3) lengths do not display this asymmetry for the chelate. With bond distances between 1.32 and 1.34 Å, these values fall between

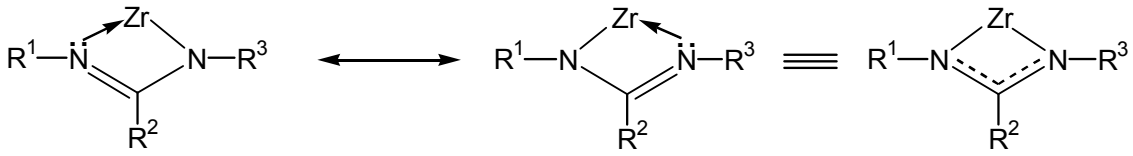

Scheme 25. Illustration of resonance modes allowing for charge delocalization along the amidinate moiety.

those for an *sp*^{2} C-N bond (1.38 Å) and a C=N bond (1.28 Å), illustrating the delocalization of the charge within the NCN moiety applicable to all Cp*ZA's of **6**.

Figure 7 shows the solid state structures of several selected Cp*ZA's which illustrate the variety of different R^2 substituents which have been investigated. With this set of structures, it is possible to ascertain in what ways steric interactions of the carbon substituent of the amidinate impact overall stucture. With R^2 = H, the smallest possible substituent, the N-alkyl substituents are able to "relax" back toward this small group as evidenced by the N-C-N angle being the most open of the series at 116.79(10) ° for **11a** (cf., 112.2(3) ° for **6a** and 109.2(4) ° for **12**). In conjunction with this, the bite angle of the amidinate is slightly more obtuse, with the N-Zr-N angle being 58.94(3) ° for **11a**, as

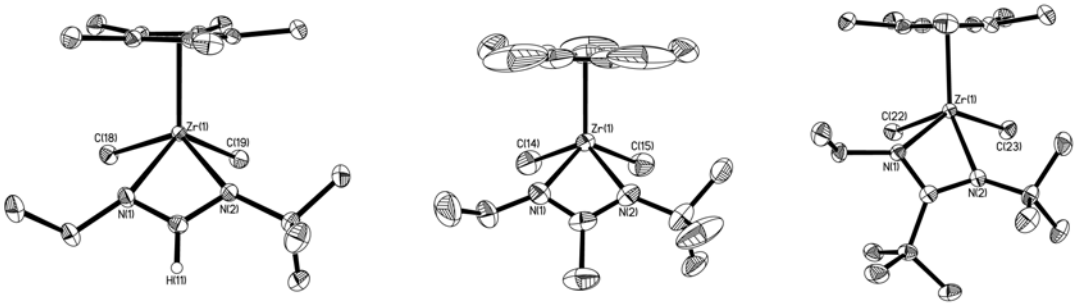

11a **6a** **12**

Figure 7. Selected solid state structure of Cp*ZA's illustrating various R^2 groups. Hydrogen atoms, except for H(11) in **11a**, have been omitted for the sake of clarity.

compared to 58.40(9) ° and 57.50(13) ° for **6a** and **12**, respectively. To minimize non-bonding steric interactions, a pyramidal distortion occurs for all N atoms, being in all cases larger for N(1) than N(2). Although only minimal in many cases, the largest divergence occurs for N(1) of **12**, being 348.7 °. In conjunction with this, steric congestion can be modified through the amount of bend, or pucker, found within the binding mode of the amidinate. While most amidinate metallacycles exist in planar environments, others are known that deviate from planarity.[12] This interplane deviation, identified as the dihedral angle between planes defined by N-C-N and N-Zr-N, is largest for **12** with a value of 34.7 °, compared to 20.7 ° for **11a** and 18.3 ° for **6a**. Two such large groups ($R^2 = R^3 = {}^tBu$ in **12**) on neighboring portions of the amidinate appear to induce major strain on the amidinate structure, necessitating both sets of non-planar surroundings. By contrast, moving the large groups further from eachother by increasing the overall bulk of R^1 and R^3, as in **6c**, brings the two planes closer to unity with an interplane angle of 1.0 °.

2.4. Solution Behavior and Properties of Cp*ZA's.

It is readily apparent from ^1H NMR spectra of Cp*ZA's that these molecules are highly fluctional in solution. This is not without precedent for other amidinate complexes have also displayed configurational fluxionality in solution.[35-38] For a series of titanium Cp*ZA's, it was established that configurational instability was inherent to this family of mixed ligand molecules.[26] As mentioned earlier, when $R^1 \neq R^3$, the molecule is C_1-symmetric and obtained as a mixture of enantiomers. For these asymmetric derivatives, it was found that two resonances were present in the low temperature ^1H NMR spectra corresponding to the diastereotopic methyl groups attached to the chiral Ti atom at the slow exchange limit for racemization. Although the precise mechanism by which these

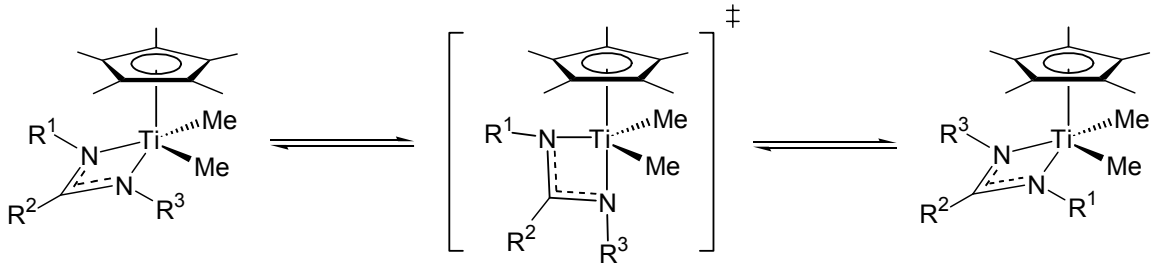

Scheme 26. Facile racemization of Cp*ZA's via amidinate ring flipping.

methyl groups equilibrate at the fast exchange limit is not precisely known, amidinate "ring flipping" in which one nitrogen totally or partially dissociates from the metal, as shown in Scheme 26, has been offered as the method that allows for this interchange.[37,38] Other methods of exchange have been proposed for other amidinate complexes.[17]

Upon inspection of the partial ^{1}H NMR spectra of **6a** shown in Figure 8, similar fluxional behavior is evident. At 293 K, the environments about the hydrogens is averaged, and the two methyl groups appear as one singlet while the methylene of the N-ethyl group appears as a quartet, illustrating that amidinate ring flipping is a facile process. Upon cooling, both resonances broaden then decoalesce to form two singlets and two doublets of quartets, respectively, at the slow exchange limit (193 K). This can be better appreciated by viewing the equilibrium also shown in Figure 8. At low temperature, once the dynamic processes, save Cp* rotation, have been frozen out, the environments around each respective Zr-Me group are noticeably different, with one residing on the N-^{t}Bu side and the other on the N-Et side of the amidinate. As such, the chemical surroundings are effectively different resulting in two singlets. For the ethyl group at the fast exchange limit, the hydrogens of the methylene group interconvert upon ring flipping; however, H_a and H_b no longer interconvert at low temperature,

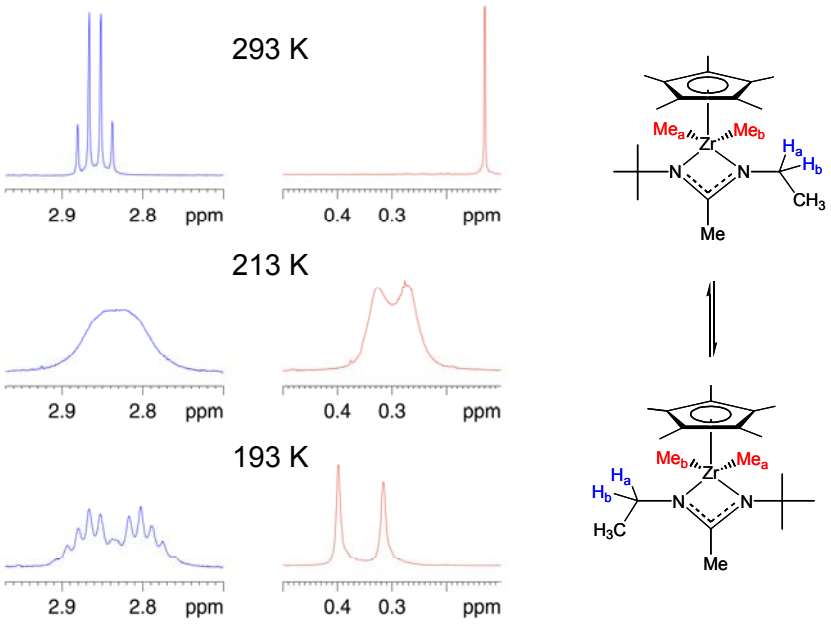

$\Delta G^{\ddagger}$ = 10.9 kcal mol^{-1}, T_c = 223 K

Figure 8. Partial low temperature ^{1}H NMR spectra (C_7D_8, 400 MHz) of **6a**.

leading to distinct resonances for both hydrogen atoms. Analysis of the series of spectra provides a barrier to racemization for **6a** at the coalescence temperature, $\Delta G_c^{\ddagger}$, of 10.9 kcal / mol. Similarly, the same parameter for **6b** was found to be 12.8 kcal / mol, indicative of a larger barrier to racemization upon increasing steric bulk opposite to the N-^{t}Bu group (i.e. from R^3 = Et to Cy). By comparison, these compounds contain a lower barrier to metal-centered epimerization (amidinate ring flipping is faster) for the series of **6** compared to their titanium analogues having $\Delta G_c^{\ddagger}$ values of 14.9 and 15.2 kcal mol^{-1} for Cp*TiMe$_2$[^{t}BuNC(CH$_3$)NEt] and Cp*TiMe$_2$[^{t}BuNC(CH$_3$)NCy], respectively.[26]

In terms of stability, compounds **6** are quite stable at RT in C_6D_6 under N_2 for days without change. The formamidinates are not nearly so, with **11a** decomposing under the same conditions within ~24 hours. As for **12**, sitting in solution overnight did

not alter the ^{1}H NMR spectrum at all, while heating to 80 °C for 3 hours offered a small amount of evidence that the material was decomposing.

2.5. Cyclopentadienyl Zirconium Acetamidinates (CpZA's).

2.5.1. Synthesis. With a number of modifications made to the R groups present in the amidinate group, it was next necessary to assess another source for manipulation, specifically the cyclopentadienyl ligand. The simplest approach to varying the structure of the (η^5-C_5R_5) ligand was to transition from the previously discussed R = Me to R = H. The resulting CpZA's will provide another piece toward understanding structure / property relationships within this collection of complexes.

While for Cp*ZA's the trimethyl Cp*$ZrMe_3$, **5**, was attainable as an isolable solid and could be used for subsequent carbodiimide insertion, the related $CpZrMe_3$ is known to be thermally and chemically unstable, in fact never being isolated in pure form. Fortunately, the need to contend with this compound is bypassed due to the ability in preparing CpZA's through the one pot, two-step carbodiimide insertion approach highlighted in the preparation of Cp*ZA's **6**.

As shown in Scheme 27, the unstable $CpZrMe_3$ is produced *in situ* through methylation of $CpZrCl_3$ at low temperature. Upon quenching excess MeLi, introduction of carbodiimide and slowly warming to RT supplies the desired compounds **15** in good yields.[39] Diligent care must be taken in the synthesis of these complexes. Imprecision in the amount of MeLi drastically affects the products of the reaction. In the synthesis of **15c**, a very slim amount of product was found if the reaction is performed in the presence of a slight excess of MeLi. In this case the major products of reaction were the dimethyl bisamidinate, [^{i}PrNC(Me)N^{i}Pr]$_2$$ZrMe_2$ (**16**), and Cp_2ZrMe_2 (**17**).[13] Tight control of the amount of MeLi employed and quenching any potential excess with TMSCl prior

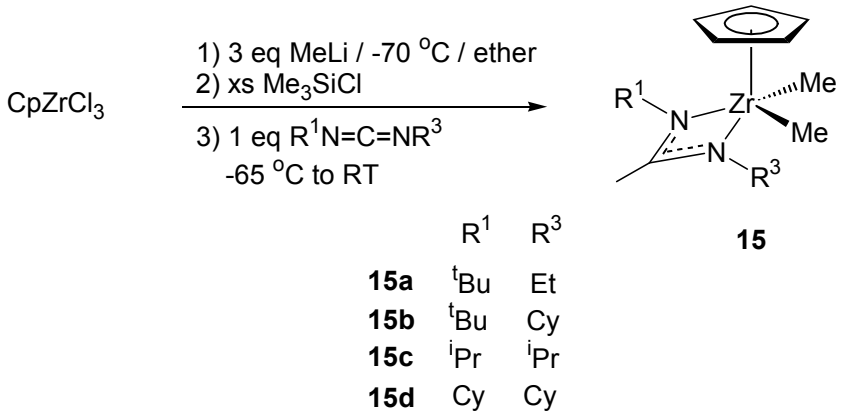

	R^1	R^3
15a	^{t}Bu	Et
15b	^{t}Bu	Cy
15c	^{i}Pr	^{i}Pr
15d	Cy	Cy

15

Scheme 27. Preparation of CpZA's **15** via one pot method.

to carbodiimide addition serves as the best method for production of CpZA's with few to no coproducts. Equally critical to this synthesis is the type of solvent. Ether is by far the top choice in terms of solvent, for reactions in THF provided the bisinserted complexes, Cp ZrMe[^{t}BuNC(Me)NEt]$_2$ (**19a**) and CpZrMe[^{i}PrNC(Me)N^{i}Pr]$_2$ (**19b**), as the only identifiable products, and the only isolable product from pentane, while providing evidence of **15a** in the crude product as compared to THF, was Cp_2ZrMe_2.

2.5.2. Other Synthetic Methods. The salt elimination method successfully observed with Cp*ZA's was applied toward the synthesis of dichloro CpZA's. Following the course defined in Scheme 22 and using $CpZrCl_3$ instead of Cp^*ZrCl_3, the major product of the reaction was the monocyclopentadienyl bisamidinate, Cp[R^1NC(Me)NR^3]$_2$ZrCl, with a trace of monoamidinate product. By comparison, switching conditions proved advantageous, with a modest yield of the dichloro product, Cp[R^1NC(Me)NR^3]$ZrCl_2$ (**21**), being obtained in toluene at RT.

The metathesis scheme outlined earlier proved much less effective for the preparation of dichloro formamidinates of Cp. Upon introduction of the N-silylated formamidine to $CpZrCl_3$, a myriad of products were obtained, none of which appeared to

be the desired product. Recrystallization simply provided a fine powdery precipitate containing similar species as seen in the crude reaction mixture.

For preparation of dimethyl precatalysts, the dichloro species **21** were subjected to alkylation conditions. Unfortunately, even with care taken to use stoichiometric amounts of MeLi, attempts in this manner failed, yielding the same products as seen from the one-pot method in which excess MeLi was used, namely **16** and **17**. It appears then that MeLi can catalyze the intermolecular ligand exchange to form these products from both synthetic pathways.[13]

2.6. Solid State Structures of CpZA's.

Low temperature recrystallization afforded single crystals of **15** suitable for X-ray analysis. Several structures are reproduced in Figure 9. Other reports of cyclopentadienyl Group IV amidinates have appeared,[13,14,16,40] although they only represent the symmetric benzamidinate featuring two N-$SiMe_3$ groups, and only one of those contains a dimethyl derivative.[13] Within the subset of structures shown, only very subtle changes in bond length or bond angles are evident upon comparison to the CpZA Cp[$Me_3SiNC(Ph)NSiMe_3$]$ZrMe_2$ (**20**). The parameters that deviate the greatest between structures of **15** and **20** are related to perturbations within the ZrN_2C metallacycle: the amidinate angle, NCN, and the degree of nonplanarity within the four-membered ring. For the former which outlines the angle within the amidinate itself, the bond angle of the NCN moiety is 115.9(2) ° for **20** which exceeds those for **15a**, **15b**, and **15c** (111.40(12) °, 112.4(2) °, and 112.20(13) °, respectively. Interplane angles of 9.7 ° for **15a**, 3.9 ° for **15b**, and 9.7 ° for **15c** contrast the larger 17.1 ° for **20**. These factors illustrate that the amidinate fragment can flex more to alleviate some of the steric congestion caused

between large R^1 and R^3 groups and the Cp ring. This may perhaps be facilitated by the fact that the phenyl ring in **20** lies orthogonal to the N-C-N plane.[13]

Compared to the sterically more encumbering Cp* derivatives **6**, the CpZA's **15** are not dramatically different, except in terms of planarity about the amidinate. For instance, evaluation of compounds similar in structure though only differing between Cp

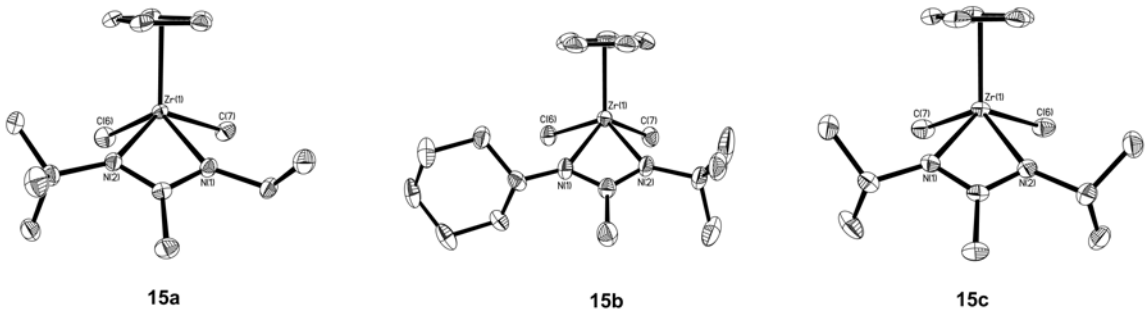

Figure 9. Selected solid state structures of several CpZA's. Hydrogen atoms have been omitted for the sake of clarity.

and Cp* (i.e. **6a** vs **15a**) reveal analogous bond angles for CH_3-Zr-CH_3, N-Zr-N, N-C-N, centroid-Zr-C, average centroid-Zr-N, and average N-Zr-CH_3, as well as related bond lengths for Zr-centroid, average Zr-CH_3, and average Zr-N. Pertinent differences, however, dwell within the conformations that the amidinate ring adopts, specifically for the degree of pucker and the pyramidalization of the amidinate nitrogens as mentioned previously. The dihedral angle for **15a** is much less severe than in **6a** (i.e. 9.7 ° vs 18.3 °). In tandem with this, a closer look at the N atoms reveals that they undergo a more significant pyramidal distortion (cf. $\Sigma\theta_N$ = 353.5 ° for N(1) and 357.3 ° for N(2)) in **6a** compared to their trigonal coplanar counterparts in **15a** (359.6 ° for N(1) and 359.3 ° for N(2)). With this in mind, it appears that the Cp* ligand is more sterically encumbering

than Cp, thus requiring the amidinate ligand to position itself in a manner that minimizes nonbonding steric interactions.

Finally, in regard to a comparison of amidinates to Cp ligands, the angle outlined by the two methyl groups attached to the metal, C-Zr-C, for **17** is 95.6(12) °,[41] larger than for Cp / Cp*ZA's having R^2 = Me (cf., average C-Zr-C angle of 88 °). This may indicate that the amidinate ligand imposes greater steric requirements for coordination, thus necessitating a narrower pocket. Meanwhile, an evaluation of Zr-C bond lengths indicates that the distances are virtually identical, if only slightly shorter for these amidinate complexes (average difference approximately 0.01 Å).

2.7. Solution Behavior and Properties of CpZA's.

The symmetry of the dimethyl complexes **15** is directly related to the nature of R^1 and R^3 (i.e. $R^1 = R^3$ provides C_s-symmetry and $R^1 \neq R^3$ provides C_1-symmetry). As with **6**, dissymmetric derivatives of **15** provide ^{1}H NMR spectra which contain one singlet for the two formally diastereotopic methyl groups. Though barriers to racemization were not quantified for these Zr analogues, similar Ti species displayed higher energy barriers upon going from Cp to Cp*.

In terms of stability, the CpZA's **15** were found to be remarkably stable. For instance, in an NMR tube under N_2, a C_6D_6 solution of **15a** was found to only marginally decompose after heating the sample to 80 °C for 15 hours.

2.8. Conclusions.

A series of Cp*ZA's and CpZA's featuring R^2 = Me are readily prepared through a facile carbodiimide insertion into a Zr-methyl bond of **5**. The need to contend with the sensitive materials **5** and $CpZrMe_3$ is sidestepped by utilizing them in a one-pot,

two step synthetic method which takes advantage of them *in situ*. This method is quite useful since a range of **6** and **15** can be prepared in this way from readily available starting materials. Further, additional varieties of dimethyl Cp*ZA's (**11**, **12**, and **13**) can be synthesized through previously detailed synthetic means.

Single crystal X-ray analysis of many Cp and Cp*ZA's revealed that all were monomeric in the solid state with no unusual bond lengths or bond angles. Upon inspection of structures varying only in their R^2 substituent, it appears that having a smaller group on the back of the amidinate tends to provide room for the R^1 and R^3 groups to tuck back further, exposing more efficiently the $ZrMe_2$ portion of the molecule. Moving from Cp* to Cp rings lessens the severity of the steric constraints on the amidinate fragment, permitting more acute interplane angles and bond angles about the two N's providing a near trigonal coplanar atmosphere.

Solution studies showed dramatic configurational instability of the amidinate on the NMR timescale. Amidinate ring flipping was shown to be a remarkably facile process for a series of racemic **6** which served to equilibrate the diastereotopic methyl groups bound to zirconium.

2.9. References.

(1) Angermund, K.; Fink, G.; Jensen, V. R.; Kleinschmidt, R. *Chemical Reviews* **2000**, *100*, 1457.

(2) Chen, E. Y. X.; Marks, T. J. *Chemical Reviews* **2000**, *100*, 1391.

(3) Rappe, A. T.; Skiff, W. M.; Casewit, C. J. *Chemical Reviews* **2000**, *100*, 1435.

(4) Resconi, L.; Cavallo, L.; Fait, A.; Piemontesi, F. *Chemical Reviews* **2000**, *100*, 1253.

(5) Alt, H. G.; Koppl, A. *Chemical Reviews* **2000**, *100*, 1205.

(6) Coates, G. W. *Chemical Reviews* **2000**, *100*, 1223.

(7) McKnight, A. L.; Waymouth, R. M. *Chemical Reviews* **1998**, *98*, 2587.

(8) Ittel, S. D.; Johnson, L. K.; Brookhart, M. *Chemical Reviews* **2000**, *100*, 1169.

(9) Britovsek, G. J. P.; Gibson, V. C.; Wass, D. F. *Angew. Chem., Int. Ed. Engl.* **1999**, *38*, 428.

(10) Gibson, V. C.; Spitzmesser, S. K. *Chemical Reviews* **2003**, *103*, 283.

(11) Barker, J.; Kilner, M. *Coordination Chemistry Reviews* **1994**, *133*, 219.

(12) Edelmann, F. T. *Coordination Chemistry Reviews* **1994**, *137*, 403.

(13) Gomez, R.; Duchateau, R.; Chernega, A. N.; Meetsma, A.; Edelmann, F. T.; Teuben, J. H.; Green, M. L. H. *J. Chem. Soc., Dalton Trans.* **1995**, 217.

(14) Gomez, R.; Duchateau, R.; Chernega, A. N.; Teuben, J. H.; Edelmann, F. T.; Green, M. L. H. *Journal of Organometallic Chemistry* **1995**, *491*, 153.

(15) Gomez, R.; Green, M. L. H.; Haggitt, J. L. *J. Chem. Soc., Chem. Commun.* **1994**, 2607.

(16) Chernega, A. N.; Gomez, R.; Green, M. L. H. *J. Chem. Soc., Chem. Commun.* **1993**, 1415.

(17) Duchateau, R.; van Wee, C. T.; Meetsma, A.; van Duijnen, P. T.; Teuben, J. H. *Organometallics* **1996**, *15*, 2279.

(18) Littke, A.; Sleiman, N.; Bensimon, C.; Richeson, D. S.; Yap, G. P. A.; Brown, S. J. *Organometallics* **1998**.

(19) Edelmann, F. T. *Journal of Organometallic Chemistry* **1992**, *426*, 295.

(20) Richter, J.; Edelmann, F. T.; Noltemeyer, M.; Schmidt, H. G.; Shmulinson, M.; Eisen, M. S. *Journal of Molecular Catalysis A: Chemical* **1998**, *130*, 149.

(21) Drew, M. G. B.; Wilkins, J. D. *J. Chem. Soc., Dalton Trans.* **1974**, 1579.

(22) Gambarotta, S.; Strologo, S.; Floriani, C.; Chiesi-Villa, A.; Guastini, C. *Inorg. Chem.* **1985**, *24*, 654.

(23) Gambarotta, S.; Strologo, S.; Floriani, C.; Chiesi-Villa, A.; Guastini, C. *Journal of the American Chemical Society* **1985**, *107*, 6278.

(24) Coles, M. P.; Swenson, D. C.; Jordan, R. F. *Organometallics* **1997**, *16*, 5183.

(25) Coles, M. P.; Swenson, D. C.; Jordan, R. F.; Young Jr., V. G. *Organometallics* **1998**, *17*, 4042.

(26) Sita, L. R.; Babcock, J. R. **1998**, *17*, 5228.

(27) Koterwas, L. A.; Fettinger, J. C.; Sita, L. R. **1999**, *18*, 4183.

(28) Babcock, J. R.; Incarvito, C.; Rheingold, A. L.; Fettinger, J. C.; Sita, L. R. **1999**, *18*, 5729.

(29) Wolczanski, P. T.; Bercaw, J. E. *Organometallics* **1982**, *1*, 793.

(30) Jayaratne, K. C.; Sita, L. R. *Journal of the American Chemical Society* **2000**, *122*, 958.

(31) Babcock, J. R.; Sita, L. R. **1998**, *120*, 5585.

(32) Ojima, A.; Inaba, S. I. *Journal of Organometallic Chemistry* **1977**, *140*, 97.

(33) Maier, S.; Hiller, W.; Strahle, J.; Ergezinger, C.; Dehnicke, K. *Naturforsch.* **1988**, *43b*, 1628.

(34) Fenske, D.; Baum, G.; Zinn, A.; Dehnicke, K. *Naturforsch.* **1990**, *45b*, 1273.

(35) Brunner, H.; Agrifoglio, G. *Journal of Organometallic Chemistry* **1980**, *202*, C43.

(36) Brunner, H.; Lukassek, J.; Agrifoglio, G. *Journal of Organometallic Chemistry* **1980**, *195*, 63.

(37) Wedler, M.; Knosel, F.; Edelmann, F. T.; Behrens, U. *Chem. Ber.* **1992**, *125*, 1313.

(38) Stewart, P. J.; Blake, A. J.; Mountford, P. *Organometallics* **1998**, *17*, 3271.

(39) Keaton, R. J.; Jayaratne, K. C.; Henningsen, D. A.; Koterwas, L. A.; Sita, L. R. *Journal of the American Chemical Society* **2001**, *123*, 6197.

(40) Sotoodeh, M.; Leichtweis, I.; Roesky, H. W.; Noltemeyer, M.; Schmidt, H. G. *Chem. Ber.* **1993**, *126*, 913.

(41) Hunter, W. E.; Hrncir, D. C.; Bynum, R. V.; Pentilla, R. A.; Atwood, J. L. *Organometallics* **1983**, *2*, 750.

Chapter 3

Olefin Polymerization Characteristics of Zirconium Amidinates

3.1. Introduction.

With a multitude of Cp and Cp*ZA's readily available from simple synthetic manipulations, exploring their capabilities toward the Ziegler-Natta polymerization of α-olefins was explored. Like metallocenes, it is possible to change the symmetry of the amidinate complexes via appropriate choice of R^1 and R^3, and if they did indeed prove to be active, whether the symmetry of these complexes matched the outcome of polymerizations with metallocenes of similar symmetry would be quite interesting. Also, these amidinate species may be able to change the history of amidinates for polymerization, which to this point has not seen great success.

Group IV monoamidinates (**1**) are known to be active Ziegler-Natta catalysts when activated with MAO. Styrene was polymerized to highly syndiotactic PS regardless of the symmetry of the catalyst involved, using either chiral[1] or nonchiral[2] monobenzamidinate complexes. Changing the bulkiness of the amidinate nitrogen substituents ($SiMe_3$ to Me) did affect the stereochemical outcome, producing a yield of syndiotactic PS that was noticeably smaller.[2] These catalysts are also capable of polymerizing ethylene, although no activity is typically seen for propylene at low pressures.[3] Propylene polymerization at RT and 5 atm showed good activity for a C_1-symmetric zirconium monobenzamidinate, although the PP so produced was not very stereoregular (*mmmm* = 35%).[1]

Tris(amidinate) complexes (**3**) plus MAO have also shown catalytic activity for olefin polymerization. The tris(benzamidinate), $[RNC(Ph)NSiMe_3]_3ZrCl$ (where R is a chiral, bulky alkyl group), provides isotactic PP via site control above 5 atm of propylene.[1] Curiously, using a more polar solvent, such as CH_2Cl_2 in place of toluene, dramatically altered the polymer microstructure, yielding atactic PP. Increasing the amount of MAO, and thus the ratio of Al : Zr, lead to a decrease in polymerization activity and in polymer molecular weight. This can be better appreciated upon investigation of the NMR spectra of the resulting polymers, which were devoid of olefinic resonances attributable to β-hydride or β-methyl elimination. The lone termination event during polymerization appears then to be chain transfer to aluminum, which would be more favored at higher MAO concentrations.

For the pseudo-octahedral, C_2-symmetric bis(benzamidinate) complexes, **2**, high density PE is generated from polymerizations with MAO.[4,5] Raising the temperature at which the polymerization is run, as well as increasing the ethylene pressure, both serve to increase the catalysts activity, the polymer molecular weight, and the polymer melting point. Beyond a particular Al : Zr ratio, activities and molecular weights appear to level out, in contrast to that mentioned above. Switching to the Ti catalyst, the authors discovered a higher activity for PE production as compared to the Zr analogue.[5] Substitution of the amidinate phenyl group for a *para*-tolyl group nearly halved the activity and the molecular weight of the PE.[4] This was described as a change in the electrophilic nature of the metal center. The methyl group serves to heighten the electron donating capabilities of the phenyl ring, decreasing the positive charge on the metal center, thus reducing polymerization activity.

In terms of PP formation, characteristic NMR evidence for end groups indicative of vinyl and ^{i}Bu groups are present with no resonances matching those for vinylidene or ^{n}Pr groups. This points to β-Me elimination as the primary elimination pathway for these

benzamidinates.[6,7] From polymerizations in toluene at atmospheric pressure, atactic oils are isolated from the polymerization mixture using MAO, and ^{13}C NMR spectra indicate the presence of 2,1- and 1,3-insertions. When the polymerization was performed with $B(C_6F_5)_3$ as cocatalyst under the same conditions, the activity was slightly lowered, but most importantly, highly isotactic PP was obtained, as is predicted by the C_2-symmetry of the catalyst. At higher pressures, toluene had to be abandoned due to the production of two different polymer fractions, isotactic and atactic PP, when utilizing either MAO or borane cocatalysts. The authors argued that two different catalysts were present in solution, though the structure of the one which produced the stereoirregular polymer was not speculated on. This was unfortunate, for toluene, which is believed to competitively bind to the metal center in an η^6-manner,[8,9] produced PP of higher molecular weight and narrower PDI. However, an activity increase, and a more uniform type of polymer production, was accomplished with the more polar CH_2Cl_2 as solvent. The greater activity is a consequence of the ability for CH_2Cl_2 to more efficiently stabilize the separated ions. With the switch in solvent and greater propylene pressures, these bis(amidinate) / MAO systems were capable of producing istotactic PP devoid of the misinsertions that were present at lower monomer concentrations. The authors implicated chain-end epimerization as the cause for the generation of atactic PP at low pressure.[6,7,10]

Green and coworkers have prepared several mixed ligand systems, similar to Cp* and CpZA's, employing benzamidinate ligands with TMS substituted nitrogen groups.[11-13] Polymerizations performed at RT in toluene using $Cp[PhC(NSiMe_3)_2]MCl_2$ / MAO, where M is either Ti or Zr, were competent for both ethylene and propylene polymerization. Activity for ethylene was higher than that for propylene, the latter of which was obtained as an atactic oil. Remarkably, both the Ti and Zr analogue had exactly the same activity and yield of polymer for both monomers at the only reported

pressure of 2 atm.[11,13] The molecular weights of the polymers so produced, as well as the molecular weight distributions, were not reported. Also of note, the analogous dimethyl or dibenzyl zirconium CpZA's, with $[Ph_3C][B(C_6F_5)_4]$ as cocatalyst, were not successful toward ethylene polymerization.[12]

3.2. Polymerization with Cp*ZA's.

While analogous mixed ligand systems were active for the Ziegler-Natta polymerization of α-olefins, control over features of the polymerization in terms of activity, stereoregularity, and living nature, still left much to be desired. After activation of the Cp*ZA's prepared in Chapter 2 with either $[Ph_3C][B(C_6F_5)_4]$ or $[PhNHMe_2][B(C_6F_5)_4]$, the polymerization of 1-alkenes was accomplished at -10 °C in chlorobenzene. Although polymerizations could also be performed at higher temperatures, higher molecular weights and narrower PDI were achieved at the lower polymerization temperature. Polymeric materials prepared can range from oligomers (M_n ~ 2000) to very high molecular weights (M_n ~ 500,000).

The choice of cocatalyst was quite important within polymerizations using these Cp*ZA's. While metallocenes are typically activated with MAO, Cp*ZA's of **6** provide broad GPC traces, loss of stereoselectivity, as well as evidence of vinylidene end groups when utilizing this cocatalyst. The borane, $B(C_6F_5)_3$, may also be used, though catalyst activity is decreased. The borates, $[PhNHMe_2][B(_6F_5)_4]$ and $[Ph_3C][B(_6F_5)_4]$, when used in conjunction with the dimethyl Cp and Cp*ZA's, generate systems with the greatest activity and reproducibility.

Finally, chlorobenzene proved to be the best solvent for polymerization tested to date. Attempts with pentane and toluene provided catalyst systems that gave quite low activity and polymer yield. These factors are accounted for due to the instability of the

solvent separated ions of the cation and anion, which would precipitate out of solution as viscous oils during polymerization. The more polar chlorobenzene most likely is a better solubilizing solvent, and more efficiently stabilizes the separate ion pairs. Along this trend, replacing the CH_3 group in toluene for a CF_3 was also attempted as an option for a polar solvent, and it also was not compatible with this catalyst system, potentially undergoing F^- abstraction from the solvent.[14,15]

3.2.1. 1-Hexene. The following discussion of the Ziegler-Natta polymerization of α-olefins via Cp*ZA's will revolve mostly around 1-hexene, unless otherwise indicated, since the bulk of the work was based on this monomer. However, 1-butene, 1-pentene, 1-octene, 1-decene, and 1-dodecene typically show similar behavior under identical conditions. Propylene will be the subject of a separate discussion (see Section 3.5).

3.2.1.1. Living Polymerization. In chlorobenzene at -10 °C, the polymerization of 1-hexene with the combination of **6a** and $[PhNHMe_2][B(C_6F_5)_4]$ was accomplished in a stereospecific and living fashion.[16] The living nature of this polymerization was established through a very narrow polydispersity of the PH produced (PDI = 1.03). Also, a kinetic analysis of the polymerization also favored a living system. As shown in Figure 10, a linear relationship was found to exist between molecular weight and conversion of monomer. Also shown is the fact that monomer consumption goes to completion, for 400 eq of 1-hexene, within 2 hours. Inspection of the ^1H and ^{13}C NMR spectra of polymers obtained in this manner were devoid of olefinic resonances, suggesting that β-hydride eliminations are not prevalent at this temperature. Molecular weights were tunable by the ratio of the monomer to initiator to a predetermined degree

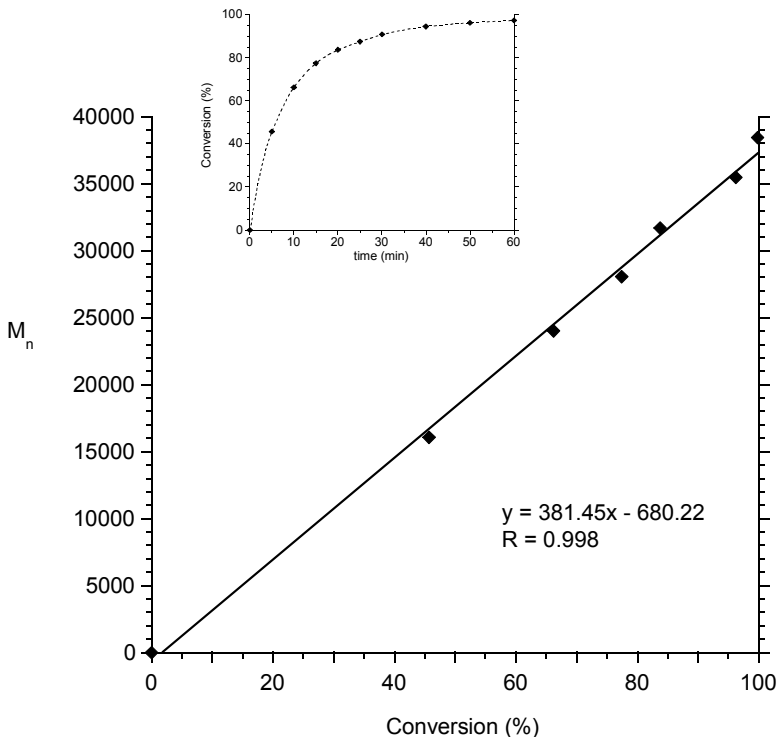

Figure 10. Kinetic analysis of living 1-hexene polymerization with **6a**.

of polymerization. Finally, to be discussed shortly, block copolymers can also be synthesized from sequential addition of monomer upon exhaustion of the preceding olefin. Polymerizations at higher temperatures also provided polymer, although molecular weights were lower and polydispersities increased. In terms of other acetamidinate derivatives, the meso complexes **6d** and **6e** proved to be equally living for 1-hexene under identical conditions. For the other racemic derivatives, **6b** and **6c**, only low molecular weight PH was obtained, potentially due to greater steric congestion from the ligand framework affecting monomer coordination.

Knowing that a tertiary carbon atom attached to the nitrogen of the acetamidinate NR^1 group, when combined with the quaternary NR^3 fragment as a $N(^tBu)$, results in severely reduced polymerization activity, further elaboration of this steric effect is necessary. Other work by Dr. Denis Kissounko has involved the systematic alteration of

the substitution at the β-carbon atom of one of the acetamidinate nitrogen alkyl groups, while maintaining NR^3 as a N(^{t}Bu) group.[17] Table 1 displays the results of polymerizations within this regime of precatalysts. Going from the N substituents Et

Precatalyst (R^1)	M_n	PDI
6a (Et)	19,800	1.03
6f (^{i}Bu)	7940	1.03
6g (neopentyl)	No polymer	
6h (benzyl)	19,340	1.10
6i (CH_2-2-Cl-phenyl)	No polymer	
6j (CH_2-3-Me-phenyl)	23,580	1.48
6k (CH_2-Mes)	No polymer	

Table 1. Effect of the β-carbon atom substitution of R^1 on polymerization capabilities.

(**6a**), ^{i}Bu (**6f**), to neopentyl (**6g**), a transition in the substitution of the β-carbon atom from primary to tertiary to quaternary, results in a steady loss of 1-hexene polymerization activity. This effect is so severe that in the case of the largest group, **6g**, no polymer is obtained. PH obtained in this manner decreased in molecular weight from 19,800 for **6a** to 7940 for **6f**, while polydispersities for both are quite narrow. It appears that a substitution greater than tertiary provides a crowded environment through which polymerization is curtailed, although the living nature of the polymerization seems to be retained for the ^{i}Bu derivative.

Interestingly, employing an sp^2 hybridized β-carbon as part of a benzyl group for **6h** induced a polymerization of 1-hexene that was virtually indistinguishable from that

with **6a** in terms of M_n, PDI, and polymer yield.[17] However, substitution of the phenyl ring provided results that were not encouraging. With a 2-Cl substituent on the ring (**6i**) or if the ring is a Mes (**6k**), no polymer can be isolated from the polymerization. If instead a 3-Me substituent is present on the phenyl ring as in **6j**, polymerization occurs and PH can be isolated in good yield, although as the polydispersity value denotes (PDI = 1.48), polymerization with this precatalyst is not living. The instability of polymerizations employing **6j** and **6k** may be attributable to decomposition of the cation for each due to C-H bond activation of a CH_3 group of the ligand framework, which has been seen before.[18,19]

In addition to manipulation of R^1 and R^3 of the amidinate moiety, polymerizations with a range of precatalysts which varied in the R^2 group were also performed. As mentioned, bis(benzamidinate) complexes have had mixed success for propylene polymerization.[7] However, the mixed ligand systems with Cp and benzamidinate prepared by Green had little success toward α-olefin polymerization.[11,13] The benzamidinate **13**, by contrast, proved to be capable of performing the living polymerization of 1-hexene. The molecular weight of the PH, the polydispersity, and polymer yield were essentially identical to that obtained from **6a** under identical conditions (Table 2).

Precatalyst	M_n	PDI
6a	18,700	1.06
11a	14,400	1.40
11b	36,100	1.21
12	No polymer	
13	19,600	1.02

Table 2. Polymerization data for Cp*ZA's with different R^2 substituents.

Diverging from the similarities with **6a** are the formamidinates, **11**, and the ^{t}Bu substituted amidinate **12**. Ethylene polymerization has been reported for a bisamidinate complex with a ^{t}Bu substituent.[20] The researchers found that higher molecular weights were obtained from this system, as well as narrower molecular weight distributions, when compared to their methyl counterparts, although the systems are far from living (PDI $\geq$ 15). Remarkably, when **12** was activated for polymerization by $[PhNHMe_2][B(C_6F_5)_4]$, no PH was obtained. This may be due to the bulky ^{t}Bu group forcing the R^1 and R^3 substiuents on the N atoms forward, as such crowding the coordination site. On the other end of the size spectrum, the formamidinates,**11a** and **11b**, where R^2 is a H, were competent toward 1-hexene polymerization. Though activity was regained, the yields of polymer after 2 hours were consistently around 40 %, and polydispersities were slightly broadened. The molecular weight for polymerization with **11b** was over twice that for **11a**, although the former maintained a narrower molecular weight distribution. No literature exists for a formamidinate which has been utilized for olefin polymerization.

In one final comparison of factors that may affect polymerization within Cp*ZA's, the nature of the R group bound to Zr was varied while maintaining the remaining ligand environment. For this experiment, instead of the methyl groups in **6a**, a precatalyst with two ^{i}Bu groups serving as σ-donor ligands was employed. Activation of Cp*[^{t}BuNC(Me)NEt]Zr(^{i}Bu)$_2$ (**38a**) with $[PhNHMe_2][B(C_6F_5)_4]$ produced a PH with a narrow molecular weight distribution (1.02) and a molecular weight of 20,300. Under identical polymerization conditions, **6a** produced a living polymerization system with a M_n value of 18,700. This stands in stark contrast to the discoveries of Schrock and coworkers, which will be discussed in greater detail later, who discovered a dramatic effect toward polymerization of 1-hexene with the [MesNpy]ZrR_2 system, where R is Me or ^{i}Bu.[21]

Finally, 1-hexene polymerization with **6a**, which was found to be living at -10 °C, was matched against the highly active and stereospecific ansa-bridged metallocene, *rac*-EBIZrMe$_2$, **17**. With a calculated degree of polymerization of 200 (M_n (theor.) = 17,600), the metallocene displayed a higher molecular weight (M_n = 25,8000) and a broader polydispersity (PDI = 1.50) due to some degree of termination, evident in the ^{13}C NMR spectrum as olefinic resonances.

3.2.1.2. Structure / Property Relationships. Polymerization of 1-hexene at -10 °C with **6d** or **6e** as precatalyst provided tacky oils that, upon investigation of NMR spectra, were clearly devoid of any resonances attributable to β-hydride elimination. Inspection of the ^{13}C NMR spectrum of one of these polymers, as illustrated in Figure 7b for **6d**, showed a definite lack of stereocontrol over polymer enchainment as seen previously with benzamidinate CpZA's employed for propylene polymerization.[11-13] Interesting to note is that even though the precatalyst has C_s-symmetry, syndiotactic PH[22] is not produced as would be predicted from metallocene symmetry rules.[23]

The C_1-symmetric acetamidinate precatalysts **6a**, **6b**, and **6c** do not provide similar results for the polymers produced. Only oligomeric PH is produced for the latter two due to the slow activity. While for **6a**, which showed excellent activity and living characteristics, analysis of the PH obtained at -10 °C surprisingly showed a polymer microstructure that was highly isotactic (Figure 7c). The zirconium amidinate, **6a**, represents the first reported catalyst that contains the highly desirable characteristics of livingness and stereospecificity. This is quite unexpected, since the precatalyst was shown to be highly configurationally unstable (see Section 3.2.1.3.).

For the sake of comparison, also included in Figure 11a is a purely atactic PH (M_n = 19,730, PDI = 1.01) produced from a non-face selective polymerization system of

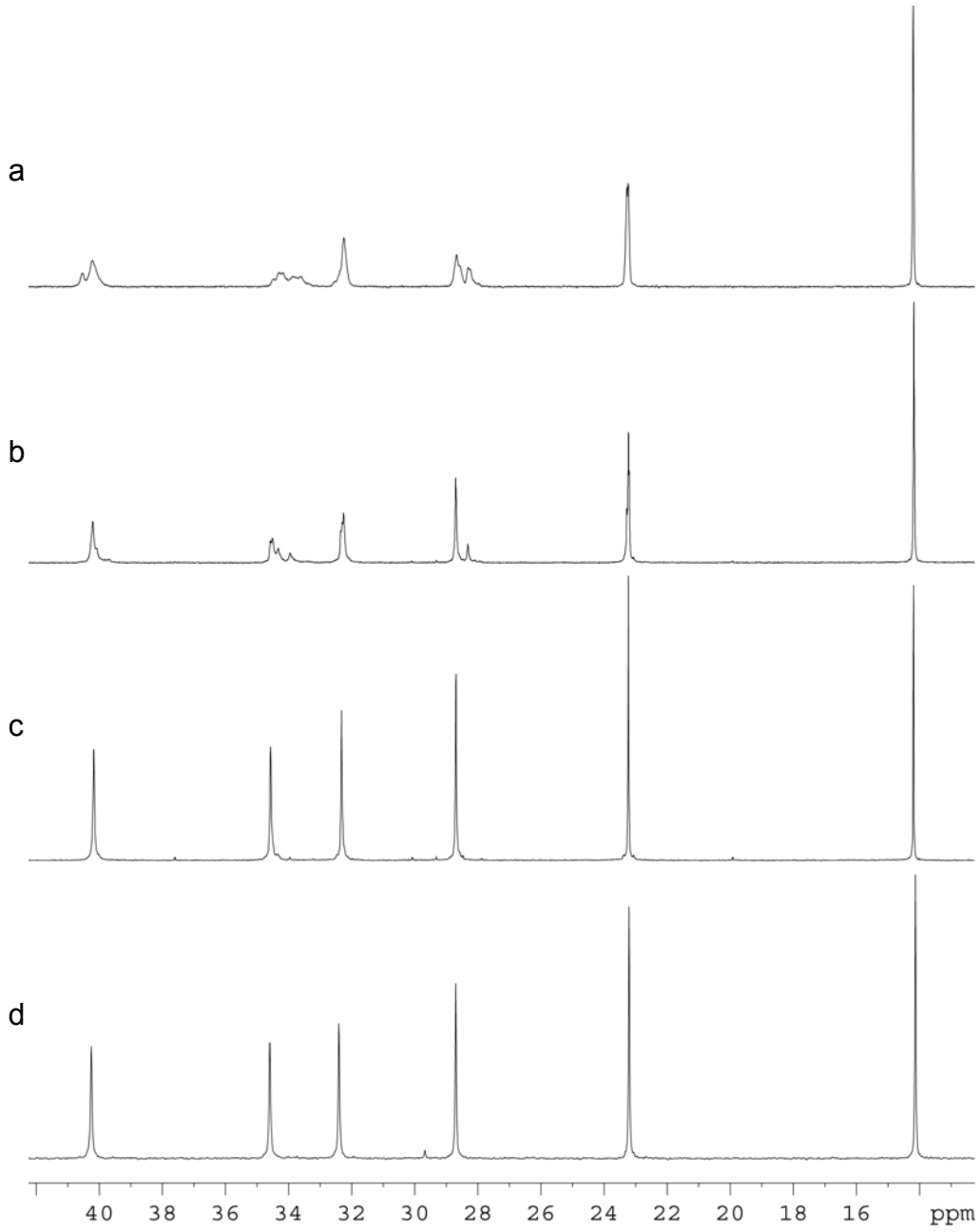

Figure 11. ^{13}C NMR spectra (100MHz, $CDCl_3$, 23 °C) of (a) atactic PH, (b) stereoirregular PH from **6d**, (c) isotactic PH from **6a**, and (d) isotactic PH from *rac*-**17**.

Schrock.[24] For PH, the resonance for the C3 carbon atom in ^{13}C NMR spectra (δ 34.5 ppm), which is the first methylene of the pendant alkyl group off the polymer backbone, carries much of the information about polymer microstructure.[25,26] In highly isotactic PH

(Figure 11c), only one narrow signal is evident, indicative of uniform relative stereochemistry between adjacent asymmetric centers from a stereospecific polymerization as with **6a**. Also exemplifying this quality is the spectrum shown in Figure 11d, which is an isotactic PH produced from the ansa-bridged metallocene, *rac*-**17**.[26] By contrast, atactic PH (Figure 11a) carries numerous resonances for C3 attributable to the lack of consistent stereochemistry along the polymer backbone.

Compared to other Cp*ZA's, **6a** is only matched in stereospecificity by **6h** and **6j**. The remaining Cp*ZA's have ^{13}C NMR spectra very similar to those shown in Figure 12 for **11a** and **13**. Although the spectra do not indicate the production of an atactic

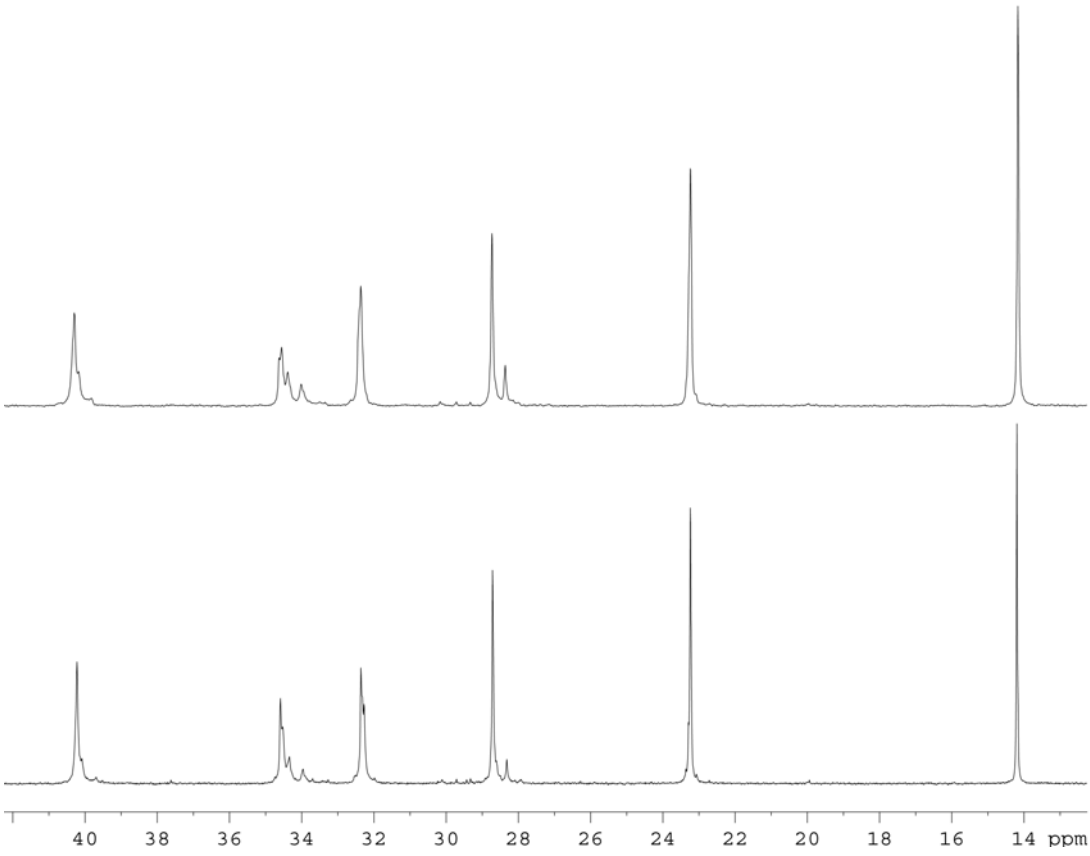

Figure 12. ^{13}C NMR spectra (100MHz, $CDCl_3$, 23 °C) of PH produced from (top) **13** and (bottom) **11a**.

polymer, like that in Figure 11a, they appear to be similar in microstructure to PH produced from the C_s-symmetric **6d**. Qualitatively, it appears that there is a greater degree of stereocontrol induced by **11a** over that of **13**.

3.2.2. 1-Butene. Polymerization of 1-butene was also attempted with **6a** and **6e**. At -10 °C for the former precatalyst, the living polymer precipitates out of solution within 30 minutes due to the crystallinity of the isotactic chains. If the polymerization is continued for a total of 9 hours, the polymer obtained has a molecular weight of 32,600 and the polymer yield is only 20 %. Also, the PDI is 1.58, though no vinyl end groups are present in the ^{1}H or ^{13}C NMR spectra. The inhomogeneity of the polymerization mixture detrimentally affects the concentration of propagating centers, creating heterogeneous species that may have different rates of propagation as compared to their soluble counterparts, creating the larger dispersity in molecular weights. Only upon going to extremely low molecular weight could poly(1-butene) (PB) be obtained as a narrow molecular weight distribution material. For instance, set to a DP of 15, **6a** produced an oligomeric PB sample with an M_n of 2820 and a low PDI of 1.005.

For the C_s-symmetric precatalyst **6e**, the situation improves greatly. High molecular weight PB can be obtained in a living fashion at -10 °C. No precipitation from solution was noticed at any point during the polymerization. The molecular weight was higher (M_n = 38,300) and the polydispersity narrower (PDI = 1.07) within only 6 hours under otherwise identical conditions to **6a**. Along with this, the polymer yield was higher, being near 50 %. The greater solubility of the less-tactic polymer backbone imparts a higher activity and living capability to the polymerization. Interestingly, PB from **6a** is a white powder while that from **6e** is tough, colorless oil.

Although in high molecular weight PH prepared from **6d** the stereoerrors are difficult to characterize, these separate resonances are more easily recognized in ^{13}C NMR spectra for samples of PB. Inspection of the PB from **6a** (Figure 13), and in particular the C3 resonance at δ 27.0, provides insight into the degree of stereocontrol exhibited for this polymerization. Slightly upfield from this signal, small resonances can be seen which are assigned to the insertion of the wrong enantioface of the 1-butene monomer.[25] Taking into account these signals, the strong *mmmm* pentad resonance accounts for 95 % of the overall signal attributable to the pendant methylenes of PB.

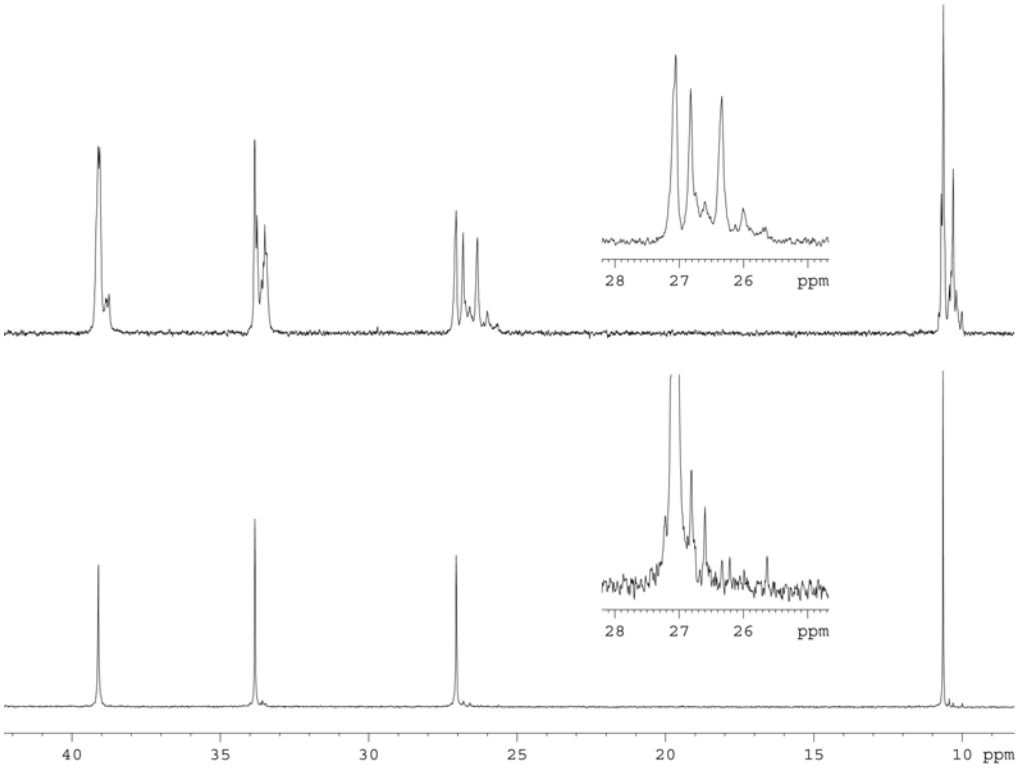

Figure 13. ^{13}C NMR spectra (100 MHz, $CDCl_3$, 23 °C) of PB prepared with (a) **6a** and (b) **6e**. Inset is the expanded region of the C3 resonance, highly magnified for isotactic PB.

3.2.3. Non-conjugated Dienes. The first report of the cyclopolymerization of non-conjugated dienes was reported for a heterogeneous system in 1958.[27] Using Al^iBu_3 with $TiCl_4$, the authors determined that very few (< 10%) of the monomer units incorporated, either 1,5-hexadiene or 1,6-heptadiene, retained a pendant double bond. Also, they deduced that the most likely structure of the polymer created was consecutive 1,3-disubstituted cyclopentane and cyclohexane rings, respectively, which were separated by a methylene group formed through cyclopolymerization (Scheme 28). Most interestingly, intramolecular cyclization was shown to be favored over subsequent 1,2-addition of another monomer unit.

Stereoselective cyclopolymerization was achieved by Waymouth via Cp_2ZrX_2 (X = Cl or Me) or Cp^*ZrCl_2 activated by MAO.[28] At about RT, polymerization of 1,5-

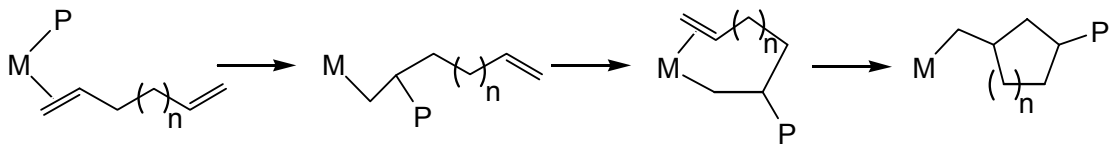

Scheme 28. Mechanism of cyclopolymerization for non-conjugated dienes to form the methylene cycloalkane repeat unit.

hexadiene afforded poly(methylene-1,3-cyclopentane) (PMCP) with 80 % trans and 70 % cis rings for the Cp and Cp* derivatives, respectively. Lowering the temperature increased the selectivity, being 91 % for trans and 86 % for cis. As such, it can be noticed that the more sterically hindered system, Cp^*ZrCl_2, yields polymer with a greater frequency of cis arrangements. In order to gain greater control over the relative tacticity of the resulting rings, Waymouth next utilized a precatalyst that could more selectively control olefin insertion, thus turning to a derivative of *rac*-EBTHIZrX$_2$.[29] Polymerization of 1,5-hexadiene with the two separate enantiomers of the racemic catalyst afforded

PMCP with only 63-72 % trans rings, though the polymers were indeed optically active (see below).[30] It seems then that since insertion of α-olefins with activated *rac*-EBTHIZrCl_2 is isospecific, the inability to exclusively produce one type of ring conformation suggests that the specificity of the cyclization step for production of solely cis or trans rings is lacking.[31]

Preparation of poly(1,5-hexadiene) in this manner, which maintains the repeat unit methylene-1,3-cyclopentane, provided the first example of this optically active polymer. Figure 14 illustrates the four microstructures of highest order from 1,5-hexadiene cyclopolymerization. Featuring a catalyst with a stereoselective active site will fix the tacticity of the polymer, while the cyclization step will determine whether the rings are formed with cis or trans arrangements. Three of the four microstructures contain a mirror plane; isotactic- and syndiotactic-cis have them splitting the five-membered ring, and isotactic-cis and syndiotactic-trans have them on the bridging methylene. The one without the mirror plane of symmetry is the isotactic-trans configuration, and is thus optically active.

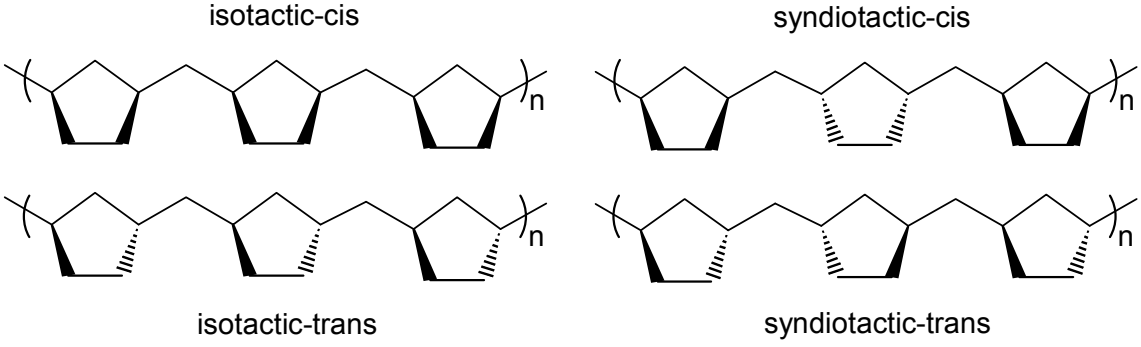

Figure 14. Schematic representation of the four possible highest ordered microstructures of PMCP. Only the isotactic-trans polymer is optically active by lack of a mirror plane.

3.2.2.1. Living Cyclopolymerization. As seen for 1-hexene, polymerization of 1,5-hexadiene at -10 °C in PhCl, for the precatalysts **6a**, **6b**, and **6d**, provided narrow molecular weight distribution polymers when activated by $[PhNHMe_2][B(C_6F_5)_4]$.[32] Evidence of β-hydride elimination was not apparent in NMR spectra of the PMCP samples. Under pseudo-first order conditions, the kinetics of polymerization were obtained with **6a**, and the linear plot of $\ln([M_o] / [M_t])$ vs time is shown in Figure 11. The linear fit denotes that a constant concentration of propagating species is present during polymerization, and that irreversible termination is not present.[33] Also plotted in Figure 15 is a kinetic anaylsis of the same precatalyst for 1-

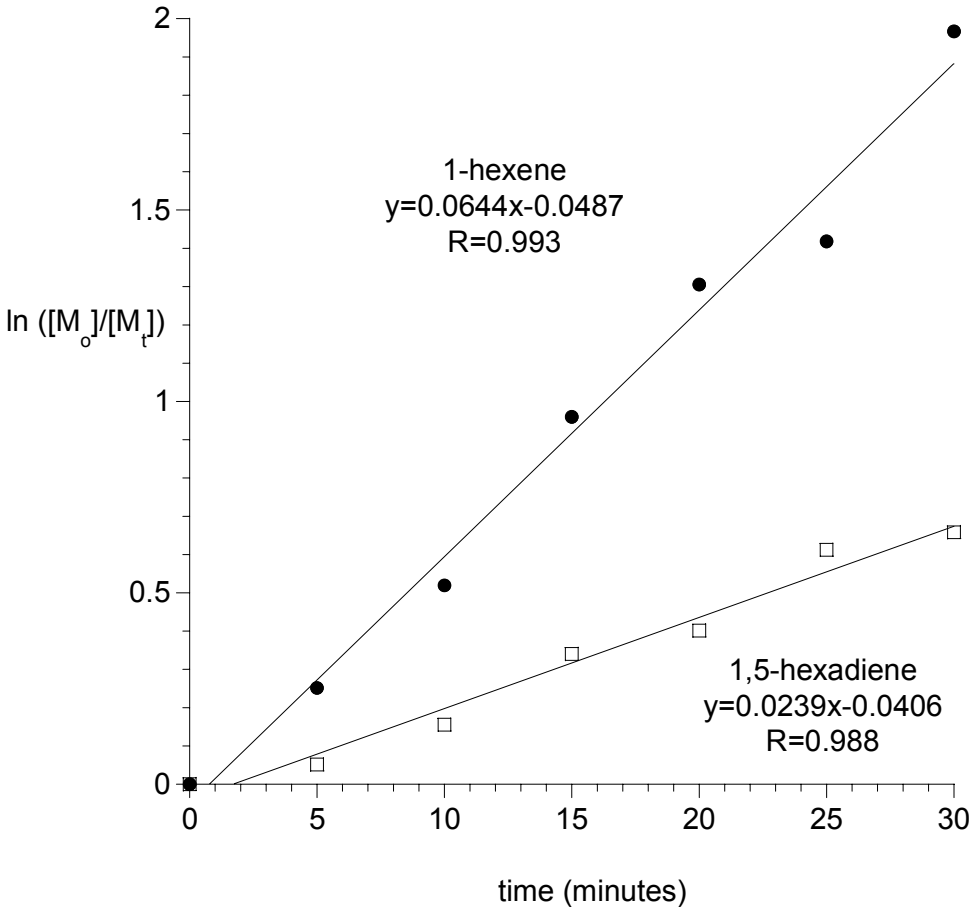

Figure 15. Polymerization kinetics for 1-hexene and 1,5-hexadiene with **6a**.

hexene under identical conditions. The differences in observed rate constants serves to show that cyclopolymerization is slower than linear 1,2-polymerization. This may reflect a difference in rate determining steps for the two polymerizations, which for α-olefins is 1,2-insertion, while for nonconjugated dienes, it may be cyclization.

Toward the cyclopolymerization, **6b** showed the slowest rate for monomer consumption. At high monomer concentrations, a molecular weight of only 14,000 was achieved after almost 4 hours of polymerization. Importantly, the living nature of the polymerization was not adversely affected, for the PDI was still very narrow (1.03). At similar monomer concentrations, **6d** effected the polymerization of PMCP to a molecular weight of 25,000 in only one hour. For these polymerizations, the reaction was not taken to complete conversion. Unlike these Cp*ZA's, cyclopolymerization employing Cp_2ZrCl_2 / MAO at high monomer concentration (bulk monomer) proceeded to 100 % conversion within one hour, though with nearly 60 % of the polymer being highly crosslinked from incomplete cyclization and polymerization of the pendant olefin.[29]

3.2.2.2. Structure / Property Relationships. Similar to *rac*-EBTHIZrCl_2 / MAO, the Cp*ZA **6a** was highly stereospecific for isotactic olefin polymerization. It has been pointed out previously that an isospecific catalyst is a prerequisite for production of optically active PMCP.[29] As such, only the effect of cyclization would not allow for formation of optically active PMCP with this precatalyst. First, the active catalysts had a high affinity for cyclopolymerization, with all performing the cyclization greater than 98% of the time. Also, all catalysts exhibited a selectivity toward trans ring formation. For **6a**, the selectivity for trans rings was only 64 %, meaning the cyclization was not diastereoselective. However, by steadily increasing the steric bulk around the metal, upon going to precatalysts **6d** and **6b**, the trans content steadily rose to 78 % and 82 %, respectively. This was an unfortunate turn, for the latter

two are not stereoselective for monomer insertion, and though the trans ring content is met, the isotactic portion of the polymer is not present to allow for optical activity.

3.3. Polymerization with CpZA's.

3.3.1. 1-Hexene.

3.3.1.1. Living Polymerization. With the living Ziegler-Natta polymerization of α-olefins being demonstrated for Cp* derivatives, the extension of these results toward CpZA's was investigated. Activation of **15b**-**d** with $[PhNHMe_2][B(C_6F_5)_4]$ produced a highly active polymerization system in chlorobenzene at -10 °C which also maintained the living characteristics seen for Cp*ZA's.[34] Data shown in Table 3 show that polydispersities of the PH produced were quite narrow, and

Precatalyst	M_n	PDI
15b	21,700	1.05
15c	20,800	1.03
15d	23,500	1.06

Table 3. Polymerization of 1-hexene with CpZA's.

molecular weights matched well with the expected degree of polymerization, or $[M]_o$ / $[I]_o$. Monomer consumption, shown in Figure 16, was quite rapid for the C_s-symmetric derivatives, with 79 and 53% of 1-hexene being consumed in the first two minutes of polymerization using **15c** and **15d**, respectively. As a testament to the rapid incorporation of monomer with **15c**, PH, with M_n over 200,000 (corresponding to a DP of ~ 2400 units) and a PDI of 1.09, could be prepared in only 15 minutes. With **15b**, the rate of propagation was now curtailed sufficiently such that dependable kinetic

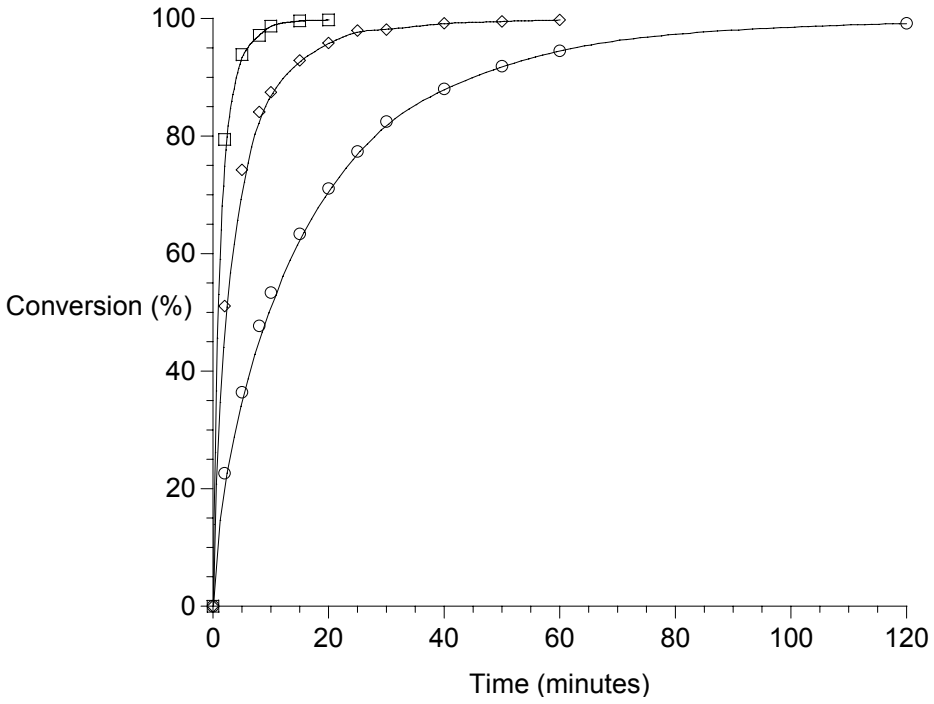

Figure 16. Consumption of 1-hexene as a function of time for the CpZA's (○) **15b**, (□) **15c**, and (◊) **15d** at -10 °C.

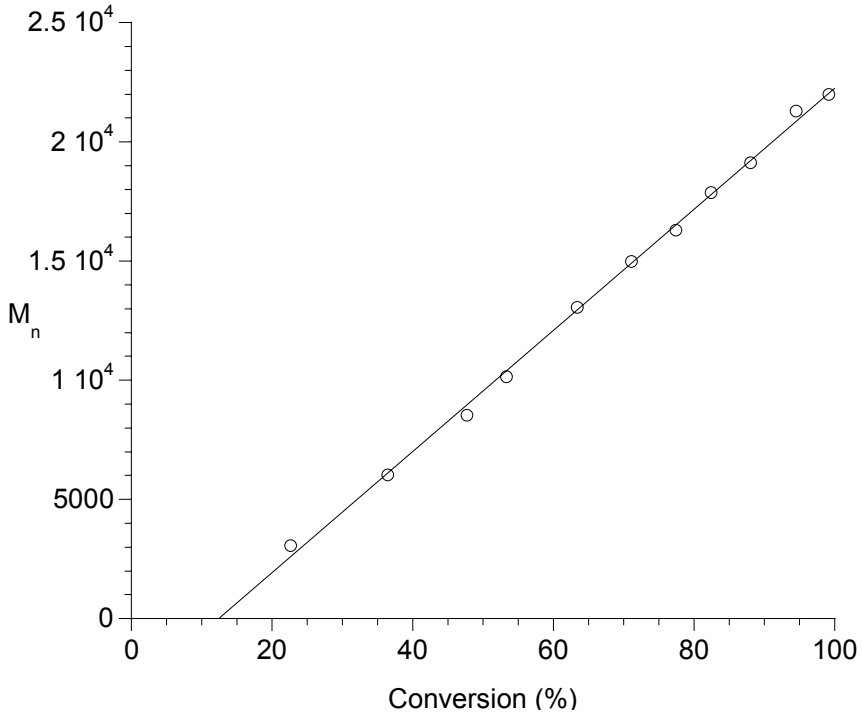

Figure 17. M_n vs percent conversion for 1-hexene polymerization with **15b**.

measurements could be made. Analyzing aliquots from the polymerization provided a linear correlation between number average molecular weight and percent conversion (Figure 17), a good indication of a living polymerization.[33,35]

The news is not nearly as good for polymerizations with **15a**. Polymerization of 1-hexene at -10 °C with this precatalyst always bore yields of polymer which were considerably lower than comparable polymerizations with other CpZA's, and molecular weights that were higher than was calculated from $[M]_o / [I]_o$. Also, polydispersities were consistently greater than 1.1, though the GPC traces were always monomodal with a long low molecular weight tail. Still no evidence existed for products of β-hydride elimination in NMR spectra of the polymers. If **15a** and $[PhNHMe_2][B(C_6F_5)_4]$ are mixed for 15 minutes before addition of monomer, the PH has a M_n value double that seen from when they are mixed for only approximately one minute. It appears that the Zr-Me cation is quite unstable (Section 4.3.), leading to a system with non-living characteristics.

3.3.1.2. Structure / Property Relationships. As seen with Cp*ZA's, C_1-symmetric precatalyst **6a** provided isotactic PH, while C_s-symmetric species proved to be nonstereospecific for either isotactic or syndiotactic polymerization. Inspection of ^{13}C NMR spectra of PH produced from **15c** and **15d** (Figure 18) confirm similar findings for the CpZA's with relation to C_s-symmetric precatalysts. In actuality, it seems that these Cp derivatives provide polymer that, more so than from Cp*ZA's, more closely resembles truly atactic PH shown previously in Figure 11a. For PH from **15a** and **15b**, a surprisingly similar microstructure to the C_s-symmetric counterpart **6d** is observed (Figure 14b). Accordingly, a Cp* group appears to be necessary for stereodifferentiation of 1-hexene enantiofaces in order to produce isotactic polymer from C_1-symmetric derivatives.

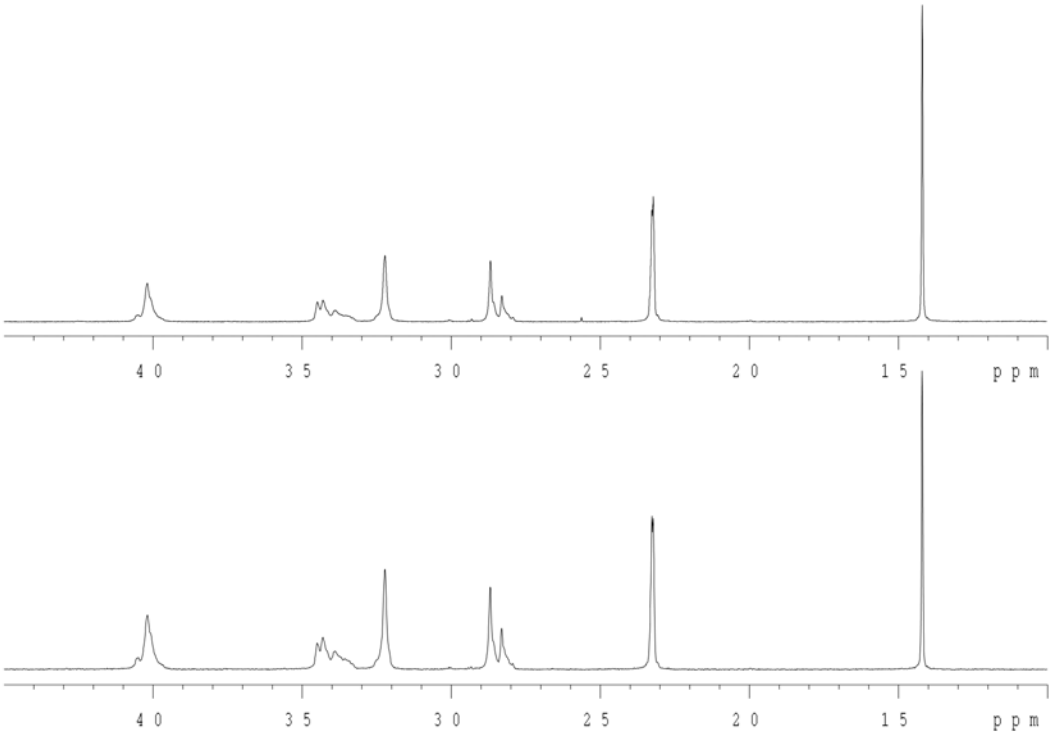

Figure 18. ^{13}C NMR spectra (100 MHz, $CDCl_3$, 23 °C) of PH produced from polymerization with (top) **15c** and (bottom) **15b**.

3.3.2. Vinylcyclohexane. With a reduction in steric hindrance of the cyclopentadienyl ligand, polymerizations of more sterically encumbered olefins may be possible to perform in a living manner. One monomer which affords a crystalline polymeric material with interesting industrial potential, most notably a very high melting point (> 300 °C), is vinylcyclohexane (VCH). PVCH is most commonly prepared from the hydrogenation of PS.[36] Heterogeneous Ziegler-Natta catalysts are known to polymerize VCH and other monomers with branch points at the allylic carbon atom, such as 3-methyl-1-pentene.[37-39] The polymerization rates for these olefins containing branched pendant alkyl groups are slower than their linear straight chain counterparts. For homogeneous metallocene catalysts, VCH is usually copolymerized with ethylene or another α-olefin for enhanced mechanical properties.[40,41] To illustrate how sluggishly

metallocenes perform the homopolymerization of VCH, the well-renowned $EBIZrCl_2$ / MAO (Al : Zr ratio 1000 : 1) system produces only 50 mg of isotactic PVCH after 300 hours at 20 °C, while only dimers could be isolated from the catalyst for syndiospecific propylene polymerization, $[SiMe_2(Cp)(fluorenyl)]ZrCl_2$.[42]

3.3.2.1. Living Polymerization. The polymerization of VCH could be achieved at 25 °C using **6a** to produce highly isotactic PVCH. However, the polydispersity of this polymer was 1.3, indicating non-ideal living behavior. Cooling down to -10 °C to gain greater living behavior only served to severely retard the rate of propagation, producing essentially no polymer during the typical 120 minute polymerization. However, the CpZA's show a heightened rate constant for VCH polymerization as previously seen for 1-hexene. Along with faster monomer consumption, the polymerizations are living for **15c** and **15d** as shown through narrow polymer polydispersities and linear correlations of ln ($[M]_o$ / $[M]_t$) vs time as shown below in Figure 19.

One factor that may be severely affecting all polymerizations up to this point, yet is easily overlooked, is the product of precatalyst activation. The two cocatalysts employed have different methods of activation, with $[Ph_3C]^+$ abstracting a methyl group from Zr, and $[PhNHMe_2]^+$ protonating a methyl group to produce methane. The soluble coproducts of activation, then, are Ph_3CCH_3 and $PhNMe_2$, the latter of which could serve as an efficient Lewis base that must be displaced by monomer. This interaction has been observed previously with other homogeneous Ziegler-Natta catalysts.[43,44] To test this, the kinetics of VCH polymerization using **15d** were investigated under identical conditions only varying the type of cocatalyst. This is shown in Figure 19. The similarity between the observed rate constants for propagation for the two cocatalysts, 0.0245 and

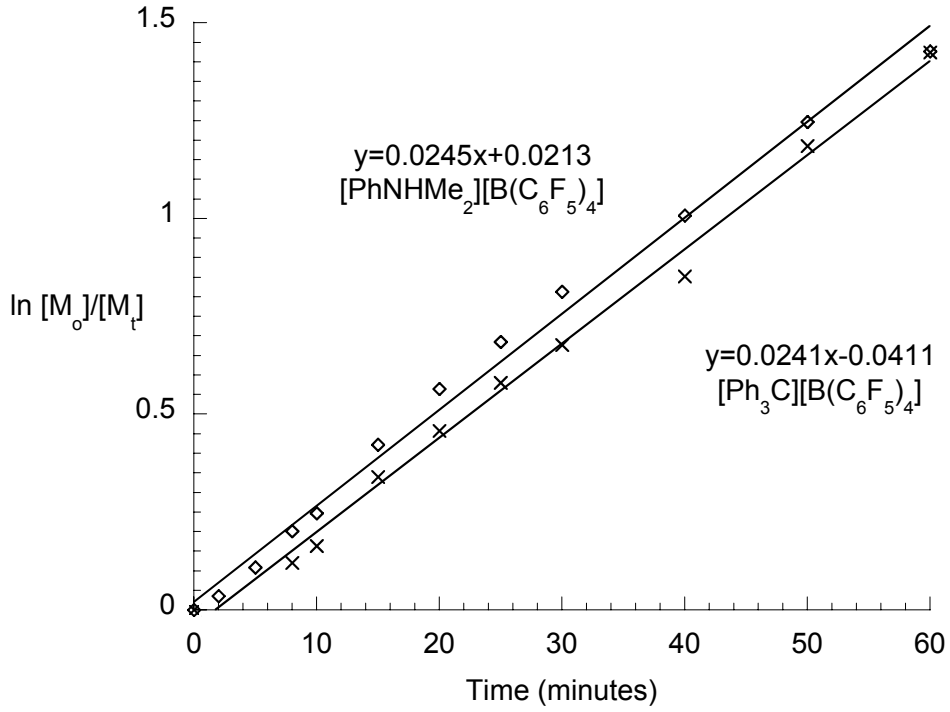

Figure 19. VCH polymerization kinetics of **15d** when activated by two different borates.

0.0241 s^{-1}, suggests that, if coordination of dimethylaniline is occurring, it does not detrimentally affect the rate of propagation.

3.3.2.2. Structure / Property Relationships. Figure 20a shows the isotactic PVCH prepared at RT from racemic **6a** having six resonances in the ^{13}C NMR spectrum for the stereoregular polymer. For comparison, the PVCH isolated from polymerization with the achiral **15c** at -10 °C is also shown in Figure 20b. Interestingly, the polymer microstructure is quite highly isotactic, unlike that seen from 1-hexene polymerizations, which was nearly atactic for CpZA's. This result implies that the ligand framework is not playing a role in determining the enantiofacial selectivity of the incoming monomer, which is indicative of a polymerization under chain-end control.[45,46]

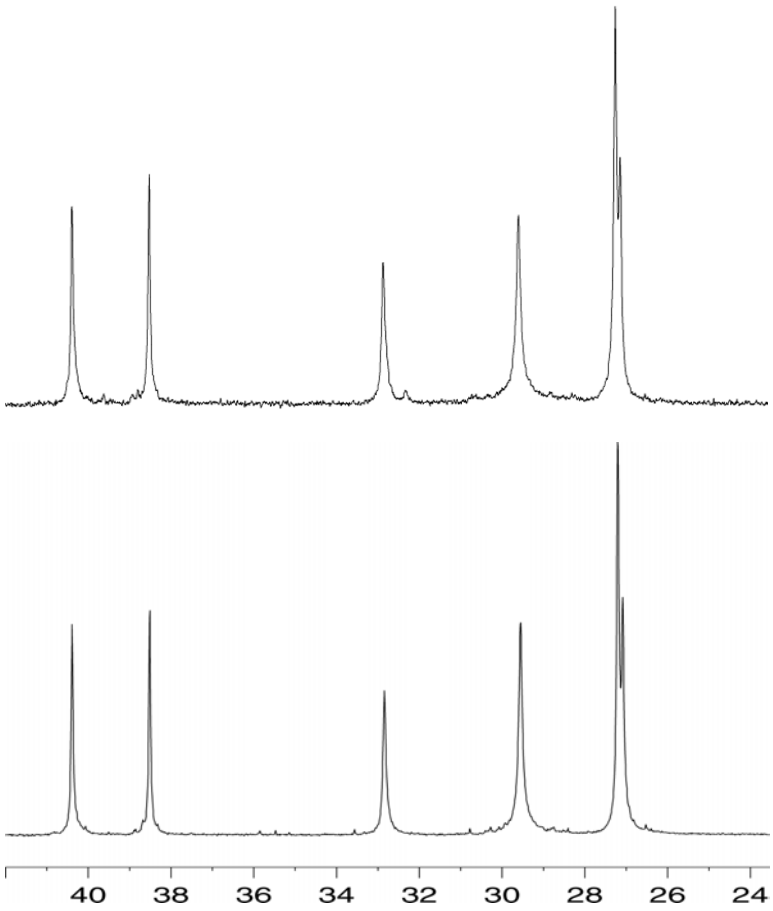

Figure 20. ^{13}C NMR spectra (100 MHz, $CDCl_3$, 23 °C) of PVCH prepared from (top) **6a** at 25 °C and (bottom) **15c** at -10 °C.

3.4. Block Copolymers.

One major development within the non-metallocene family is the elucidation of catalysts capable of performing the living polymerization of monomers, previously known primarily for ionic and radical polymerization mechanisms. Worthy of note is the trend that despite the lucrative history of metallocenes, a far greater number of living polymerization catalysts exist for those based on heteroatom containing ligands. Having systems devoid of irreversible termination, one of the greatest attributes of a living polymerization is the capability to form well-defined block copolymers from consecutive monomer additions. These polymers can combine the advantageous characteristics of

the two homopolymers into the same material, instead of mixing the two preprepared polymers into a blend which can completely separate upon annealing. Combining an amorphous block with a highly crystalline block can lead to micro-phase separation upon annealing which can be characterized through phase-sensitive tapping mode atomic force microscopy (AFM).[47]

Proof of block copolymer formation was first revealed through polymerization of 1-hexene.[16] Reacting 180 eq of 1-hexene with **6a** / $[PhNHMe_2][B(C_6F_5)_4]$ at -10 °C produced a polymer with M_n of 20,732 and a narrow PDI (1.03). After monomer consumption was complete, exposing the solution to an additional 180 eq lead to a

With **6a**, the diblock copolymerization of 1-hexene with 1,5-hexadiene was also accomplished.[32] Incorporating first 90 eq of 1-hexene then cyclopolymerizing the same amount of the diene yielded a diblock copolymer with a narrow PDI (1.05) and a monomodal GPC trace (run 2). Performing virtually the same reaction, except adding another block of 1-hexene after the 1,5-hexadiene block, generated a triblock copolymer with a higher molecular weight than the diblock (compare runs 2 and 3) yet still maintaining a narrow PDI.

Run	Precatalyst	Monomer #1	Monomer #2	Monomer #3	M_n	PDI
1	**6a**	1-hexene	1-hexene		35,000	1.13
2	**6a**	1-hexene	1,5-hexadiene		22,800	1.05
3	**6a**	1-hexene	1,5-hexadiene	1-hexene	30,900	1.10
4	**15d**	VCH	1-hexene	VCH	24,400	1.08

Table 4. Diblock and triblock copolymerization data employing Cp and Cp*ZA's.

polymer with greater molecular weight (M_n = 35,372) and still narrow molecular weight distribution of 1.13 (see Table 4, run 1).

Copolymerization of VCH with 1-hexene was accomplished with **15d**.[48] Via addition of 40 eq of VCH followed by 150 eq of 1-hexene and finishing with another 40 eq of VCH provided an elastomeric material after ~5 hours of polymerization (run 4). This reaction pointed out that the monomer producing the crystalline domain of the copolymer did not necessarily have to be in between two amorphous PH chains, illustrating the fact that the sequence of monomer addition did not affect polydispersities of the resultant polymers

3.5. Ethylene and Propylene.

While the ability to polymerize a wide variety of monomers is important, to truly test the mettle of a catalyst system ethylene and propylene polymerizations must be run since these are the most industrially relevant monomers. Although this lab was not adequately equipped to embark on a lengthy experimental exploration with these monomers, a few preliminary results need to be put forth.

At room temperature, ethylene and propylene could both be polymerized in a Fisher-Porter bottle. Large exotherms were apparent during the polymerization which were not performed under temperature controlled conditions. Under identical conditions, **15c** had an activity twice that of **6a** for production of PE. Polymerization with **6a** provided PE with a high molecular weight (M_n = 41,000), though with a broad molecular weight distribution of 2.11. As for PP at RT, employing **6a** provided semicrystalline polymer within an hour with a low M_n value of 2860 and a PDI of 1.73, still indicative of a single-site catalyst, yet showing considerable catalyst deactivation. By comparison, performing the same polymerization at 0 °C for one hour, then warming to room temperature, provided a higher molecular weight material, M_n = 11,110, though with a broader PDI (2.15).

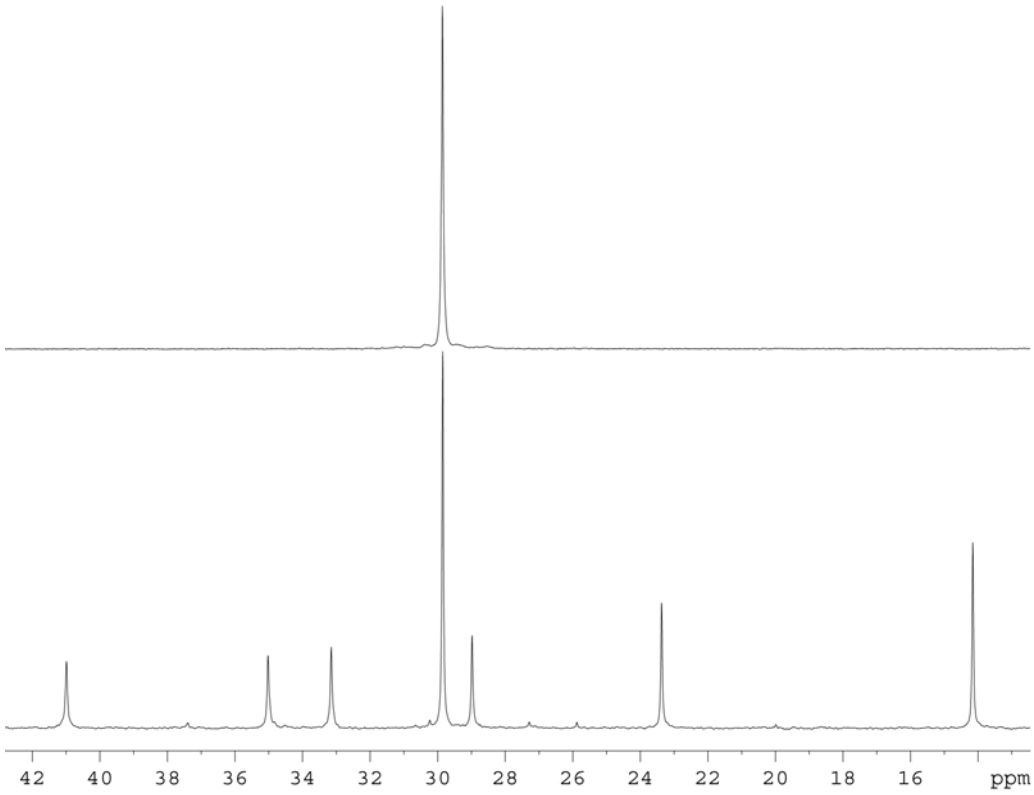

Figure 21. ^{13}C NMR spectrum for (top) PE prepared with **6a** at RT (100 MHz, 5 eq 1,2,4-trichlorobenzene : 1 eq C_6D_6, 120 °C) and (bottom) of an isotactic-PH-block-PE (100 MHz, $CDCl_3$, 23 °C).

High temperature NMR analysis of the PE produced from **6a** showed a highly linear polymer microstructure with no apparent branches (Figure 21). In fact, other than solvent resonances, the only signal present in the $^{13}C\{^1H\}$ NMR was at 29.9 ppm due to the numerous consecutive methylene groups in the polymer chain. The molecular weight was sufficiently high enough that no methyl end groups could be seen. In an attempted block copolymerization, 200 eq. of 1-hexene was first polymerized with **6a** / $[PhNHMe_2][B(C_6F_5)_4]$ at -10 °C. This living polymer solution was then subjected to ethylene for ~2 minutes before quenching with MeOH. Homopolymers of PH are quite soluble in tetrahydrofuran (THF), but no material was soluble in THF for the isolated

material, pointing to a covalently linked diblock copolymer and not a mixture of two separate homopolymers. Evaluation of the $^{13}C\{^{1}H\}$ NMR of the isolated diblock copolymer showed simply an overlay of homopolymers of PH and PE (Figure 21).

For propylene polymerizations also utilizing **6a**, NMR analysis did not display any evidence for vinyl end groups from polymerizations performed between -10 and 25 °C, indicating that β-hydride elimination is not a dominant pathway for chain termination. The main signals in the ^{13}C NMR spectrum are shown in Figure 22. Microstructure analysis shows that the polymerization was under site control by the presence of a 2 : 2 : 1 ratio of *mmmr* : *mmrr* : *mrrm* pentads.[45,46] Within the same temperature regime, the amount of stereoerrors produced at RT is higher than those produced at lower temperatures, with *mmmm* pentad distributions of 67.2 and 81.4 %, respectively. At ambient temperature, a higher number of 2,1-misinsertions are evident as compared to polymers prepared at low temperature.

3.6. Additional Monomers.

With the success seen with zirconium amidinates for stereospecific and living α-olefin polymerization, application to a broader range of monomers was investigated. Toward this, forming polymeric materials with interesting physical properties was of utmost interest. With **6a** and $[PhNHMe_2][B(C_6F_5)_4]$, 4-methyl-1-pentene was efficiently polymerized at -10 °C. This polymer is of great interest for its thermal stability, similar to PVCH, although it proved to be highly insoluble.[49] Success seen with VCH lead toward similar derivatives with acyclic γ-substituted α-olefins. Investigation in this regard allowed polymerization of β-citronellene with **15c**. The material obtained from such a venture was more easily characterized and the ^{13}C NMR spectrum for this semicrystalline powder is shown in Figure 23. This polymer, with M_n = 36,000 and PDI

= 1.06, displays the chemoselectivity for insertion of monosubstituted olefins as opposed to the trisubstituted group also present in the monomer.

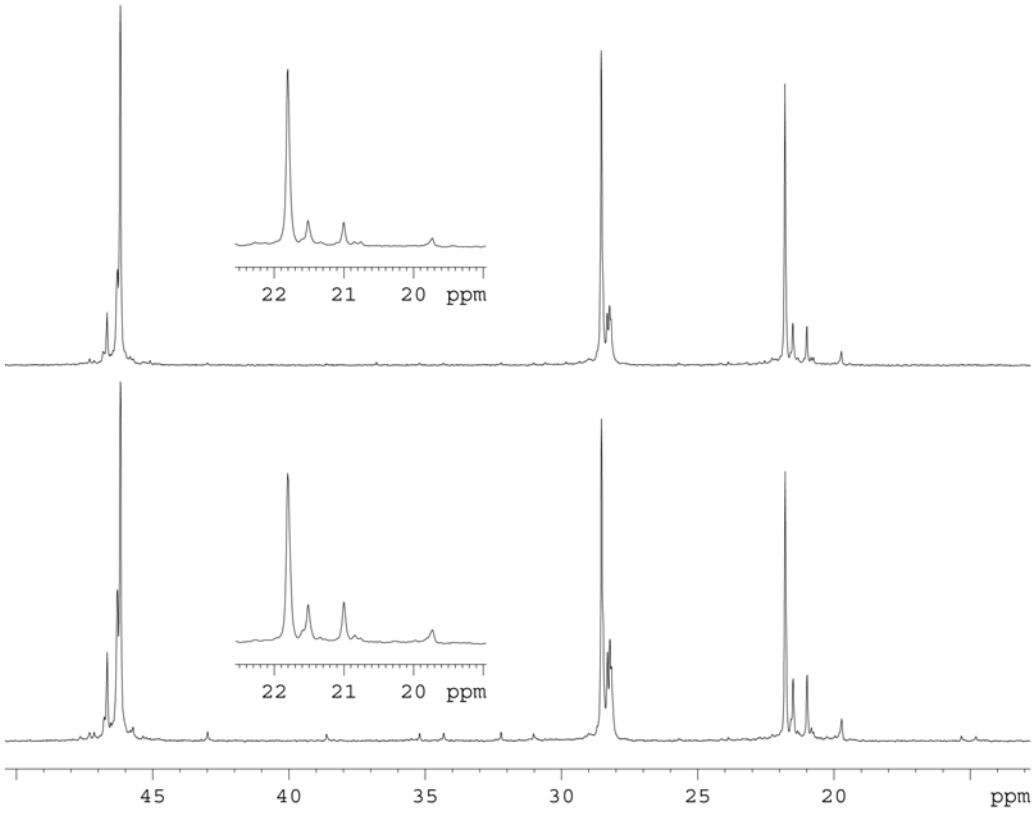

Figure 22. ^{13}C NMR spectra (100 MHz, $C_2D_2Cl_4$, 100 °C) of isotactic-PP prepared with **6a** at (top) –10 °C with temperature control and (bottom) RT without temperature control. The inset shows the resonances for the pendant methyl group.

The ability for Cp and Cp*ZA's to polymerize monomers other than those listed above becomes nearly negligible. Table 5 summarizes the monomers attempted along with the catalyst employed. The lone remaining success was 1,7-octadiene cyclopolymerization with **6a**. Beyond this, cyclopolymerization was not seen toward diallylaniline, diallylether, or 1,5-cyclooctadiene. Similar to the latter, other 1,2-disubstituted alkenes also did not prove to be active toward polymerization, even after

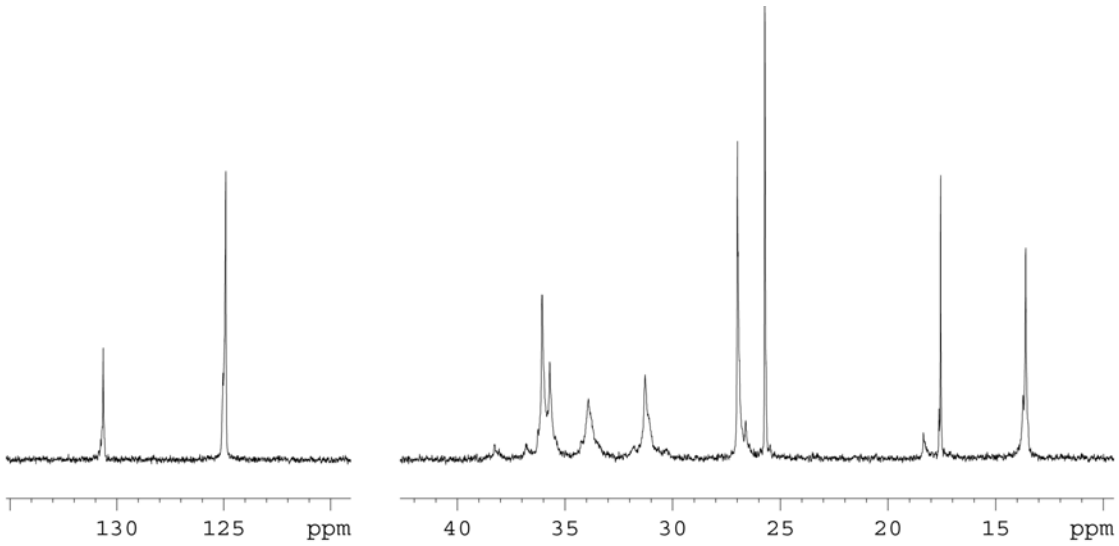

Figure 23. ^{13}C NMR spectrum (100MHz, $CDCl_3$, 23 °C) of poly-(β-citronellene).

long polymerization times. Inactivity toward isobutylene, in conjunction with other disubstituted alkenes, suggests that only monosubstituted alkenes will be tolerated by

Monomer	Precatalyst	Monomer	Precatalyst
cis-2-butene	**6a**	diallylaniline	**6a**
norbornene	**6a**, **15d**	diallylether	**6a**
1,5-cyclooctadiene	**6a**	styrene	**6a**, **15d**
cyclopentene	**6a**, **15c**	phenylacetylene	**6a**, **15d**
isobutylene	**6a**	nonafluoro-1-hexene	**6a**, **15c**

Table 5. Monomers inactive for polymerization with the corresponding precatalysts.

the Cp* framework. Styrene and phenylacetylene, perhaps due to structural similarity to VCH, were not polymerized. Finally, nonafluoro-1-hexene was shown to be totally inactive, even at 60 °C.

3.7. Conclusions.

The Cp and Cp*ZA's discussed in this chapter have proven to be much more successful toward the Ziegler-Natta polymerization of α-olefins than analogous derivatives reported in the literature. The stereospecific and living polymerization of 1-hexene has been realized using **6a**. The living cyclopolymerization of 1,5-hexadiene can also be accomplished with **6a**, **6b**, and **6c**, with a high trans ring content present for the more sterically bulky systems. The stereospecific and living polymerization of VCH can be performed with the CpZA's **15b**, **15c**, and **15d**. Due to the living nature of the polymerizations, di- and triblock α-olefin copolymers can be prepared which have interesting physical properties.

Acetamidinates of **6** and **15** appear to afford the best balance between electronics and sterics to attain both stereospecific and living polymerization characteristics. The formamidinates **11** provide low activity, low molecular weight, and broad polydispersities, along with a lack of stereocontrol for PH production. The benzamidinate, **13**, regained the advantageous attributes of a living polymerization, although the stereocontrol was still lacking. Lastly, for the ^{t}Bu amidinate **12**, no activity toward 1-hexene polymerization was noticed, implying that this group is simply too encumbering to allow polymer formation.

3.8. References:

(1) Averbuj, C.; Tish, E.; Eisen, M. S. *J. Am. Chem. Soc.* **1998**, *120*, 8640.

(2) Flores, J. C.; Chien, J. C. W.; Rausch, M. D. *Organometallics* **1995**, *14*, 1827.

(3) Walther, D.; Fischer, R.; Gorls, H.; Koch, J.; Schweder, B. *J. Organomet. Chem.* **1996**, *508*, 13.

(4) Herskovics-Korine, D.; Eisen, M. S. *J. Organomet. Chem.* **1995**, *503*, 307.

(5) Richter, J.; Edelmann, F. T.; Noltemeyer, M.; Schmidt, H.-S.; Shmulinson, M.; Eisen, M. S. *J. Molec. Catal. A: Chem.* **1998**, *130*, 149.

(6) Volkis, V.; Shmulinson, M.; Averbuj, C.; Lisovskii, A.; Edelmann, F. T.; Eisen, M. S. *Organometallics* **1998**, *17*, 3155.

(7) Volkis, V.; Nelkenbaum, E.; Lisovskii, A.; Hasson, G.; Semiat, R.; Kapon, M.; Botoshansky, M.; Eishen, Y.; Eisen, M. S. *J. Am. Chem. Soc.* **2003**, *125*, 2179.

(8) Lancaster, S. J.; Robinson, O. B.; Bochmann, M.; Coles, S. J.; Hursthouse, M. B. *Organometallics* **1995**, *14*, 2456.

(9) Eisen, M. S.; Marks, T. J. *Organometallics* **1992**, *11*, 3939.

(10) Averbuj, C.; Eisen, M. S. *J. Am. Chem. Soc.* **1999**, *121*, 8755.

(11) Chernega, A. N.; Gomez, R.; Green, M. L. H. *J. Chem. Soc., Chem. Commun.* **1993**, 1415.

(12) Gomez, R.; Green, M. L. H.; Haggitt, J. L. *J. Chem. Soc., Chem. Commun.* **1994**, 2607.

(13) Gomez, R.; Duchateau, R.; Chernega, A. N.; Teuben, J. H.; Edelmann, F. T.; Green, M. L. H. *J. Organomet. Chem.* **1995**, *491*, 153.

(14) Ferraris, D.; Cox, C.; Anand, R.; Lectka, T. *J. Am. Chem. Soc.* **1997**, *119*, 4319.

(15) Kraft, B. M.; Lachicotte, R. J.; Jones, W. D. *J. Am. Chem. Soc.* **2001**, *123*, 10973.

(16) Jayaratne, K. C.; Sita, L. R. *J. Am. Chem. Soc.* **2000**, *122*, 958.

(17) Kissounko, D. A.; Fettinger, J. C.; Sita, L. R. *Inorg. Chim. Acta* **2002**, *00*, 1.

(18) Schrock, R. R.; Bonitatebus, P. J.; Schrodi, Y. *Organometallics* **2001**, *20*, 1056.

(19) Yang, X. M.; Stern, C. L.; Marks, T. J. *J. Am. Chem. Soc.* **1994**, *116*, 10015.

(20) Littke, A.; Sleiman, N.; Bensimon, C.; Richeson, D. S.; Yap, G. P. A.; Brown, S. J. *Organometallics* **1998**, *17*, 446.

(21) Mehrkhodavandi, P.; Bonitatebus, P. J.; Schrock, R. R. *J. Am. Chem. Soc.* **2000**, *122*, 7841.

(22) Hagihara, H.; Shiono, T.; Ikeda, T. *Macromolecules* **1998**, *31*, 3184.

(23) Ewen, J. A. *J. Mol. Catal. A: Chem.* **1998**, *128*, 103.

(24) Mehrkhodavandi, P.; Schrock, R. R. *J. Am. Chem. Soc.* **2001**, *123*, 10746.

(25) Asakura, T.; Demura, M.; Nishiyama, Y. *Macromolecules* **1991**, *24*, 2334.

(26) Babu, G. N.; NewMark, R. A.; Chien, J. C. W. *Macromolecules* **1994**, *27*.

(27) Marvel, C. S.; Stille, J. K. *J. Am. Chem. Soc.* **1958**, *80*, 1740.

(28) Resconi, L.; Waymouth, R. M. *J. Am. Chem. Soc.* **1990**, *112*, 4953.

(29) Coates, G. W.; Waymouth, R. M. *J. Am. Chem. Soc.* **1991**, *113*, 6270.

(30) Coates, G. W.; Waymouth, R. M. *J. Am. Chem. Soc.* **1993**, *115*, 91.

(31) Coates, G. W.; Waymouth, R. M. *J. Mol. Catal.* **1992**, *76*, 189.

(32) Jayaratne, K. C.; Keaton, R. J.; Henningsen, D. A.; Sita, L. R. *J. Am. Chem. Soc.* **2000**, *122*, 10490.

(33) Matyjaszewski, K. *J. Phys. Org. Chem.* **1995**, *8*, 197.

(34) Keaton, R. J.; Jayaratne, K. C.; Henningsen, D. A.; Koterwas, L. A.; Sita, L. R. *J. Am. Chem. Soc.* **2001**, *123*, 6197.

(35) Quirk, R. P.; Lee, B. *Polym. Int.* **1992**, *27*, 359.

(36) Soga, K.; Nakatani, H.; Shiono, T. *Macromolecules* **1989**, *22*, 1499.

(37) Endo, K.; Otsu, T. *J. Polym. Sci. A: Polym. Chem.* **1992**, *30*, 679.

(38) Ammendola, P.; Tancredi, T.; Zambelli, A. *Macromolecules* **1986**, *19*, 307.

(39) Zambelli, A.; Ammendola, P.; Sivak, A. J. *J. Am. Chem. Soc.* **1984**, *17*, 461.

(40) Mani, R.; Burns, C. M. *Polymer* **1993**, *34*, 1941.

(41) Marques, M.; Yu, Z.; Rausch, M. D.; Chien, J. C. W. *J. Polym. Sci. A: Polym. Chem.* **1995**, *33*, 2787.

(42) Longo, P.; Grassi, A.; Grisi, F.; Milione, S. *Marcomol. Rapid Comm.* **1998**, *19*, 229.

(43) Horton, A. D.; de With, J.; van der Linden, A. J.; van de Weg, H. *Organometallics* **1996**, *15*, 2672.

(44) Baumann, R.; Davis, W. M.; Schrock, R. R. *J. Am. Chem. Soc.* **1997**, *119*, 3830.

(45) Resconi, L.; Abis, L.; Franciscono, G. *Macromolecules* **1992**, *25*, 6814.

(46) Hagihara, H.; Shiono, T.; Ikeda, T. *Macromol. Chem. Phys.* **1998**, *199*, 2439.

(47) Bates, F. S. *Science* **1991**, *251*, 898.

(48) Keaton, R. J.; Jayaratne, K. C.; Henningsen, D. A.; Koterwas, L. A.; Sita, L. R. *J. Am. Chem. Soc.* **2001**, *123*, 6197.

(49) Ferraris, G.; Corno, C.; Priola, P.; Cesca, S. *Macromolecules* **1977**, *10*, 188.

Chapter 4

Characterization of Active Cationic Initiators

4.1. Introduction.

As mentioned in Chapter 1, for greater characterization of active mechanisms or any intermediates present during polymerization, highly soluble catalysts needed to be developed. Metallocenes first met this demand, followed by hetero-atom containing non-metallocenes, with many of the latter being highlighted as living polymerization catalytic species.[1] While the microstructure of the polymers provided a detailed record of each step of the reaction, it was becoming clearer that the widely accepted dogma around cationic Group IV alkyls as the catalytically active species in solution was gaining credence. Characterization of such intermediates has enhanced our appreciation and understanding of the subtleties behind Ziegler-Natta polymerizations.

4.2. Solid State Structures.

Although various experimental results have argued in favor of cationic Group IV alkyls as the active species in Ziegler-Natta polymerizations, the exact structure of these intermediates was not precisely known. Mentioned in Chapter 1 was the chemical trapping of the methyl cation with an alkyne.[2] Electrochemical experiments showed that Cp_2ZrCl_2, $Cp_2ZrMeCl$, and Cp_2ZrMe_2 when combined with MAO, all provided a species with the exact same binding energy before and after addition of ethylene.[3] The fact that the energies were higher than that of the neutral precursors points to a more electron deficient metal being present. While these systems allowed the assumption of a cationic Zr-Me, the exact structure of the activated complex was not yet solidly established.

Early attempts at crystallization of active species only provided decomposition products from the combination of Cp_2TiCl_2 / $AlEt_3$.[4] With the simplistic system $Cp_2Zr(CH_3)_2$, Jordan was able to structurally characterize the Lewis-base stabilized methyl cation, $[Cp_2Zr(CH_3)(THF)][BPh_4]$ (**ii**), upon addition of $AgBPh_4$ and recrystallization in THF.[5] This molecule displayed shorter distances for the remaining Zr-Me and Cp-Zr bonds compared to the neutral predecessor. In CH_2Cl_2, this cation polymerizes ethylene much more slowly than the base free cation, $[Cp_2ZrCH_3]^+$, the former of which is undoubtedly hindered due to competitive binding of THF.

First mentioned in Chapter 1, a base free cationic Th adduct, from the reaction of $Cp^*_2ThMe_2$ and $[Bu_3NH][B(C_6F_5)_4]$, was isolated by Marks.[6] Exposure of the adduct to ethylene and 1-hexene resulted in polymerization and dimerization, respectively. Subsequent work from the same group described the molecular structures of a multitude of simple zirconocenes activated by $B(C_6F_5)_3$.[7,8] Unlike the Th cation with the less coordinating borate anion, the Zr cations were in close contact with the bridging methyl groups of the $MeB(C_6F_5)_3^-$ anion. Many of the latter were highly active for ethylene polymerization.

Identification of similar products from Cp*ZA's was attempted through addition of stoichiometric amounts of **6a** and $[PhNHMe_2][B(C_6F_5)_4]$ in chlorobenzene at low temperature, presumed to yield the ion pair, $[Cp^*ZrMe(^tBuNC(Me)NEt][B(C_6F_5)_4]$, **22a**. In the case where a small amount of Et_2O was added to the solvent, single crystals of the Lewis base stabilized cation **22a**·(Et_2O) were obtained.[9] The molecular structure of this complex is shown in Figure 24 and pertinent bond angles and bond lengths are provided in Table 6. For the base stabilized adducts **ii** and **22a**·(Et_2O), differences in the Zr-Me bond lengths are matched between neutral[10] and cationic complexes at ~ 0.02 Å. However, the decrease in the Cp-Zr distance for the metallocene adduct (0.04

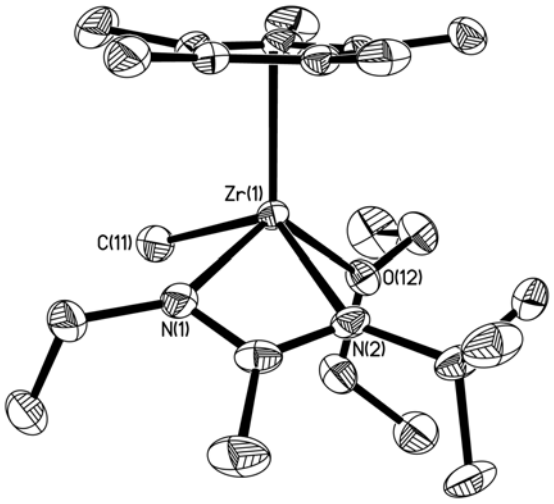

Figure 24. Molecular structure of **22a**·(Et_2O) with 30 % thermal ellipsoids. The hydrogen atoms and the borate anion have been removed for clarity.

	6a	**22a**·(Et_2O)	**22a-1**	**22a-2**	**23**	**24**
Zr-N(1)	2.251(3)	2.171(3)	2.135(4)	2.146(2)	2.157(3)	2.226(3)
Zr-N(2)	2.265(2)	2.258(3)	2.199(3)	2.222(2)	2.123(3)	2.252(3)
Zr-X	2.273(3)	2.255(4)	2.441(5)	2.372(3)	2.203(4)	2.302(3)
X	C14	C11	C11	C11	C22	C11
Zr-Y	2.272(3)	2.233(2)	2.453(4)	2.415(3)		2.302(4)
Y	C15	O	C11A	C11A		C11a

Table 6. Selected bond lengths (Å) for structurally characterized Cp*ZA cations and **6a**.

Å) is not found to be as severe between **6a** and **22a**·(Et_2O) (0.01 Å). Instead, the amidinate Zr-N bond lengths experience a shortening, expected for a more electron deficient metal center. This may prove quite advantageous for polymerizations employing **6a**. Since **6a** has been found to be stereospecific, it may be assumed that the shorter bond lengths found in **22a**·(Et_2O) increase the barrier to amidinate ring flipping, providing a more stable ligand framework for stereoregular polymer production.

Ansa-bridged metallocenes are very popular for just this reason. As a final note, the molecule of ether in this structure is located closest to the ^{t}Bu side of the amidinate ligand. It cannot be stated with certainty that this site is the same which allows olefin coordination.

For isolation of a base-free adduct, Et_2O was left out of the recrystallization mixture. From this, slow growth of light tan crystals was noticed which proved to be the dimethyl bridged dimeric dication of **22a**. From the same batch of crystals, three different structures are present and were separately identified, though two are very similar, having bond lengths and angles that fall within experimental error of eachother. The two significantly different solid state structures of the dimer are depicted in Figure 25 and other features are listed in Table 6. All of the dimeric structures contain bridging methyl groups. In the first isomer, **22a-1**, within the four membered ring that forms the bridge reside two crystallographically located hydrogen atoms, H(11C) and H(11F). With close proximity of these atoms to the electrophilic metal center (cf., Zr-H(11C)

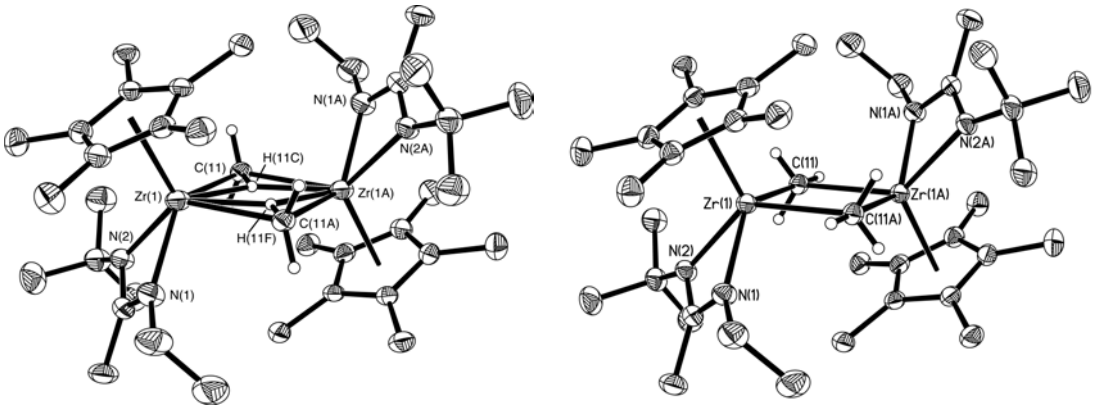

Figure 25. Two crystallographically identified molecular structures of the dimeric dication, (left) **22a-1** and (right) **22a-2**, with 30 % ellipsoids for both. Hydrogen atoms, except those for the bridging methyl groups, and the borate anions have been removed for clarity.

1.899(19) Å and Zr-H(11F) 1.95(2) Å), it appears that the hydrogens are agostically interacting with both Zr centers.[11,12] This can be further verified through inspection of the Zr-C bond distances, which are longer than in either the neutral **6a** or the ether stabilized structure, from which it can be assumed that the agostic interactions balances this out. Further, the four membered metallacycle is not symmetric, with Zr-C bond distances being slightly inequivalent. With the lack of a coordinating Lewis base, the Zr-N bond lengths are even shorter compared to **22a**·(Et_2O) in order to compensate for the lack of the electron donating group.

In Chapter 1, the Cossee mechanism for chain elongation during Ziegler-Natta polymerization was discussed. Improvements on this mechanism from detailed mechanistic studies have implied that α-hydrogen agostic interactions within a mononuclear species may serve to lower the insertion barrier for chain elongation.[13] Therefore, **22a-1** may be showing that the agostic interactions serve to lengthen the Zr-C distance allowing for more facile olefin insertion.

The second structure of the dimeric dication, **22a-2**, maintains the four membered bridging ring, though now the agostic interactions are missing. In this species, the closest C(11) hydrogen contact to a Zr center is 2.39(4) Å, which is outside of typical distances for either bridging (2.0 Å)[12] or agostic (2.16 Å)[14] distances. The agostic interactions may not be possible due to the more tetrahedral environment about C11 ($\Sigma\theta_{C11}$ = 315 °) as compared to **22a-1** ($\Sigma\theta_{C11}$ = 358 °). Without the intervention of α-agostics, the Zr-C bond lengths are appreciably smaller, while the Zr-N lengths are slightly elongated, though the latter are still not as long as those in **6a**.

An interesting feature in these studies is the existence of dimeric dications. Typically, the catalytically active species is denoted as L_2MR^+, or rather to say, a mononuclear species. Previous crystal structures from other Group IV Ziegler-Natta

systems have utilized either stabilizing bases or more strongly coordinating anions to aid in crystallization.[5,8,14,15] Results with **22a** demonstrate that the dimeric nature can be disrupted by the presence of a highly coordinating Lewis base. Thus the roles of dimers during polymerization cannot be readily dismissed.

This is not the first instance where existence of dimers has been suggested during Ziegler-Natta polymerizations. The first type of dimer evolves from the generation of a M-Me cation which then is stabilized not by solvent or the counterion, but by a molecule of neutral dimethyl species (Scheme 29).[6,16] These species can be produced during activation of the dimethyl precatalyst, where dimer formation competes or is faster than activation While these species are typically observed via NMR spectroscopy, Marks was able to gain crystallographic evidence for just such a species.[17] It should not be assumed, however, that continued addition of cocatalyst will abstract another Zr-Me group to break apart the dimer and generate another equivalent of the methyl cation. Bochmann found that generation of the monocationic dimer for $Cp^*_2ZrMe_2$ was quite facile at –60 °C, and that full activation by the other half equivalent of borate cocatalyst occurred at –40 °C.[18] However, the dimer from the $SiMe_2$-bridged version of *rac*-**18** remains even at RT, though continued reaction with cocatalyst does occur slowly. Schrock has observed the dimerization of a nonmetallocene dimethyl complex that would not react with excess Ph_3C^+.[19]

The second type of dimer proposed in the literature is more applicable to the molecular structures of **22a-1** and **22a-2**. This version of the multinuclear species

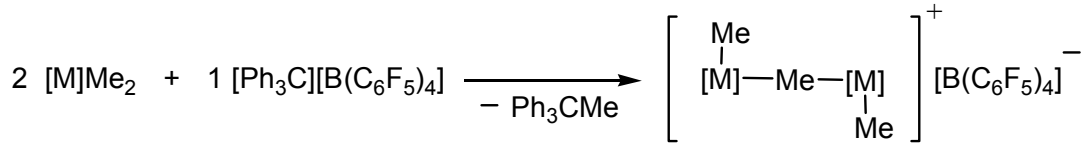

Scheme 29. Formation of dinuclear monocationic methyl bridged species.

involves interaction of two fully cationic species during Ziegler-Natta polymerization. Mülhaupt proposed that a two-step deactivation process was active within propylene polymerizations with Cp_2ZrCl_2 / MAO.[20] Though no explicit intermediates were named, two catalytically active species were projected to reversibly form a dormant species, at which point this latter species could irreversibly deactivate. At the beginning of the polymerization, only the catalytically active complex is present, and the productivity as a function of time slackened as the inactive species built up. At lower temperatures, this equilibrium is established much more slowly as evidenced through a greater initial productivity at early reaction times.

Brintzinger and coworkers performed NMR experiments to establish the nature of cation-anion pairs in solution.[21] This work detailed that aggregation of ion pairs was evident in C_6D_6 solutions, and that they varied slightly depending on the type of metallocene complex and whether a borane or a borate cocatalyst was employed. These aggregates, which were termed ion quadruples, are shown in Scheme 30. These species were theorized based on the fact that the ions had volumes in solution that were twice that expected. Support for this came from similarities between values for a proposed ion quadruple and one of the dinuclear methyl bridged monocations discussed earlier. Brintzinger was also able to show that rapid anion swapping of $B(C_6F_5)_4^-$

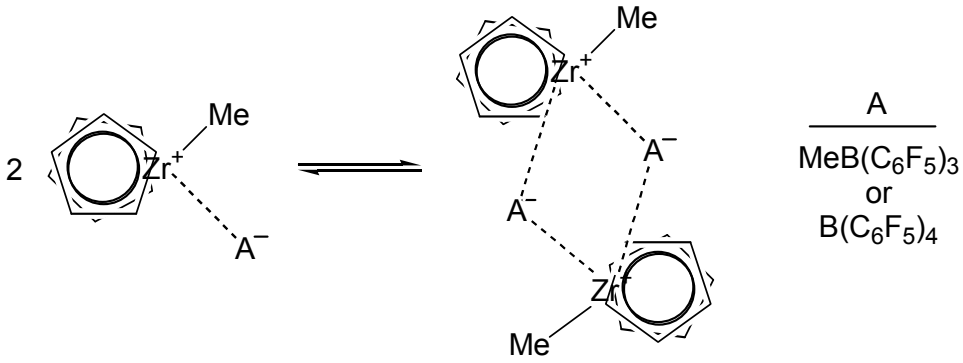

Scheme 30. Dimerization of ion pairs in solution producing ion quadruples.

between ion pairs occurs in solution, and that it is 5000 times faster than with the more coordinating $CH_3B(C_6F_5)_3^-$ anion.[22]

While dimers were prevalent from protonolysis from **6a**, it was of interest to disrupt dimerization in order to achieve a lone monomeric cation. This was achieved through reaction of the ^{t}Bu amidinate derivative **12** with $[PhNHMe_2][B(C_6F_5)_4]$. Single crystals were obtained and the structure is shown in Figure 26 with selected parameters located in Table 6. No α-agostic interactions were obvious, and no close contacts with

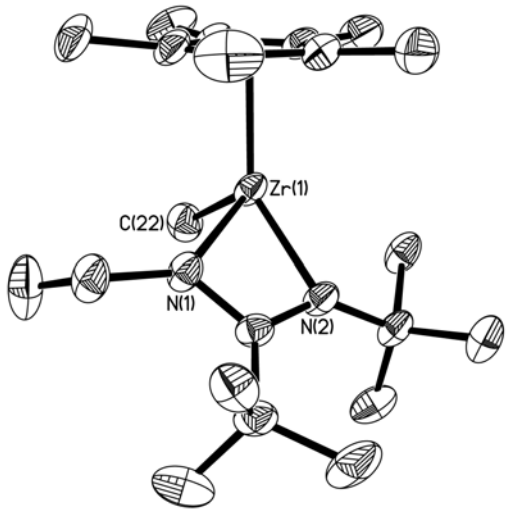

Figure 26. Molecular structure of monomeric amidinate cation **23** with 30 % thermal ellipsoids. Hydrogen atoms and the borate anion have been removed for clarity.

any of the F atoms of the borate anion were apparent. Of immediate interest is the significant shortening of the Zr-C and Zr-N bond distances compared to the dimeric dications. With the Zr-N(2) distance, defined as the N^{t}Bu side of the amidinate, being the shortest seen, the binding of the amidinate to Zr is forced to be quite asymmetric to minimize steric congestion, with the angles defined by CT-Zr-N (CT is the centroid of the Cp* ring) of 116.87(9) and 135.84(9) ° for N(1) and N(2), respectively. This is quite a

deviation when compared to the same angles in **22a-1** (114.28(16) and 119.13(13) °) and **22a-2** (112.68(12) and 117.86(9) °). This perturbation may prohibit monomer coordination through a detrimental transformation of the binding pocket, explaining why polymerizations with **12** did not produce polymer. Another reason for the lack of activity may revolve around the length and strength of the Zr-C bond. Without additional electron donation from a dimeric structure or agostic interactions, this bond may be thermodynamically more stable and more difficult to break in the transition state. This same rationale is employed to explain why Hf complexes have lower activities and produce higher molecular weight polymers than Ti and Zr.

Attempts at single crystal growth from solutions of **22a** at RT provided, instead of the dimeric dication, another dinuclear species in which one of the bridging carbon atoms has been deprotonated.[9] The molecular structure for this μ-CH_2, μ-CH_3 dimer, **24**, is illustrated in Figure 27. The reduction of this complex as compared to those of **22a** is evident through the presence of a single borate anion for charge balance. This net reduction in charge is exemplified through lengthened Zr-N distances, longer even than in **22a**·(Et_2O) and approaching the values seen for **6a**. Devoid of agostic interactions, possibly as a result of the decrease in the metal electrophilic nature, the Zr-C bond distance is still quite short (the Zr-C values are averages for the positionally disordered mixture of μ-CH_2 and μ-CH_3). Although the mechanism for this decomposition has not yet been firmly established, it is possible that the *in situ* generated Lewis base $PhNMe_2$, which was shown not to affect the rates of propagation, may in this case deprotonate a bridging methyl group of **22a-1** or **22a-2** producing this termination product. Bochmann has reported characterization via NMR of a similar μ-CH_2, μ-CH_3 dinuclear monocationic dimer, though the decomposition evolved CH_4 and the system did not contain $PhNMe_2$.[9,23]

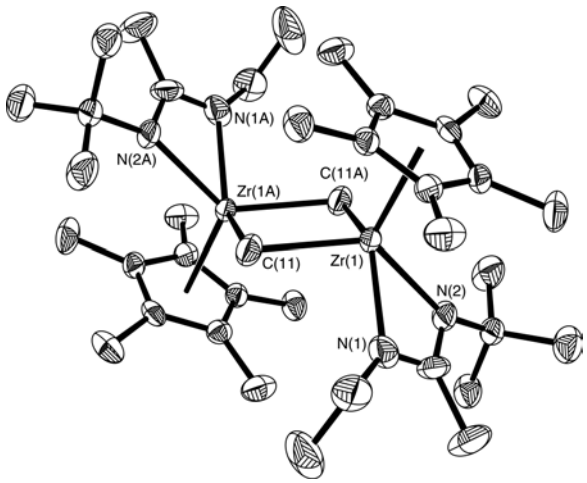

Figure 27. Molecular structure of deprotonation product **24** with 30 % thermal ellipsoids. Hydrogen atoms and the borate anion have been removed for clarity.

Warming PhCl solutions of the cation **22a** to RT also leads to formation of yet another dimeric dicationic species, though this time the product was the highly insoluble dark red crystals of the dichloro bridged dimer, **25** (Figure 28). This appears to be the ultimate product of decomposition from **22a**, with **24** perhaps serving as an intermediate. Instability of Group IV complexes in chlorinated solvents has been seen previously.[5,24] This same species is more readily prepared from solutions of CH_2Cl_2, even at low temperatures. Formation of **25** requires the abstraction of a Cl atom from either solvent. Like **22a**, both Zr atoms in **25** are still in the Zr^{4+} oxidation state with two borate anions present in the unit cell. Other work in this lab has resulted in the isolation of the same bridging dichloro dication from the Hf derivative of **6a**, as well as the formamidinate version from activation of **11b**. Green has also observed a dichoro-bridged dimer with a zirconium benzamidinate upon attempts to isolate the base free cation with a weakly coordinating anion from activation of the dimethyl precursor with $[Ph_3C][B(C_6F_5)_4]$.[25] Analogous derivatives could be isolated from the dibenzyl zirconium precatalyst or the $B(C_6F_5)_3$ cocatalyst.

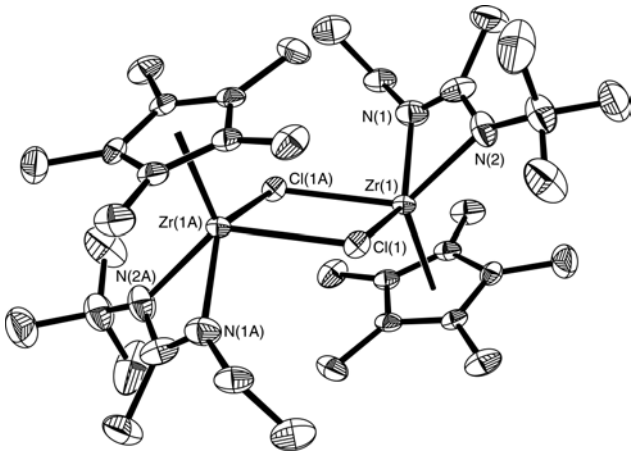

Figure 28. Molecular structure of the decomposition product **25** with 30 % thermal ellipsoids. Hydrogen atoms and the borate anions have been removed for clarity.

4.3. Solution Studies.

With the isolation of several cationic Cp*ZA's, interest grew toward the behavior of the cations in solution in an attempt to explain polymerization characteristics. The isotactic behavior of polymerizations with cation **22a** was still an enigma considering the fluxionality of the neutral **6a**. The broad polydispersities obtained from several polymerization systems was not straightforward. Assessment of NMR spectra of the methyl cations may offer a basis for these findings.

The ^{1}H NMR spectrum of the Zr-Me cation **22a** produced from the combination of ^{13}C-labeled **6a** (^{13}C-**6a** is synthesized from carbodiimide insertion into Cp*Zr($^{13}CH_3$)$_3$) and the borate [Ph_3C][$B(C_6F_5)_4$], is displayed in Figure 29. A slight stoichiometric excess of the cocatalyst was used to ensure that no residual **6a** remained in solution. From the NMR spectrum, it is apparent that quantitative formation of ^{13}C-**22a** has occurred. If a monomer-dimer equilibrium is active, this process is quite rapid even down to the temperature limit of the chlorobenzene-d_5 solvent (~233 K). The Zr bound methyl group shows a doublet in the ^{1}H NMR spectrum at δ 0.47 ppm with a coupling of $^{1}J_{CH}$ = 117

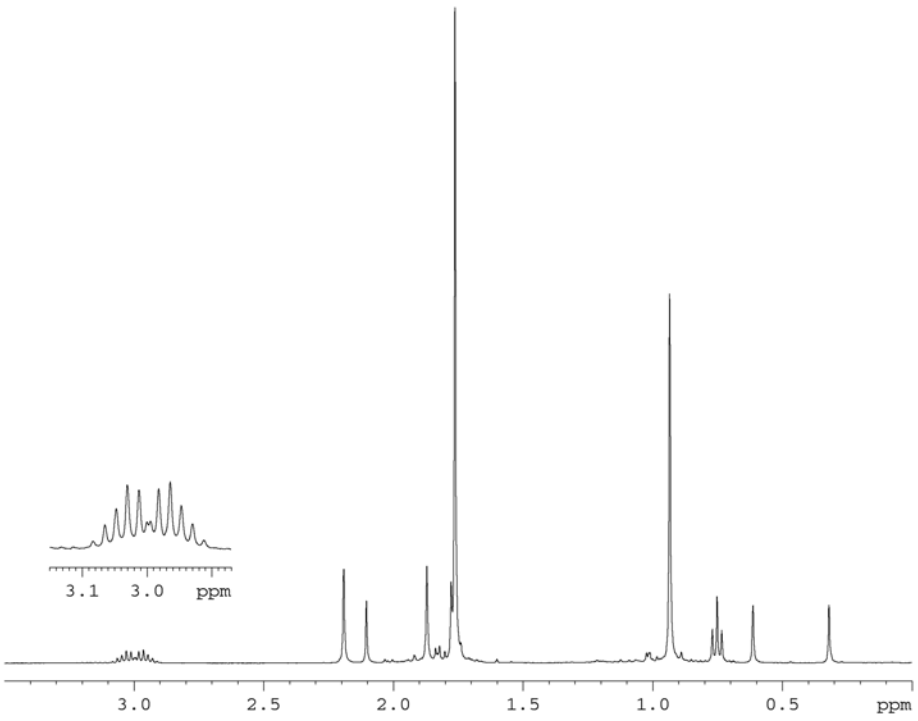

Figure 29. ^{1}H NMR spectrum (500MHz, PhCl-d_5, RT) of ^{13}C labeled **22a**.

Hz. Also split are the acetamidinate C($^{13}CH_3$) (δ 1.93 ppm and $^{1}J_{CH}$ = 124 Hz) and the product of methide abstraction, $Ph_3C^{13}CH_3$ (δ 2.03 ppm). For the methylene of the amidinate ethyl group, two separate resonances are present for the diastereotopic hydrogens around δ 3.0 ppm . The spectrum in Figure 29 is for the cation at RT, and even at this temperature, which is higher than conventional polymerization conditions, it appears that amidinate ring flipping has been frozen out. Recall that very low temperatures were required to freeze out amidinate ring flipping for the neutral dimethyl complex **6a**. This matches well with the discovery that in the solid state, the Zr-N bond lengths are much shorter due to the greater electron deficiency of the cationic metal which should provide greater configurational stability to the complex. This less fluctional structure should allow for stereoregular polymer formation. This feature is quite notable,

since metallocenes require rigidity supplied from the ansa-bridges to produce stereoregular polymers.

Further examples of configurationally stable cations were provided through additional work in this lab by Dr. Denis Kissounko on the cations of **6f**-**h**.[26] At –10 °C, distinct resonances for each methylene hydrogen are again evident. However, the cation from **6i** was discovered to be highly fluctional by NMR, indicating that potential intramolecular coordination of the para-substituted Cl atom of the phenyl ring may be occurring. Along these lines, protonolysis of one of the methyl groups from **6j** and **6k** produced cations that were chemically unstable at –10 °C. Similar instability is seen after reaction of **6c** with $[Ph_3C][B(C_6F_5)_4]$. Several examples exist in which cations react with the ligand framework through C-H bond activation processes.[8,27,28] These potential side reactions could be responsible for the decreased activity, or lack thereof, seen with these precatalysts.

The ^{1}H NMR spectrum reproduced in Figure 30 represents the cationic species, **26**, prepared from **12**. Similar to **22a**, **26** shows that the two N-Et methylene hydrogens are inequivalent due to the lack of amidinate ring flipping. At –10 °C, the Zr-Me group produces a broad signal which at RT is quite sharp, potentially from the more crowded steric environment. The cations **27a** and **27b**, prepared from the formamidinates **11a** and **11b**, respectively, are indefinitely stable when maintained at –10 °C. Diastereotopic hydrogens are again present for the amidinate ethyl group within **27a**, although at RT the signals overlap. Whether this feature arises through coincidental chemical shifts or actual coalescence has not been studied. It does not appear that **26** decomposes readily at –10 °C, yet both cationic formamidinates do decompose rather quickly at RT, with **27a** qualitatively being the quickest. Work on the formamidinates was done in conjunction with Erin K. Reeder.

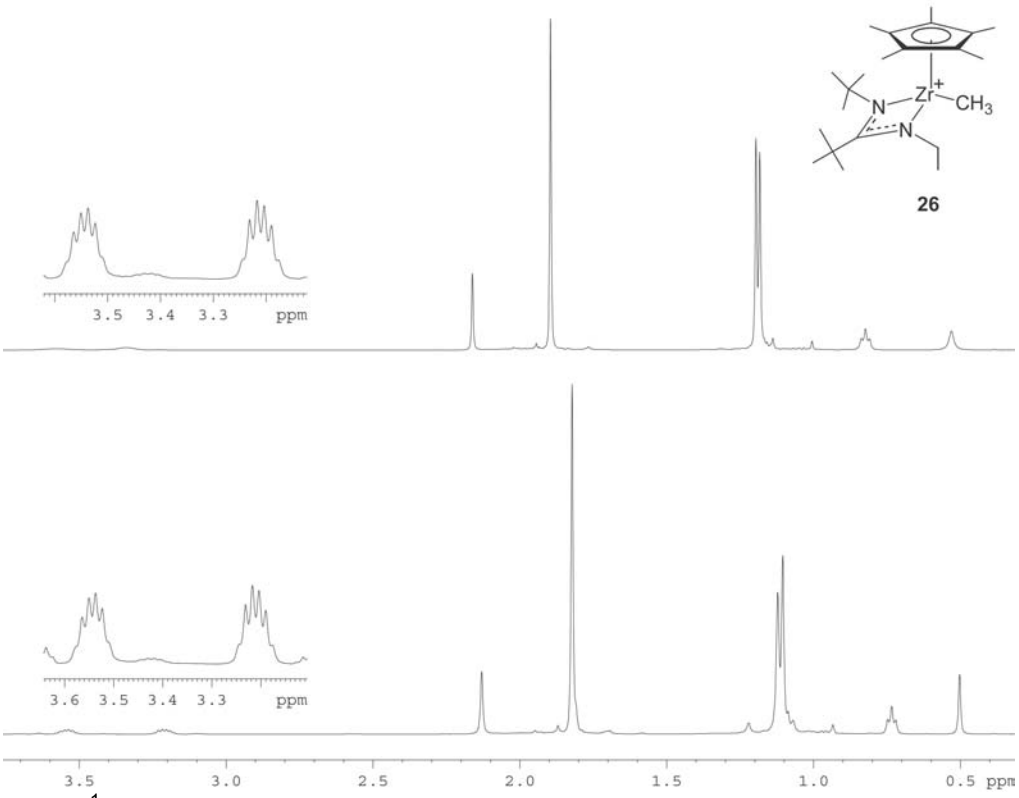

Figure 30. ^{1}H NMR spectra of **26** at (top) –10 °C (500 MHz, PhCl-d_5) and (bottom) RT (400 MHz, PhCl-d_5).

For CpZA's, living polymerizations were accomplished with **15b**-**d**. The cations derived from them would presumably be quite stable. Addition of $[Ph_3C][B(C_6F_5)_4]$ to **15c** and **15d** at –10 °C yielded **28c** and **28d** whose ^{1}H NMR spectrum were quite clean and revealed signals for the zirconium bound methyl group at 0.74 and 0.61 ppm, respectively. Both species were fairly stable at RT, with **28c** disappearing more rapidly than **28d**, which barely decomposed after 24 hours at RT.

Polymerizations with **15a** produced broad polydispersity PH with a loss of stereocontrol. Generation of the cation **28a** from **15a** and $[Ph_3C][B(C_6F_5)_4]$ yielded a ^{1}H NMR spectrum that did not contain a Zr-CH_3 resonance. Equally, the ^{13}C NMR spectrum only showed resonances attributable to the Cp and amidinate framework, as well as the coproduced Ph_3CCH_3. This species, **29**, is proposed to be the Cp version of

25. This compound was also evident from an NMR scale reaction between **28a** and 1-hexene. In an attempt to prevent decomposition, the cation was generated at –30 °C in the presence of excess Et_2O. The ^1H NMR spectrum from this reaction is shown in Figure 31a. With the ether molecule present, reaction with solvent is inhibited, and the Zr-Me group can be seen (δ 0.61 ppm) which integrates similarly to the CH_3 groups of the amidinate and Ph_3CCH_3. Figure 31b represents the ^1H NMR spectrum from the production of **28a**, which sat in solution for 10 minutes before addition of excess Et_2O. The changes in the two spectra represent a rapid decomposition of **28a** in the absence of base. In the spectrum of **28a**, signals assignable to **29** are present, though they do not appreciably grow with time.

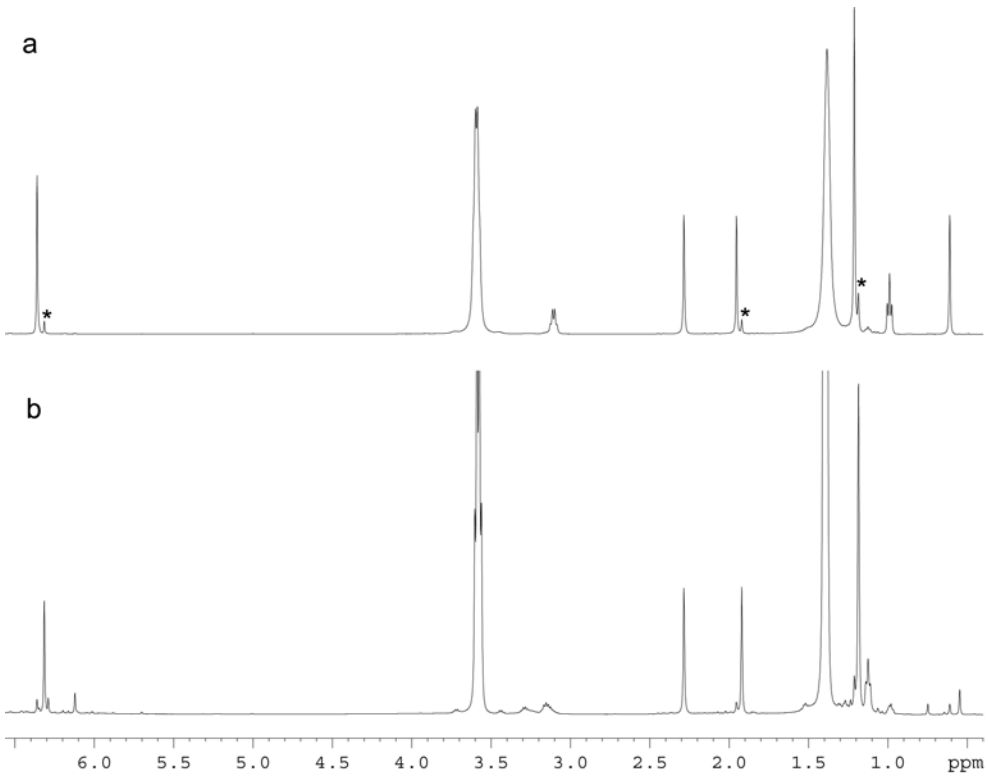

Figure 31. ^1H NMR spectra (500 MHz, PhCl-d_5, -30 °C) of the ether stabilized cations (a) **28a** and (b) **29**. The asterisk in the spectrum for **28a** denotes a small amount of **29**.

4.4. Conclusions.

The demethylation of Cp*ZA's produces Zr-Me cations that are readily characterized. Remarkably, single crystals can be obtained through careful recrystallization of the activated precatalyst, allowing visualization of the initiator in the solid state. The ether stabilized cation, **22a**·(Et_2O), can be realized if the cation is exposed to a small amount of the Lewis base during recrystallization. In the absence of base, the cation, **22a**, adopts a dimeric structure in the solid state with no close contacts with the anion. A monomeric Zr-Me cation structure was found from the sterically more encumbering ^{t}Bu amidinate **23**, in which the Zr-C and Zr-N bond distances were the shortest of all initiators crystallographically characterized. Evidence exists which suggests that the $PhNMe_2$ produced upon protonation of one of the Zr bound methyl groups in **6a** is not totally innocent in solution and may be a source of deactivation of the cation. The possibility exists that it may attack one of the acidic bridging methyl groups, and upon deprotonation, a new dimeric structure is obtained, **24**, in which the metallacycle is formed via one bridging methylene and one bridging methyl group. Ultimate decomposition leads to the dichloro bridged dimer **25**, resulting from halide abstraction from the solvent, although the precise mechanism by which this proceeds has not yet been determined.

In PhCl-d_5 solution, **22a** is found to be configurationally stable at RT which is in accord with the shortened Zr-N distances found in the solid state. This more rigid ligand skeleton supports an environment that more judiciously aids the selection of enantiofaces of an incoming monomer, producing isotactic polymer. However, the dimeric evidence in the solid state is not mirrored in solution, such that dimers either do not form or their formation and dissociation is more rapid than the NMR time scale. From other C_1-symmetric precatalysts, the cations **23** and **27a** also appear to be configurationally stable at –10 °C.

For CpZA's, the cations **28c** and **28d**, from C_s-symmetric dimethyl precatalysts, were quite stable in PhCl-d_5 solution. However, the methyl cation, **28a**, derived from **15a** was quite unstable at –10 °C. Only upon preparation of **28a** in the presence of a highly coordinating Lewis base could evidence be seen that the methyl cation was even being produced.

4.5. References.

(1) Coates, G. W.; Hustad, P. D.; Reinartz, S. *Angew. Chem., Int. Ed.* **2002**, *41*, 2237.

(2) Eisch, J. J.; Piotrowski, A. M.; Brownstein, S. K.; Gabe, E. J.; Lee, F. L. *J. Am. Chem. Soc.* **1985**, *107*, 7219.

(3) Gassman, P. G.; Callstrom, M. R. *J. Am. Chem. Soc.* **1987**, *109*, 7875.

(4) Natta, G.; Pino, P.; Mazzanti, G.; Giannani, U. *J. Am. Chem. Soc.* **1957**, *79*, 2975.

(5) Jordan, R. F.; Bajgur, C. S.; Willett, R.; Scott, B. *J. Am. Chem. Soc.* **1986**, *108*, 7410.

(6) Yang, X. M.; Stern, C. L.; Marks, T. J. *Organometallics* **1991**, *10*, 840.

(7) Yang, X. M.; Stern, C. L.; Marks, T. J. *J. Am. Chem. Soc.* **1991**, *113*, 3623.

(8) Yang, X. M.; Stern, C. L.; Marks, T. J. *J. Am. Chem. Soc.* **1994**, *116*, 10015.

(9) Keaton, R. J.; Jayaratne, K. C.; Fettinger, J. C.; Sita, L. R. *J. Am. Chem. Soc.* **2000**, *122*, 12909.

(10) Hunter, W. E.; Hcnzir, D. C.; Bynum, R. V.; Penttila, R. A.; Atwood, J. L. *Organometallics* **1983**, *2*, 750.

(11) Jordan, R. F.; Bradley, P. K.; Baenziger, N. C.; LaPointe, R. E. *J. Am. Chem. Soc.* **1990**, *112*, 1289.

(12) Jones, S. B.; Peterson, J. L. *Inorg. Chem.* **1981**, *20*, 2889.

(13) Grubbs, R. H.; Coates, G. W. *Acc. Chem. Res.* **1996**, *29*, 85.

(14) Jordan, R. F.; Bradley, P. K.; Baenziger, N. C.; LaPointe, R. E. *J. Am. Chem. Soc.* **1990**, *112*, 1289.

(15) Lancaster, S. J.; Robinson, O. B.; Bochmann, M.; Coles, S. J.; Hursthouse, M. B. *Organometallics* **1995**, *14*, 2456.

(16) Bochmann, M.; Lancaster, S. J. *J. Organomet. Chem.* **1992**, *434*, C1.

(17) Chen, Y. X.; Stern, C. L.; Yang, S. T.; Marks, T. J. *J. Am. Chem. Soc.* **1996**, *118*, 12451.

(18) Bochmann, M.; Lancaster, S. J. *Angew. Chem., Int. Ed. Engl.* **1994**, *33*, 1634.

(19) Mehrkhodavandi, P.; Bonitatebus, P. J.; Schrock, R. R. *J. Am. Chem. Soc.* **2000**, *122*, 7841.

(20) Fischer, D.; Mulhaupt, R. *J. Organomet. Chem* **1991**, *417*, C7.

(21) Beck, S.; Geyer, A.; Brintzinger, H. H. *Chem. Commun.* **1999**, 2477.

(22) Beck, S.; Lieber, S.; Schaper, F.; Geyer, A.; Brintzinger, H. H. *J. Am. Chem. Soc.* **2001**, *123*, 1483.

(23) Bochmann, M.; Cuenca, T.; Hardy, D. T. *J. Organomet. Chem.* **1994**, *484*, C10.

(24) Vollmerhaus, R.; Rahim, M.; Tomaszewski, R.; Xin, S. X.; Taylor, N. J.; Collins, S. *Organometallics* **2000**, *19*, 2161.

(25) Gomez, R.; Green, M. L. H.; Haggitt, J. L. *J. Chem. Soc., Chem. Commun.* **1994**, 2607.

(26) Kissounko, D. A.; Fettinger, J. C.; Sita, L. R. *Inorg. Chim. Acta* **2003**, *345*, 121.

(27) Chen, Y. X.; Marks, T. J. *Organometallics* **1997**, *16*, 3649.

(28) Schrock, R. R.; Bonitatebus, P. J.; Schrodi, Y. *Organometallics* **2001**, *20*, 1056.

Chapter 5

Chemistry of Cationic Zirconium Initiators

5.1. Introduction.

Many side reactions occur during the Ziegler-Natta polymerization of α-olefins other than initiation, propagation, and termination, yet the only manner typically available in which to ascertain what occurs in solution is to heavily scrutinize the polymer backbone. Nonetheless, now with highly soluble initiators, greater characterization techniques, and the ability to tune the capabilities of a polymerization system, viewing intermediates present during polymerization or unexpected side reactions has become much more viable. This ability allows a greater appreciation for the observed polymer microstructures that are achieved, and generates new models that expand the utility of Ziegler-Natta systems.

Stereoblock polyolefins, like those derived from the oscillating catalyst of Waymouth (See Chapter 8.1.),[1] have been of great technological interest. One method employed for preparing such materials revolves around the use of trialkyl aluminums for polymer group transfer within binary mixtures of catalysts which have different stereoselectivities.[2,3] Bypassing the necessity of the aluminum complex as a transfer reagent, the proposition of direct polymer group exchange between zirconium cations bearing polymer chains was made by Chien and Rausch.[4] In support of this, several groups have reported methyl group exchange between Zr-Me cations and their respective dimethyl precatalysts through a dimeric methyl bridged cation.[5-8] With evidence present for Cp*ZA's to form dimeric structures, the study of exchange

reactions may further strengthen the repertoire of synthetic polymers attainable with this set of precatalysts.

Studies of the minute details of a polymerization aid in elucidation of the polymer microstructure, as evidenced from cyclic olefin polymerization with metallocenes. In early studies with cyclopentene, *rac*-EBIZrCl$_2$ / MAO systems polymerized this monomer without ring opening to yield a highly insoluble, crystalline material.[9] The microstructure assigned to this polymer was based on simple and consecutive 1,2-insertions of the monomer. Subsequent oligomerization studies by Collins proved that the initial proposition of poly(cyclopentene) as a series of 1,2-enchainments was incorrect. The oligomers Collins prepared pointed to an isotactic *cis*-1,3-enchainment of cyclopentene by the C_2-symmetric metallocene.[10-12] The same steps applied to chain end epimerization are applied to cyclopentene polymerization to explain the 1,2- to 1,3-isomerization: β-hydride elimination, olefin rotation, and 2,1-insertion into the Zr-H bond. The isomerization process must be quite facile for no spectroscopic evidence of the 1,2-inserted product has been put forward. Indeed, even with late transition metal complexes at –80 °C, the product of cyclopentene insertion with the Ni or Pd methyl cations is the 1,3-isomer.[13] In this chapter, the reaction of **6a** with cyclopentene will be discussed, wherein the product of insertion is the elusive *cis*-1,2-isomer, and warming the solution induces the isomerization to the *cis*-1,3-product.

5.2. Methyl-Methyl and Methyl-Polymeryl Group Exchange.

With the stability of Cp*ZA based initiators established in Chapter 4, determining the capacity and extent of methyl group exchange was to be performed via a series of NMR experiments.[14] This work was performed by Dr. Kumudini Jayaratne. To aid in differentiating methyl group exchange, the ^{13}C labeled derivative of **22a** was used. The

methyl group resonances for **22a** and **22e** differ in ^{1}H NMR chemical shift by ~ 0.3 ppm such that swapping of the methyl groups between the two initiators should be readily evident. To ensure that no exchange was being mediated by any residual **6a** or **6e** that was unactivated, each cation was generated in the presence of an excess of the cocatalyst, $[Ph_3C][B(C_6F_5)_4]$.

Mixing together equimolar ratios of ^{13}C-**22a** (Figure 32a) and unlabeled **22e** (Figure 32b) at –10 °C leads to facile exchange of the label between both initiators as illustrated in Scheme 31 with the ^{1}H NMR spectrum for this reaction shown in Figure32c. As seen, the Zr-$^{13}CH_3$ can be found on both **22a** and **22e**. With this process being

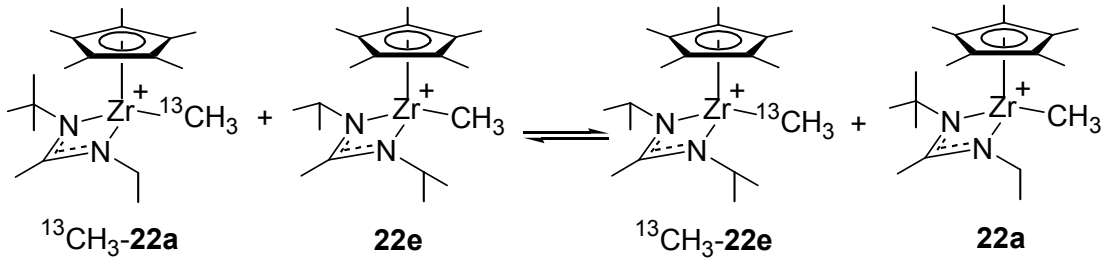

$^{13}CH_3$-**22a** **22e** $^{13}CH_3$-**22e** **22a**

Scheme 31. Methyl group exchange placing a $^{13}CH_3$ group on unlabeled **22b**.

quite facile, extrapolation of this methodology toward methyl-polymer group exchange was of interest. Towards this end, adding ~ 15 eq of 1- decene to **22e** produced the living polymeric species, LP-**22e**. Upon quantitative consumption of the monomer, 2 eq of ^{13}C-**22e** was next added, and rapid methyl polymer group exchange occurred as seen in Figure 32d. In this spectrum, two doublets are present for the ^{13}C-**22a** and the *in situ* generated ^{13}C-**22e** upon exchange which have $^{1}J_{CH}$ values of 117 and 118 Hz, respectively. This spectrum also exhibits the lack of resonances for the Zr-$^{12}CH_3$ isotopomer at the centerpoint of each doublet, pointing to clean generation of **22e** prior to monomer addition and total consumption of **22e** upon reaction with 1-decene.

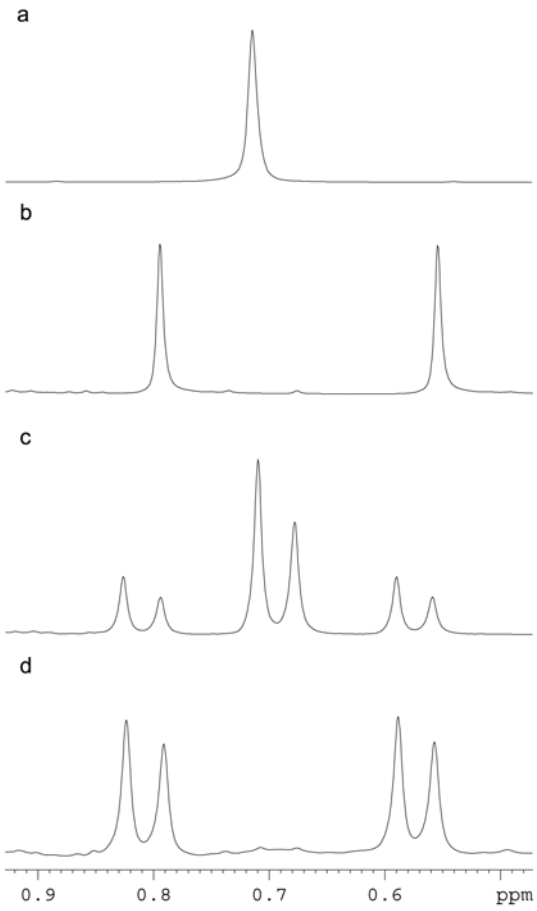

Figure 32. ^{1}H NMR spectra (500 MHz, d_5-PhCl, -10 °C) of Zr-CH_3 resonances for (a) **22e**, (b) ^{13}C-**22a**, (c) a mixture of **22e** and ^{13}C-**22a**, and (d) a mixture of LP-**22e** and 2 eq of ^{13}C-**22a.**

With evidence in place for transfer of the methyl group, it was next necessary to prove that the polymer bound to the metal gets transferred to a new metal center. In this regard, 1-^{13}C-1-decene was employed to provide a marker with which to follow through ^{13}C NMR. Addition of the labeled monomer (~ 15 eq) to **22e** and **22a** produced the living polymeric species LP-**22e** and LP-**22a** shown in Figures 33a and b, respectively. Examining the differences in the two spectra illustrates that for LP-**22e**, the chains on the metal are not stereoregular and illicit a number of resonances for the Zr bound

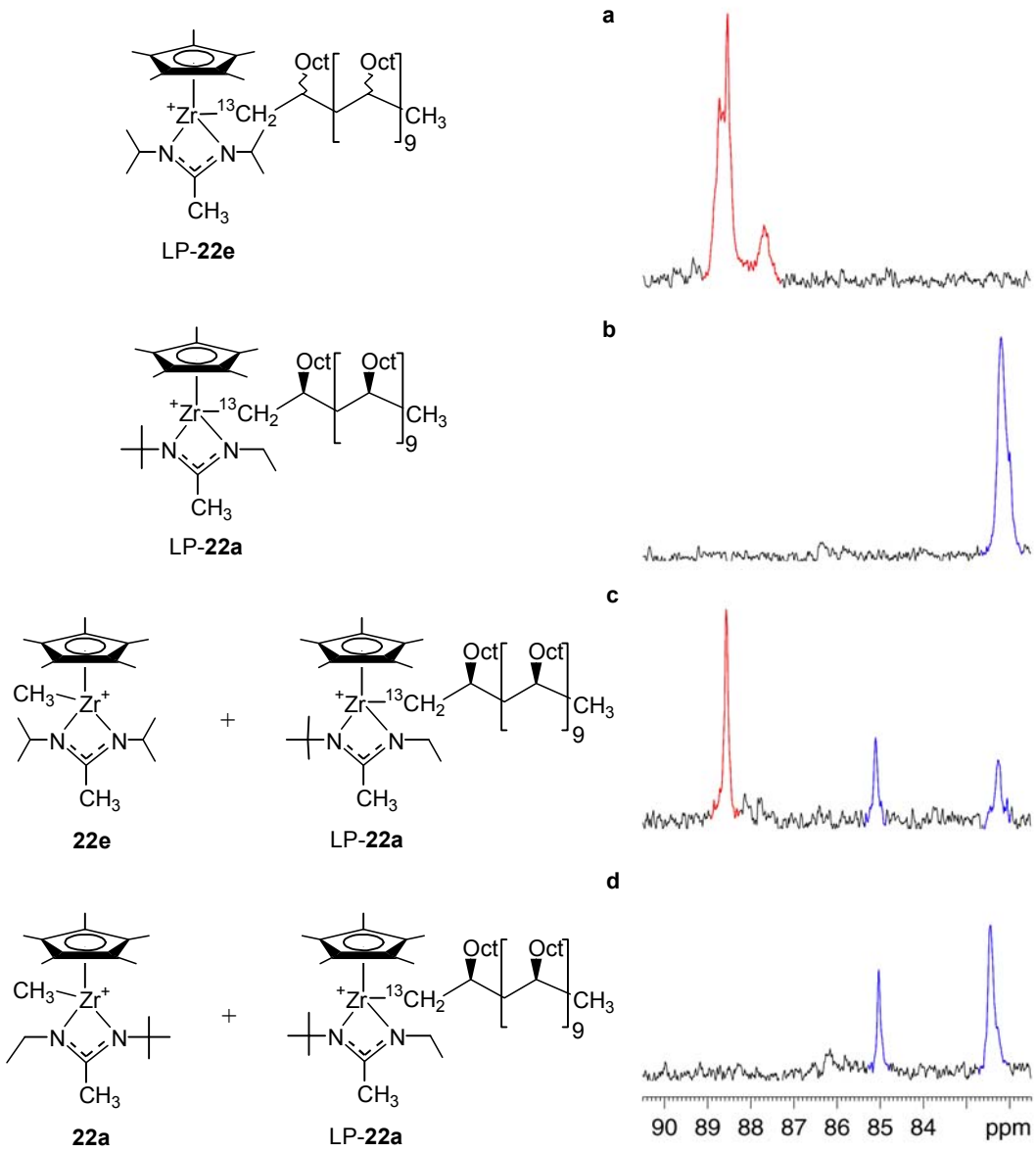

Figure 33. Partial ^{13}C NMR spectra (125 MHz, d_5-PhCl, -10 °C) of (a) LP-**22e**, (b) LP-**22a**, (c) a mixture of **22e** and LP-**22a**, and (d) a mixture of **22a** and LP-**22a**.

methylene carbon atoms. However, for LP-**22a**, a single resonance is observed which represents the enantiomeric pair of propagating species containing the highly symmetric backbone of the isotactic growing polymer that is typically produced from **22a**. With time, the latter spectrum will exhibit growth of another resonance at δ 85.0 ppm ($t_{1/2}$ = 8

hrs) that is assigned to the newly formed diastereomeric pair, presumably through amidinate ring flipping and not exchange.

Figure 33c is the spectrum obtained from exchange between equimolar amounts of LP-**22a** and **22e**. This highlights one of the most important aspects of this methodology, that a highly stereospecific polymer chain can be rapidly transferred to a nonstereoregular propagating center. Also manifest in the spectrum is the resonance for the diastereomeric pair of LP-**22a**, which can theoretically evolve from additional exchange from the two newly formed species LP-**22e** and **22a**, or from exchange between the latter and LP-**22a**. Facile exchange between LP-**22a** and **22a** to form the diastereomeric propagating species is supported by Figure 33d, in which LP-**22a** and **22a** have been mixed for 30 minutes at –10 °C.

The simple illustrations discussed above represent a new methodology for the production of stereoblock polyolefins. However, the two propagating centers in solution will not necessarily have the same activity nor the same molecular weight upon further addition of monomer, for one already has a polymer chain while the other is still the Zr-Me initiator. Also, if nonidentical ligand frameworks are used, the rates of propagation will be dramatically different producing multimodal GPC curves for the polymer so obtained. Indeed, mixtures of Cp*ZA's and CpZA's have produced bimodal and trimodal materials.[15]

5.3. Insertion of Cyclopentene.

The methyl cation **22a** polymerizes a multitude of various monomers, though they are all terminal olefins. Expanding the repertoire to include cyclic olefins was not a guaranteed success. Indeed, even RT reactions of **22a** with large excess of cyclopentene and cyclohexene provided no polymer. To gain insight into the lack of

activity for these monomers, experiments were conducted on the NMR scale to ascertain what may be happening in solution.

To a d_5-PhCl solution of **22a** at low temperature was added a slight stoichiometric excess of cyclopentene.[16] The ^{1}H NMR spectrum (Figure 34) shows complete consumption of the methyl cation and the quantitative appearance of a new series of signals attributed to a single new amidinate species that is indefinitely stable at –30 °C. Through extensive NMR analysis, this species, **30a**, was determined to be the product of *cis*-1,2-insertion of cyclopentene into the Zr-Me bond. In stark contrast, cation **23** does not decrease in intensity even after several hours at RT in the presence of excess cyclopentene. All hydrogen atoms for **30a** have been located though a 2D ^{1}H-^{1}H COSY NMR experiment. Several 1D nOe ^{1}H NMR and 2D ^{1}H-^{1}H NOESY experiments were performed to ascertain the structure of this elusive insertion product in

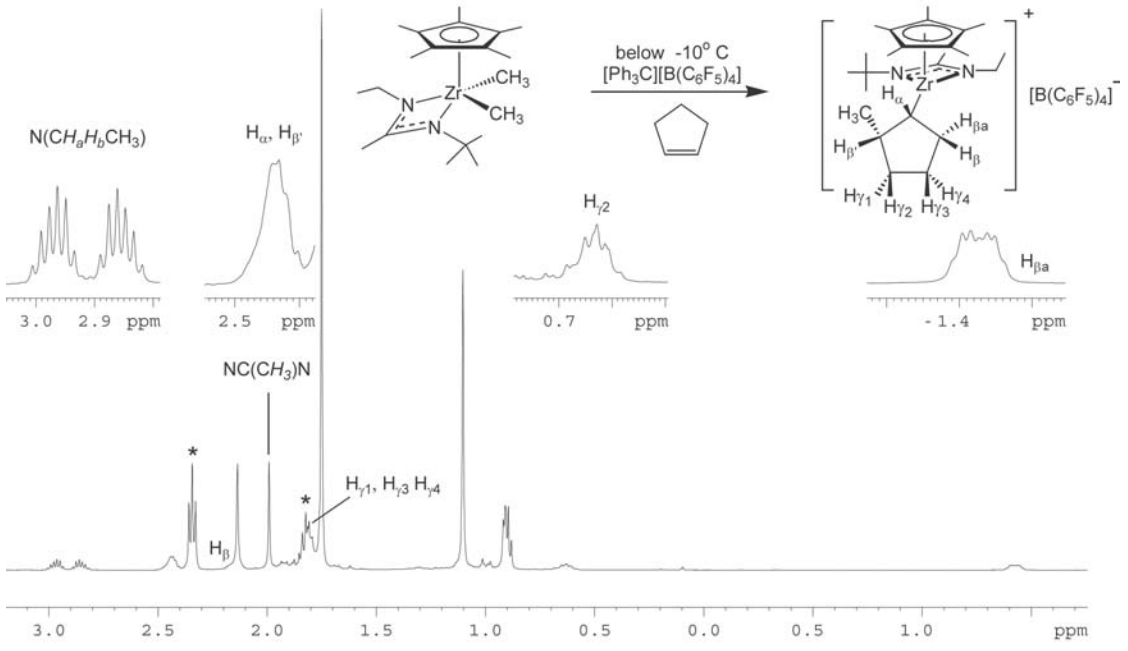

Figure 34. ^{1}H NMR spectrum (500 MHz, d_5-PhCl, -30 °C) of the *cis*-1,2-insertion product of cyclopentene insertion, **30a**. The asterisk (*) denotes excess cyclopentene.

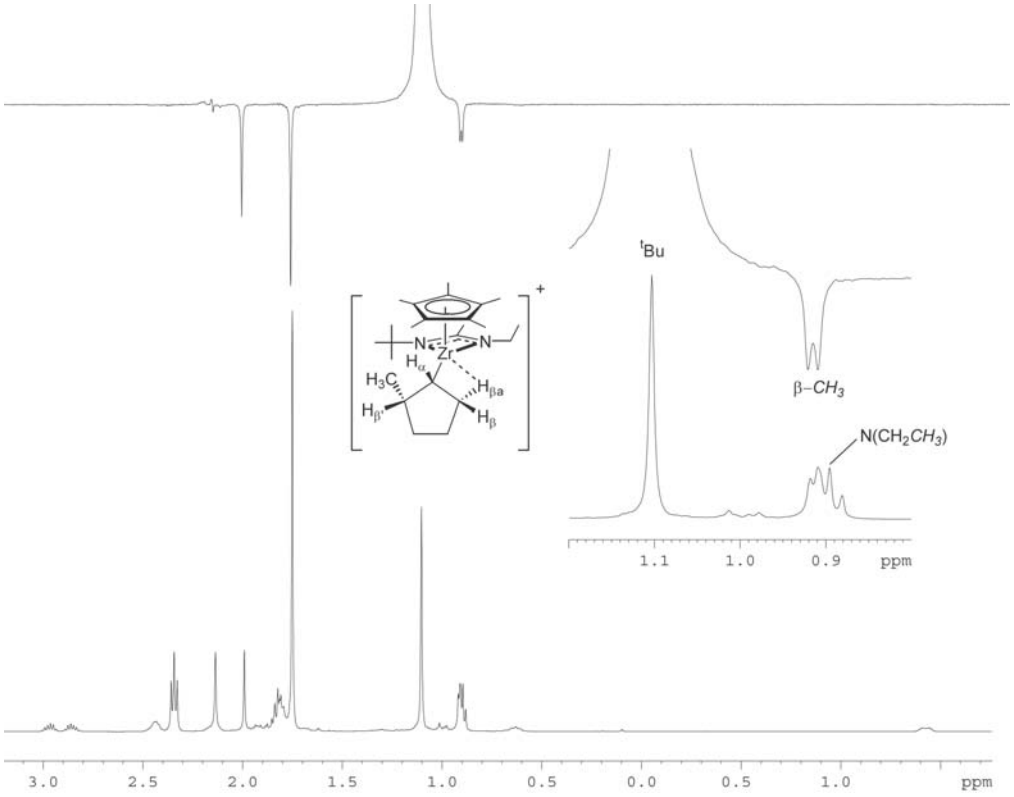

Figure 35. 1D nOe ^{1}H NMR experiment (500MHz, d_5-PhCl, -30 °C) for the cis-1,2-insertion product of cyclopentene upon irradiation of the N^{t}Bu group.

solution. Reproduced in Figure 35 is one such spectrum, in which the singlet of the ^{t}Bu group of the amidinate has nOe effects with the acetamidinate CH_3, the Cp* ligand, and most notably, the doublet assigned to the β-CH_3 group of the five-membered ring. This spatial relationship suggests that the cyclopentene monomer binds to the metal closer to the Et side of the amidinate moiety, forcing the Me group closer to the ^{t}Bu group. It should be pointed out here that this insertion occurs on the opposite side as that supported from the solid state structure of **22-**(Et_2O), in which the Et_2O molecule was bound to the metal on the N^{t}Bu side of the amidinate. One of the β-hydrogens of the ring is engaged in a strong agostic interaction, providing the hydrogen with an upfield ^{1}H NMR chemical shift (δ -1.4 ppm) and a low carbon-hydrogen coupling constant ($^1J_{CH}$ =

87.7 Hz). Along with this result, the geminal partner of this agostic hydrogen has a heightened $^1J_{CH}$ of 146.2 Hz. This is not uncommon within agostic interactions, for one low and one high set of coupling constants associated with geminal hydrogens to exist.[17,18] Also notably larger than the average coupling of an sp^3 carbon atom is the value found for the single hydrogen of the methine carbon bound to Zr, which was 141.3 Hz.

As seen earlier for **22a**, the amidinate ligand within this cationic species appears to be quite static; that is to say, amidinate ring flipping appears to be frozen out. While a gain in electron density on the metal should facilitate this process, the observed effect in **30a** may be related to the strength of the β-hydrogen agostic interaction which may impose a preferred orientation of the amidinate fragment. In fact, warming the solution does not significantly affect the line shape of any of the resonances in the ^{1}H NMR spectrum. What does occur, however, is the steady disappearance of these signals at the expense of the growth of a single new set. Quantitative conversion of the *cis*-1,2-product leads to the formation of the *cis*-1,3-isomerization product, **30b**, in a clean, first order process. The ^{1}H NMR spectrum for this cationic complex is displayed in Figure 36. Of great import, a slightly upfield shifted resonance still appears at δ -1.5 ppm, shifted slightly compared to that of **30a**. This hydrogen, $H_{\beta a}$, is agostically interacting with the Zr metal, exhibiting a decreased coupling constant of $^1J_{CH}$ = 97.5 Hz. In this structure, a second agostic hydrogen atom, $H_{\beta' a}$, also can be identified at δ 0.6 ppm with a slightly larger $^1J_{CH}$ value of 107.2 Hz. By way of 1D nOe ^{1}H NMR spectra, shown in Figure 37, the solution structure of the 1,3-product can be determined. Interestingly, the stronger agostic hydrogen, $H_{\beta a}$, is located on the more sterically accessible portion of the metal center, that being closest to the NEt fragment of the amidinate. The weaker agostic hydrogen, $H_{\beta' a}$, is in close proximity to the N^{t}Bu group as well as the γ-CH_3. The

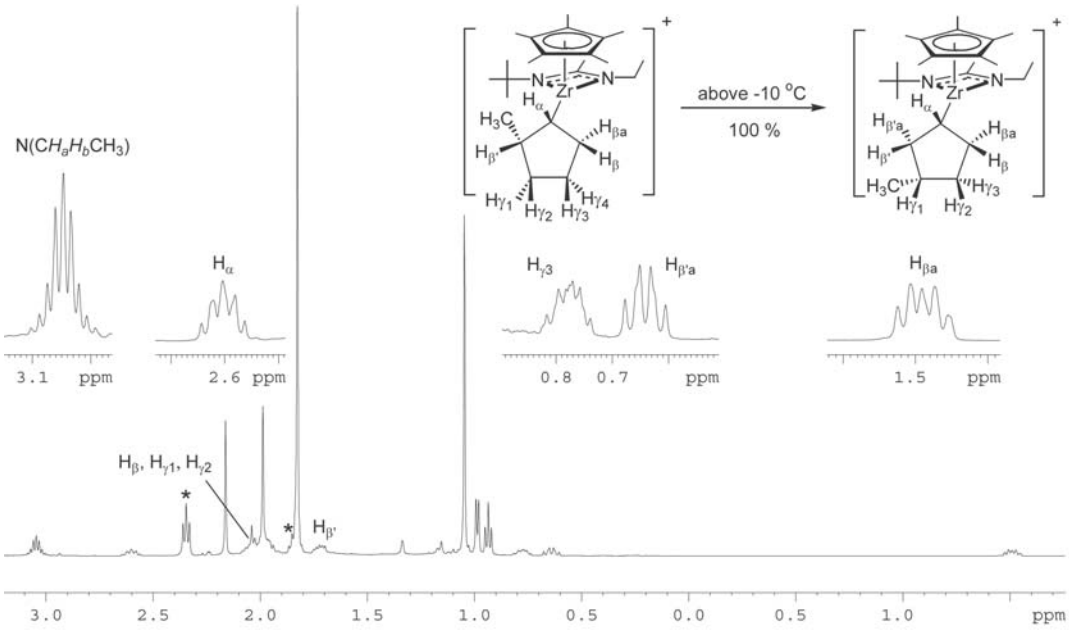

Figure 36. ^{1}H NMR spectrum (500 MHz, d_5-PhCl, -30 °C) of the *cis*-1,3-insertion product of cyclopentene insertion, **30b**. The asterisk (*) denotes excess cyclopentene.

differences in the strength of the two agostic interactions might be caused by steric concerns since the weaker agostic appears on the N^{t}Bu side. A complimentary effect from the dual agostic interactions is the striking increase in the $^{1}J_{CH}$ value for the hydrogen of the methine carbon bound to Zr bearing a value of 160.8 Hz. The above factors are worthy of mentioning again: 1) a transformation from a single agostic to a double agostic cationic complex, 2) a dramatic increase in the $^{1}J_{CH}$ value for H_{α}.

In theoretical studies on the isomerization of cationic Zr-alkyl species, two groups have discussed the migration of the Zr center between adjacent carbon atoms in terms of the classical β-hydride elimination / reinsertion route that produces chain-end epimerization in PP.[19,20] Through their calculations, along the epimerization pathway redrawn in Scheme 32, both agree that the rate determining step is the β-hydride elimination from the β-agostic resting state. Subsequent olefin rotation and 2,1-insertion

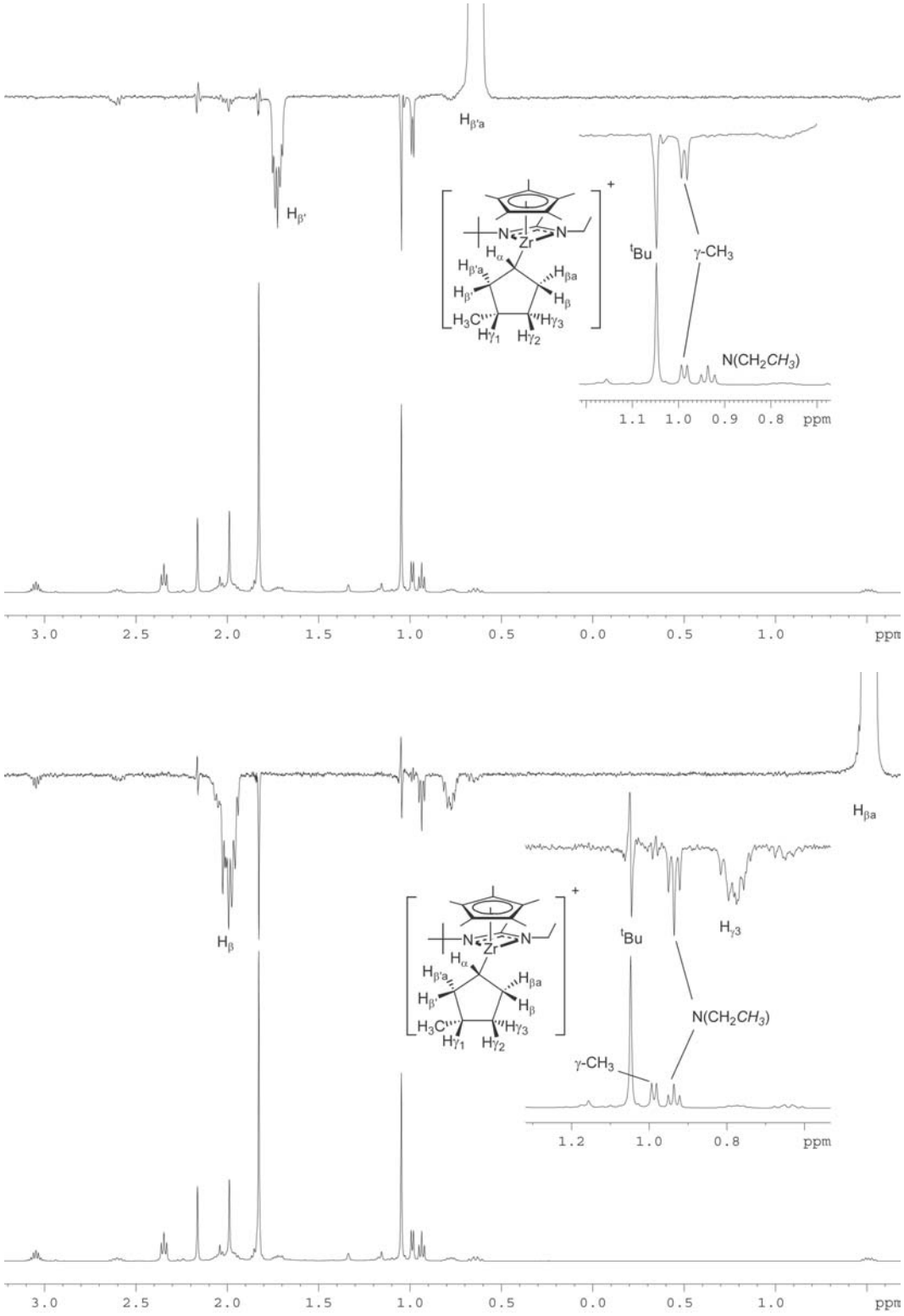

Figure 37. 1D nOe ^{1}H NMR spectra (500MHz, d_5-PhCl, -30 °C) for the cis-1,3-insertion product of cyclopentene, **30b**, upon irradiation of (top) $H_{\beta'a}$ and (bottom) $H_{\beta a}$.

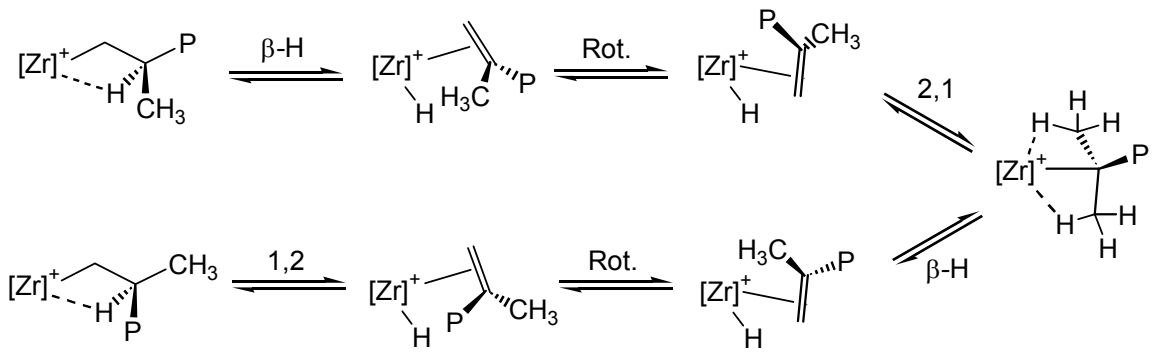

Scheme 32. Epimerization from the β-agostic resting state has an intermediate Zr-^{t}Bu cation that features two β-agostic interactions.

into the Zr-H bond would lead to the Zr-^{t}Bu cation. The ^{t}Bu complex is quite intriguing because it is believed to contain an agostic interaction with two of the methyl groups. Compared to other steps along the reaction sequence, this species is calculated to be only ca. 1.6[20] and 2.1[19] kcal / mol higher in energy than the β-agostic resting state. Prosenc and Brintzinger found that with two agostic methyl groups directed toward the metal center, the third is pointed out so as to remove any destabilizing steric effects, and this provides the α-C with a more planar environment ($\Sigma\theta_c$ = 358 °).[19] This suggests a carbon atom that is very sp^2-like, with hybridization similar to a ^{t}Bu cation, in which the $^1J_{CH}$ would be expected to be higher than that for an sp^3-hybridized center.

With precedent for this isomerization finding roots similar to chain-end epimerization, exploring the mechanism was accomplished through the preparation of cyclopentene-1,2-d_2. Depending on the path taken to reach **30b**, it would be expected that two stereochemical outcomes are possible, where either the D label becomes the agostic $H_{\beta'a}$ or its geminal partner, $H_{\beta'}$ (Scheme 33). When cyclopentene-1,2-d_2 was added to **6a** and the solution was warmed, the ^{1}H NMR spectrum of the isomerization product showed a doublet for the resonance of $H_{\beta'a}$ (Figure 38). This directly shows that

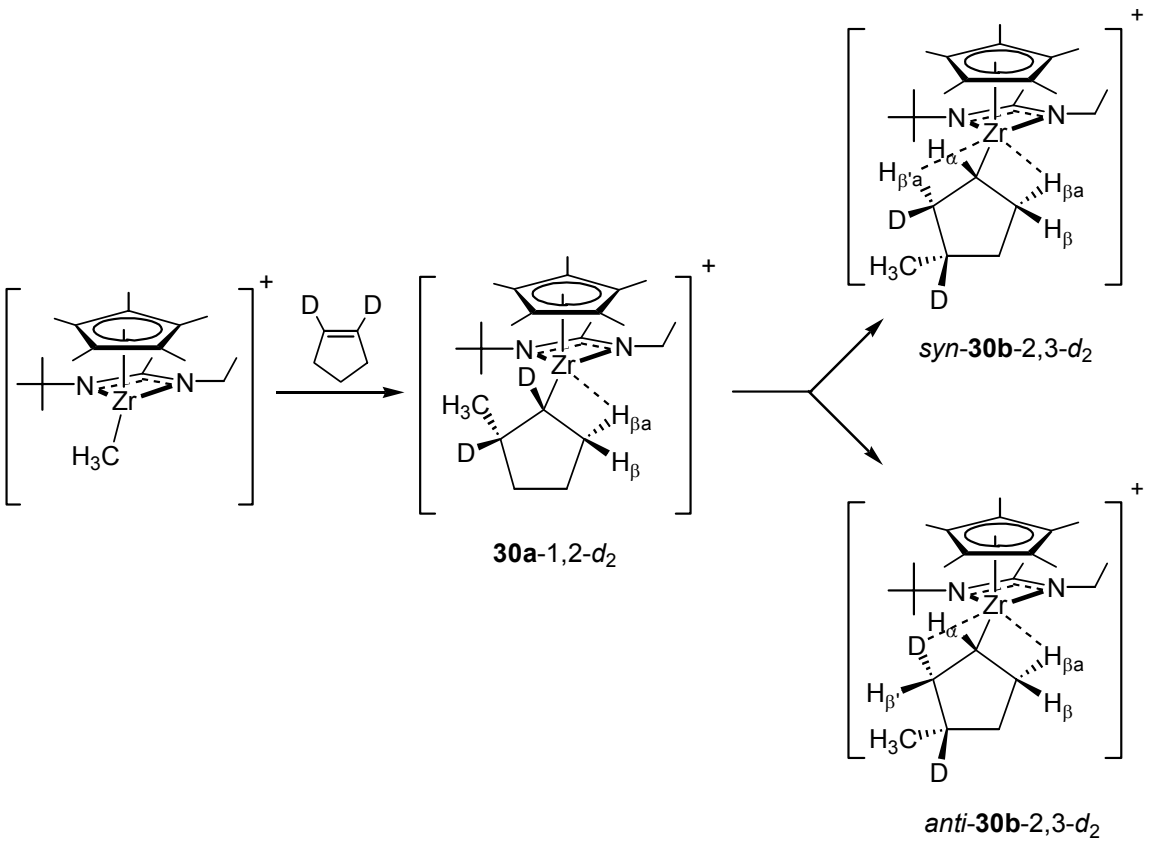

Scheme 33. Potential products from isomerization of **30a**-1,2-d_2 to form **30b**-2,3-d_2.

the lone agostic hydrogen, $H_{\beta a}$, in **30a** becomes the weaker agostic hydrogen, $H_{\beta' a}$, in **30b**. Overall, this represents a *syn*-1,2-hydrogen shift on the same side of the Zr center. Performing an Eyring analysis supplied the following activation parameters: $\Delta H^{\ddagger}$ = 21.8 (5) kcal / mol and $\Delta S^{\ddagger}$ = 8.1 (5) eu. For a mechanism in which the rate determining step is believed to be β-hydride elimination from a β-agostic resting state, it is surprising that for the isomerization of **30a** to **30b**, which is already in a prearranged position for elimination, a positive $\Delta S^{\ddagger}$ and a high enthalpic barrier are obtained.[21] With the stabilizing effect of the agostic interaction of **30a** lowering the energetics of the ground state relative to the transition state, a larger enthalpic term could be expected. The value of $\Delta S^{\ddagger}$ may be enhanced by solvent reorganization or the strength of the cation-

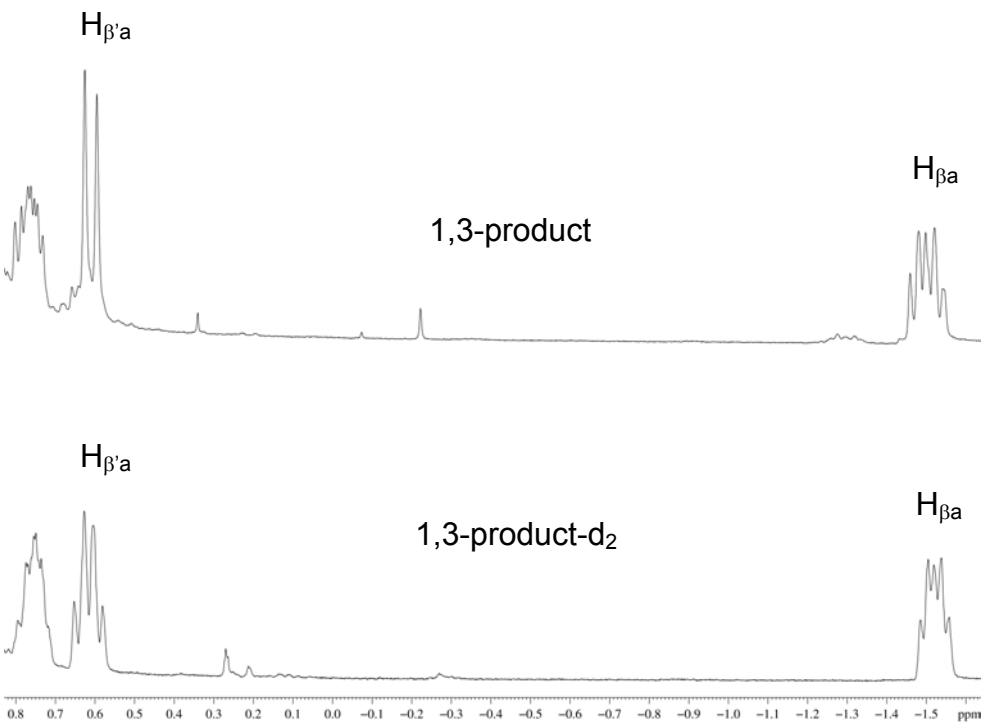

Figure 38. Partial ^{1}H NMR spectra (500 MHz, d_5-PhCl, -10 °C) of **30b** from (top) cyclopentene-1,2-d_2 and (bottom) cyclopentene.

anion interaction. Finally, it should be noted that two concerted mechanisms have been proposed for the isomerization. The first, with a transition state energy 12.8 kcal / mol above the β-agostic resting state, incorporates simultaneous breaking of the C_β-H_β bond and alkene rotation.[22] The second involves a protonated zirconocene olefin complex, where the mobile H^+ is embedded in the electron cloud of the alkene.[19] With an energy barrier of 31 kcal / mol, this mechanism seems quite unlikely when compared to the lower energy transformations associated with the traditional route of β-hydride elimination, olefin rotation, and 2,1-insertion.

5.4. Insertion of Additional Monomers.

Structurally similar to cyclopentene, cis-2-butene can also insert into **22a** to form the secondary product **31** (Scheme 34). As with **30a**, the product appears to be from cis-1,2-insertion, as opposed to rapid isomerization to the 1,3-product, which in this case would be expected to be favored due to a reduction in steric hindrance from the presence of the metal on a primary carbon atom. For **30a** and **30b**, the hydrogens that were agostically interacting with the metal featured chemical shifts that were well upfield from the remaining resonances. This also appears to be the case for **31**, with a doublet appearing δ 0.02 ppm representing the β-CH_3 group (Figure 39). If the agostic interaction is present, it is rapidly exchanging between the three hydrogens and thus washes out any evidence that may be extracted from the $^1J_{CH}$ for this signal, which appears as 122 Hz. This may be the case, since 1D nOe ^{1}H NMR spectra prove a close proximity between this doublet and the triplet of the NEt group. The methine bound to Zr exhibits a $^1J_{CH}$ coupling that is 150 Hz, quite similar to that seen from cyclopentene insertion. Opposed to cyclopentene insertion however, which occurs rapidly, cis-2-butene insertion is rather sluggish, with the resonance for the methyl group in **22a** disappearing only after 4 hours. Also, **31** is not formed cleanly for it appears to be very thermally sensitive, even at –30 °C, with decomposition to form **25** competing with its formation. Importantly, **22a** does not insert trans-2-butene even at RT.

One final insertion event that needs mentioning is the reaction between **22a** and styrene. The ^{1}H NMR spectrum for this insertion in shown in Figure 40. Although not as extensively studied as other insertion products, this species has several interesting facets. The styrene insertion product, **32**, is not the simple product of 1,2-insertion. In fact, it is the product of a secondary insertion, forming a Zr-benzyl like complex as shown in Scheme 35. Many groups have studied cationic benzyl complexes through

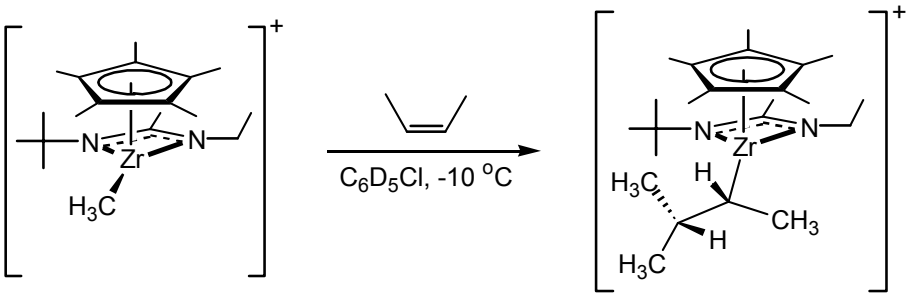

Scheme 34. Insertion of cis-2-butene into **22a** to form the secondary center on Zr.

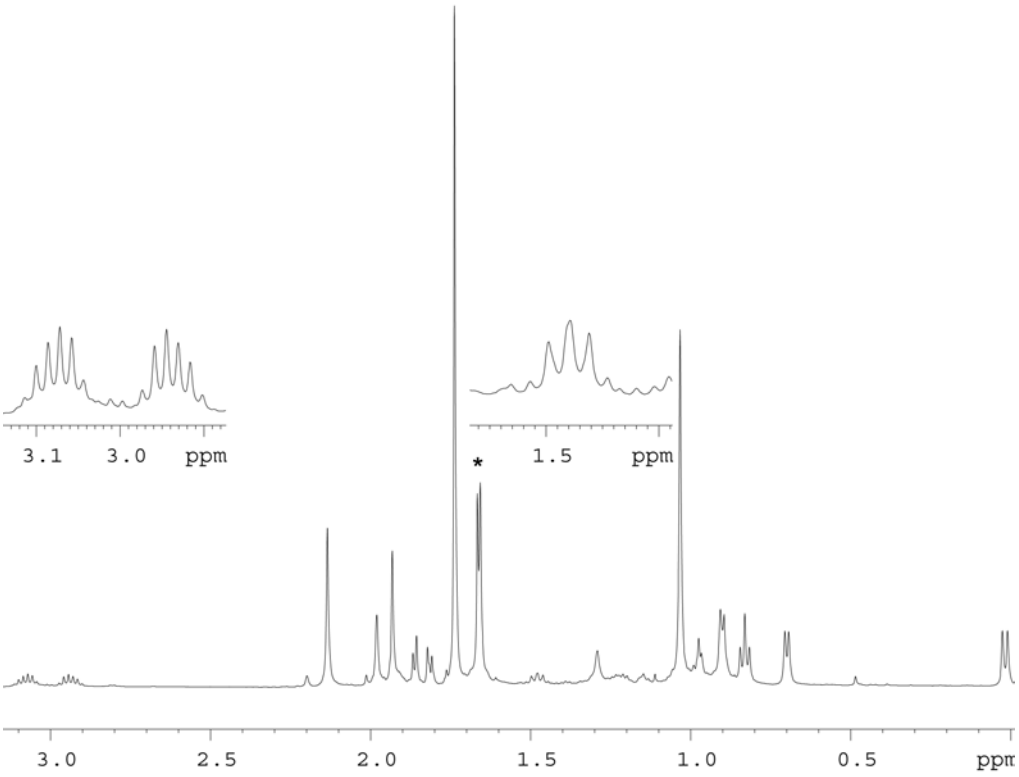

Figure 39. ^{1}H NMR spectrum (500 MHz, d_5-PhCl, -30 °C) for insertion product **31**. The asterisk (*) denotes excess cis-2-butene.

activation of metal dibenzyl complexes. In these studies, the benzyl ligand appears to be additionally stabilizing the metal center by coordinating in several potential fashions.[23-25] However, these coordination modes produce resonances for the ring H's that are shifted upfield, as far as 4.5 ppm for the ortho hydrogen.[26] In favor of similar

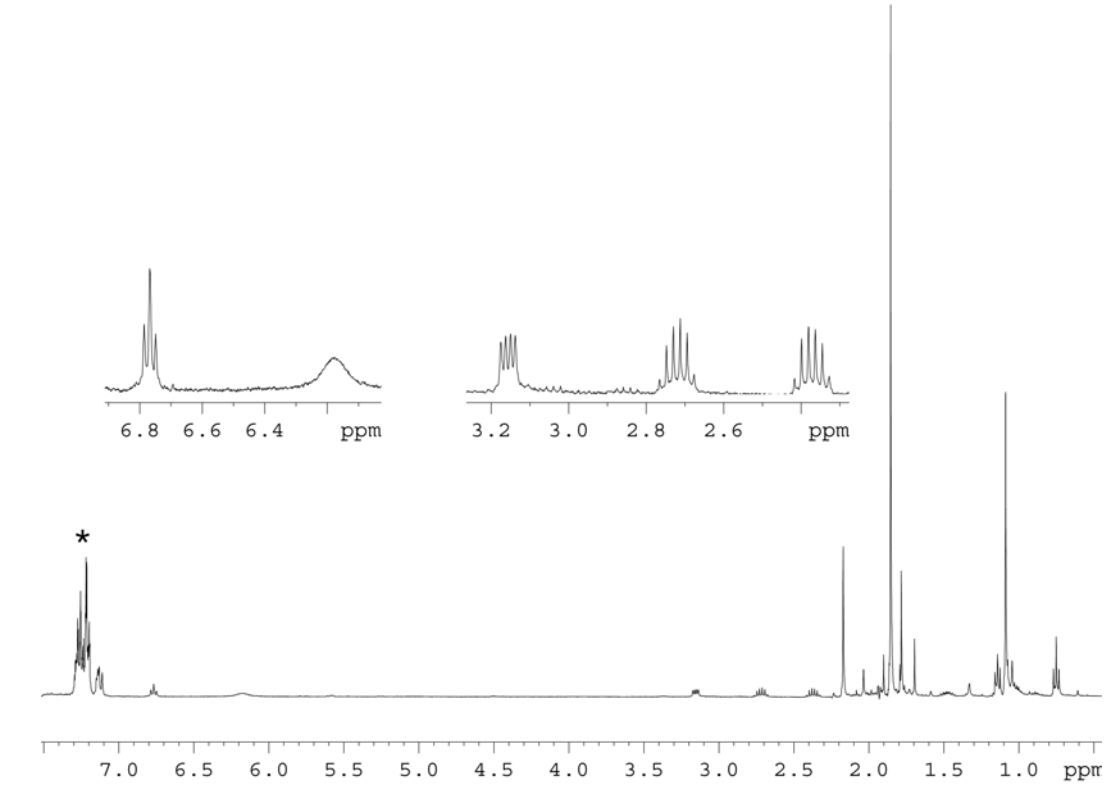

Figure 40. ^{1}H NMR spectrum (400 MHz, d_5-PhCl, RT) of styrene insertion complex **32**. The asterisk denotes signals for Ph_3CCH_3, solvent, and styrene.

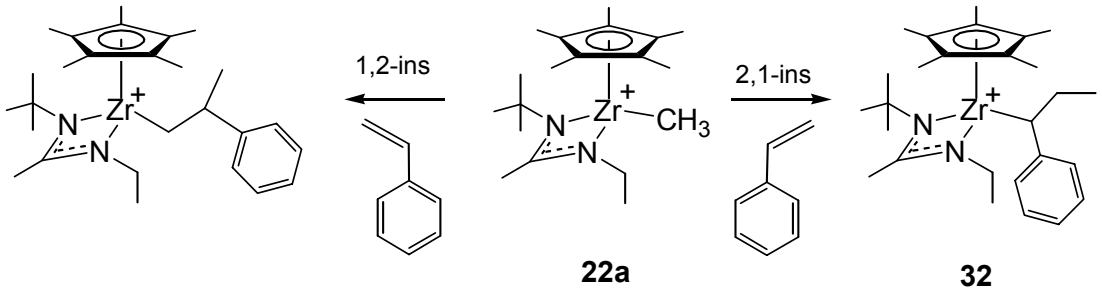

Scheme 35. Production of benzyl product **32** from 2,1-styrene insertion.

features herein, **32** contains a clean triplet at δ 6.8 and a broad resonance centered at δ 6.2 ppm that integrate to 1 and 2 H's, respectively. This interaction must be relatively strong, considering that the interaction persists even at RT.

5.5. Conclusions.

The methyl cation, **22a**, is quite dynamic, undergoing facile methyl group exchange through a dimeric dication formed with **22d**. Added to this, methyl-polymer group exchange occurs between a methyl cation and a cationic metal center with a living polymer chain. This aspect has the potential to be utilized toward the production of stereoblock polyolefins through transfer of, for instance, a stereoregular polymer chain to a non-stereospecific propagating metal center.

Insertion of cyclopentene into the Zr-Me bond of **22a** is also quite facile, and produces the cis-1,2-insertion product **30a**. This species has never before been characterized in solution, though it is thought to be the first product in metallocene and late transition metal cyclopentene polymerization from which only the 1,3-product is identified in the homopolymer chains. This species sports a strong β-hydrogen agostic interaction from a methylene group which resides on the side of the complex closest to the NEt portion of the amidinate ligand. Upon warming above –10 °C, quantitative isomerization occurs to generate the cis-1,3-product **30b** which remarkably contains two agostic interactions. The stronger of the two is located, as with **30a**, closer to the ethyl group of the amidinate. Through utilization of cyclopentene-d_2-1,2, the agostic β-hydrogen in **30a** was found to become the weaker of the two agostic hydrogens in **30b**. This is consistent with the β-hydride elimination / reinsertion scheme prevalent during chain-end epimerization during propylene polymerization. However, the thermodynamic parameters for this isomerization are not in agreement, since a positive entropic term is found, which would not be expected from a situation where β-hydride elimination is the rate determining step.

The cation **22a** can also insert styrene and cis-2-butene, with the product from the latter appearing to be quite unstable. Although the possibility exists for each

insertion product to yield a methylene bound to Zr, which would lessen any steric contacts, both generate secondary carbon centers bound to Zr, perhaps indicating that the advantageous stabilizing interactions through agostic interactions or multihapto bonding modes override steric effects

5.6. References.

(1) Coates, G. W.; Waymouth, R. M. *Science* **1995**, *267*, 217.

(2) Chien, J. C. W.; Iwamoto, Y.; Rausch, M. D.; Wedler, W.; Winter, H. H. *Macromolecules* **1997**, *30*, 3447.

(3) Lieber, S.; Brintzinger, H. H. *Macromolecules* **2000**, *33*, 9192.

(4) Song, W.; Yu, Z.; Chien, J. C. W. *J. Organomet. Chem.* **1996**, *512*, 131-140.

(5) Li, Y. F.; Ward, D. G.; Reddy, S. S.; Collins, S. *Macromolecules* **1997**, *30*, 1875.

(6) Bochmann, M.; Lancaster, S. J. *Angew. Chem., Int. Ed. Engl.* **1994**, *33*, 1634.

(7) Mehrkhodavandi, P.; Bonitatebus, P. J.; Schrock, R. R. *J. Am. Chem. Soc.* **2000**, *122*, 7841.

(8) Vollmerhaus, R.; Rahim, M.; Tomaszewski, R.; Xin, S.; Taylor, N. J.; Collins, S. *Macromolecules* **2000**, *19*, 2161.

(9) Kaminsky, W.; Spiehl, R. *Makromol. Chim.* **1989**, *190*, 515.

(10) Collins, S.; Kelly, W. M. *Macromolecules* **1992**, *25*, 233.

(11) Kelly, W. M.; Taylor, N. J.; Collins, S. *Macromolecules* **1994**, *27*, 4477.

(12) Kelly, W. M.; Wang, S. T.; Collins, S. *Macromolecules* **1997**, *30*, 3151.

(13) McLain, S. J.; Feldman, J.; McCord, E. F.; Gardner, K. H.; Teasley, M. F.; Coughlin, E. B.; Sweetman, B. J.; Johnson, L. K.; Brookhart, M. *Macromolecules* **1998**, *31*, 6705.

(14) Jayaratne, K. C.; Sita, L. R. *J. Am. Chem. Soc.* **2001**, *123*, 10754.

(15) Sita, L. R.; Keaton, R. J.; Jayaratne, K. C. In *PCT Int. Appl.*; (University of Maryland, College Park, USA). Wo, 2003, p 34.

(16) Keaton, R. J.; Sita, L. R. *J. Am. Chem. Soc.* **2002**, *124*, 9070.

(17) Jordan, R. F.; Bradley, P. K.; Baenziger, N. C.; LaPointe, R. E. *J. Am. Chem. Soc.* **1990**, *112*, 1289.

(18) Lessage, A.; Emsley, L.; Chabanas, M.; Coperet, C.; Basset, J. M. *Angew. Chem., Int. Ed. Engl.* **2002**, *41*, 4535.

(19) Prosenc, M. H.; Brintzinger, H. H. *Organometallics* **1997**, *16*, 3889.

(20) Lohrenz, J. C. W.; Buhl, M.; Weber, M.; Thiel, W. *J. Organomet. Chem.* **1999**, *592*, 11.

(21) Burger, B. J.; Thompson, M. E.; Cotter, W. D.; Bercaw, J. E. *J. Am. Chem. Soc.* **1990**, *112*, 1566.

(22) Deng, L. Q.; Margl, P.; Ziegler, T. *J. Am. Chem. Soc.* **1997**, *119*, 1094.

(23) Bochmann, M.; Lancaster, S. J.; Hursthouse, M. B.; Malik, K. M. A. *Organometallics* **1994**, *13*, 2235.

(24) Horton, A. D.; de With, J.; van der Linden, A. J.; van de Weg, H. *Organometallics* **1996**, *15*, 2672.

(25) Horton, A. D.; de With, J. *Organometallics* **1997**, *16*, 5424.

(26) Pellecchia, C.; Immirzi, A.; Pappalardo, D.; Peluso, A. *Organometallics* **1994**, *13*, 3773.

Chapter 6

Neutral and Cationic Zirconium-Alkyl Complexes

6.1. Introduction.

The development of Group IV catalyst systems of continually greater activity towards the Ziegler-Natta polymerization of α-olefins has grown by leaps and bounds in recent years.[1] Equally long strides have been made in similar systems for the polymerization of prochiral olefins (e.g. propylene) in a stereoselective or stereospecific manner.[2] With the advent of transition metal alkyl cations that are capable of performing polymerizations devoid of irreversible termination processes (i.e. β-H or β-Me elimination), understanding these polymerizations and devising methods to link them to the first two developments will produce an initiator featuring three optimal characteristics: high activity, stereospecificity, and livingness. In terms of the latter, the scarcity of detailed solution information on structural characteristics of the living propagating species has hindered their elucidation and prevents further progression for other systems.

Typically, precatalysts to these cationic initiators involve dimethyl or dibenzyl metal complexes which are quite stable, having no, or no easily removable, β-substituents. Zirconium dialkyl complexes bearing β-hydrogens have previously been shown to be thermally unstable, as well as those for mixed alkyl systems.[3-6] However, these longer chain alkyl substituents, upon activation, would prove more useful as models for metal bound living polymer chains, as opposed to models based on methyl groups mimicking polymer chains.

Herein, a discussion of the preparation and characterization of a variety of alkyl Cp*ZA's is presented. These compounds are quite stable in solution and have proven to be crystalline, allowing several to be structurally characterized by single crystal X-ray analysis. Upon generation of the Zr-alkyl cations at –10 °C, and with the benefit of their ability to ward off β-H and β-Me elimination, a multitude of NMR techniques were employed to probe the solution structural features of this class of compounds. Strong β-hydrogen agostic interactions are evident from these analyses, and further supported through X-ray crystallography. From these experiments, a rather contradictory result is established, that a larger barrier to β-hydride elimination can be achieved for those complexes that can beneficially engage in strong β-hydrogen agostic interactions between the cationic metal center and the alkyl chain.

6.2. Monoalkyl monochloro Cp*ZA's.

6.2.1. Synthesis. Previously, dialkyl versions of the Cp*ZA ligand set, in particular for dimethyl derivatives, were prepared from carbodiimide insertion into the Zr-Me bond of (η^5-C_5Me_5)$ZrMe_3$.[7] The first step towards preparing mixed alkyl systems was to synthesize the Zr(alkyl)(Cl) species through alkylation of the starting dichloride, **8**. This compound is a yellow crystalline solid which is quite thermally stable. In the ^{1}H NMR spectrum of **8**, the methylene of the amidinate ethyl group shows up as a broad quartet at δ 3.05 ppm, providing evidence that amidinate ring-flipping, the dynamic process that equilibrates these two hydrogens, is perhaps less facile than in **6**.

To –78 °C Et_2O mixtures of **8**, one equivalent of the appropriate alkyl Grignard or alkyl lithium reagent was added, and upon warming to RT, produced yellow solutions from which the alkyl/chloro species, (η^5-C_5Me_5)Zr(R)(Cl)[R^1NC(Me)NR^3], were isolated in good yields.[8,9] Scheme 36 shows the various long chain alkyl groups employed. With

the larger alkyl groups (^{t}Bu and neopentyl), alkyl lithium reagents could be employed for preparation of **33** from **8** since double alkylation was found not to occur. This was not the case for smaller R groups, and Grignard reagents, even in excess, were found only to alkylate once.

The reaction is rather rapid, with **33a** being produced after only 1 hr at –78 °C. Interestingly, Zr-^{t}Bu derivatives are known to be to be rather sensitive and difficult to prepare. While $Cp_2Hf(^tBu)(Cl)$ has been shown to be moderately stable in solution and in the solid state,[10] most typically these groups will rearrange to form Zr-^{i}Bu analogues.[11] From the starting material **8**, unidentified products are obtained with the use of ^{t}BuMgCl, and while utilizing ^{t}BuLi, low temperatures were crucial as with **33a**. At –78 °C, quenching the reaction with $(CH_3)_3SiCl$ after 40 minutes or less and removing the volatiles surprisingly provided the Zr(^{i}Bu)(Cl) derivative, **33e**. However, longer reaction times (e.g. 90 minutes) and immediate filtering of the LiCl after ether removal afforded **33g** nearly devoid of **33e**.

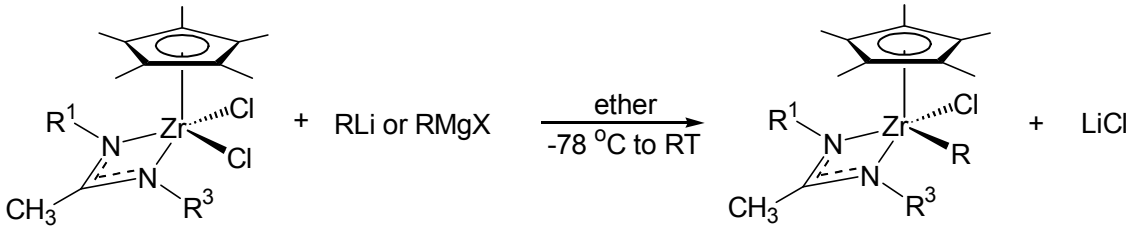

8

For $R^1 = {}^tBu$, R^3 = Et
R = Et (**33a**); ^{n}Pr (**33b**); ^{i}Pr (**33c**); ^{n}Bu (**33d**); ^{i}Bu (**33e**); ^{s}Bu (**33f**); ^{t}Bu (**33g**); neopentyl (**33h**)

For $R^1 = R^3$ = Cy
R = ^{t}Bu (**34**)

For $R^1 = R^3 = {}^iPr$
R = neopentyl (**35**)

Scheme 36. Preparation of a series of alkyl/chloro Cp*ZA complexes.

6.2.2. Characterization. For all compounds **33a**-**h**, the methylene H's of the amidinate ethyl group are inequivalent, exhibiting separate chemical shifts for the two doublets of quartets. In turn, for all monoalkyl species **33** and **35** in which a methylene group is directly bound to Zr (excluding **33c**, **33f**, and **33g**), it is interesting to note that in the ^{1}H NMR spectrum of each, these hydrogens are in fact diastereotopic, showing up as distinctly separate resonances. A low temperature ^{1}H NMR experiment in d_8-toluene using **33e** displayed minor temperature dependent chemical shift changes and very slight broadening at extremely low temperatures attributable to the viscosity of the solvent. Also, 2D ^{1}H-^{1}H EXSY NMR experiments equally did not show evidence for exchange between the diastereotopic methylene hydrogen atoms of the amidinate NEt group for any compound of **33**, nor for the two diastereomers of **33f**. It appears then that amidinate ring-flipping may be hindered for this series of compounds due to the presence of the bulkier alkyl group.

The ^{1}H NMR spectra for **33a-h** are quite straightforward, but with a few notable findings. The short chain ethyl / chloro derivative, **33a** (Figure 41), displays two upfield shifted resonances for the two Zr-bound methylene hydrogens with geminal and vicinal couplings of 13.2 Hz and 7.6 Hz, respectively. The CH_3 of this group appears further downfield at δ 1.56 ppm with a similar line shape and peak intensity to that of the amidinate ethyl CH_3. Related to this, the isopropyl group of **33c** shows a similar proclivity, with the foot methine hydrogen appearing well upfield at δ -0.20 ppm and it's two methyl groups being inequivalent doublets at δ 1.41 and 1.62 ppm (Figure 41).

Owing to their stability, high quality single crystals could be obtained for several analogues of **33**, as well as **34** and **35**. A neutral ethyl complex of Ti has previously been shown to have a β-agostic hydrogen interaction in the solid state.[12,13] As representative examples, the solid state structures of three of the four members of the

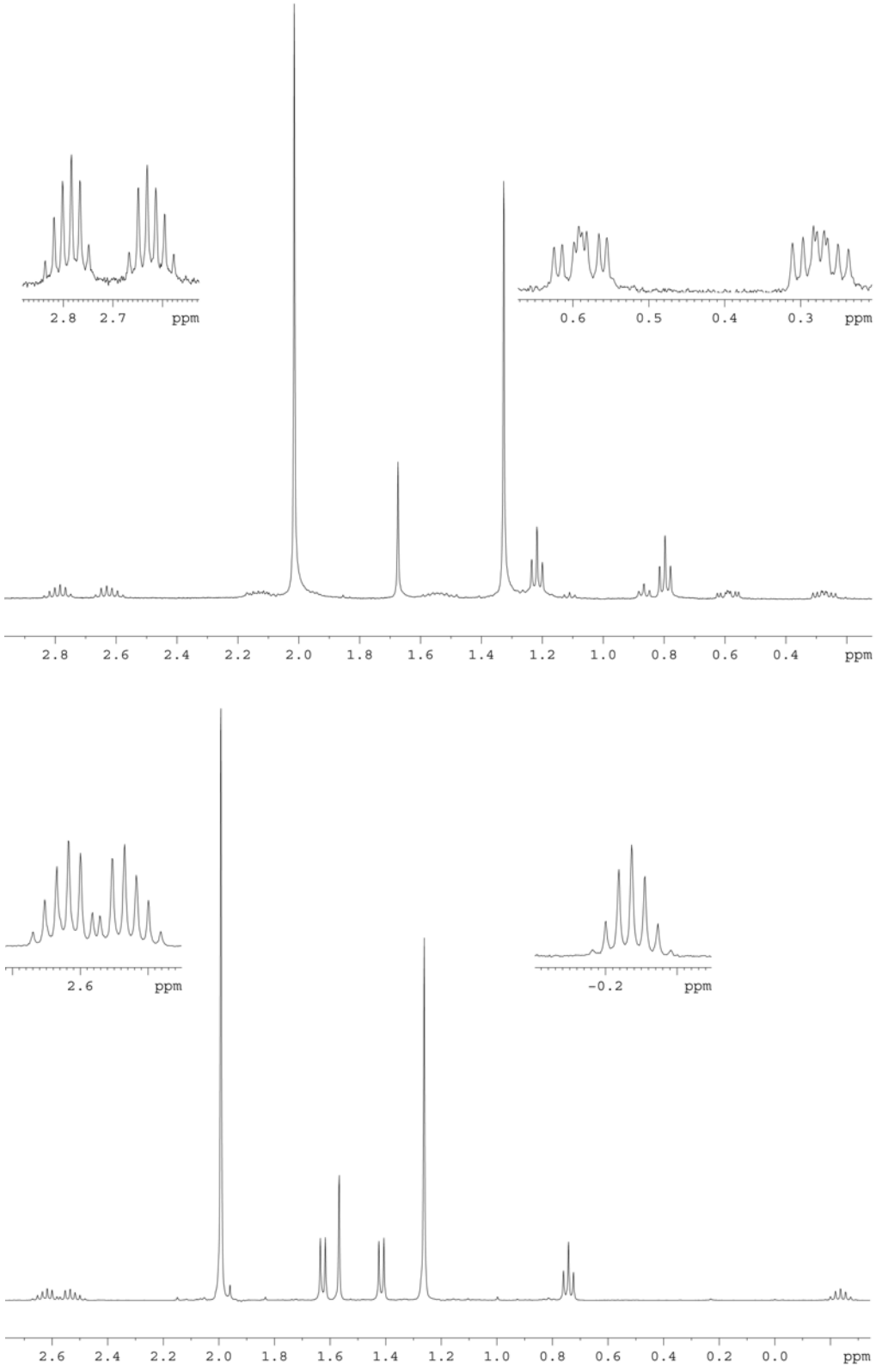

Figure 41. ^{1}H NMR spectra (400 MHz, C_6D_6, RT) of (top) **33b** and (bottom) **33c**.

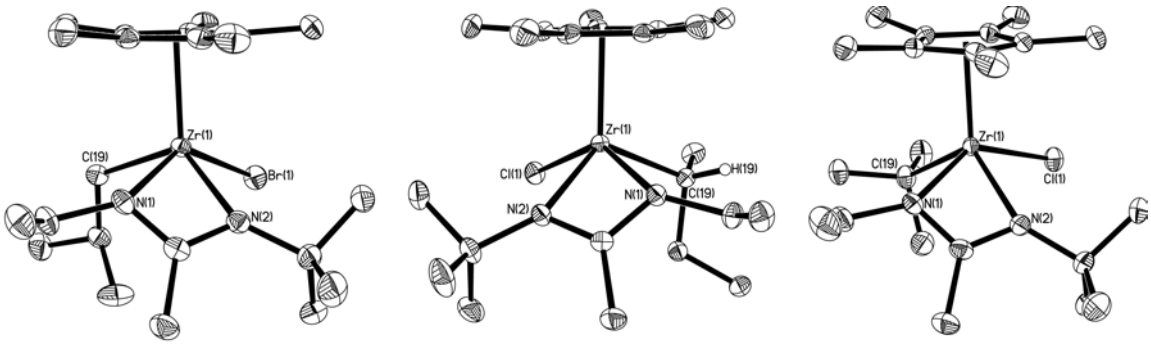

Figure 42. Solid state structures of, from left to right, **33e**, **33f**, and **33g**.

butyl series are reproduced in Figure 42. From single crystal X-ray analyses, no agostic interactions could be envisaged, for no close contacts could be found between Zr and hydrogen atoms or methyl groups of the alkyl chains. Remarkably, though **33f** is obtained as a 2 : 1 diastereomeric crude reaction mixture from alkylation of **8** with ^{s}BuMgCl, one isomer can be isolated through fractional crystallization from pentane. In all structures obtained for **33**, the alkyl group resides on the side of zirconium closest to the ethyl fragment of the amidinate, perhaps to avoid non-bonding steric interactions.

With a congested environment evident in the ^{t}Bu complexes, a low temperature ^{1}H NMR experiment was performed to attempt freezing out the rotation about the Zr-C bond. This work was done by Lisa A. Koterwas. Figure 43 shows the variable temperature ^{1}H NMR spectra performed with **33g** and **34** in toluene-d_8. Remarkably, a ^{1}H NMR spectrum at 25 °C for **34** shows that the dynamic process for the ^{t}Bu group is already quite slow. Warming the solution to 90 °C finally allows observation of a singlet that integrates to 9 hydrogens for equivalent methyl groups. These signals are well resolved singlets at lower temperatures. For **33g**, spectra at 30 °C illustrate that the rotation of the ^{t}Bu group is still quite facile compared to **34**. Lowering the temperature to –60 °C allowed the signals for the three diastereotopic methyl groups to rise out of the baseline, though they are still quite broad.

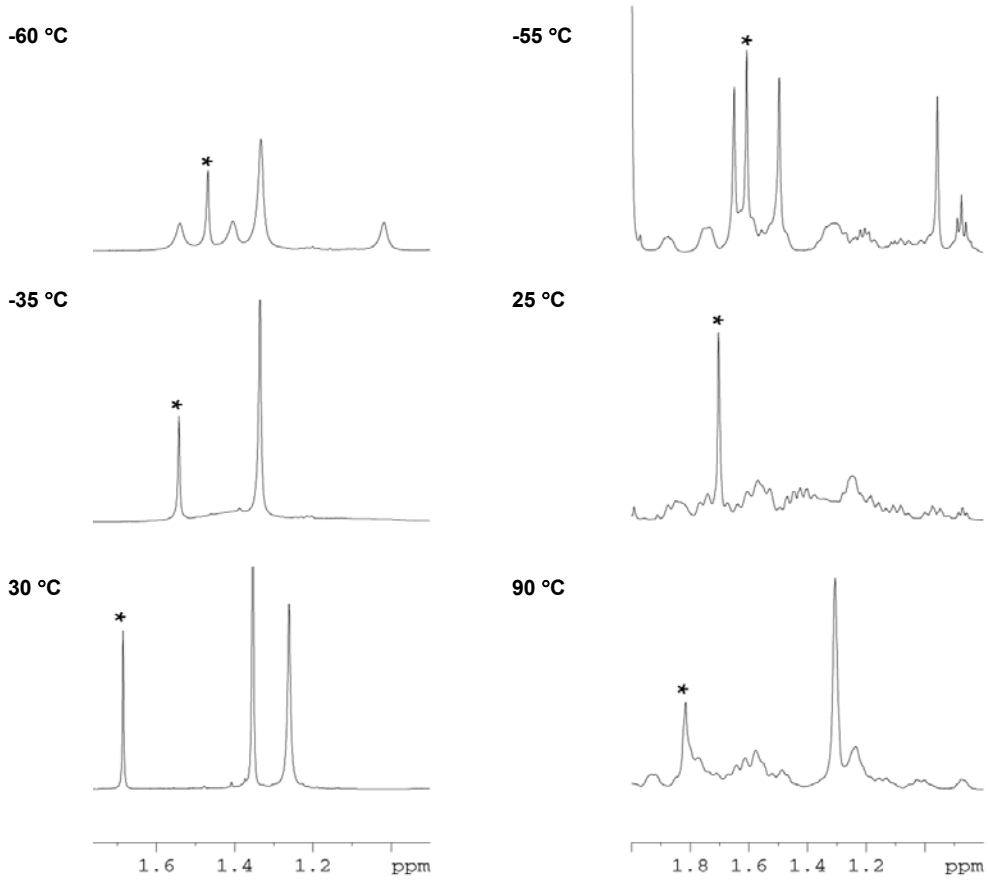

Figure 43. Low temperature ^{1}H NMR (400 MHz, toluene-d_8) of (left) **33g** and (right) **34**. The asterisk (*) indicates the amidinate CH_3 in each spectrum.

6.2.3. Stability to Isomerization and Decomposition. With regard to their stability, **33a**-**h**, **34**, and **35** are indefinitely stable in C_6D_6 solutions at room temperature. Isomerization of internal alkyl ligands within neutral metal alkyl/chloro complexes has been noted before.[14-16] However, at no point in time is evidence present that points to isomerization of **33c** to **33b** or **33f** to **33d** at RT or for **33g** to **33e** at elevated temperatures, even as high as 100 °C for **34** in toluene. Notably, if a thermolysis experiment is attempted with **33f** that is not analytically pure, slow isomerization to **33e**

is apparent. The presence of an undetectable amount of an unknown Zr species may be responsible for accelerating the isomerization in this latter case.[15]

6.3. Monoalkyl monomethyl Cp*ZA's.

6.3.1. Synthesis. As shown in Scheme 37, treatment of alkyl/chloro compounds **33** and **35** with 1 equivalent of MeLi in Et_2O at –78 °C conveniently generated the mixed alkyl systems, **36**. Methylation of even the non-straight chain alkyls, **33c**, **33e**, and **33h**, having greater steric bulk surrounding the metal center, proceeded with good success. Synthesis of the corresponding ^{t}Bu/Me version, **33g**, however, proved to be overly frustrating. Under no conditions could **33g** be methylated using MeLi, MeMgCl, $AlMe_3$, or $SnMe_4$ at low temperatures or with heating. Isomerization of **33g** to **33e** was instead noticed with heating in the presence of either $AlMe_3$ or $SnMe_4$. From all outside appearances, it seems that the ligand sphere of the monocyclopentadienyl Zr acetamidinate framework cannot accommodate such bulky alkyl groups so close to the metal center. This trend is repeated upon attempts to prepare the Zr-bis(neopentyl) product, (η^5-C_5Me_5)Zr(neopentyl)$_2$[EtNC(Me)N^{t}Bu].

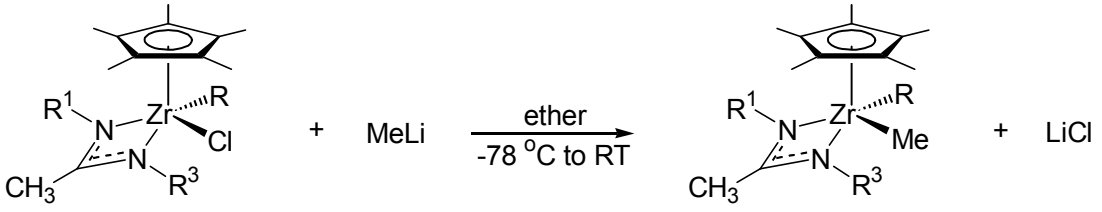

33 and **35**

For R^1 = ^{t}Bu, R^3 = Et
R = Et (**36a**); ^{n}Pr (**36b**); ^{i}Pr (**36c**); ^{n}Bu (**36d**); ^{i}Bu (**36e**); neopentyl (**36h**)

For R^1 = R^3 = ^{i}Pr
R = neopentyl (**37**)

Scheme 37. Formation of mixed dialkyl species **36**.

No reaction took place between **33h** or **35** and 1 eq. of (neopentyl)Li, but upon heating, slow decomposition to a variety of species was noticed with evolution of $C(Me)_4$.

6.3.2. Characterization. With regard to the ^1H NMR for the mixed dialkyl systems, more interesting features with regard to configurational stability about zirconium are apparent. For the straight chain alkyls **36a**, **36b**, and **36d**, all of them have effectively frozen out the dynamic racemization of the amidinate ligand. In each spectrum, one doublet of quartets representing one of the diastereotopic pair of methylene H's on the N-ethyl group is well resolved, whereas the other slightly more upfield shifted resonance appears as a broad signal with no fine structure. Also, the triplet for the CH_3 of this same group is noticeably broader in **36a** than in its preceeding counterpart, **33a**. Similarly for **36a**, the Zr-ethyl group displays a triplet for its CH_3 that is also quite broad, as well as a downfield chemical shift (1.64 ppm). In contrast, the alkyl CH_3's for **36b** and **36d** both have much narrower line widths, as well as resonances that appear at lower field strengths (1.23 and 1.09 ppm, respectively). Representative ^1H NMR spectra for several compounds of **36** are presented in Figure 44.

However, ^1H NMR spectra of **36** obtained from recrystallization showed what at first were thought to be two products cocrystallizing. Under no solvent conditions could the species be fractionally crystallized apart. The extra resonances varied in height for the different species, being the largest in **36c**, with integration denoting an approximate 2 : 1 ratio between major and minor resonances. Careful analysis of this ^1H NMR spectrum suggested that the extra species present in **36c** was actually another ^{i}Pr containing species that was not **33c**. In the case of **36e**, a 2D ^1H-^1H EXSY NMR experiment revealed exchange between the two species present in solution, suggesting

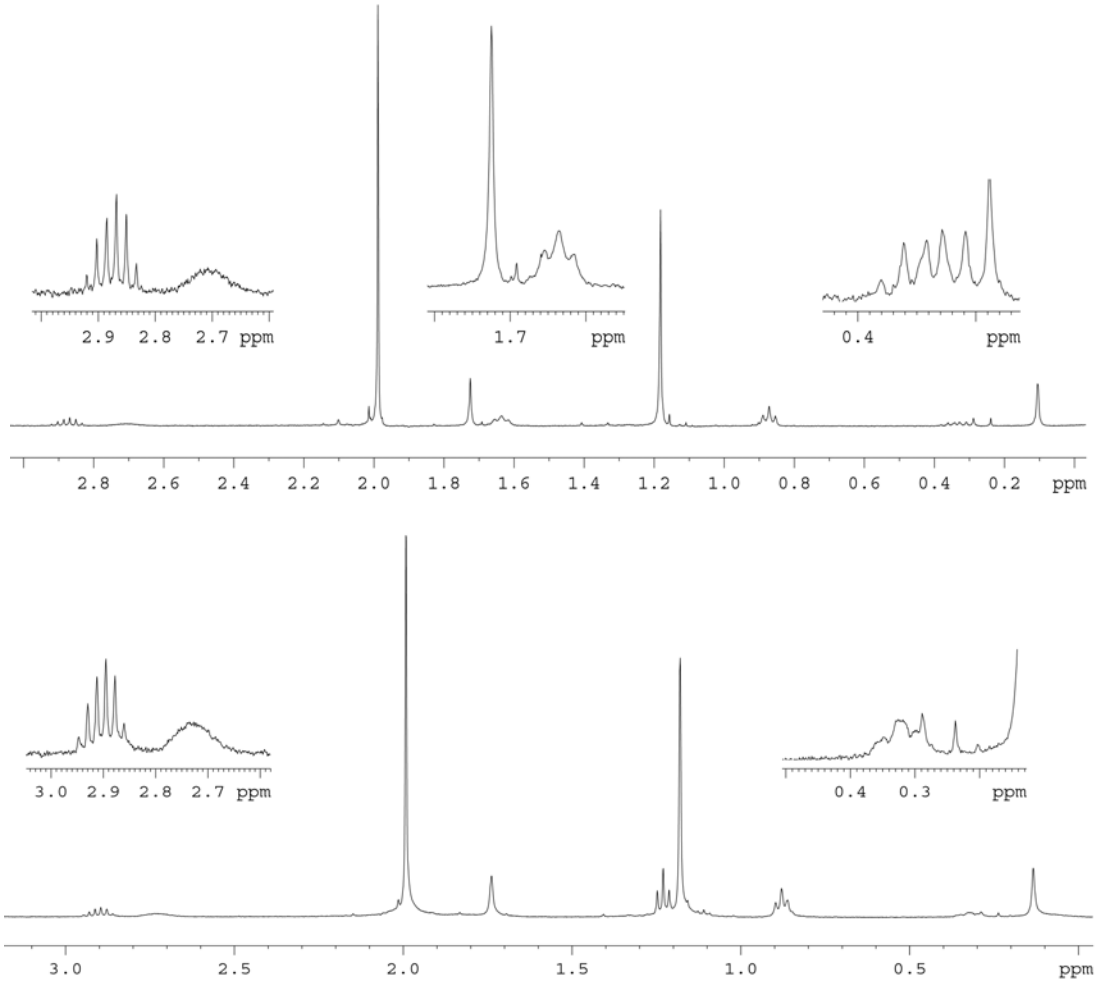

Figure 44. ^{1}H NMR spectra (400 MHz, C_6D_6, RT) for (top) **36a** and (bottom) **36b**.

a rapid equilibrium between the two structural isomers (Scheme 38).[17] Finally, performing the same experiment for **36b** did not show exchange between C_α and C_γ of the ^{n}Pr group. The latter fluctional behavior of alkyl complexes has been noted.[15]

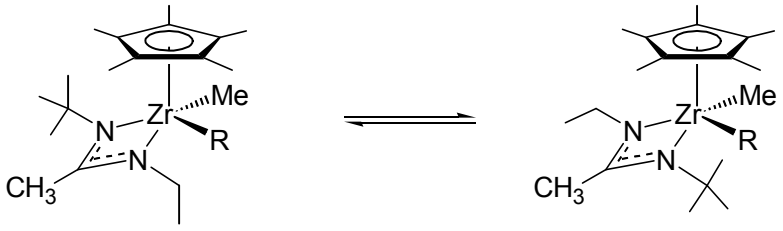

Scheme 38. Equilibration between diastereomeric isomers of **36e**.

Owing to their stability, single crystals of several of the mixed alkyl compounds have been obtained and subjected to single crystal analysis. Figure 45 shows the molecular structures for **36a**, **36c**, **36d**, and **37**, with a listing of several structural features of each provided in Table 7. In all four compounds, the alkyl group prefers to orient itself with its bulk residing "underneath" the Zr atom. This manifests itself in the orientation of C_α, which has its methylene hydrogens pointed up at the Cp* ligand, thus directing the chain away from "Cp*Zr" fragment. For the first three such structures, which feature the unsymmetric amidinate fragment with nitrogen bound ^{t}Bu and Et substituents, a common structural feature appears for each. The alkyl group, whether it be Et, ^{i}Pr, or ^{n}Bu, always appears on the same side of the structure as the amidinate ethyl group with the methyl group finding room nearest the ^{t}Bu. Bond distances for Zr-N within these compounds fall between 2.254-2.281 Å, within range of distances previously seen for similar systems.[18-20] For **36c** and **36d** the Zr-N(1) distances are longer than their Zr-N(2) counterparts [2.281 Å vs 2.259 Å for **36c** and 2.267 Å vs 2.254 Å for **36d**]. Lengthening the Zr-N(1) distance effectively removes the ^{t}Bu group further from the metal center, allowing it to avoid any steric interactions it may have with the methyl groups of the Cp* ring or the Zr methyl group. This trend is not, on the other hand, applicable to **36a** which has equivalent Zr-N bond lengths. This may be attributable to the shorter chain alkyl (Et) present in this complex.

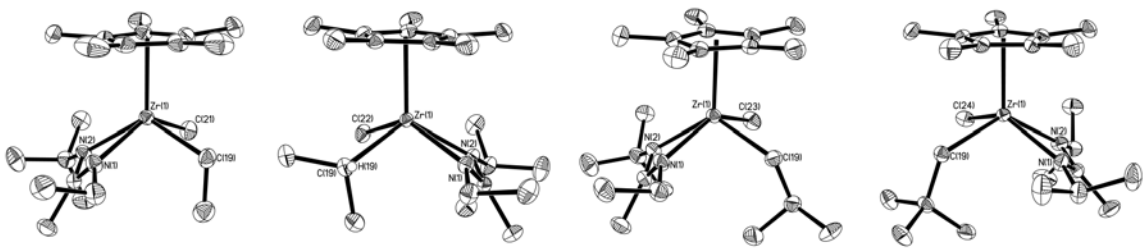

Figure 45. Solid state structures of **36a**, **36c**, **36d**, and **37**.

Compound	Zr-N(1) (Å)	Zr-N(2) (Å)	$\Sigma\theta_{N(1)}$ (°)	$\Sigma\theta_{N(2)}$ (°)	° of Pucker
36a	2.263 (3)	2.263 (3)	351.6	357.3	22.5
36c	2.259 (3)	2.281 (3)	350.7	356.9	25.0
36d	2.2601 (12)	2.2821 (12)	351.7	356.9	24.6
37	2.281 (2)	2.269 (2)	358.0	357.9	14.8

Table 7. Selected bond lengths and bond angles for monoalkyl monomethyl Cp*ZA's.

Considering the structure determined for **37**, the Zr-N bond lengths are now reversed. For this compound, which has a symmetric amidinate moiety, the Zr-N bond closest to the large alkyl group displays the greater bond distance [Zr-N(1) of 2.269 vs Zr-N(2) of 2.281 Å]. The solid-state structure of this molecule is quite perturbed, having one of its iPr groups with both methyl groups pointed toward the Zr-Me group to minimize the steric interactions with the nearby amidinate $C(CH_3)$. The other ^{i}Pr group is twisted such that only one methyl group points at the alkyl group, in this case the neopentyl, no doubt due to the steric hindrance necessary for such a ligand. Taking in the results obtained from these molecular structures, it appears that competing factors are present for this series of compounds: the need to remove the ^{t}Bu group from beneath the umbrella of the Cp* ligand, and the desire to prevent blockage of the Zr bound alkyl groups.

Upon further investigation of the four structures, the amidinate nitrogens all suffer from slight deviations from planarity. The pyramidal distortion reveals itself in the sum of the angles about nitrogen, $\Sigma\theta_N$, which are all below 360 °. Although a slight digression is necessary for N(1) in **36a**, **36c**, and **36d** [357.3 °, 356.9 °, and 357.0 °, respectively], the large chain alkyl group is provided an even wider berth with pyramidalization values for N(2) of 351.6 °, 350.7 °, and 351.1 °, respectively. Further probing of these structures revealed a nonplanarity of the Zr-amidinate four membered ring, expressed as a

difference between the two planes defined by N(1)-Zr(1)-N(2) and N(1)-C(11)-N(2). Looking at the series of **36a**, **36d**, and **36c**, an increase in the plane difference from 22.5 ° to 25.0 ° follows with the increase in alkyl ligand size in these complexes. This also relates directly to the nonplanarity about N(2), which **36c** boasted the largest deviation from 360 °. Taken together, these deviations are necessary to accommodate two non-methyl groups bound to Zr, with the greatest deformations arising to allow for a Zr-^{i}Pr.

6.3.3. Stability to Isomerization and Decomposition. Negishi has previously set a standard for stabilities of alkyl ligands with β-hydrogens.[4] For a series of $Cp_2ZrR(Me)$, he asserted that the stability of alkyl groups is dependent on the substitution at the β-position, such that stability decreases in the order β-methine > β-methylene > β-methyl. Although at higher temperatures, a set of Hf derivatives mirrored this same trend.[21] Compounds **36** and **37** are air- and moisture-sensitive, but are otherwise fairly stable, even in solution. In a room temperature C_6D_6 solution, **36a** slowly decomposes but remains the dominant species in solution even after 18 hours. Similar solutions of **36c** are also stable, showing no signs of isomerization to **36b** over extended periods of time at room temperature. Previous Group IV complexes have not proven to be stable toward such isomerizations[15] or eliminations / abstractions.[4] During a sealed NMR tube experiment, **36h** was found to be very stable at room temperature for several days without change. The first indication of decomposition was first noticed only after heating the sample at 100 °C for more than 1 hour, and after 40 hours, a significant amount of **36h** was still present in solution. This would fit well with Negishi's observations, if the list were expanded to include quaternary centers.

At no point in time during the decomposition of these compounds was there evidence in the ^{1}H NMR for the products of β-hydride elimination from **36a** (which would

provide ethylene), **36c** (propylene), or **36e** (isobutylene). Along this vein, β-methyl elimination products were also absent from solutions of **36c** (which would evolve ethylene), **36e** (propylene), and **36h** or **37** (isobutylene). Evidence is now strongly embedded that suggests that the Cp*ZA framework can be added to the list of ligand environments that are quite effective in controlling, and in fact, suppressing β-hydrogen and β-methyl abstractions / eliminations from Zr-alkyl groups.[22-25]

6.4. Synthesis and Characterization of Dialkyl Cp*ZA's.

As with the previously discussed mixed dialkyl Group IV complexes, symmetric dialkyl systems have proven equally unstable.[16,26] Negishi has discussed that in the preparation of $Cp_2Zr^nBu_2$, the dialkyl derivative could not be isolated. Instead, it appears as though the product of the reaction evolves from decomposition to form the alkene bound intermediate, $Cp_2Zr(\eta^2$-1-butene), a Zr(II) species.[27] This has been substantiated through characterization of PMe_3 stabilized olefin adducts of Zr and Hf.[10,28,29] The PMe_3-free Zr(II) species has proven useful as a reagent for organic synthesis.[27] The preparation of a thermally stable L_2ZrR_2 ($R \geq Et$) derivative[24,30,31], then, is of interest as a method to control and further heighten this synthetic methodology.

Through the utilization of a 2 : 1 stoichiometry of alkyl lithium reagent to dichloro species **8**, the doubly alkylated Zr complexes **38** and **39** (Scheme 39) can be prepared

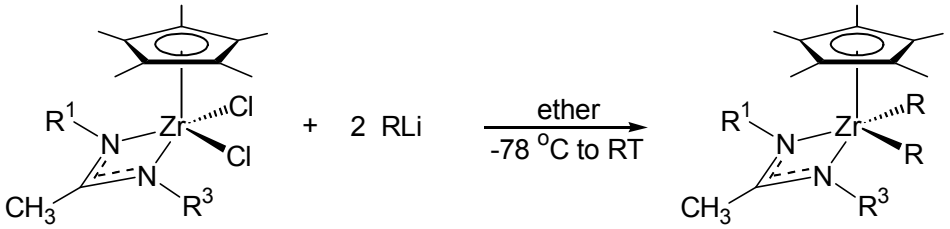

For $R^1 = {}^tBu$, $R^3 = Et$
$R = {}^iBu$ (**38a**): ^nBu (**39a**)

For $R^1 = R^3 = {}^iPr$
$R = {}^iBu$ (**38b**)

For $R^1 = R^3 = Cy$
$R = {}^nBu$ (**39b**)

Scheme 39. Doubly alkylated Cp*ZA's with identical R groups.

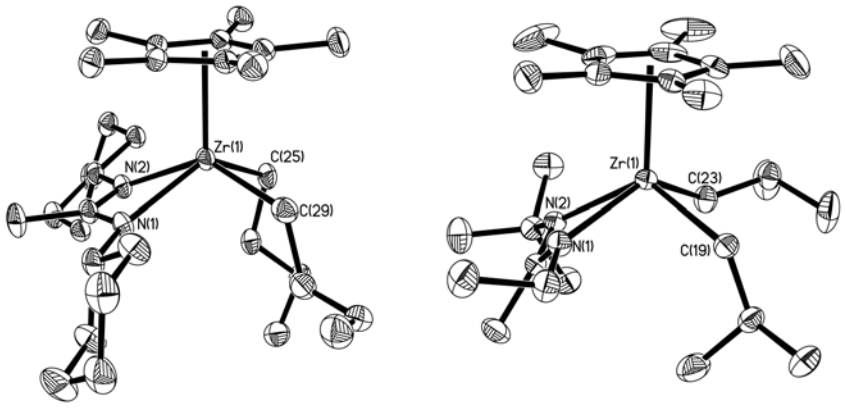

Figure 46. Molecular structures of **39b** and **38a** showing 30 % thermal ellipsoids. Hydrogen atoms have been omitted for clarity.

in good yields, the latter of which was prepared and studied by LAK.[8] The crystallinity of these complexes allowed their structural determination through single crystal X-ray analyses. The solid state structures of **38a** and **39b** are shown in Figure 46. Of import, no α-, β-, or γ- agostic interactions could be detected for either butyl complex.

In solution, it is interesting to note that, for **38**, the amidinate ligand appears to be rapidly flipping as evidenced from the methylene hydrogens appearing as a quartet in the ^{1}H NMR spectrum. As compared to complexes **33** and **36**, in which the amidinate racemization is frozen out, it appears that sterics govern this dynamic process. In other words, with identical groups bound to Zr opposite the Cp*ZA framework, as in **6**, **8**, **15**, etc., no preferential orientation is induced for the asymmetric amidinate ligand and the ring flipping will be facile. However, when the size of the two groups differs as in **33** and **36**, the amidinate appears quite static and the methylene of the ethyl group produces two separate resonances.

In terms of the decomposition of **38** and **39**, each displayed a remarkably long half-life. For instance, the Zr^nBu_2 derivatives have similar $t_{1/2}$ values of about 48 hours at 30 °C. Further, the C_1-symmetric diisobutyl derivative **38a** has a half-life of 107 min at

50 °C. The activation parameters extrapolated from an Eyring analysis (Figure 47) for this decomposition process suggest an intramolecular hydrogen atom abstraction mechanism ($\Delta H^{\ddagger}$ = 20.8 (3) kcal / mol and $\Delta H^{\ddagger}$ = -6.2 (3) eu).

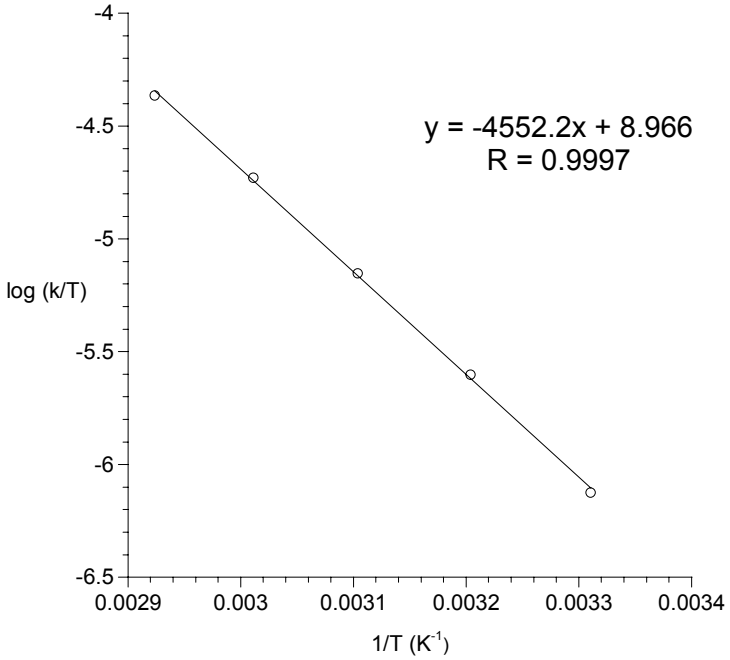

Figure 47. Eyring plot for the decomposition of **38a** between 30 and 70 °C.

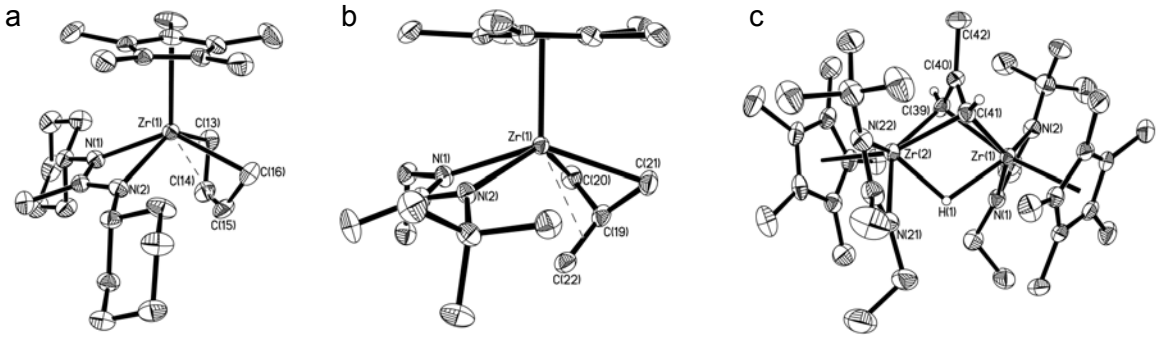

Figure 48. Molecular structures of (a) **40**, (b) **41**, and (c) **42**. Hydrogen atoms have been omitted for clarity except for the bridging H, H(1), and those on the C(39) and C(41) of the bridging C_4H_5 fragment of **42**.

For the decomposition of **39b**, the first-order decomposition cleanly afforded a single new product quantitatively, that being the zirconacyclopentene, **40**. The molecular structure of which is shown in Figure 48a. During an NMR scale thermolysis experiment, evidence for H_2 production was evident from growth of a resonance at ~ 4.5 ppm shown in Figure 49. The mechanism by which this proceeds was derived from work by Harrod describing the decomposition of $Cp_2Zr^nBu_2$.[32] As shown in Scheme 40, the first step requires a γ-hydrogen abstraction to generate butane and a zirconacyclobutane. From this species, a β-hydride elimination forms an allylic hydride intermediate which, upon another hydrogen atom abstraction, evolves one equivalent of H_2 and forms **40**.

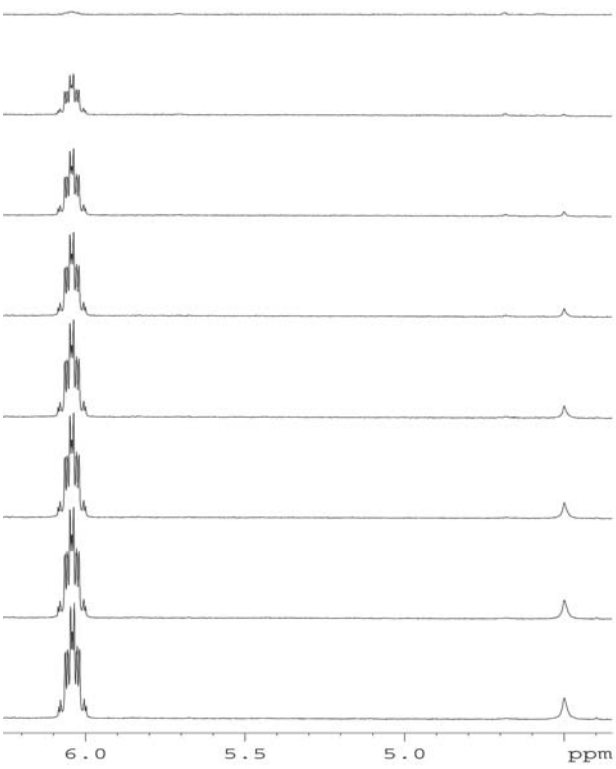

Figure 49. Partial ^{1}H NMR spectra (400 MHz, toluene-d_8, 50 °C) for the thermal decomposition of **39b**. Resonances are for **40** (6.05 ppm) and H_2 (4.5 ppm).

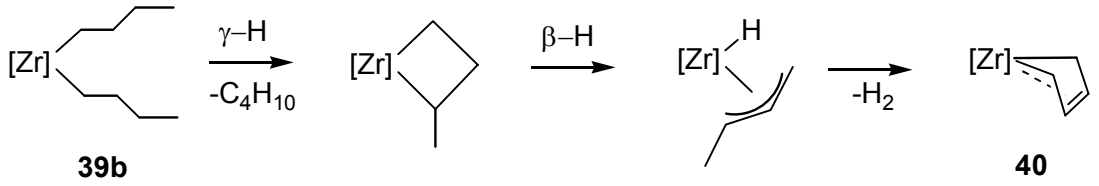

39b **40**

Scheme 40. Mechanism for production of zirconacyclopentene **40** from Zr^nBu_2, **39b**.

Thermolysis of **38a** (Scheme 41) followed a more diverse decomposition process, first through a trimethylenemethane (TMM) derivative[33], **41**, and finally into a novel dizirconium species, **42**, the molecular structures of which are shown in Figures 48b and c, respectively.[34] This pathway must eliminate 3 equivalents of isobutane before reaching the final product. Contrary to the production of **40**, H_2 does not get formed in this case. As such, the mechanism for generation of **42** is too diverse to speculate on.

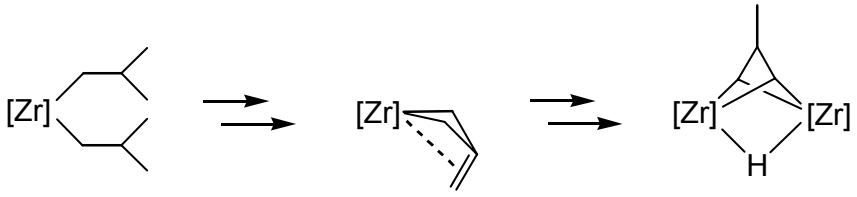

38a **41** **42**

Scheme 41. Mechanism for production of the Zr-TMM derivative **42** from Zr^iBu_2, **38a**.

6.5. Monoalkyl Zirconium Cations.

6.5.1. Activation and Characterization. Neutral d^0 zirconium alkyls are known to be the precursors to competent initiators for Ziegler-Natta polymerization.[2] Generation of the proposed active species, the cationic metal alkyl complex, $[L_2ZrR]^+$, from the starting dialkyl complex, L_2ZrR_2, proceeds smoothly upon alkyl group abstraction with $[Ph_3C][B(C_6F_5)_4]$ or protonolysis with $[PhNHMe_2][B(C_6F_5)_4]$.[35] As

exemplified in Scheme 42 for the isobutyl derivative, cationic species **43** can be created from the dialkyl systems **36** or **37** at –10 °C in PhCl-d_5. A slight excess of the borate salt, in this case, $[PhNHMe_2][B(C_6F_5)_4]$, is employed to ensure complete transformation. Use of $[Ph_3C][B(C_6F_5)_4]$ was not optimal due to competition between methide abstraction and hydride abstraction from the alkyl group, the latter of which would result in the formation of olefin plus the previously seen Zr-Me cation, **22a**. The cations were characterized by a plethora of 1- and 2D ^1H and ^{13}C NMR experiments at 500 and 125 MHz, respectively. The results obtained point to the general structure portrayed in Scheme 42. These complexes afforded the insight into models for propagating species in solution for the acetamidinate system, with **43b** and **43e** mimicking the first insertions of ethylene and propylene respectively into a Zr-Me bond, and **43c** modeling the 2,1-insertion of propylene into a Zr-H bond.

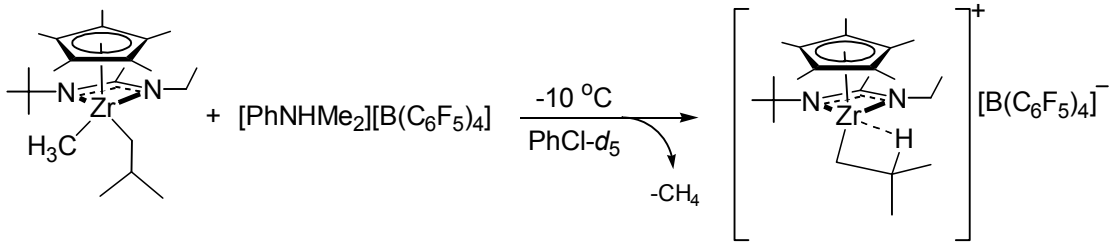

Scheme 42. Production of cationic alkyl Cp*ZA's through chemoselective protonation.

The ^1H NMR spectrum for each cationic complex, aside from the methine bearing **43c**, displays diastereotopic hydrogens, H_α, on the carbon atom, C_α, directly bonded to the zirconium center. This is shown in Figure 50 for both the ^{n}Pr and the ^{i}Bu cations, **43b** and **43e**, respectively. In addition to this, the strong β-agostic interaction (see Section 6.5.2.) leads to inequivalent β-hydrogens as well, and this is exemplified from Figure 50a for **43b**. Due to the strength of the agostic interaction, the two methyl

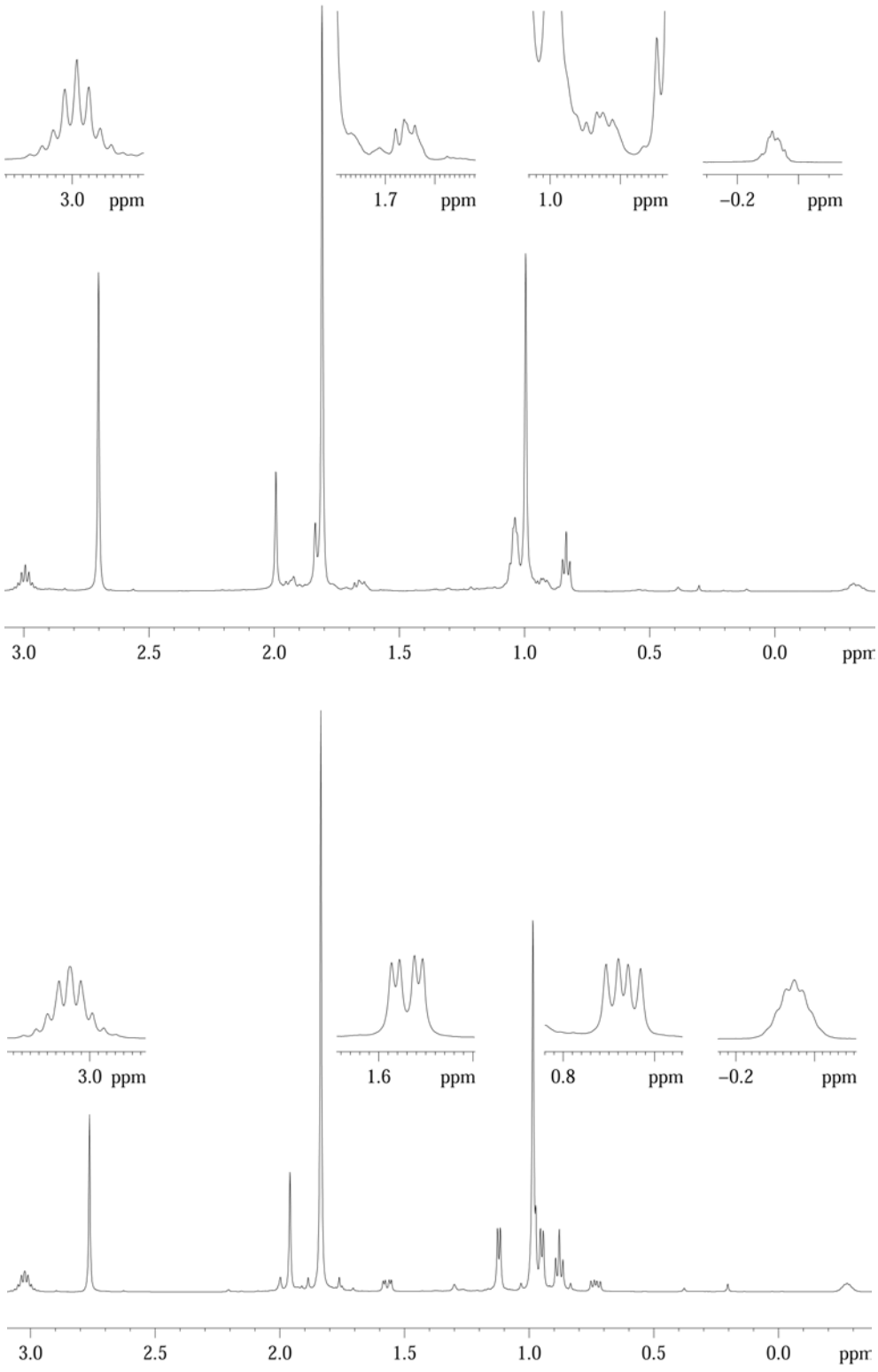

Figure 50. ^{1}H NMR spectra (500 MHz, PhCl-d_5, -10 °C) for (a) **43b** and (b) **43e**.

groups of **43e** appear as separate doublets. For the isopropyl group in **43c**, C_α instead bears diastereotopic methyl groups and its ^1H NMR spectrum is shown in Figure 51.

6.5.2. Elucidation of Cp*ZA's with Strong β-Agostic Interactions. First, each of the long chain alkyl cations, except for **43h**, possesses a strong β-agostic interaction between one of the β-hydrogens on the alkyl chain and the electron deficient zirconium atom. The values for the $^1J_{CH}$ coupling constants for the β-hydrogen containing alkyl group supports the strength which this interaction possesses. Table 8 shows that a decrease in the $^1J(^{13}C_\beta\text{-}^1H_\beta)$ value for the agostically bound H is countered, where elucidation is possible, by an increase in the value for $^1J(^{13}C_\beta\text{-}^1H_\beta)$ for its non-

R Group	$^1J(^{13}C_\alpha\text{-}^1H_\alpha)$		$^1J(^{13}C_\beta\text{-}^1H_\beta)$	
Me (**22a**)	117		No β-hydrogens	
Et (**43a**)	140	135	123	
^{n}Pr (**43b**)	144	133	110	n.o.
^{i}Pr (**43c**)	155		126	85
^{n}Bu (**43d**)	140	133	121	109
^{i}Bu (**43e**)	138	128	92	
neopentyl (**43h**)	122	107	No β-hydrogens	

Table 8. Values for $^1J_{CH}$ of Cp*ZA alkyl cations obtained from 2D $^1H\text{-}^{13}C$ NMR J-resolved HSQC experiments. (n.o. = not observable).

agostically bound geminal partner. Of importance here, **43c**, with one of the diastereotopic β-methyl groups, exhibits an agostic interaction with Zr. Also indicative of this noncovalent interaction are the values for $^1J(^{13}C_\alpha\text{-}^1H_\alpha)$, which for the entire series of

cationic species, except **43h**, proves to be larger than that normally expected for an sp^3 hybridized C atom. Recall that similar behavior was observed from cyclopentene insertion. In the case of **43h**, no β-hydrogens are present, so its stabilization of the Zr center lies down a different path, possibly through solely α-hydrogen interactions.

From the solid state structures of several of the neutral dialkyl complexes, it was found that the large alkyl chain was housed on the more sterically open side of Zr, which corresponded to the N(Et) side of the amidinate. For the cations then, it would be of use to know whether there was sufficient room for the agostic interaction to occupy space in close proximity to the ^{t}Bu side of the amidinate. To probe this, difference-1D ^{1}H nOe experiments were performed on the cations, and they revealed that the β-agostic interaction resides on the ethyl side of the molecule. With the exceptions being **43c** and **43h**, the less substituted carbon atom, C_α, resides nearest the bulky ^{t}Bu group, minimizing steric hindrance by only presenting 2 hydrogens to this part of the amidinate ligand. This positions the main chain to cross the face of the Zr atom, allowing C_β to orient H_β in close proximity to the N-ethyl substituent. Unfortunately, the H_α do not show any nOe effects with the ^{t}Bu group in any of the structures. The best illustration of this then comes from Figure 51, in which the agostically ligated methyl group of **43c** shows nOe effects with the triplet of the ethyl group, and the non-agostic methyl group possesses nOe with the ^{t}Bu singlet.

6.5.3. Solid State Evidence for Strong β-Agostic Interactions. Attributable to the strength of the agostic interaction and the innate stability of the cations at low temperature, single crystals of the ^{i}Bu cationic species **43e** were obtained. The solid state structure so obtained is displayed in Figure 52. In agreement with the low $^1J_{CH}$ found in the ^{1}H NMR for the agostic β-hydrogen, a close contact is observed

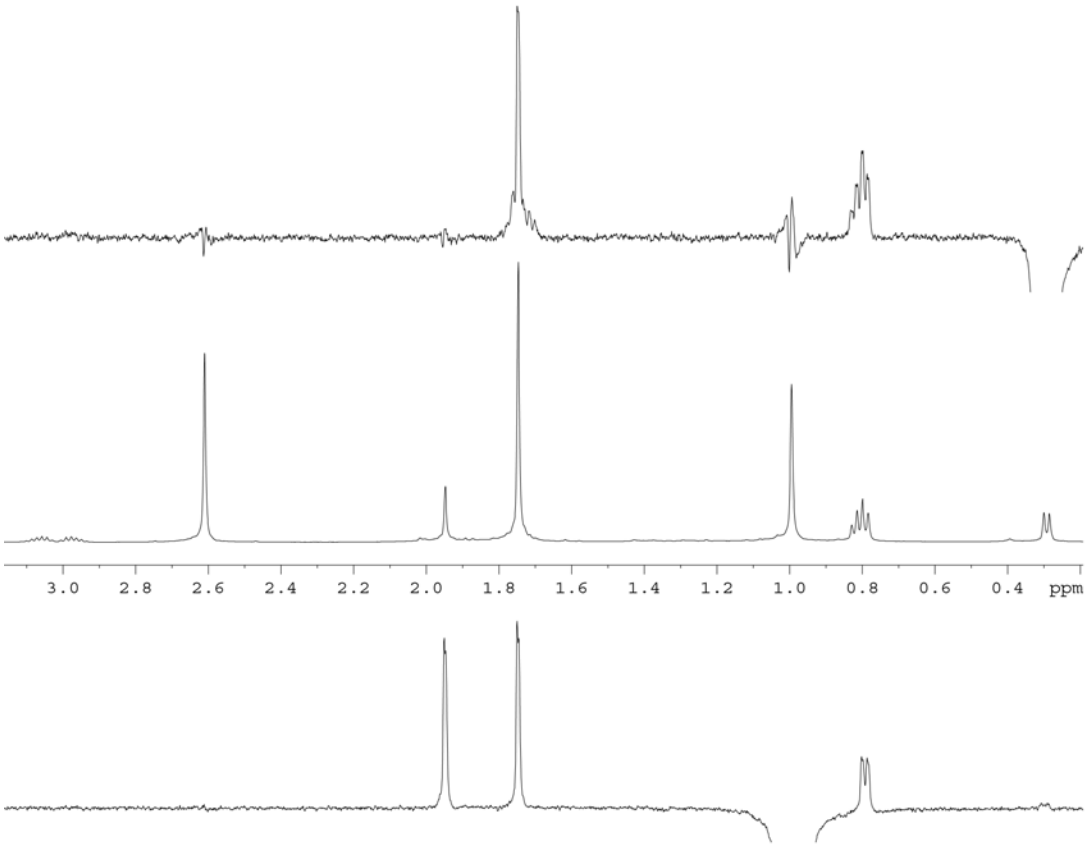

Figure 51. 1D ^{1}H nOe NMR spectra for the ^{i}Pr derivative **43c** illustrating the solution orientation of the alkyl group.

between the Zr center and the β-methine hydrogen, H(20a), at a distance of 2.25(3) Å. This distance is longer than a typical full Zr-H bond.[36,37] Also, the C(19)-C(20) bond length is 1.524(3) Å, indicative of single bond character between the two carbon atoms, which along with the agostic bond distance suggests that the species is an agostically ligated ^{i}Bu species, not an isobutylene adduct of a Zr-H cation.[38] The structure of **43e** compares best with the mononuclear cation, **23**, in most respects. However, it can be assumed that the elongation in the average Zr-N bond distances (ca. 0.02 Å) for **43e** is due to the extra electron donation from the agostic interaction.

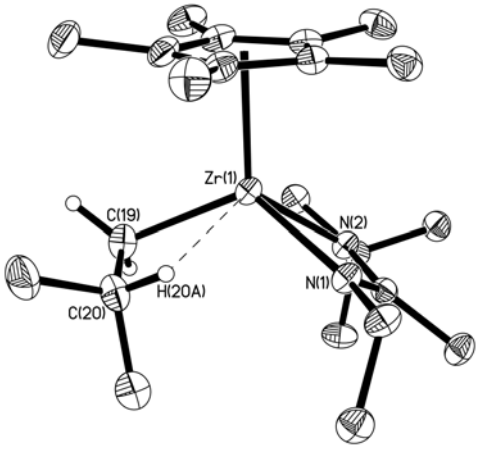

Figure 52. Molecular structure of **43e** displaying a β-hydrogen agostic interaction. The borate anion and hydrogen atoms, except of the ^{i}Bu fragment, have been removed for the sake of clarity.

6.6. Decomposition of Zr-Alkyl Cations.

We have previously shown that the polymerization of α-olefins and α,ω-nonconjugated dienes via similar Zr amidinate complexes occurs in a living and stereospecific manner at –10 °C. This knowledge lead us to test for restrictions to the stability of the cationic complexes **43** which might mimic the stability of a growing polymer chain. These compounds were found to maintain narrow line-width resonances up to room temperature, establishing that the agostic interaction is quite strong. Also, the configurational stability about Zr, with regard to racemization of the amidinate system, is maintained at temperatures above –10 °C. Additionally, the ethyl cation **43a** did not undergo β-hydrogen elimination to give ethylene, nor did the isopropyl cation **43c** eliminate to give propylene. The latter did however appear to isomerize slowly at 30 °C to **43b**. Curiously, Pd complexes have shown the opposite behavior, isomerizing from the ^{n}Pr to the ^{i}Pr cation even at –80 °C.[39]

These complexes do not possess infinite lifetimes at temperatures above –10 °C. They are observed to decompose through a slow reaction with the solvent, in this case chlorobenzene-d_5, to produce a common product, the red dimeric dicationic **25**. Qualitatively, it is possible to state that the concentration of **43e** disappears the fastest of the cations studied, having a half-life of only 15 minutes at 30 °C in C_6D_5Cl.

6.7. Conclusions.

From the starting dichloride **8**, a series of thermally stable Zr alkyl/chloro complexes, **33**, **34**, and **35**, have been prepared. The sterically superior alkyl group occupies the side of Zr nearest the ^{t}Bu moiety of the amidinate ligand. Methylation of these compounds lead to the mixed alkyl systems, **36** and **37**, which also show the same preference for housing of the large alkyl group. Both series of complexes are remarkably stable in the solid state and in solution including the ethyl and ^{i}Pr derivatives, **33a** / **36a** and **33c** / **36c**, the latter of which show no signs of isomerization to the ^{n}Pr derivatives **33b** / **36b** even after extended periods of time. At no point in time during the decomposition of these complexes was any evidence offered that hinted toward generation of olefins.

Upon protonolysis of the Zr-Me group in **36**, cationic complexes **43** were prepared that were quite stable at –10^{o} C. Characterization by various NMR techniques proved the alkyl group and the electron deficient metal were involved in strong β-hydrogen agostic interactions residing on the side of the Zr nearest the N-ethyl group of the acetamidinate. Their thermal stability is remarkable, in that the ^{1}H NMR spectra for the cations remains invariant when warmed to room temperature which seems to rule out any dynamic process involving the agostic interaction. Although these models for

living propagating species were not immortal, eventually decomposing to the bridging dichloride species, **25**, alkene decomposition products were never evident.

The generally accepted dogma involving β-agostic interactions in the living Ziegler-Natta polymerization of olefins is one in which this interaction plays the role of the antagonist. With β-hydride elimination known to be a culprit for chain termination and thus preventing a polymerization system from exhibiting living behavior, it would seem that avoiding these secondary interactions would remove the opportunity with which the chain could prematurely terminate. Conversely, the results herein balk at this proposal, instead pointing to a stabilizing feature ascribed to certain β-hydrogen agostic interactions. This electron donation to the cationic d^o metal center provides a ground state stabilization for the complex. The possibility exists that the Cp*ZA ligand set imposes an orientation of the alkyl fragment that does not lie along the typical β-hydride elimination pathway. There may exist an optimum trajectory of β-H atoms from which elimination readily occurs due to extremely favorable orbital overlap. Those complexes that cannot engage in the favorable stabilization of the electron deficient metal will be further destabilized and more fluxional without this restraining of the alkyl chain. Both of these factors will prove detrimental, such that the C_β-H bond will be able to attain the proper geometry from which elimination is favored, and the energy for this process will be far less. Within living systems, heightened awareness of the active species in solution and their attributes will aid in further development of ligand sets that retain the beneficial characteristics of living behavior and spurn terminating events, especially above ambient temperatures.

6.8. References.

(1) Alt, H. G.; Koppl, A. *Chem. Rev.* **2000**, *100*, 1205.

(2) Resconi, L.; Cavallo, L.; Fait, A.; Piemontesi, F. *Chem. Rev.* **2000**, *100*, 1253.

(3) Buchwald, S. L.; Watson, B. T.; Huffman, J. C. *J. Am. Chem. Soc.* **1987**, *109*, 2544.

(4) Negishi, E.; Nguyen, T.; Maye, J. P.; Choueiri, D.; Suzuki, N.; Takahashi, T. *Chem. Lett.* **1992**, 2367.

(5) Negishi, E.; Swanson, D. R.; Takahashi, T. *Chem. Let.* **1987**, 623.

(6) Negishi, E.; Cedarbaum, F. E.; Takahashi, T. *Tetrahedron Lett.* **1986**, *27*, 2829.

(7) Jayaratne, K. C.; Sita, L. R. *J. Am. Chem. Soc.* **2000**, *122*, 958.

(8) Keaton, R. J.; Koterwas, L. A.; Fettinger, J. C.; Sita, L. R. *J. Am. Chem. Soc.* **2002**, *124*, 5932.

(9) Zhang, Y. H.; Keaton, R. J.; Sita, L. R. *J. Am. Chem. Soc.* **2003**, *125*, 8746.

(10) Buchwald, S. L.; Kreutzer, K. A.; Fisher, R. A. *J. Am. Chem. Soc.* **1990**, *112*, 4600.

(11) Swanson, D. R.; Negishi, E. *Organometallics* **1991**, *10*, 825.

(12) Haaland, A.; Scherer, W.; Ruud, K.; McGrady, G. S.; Downs, A. J.; Swang, O. *J. Am. Chem. Soc.* **1998**, *120*, 3762.

(13) Scherer, W.; Priermeier, T.; Haaland, A.; Downs, A. J.; Boese, R.; Blaser, D. *Organometallics* **1998**, *17*, 4406.

(14) Hart, D. W.; Schwartz, J. *J. Am. Chem. Soc.* **1974**, *96*, 8115.

(15) Chirik, P. J.; Day, M. W.; Labinger, J. A.; Bercaw, J. E. *J. Am. Chem. Soc.* **1999**, *121*, 10308.

(16) Fernandez, F. J.; GomezSal, P.; Manzanero, A.; Royo, P.; Jacobsen, H.; Berke, H. *Organometallics* **1997**, *16*, 1553.

(17) Zhang, Y. H.; Keaton, R. J.; Sita, L. R. *J. Am. Chem. Soc.* **2003**, *125*, 9062.

(18) Gomez, R.; Duchateau, R.; Chernega, A. N.; Teuben, J. H.; Edelmann, F. T.; Green, M. L. H. *J. Organomet. Chem.* **1995**, *491*, 153.

(19) Gomez, R.; Duchateau, R.; Chernega, A. N.; Meetsma, A.; Edelmann, F. T.; Teuben, J. H.; Green, M. L. H. *J. Chem. Soc., Dalton Trans.* **1995**, 217.

(20) Littke, A.; Sleiman, N.; Bensimon, C.; Richeson, D. S.; Yap, G. P. A.; Brown, S. J. *Organometallics* **1998**, *17*, 446.

(21) Nishihara, Y.; Ishida, T.; Huo, S.; Takahashi, T. *J. Organomet. Chem.* **1997**, *547*, 209.

(22) Planalp, R. P.; Andersen, R. A.; Zalkin, A. *Organometallics* **1983**, *2*, 16.

(23) Buchwald, S. L.; Lum, R. T.; Fisher, R. A.; Davis, W. M. *J. Am. Chem. Soc.* **1989**, *111*, 9113.

(24) Paolucci, G.; Pojana, G.; Zanon, J.; Lucchini, V.; Avtomonov, E. *Organometallics* **1997**, *16*, 5312.

(25) Wendt, O. F.; Bercaw, J. E. *Organometallics* **2001**, *20*, 3891.

(26) Schrock, R. R.; Baumann, R.; Reid, S. M.; Goodman, J. T.; Stumpf, R.; Davis, W. M. *Organometallics* **1999**, *18*, 3649.

(27) Negishi, E.; Takahashi, T. *Acc. Chem. Res.* **1994**, *27*, 124.

(28) Negishi, E.; Holmes, S. J.; Tour, J. M.; Miller, J. A.; Cedarbaum, F. E.; Swanson, D. R.; Takahashi, T. *J. Am. Chem. Soc.* **1989**, *111*, 3336.

(29) Baumann, R.; Stumpf, R.; Davis, W. M.; Liang, L. C.; Schrock, R. R. *J. Am. Chem. Soc.* **1999**, *121*, 7822.

(30) Amor, F.; Spaniol, T. P.; Okuda, J. *Organometallics* **1997**, *16*, 4765.

(31) Mehrkhodavandi, P.; Bonitatebus, P. J.; Schrock, R. R. *J. Am. Chem. Soc.* **2000**, *122*, 7841.

(32) Dioumaev, V. K.; Harrod, J. F. *Organometallics* **1997**, *16*, 1452.

(33) Rodriguez, G.; Bazan, G. C. *J. Am. Chem. Soc.* **1997**, *119*, 343.

(34) Keaton, R. J.; Sita, L. R. *Organometallics* **2002**, *21*, 4315.

(35) Chen, E. Y. X.; Marks, T. J. *Chem. Rev.* **2000**, *100*, 1391.

(36) Pool, J. A.; Bradley, C. A.; Chirik, P. J. *Organometallics* **2002**, *21*, 1271.

(37) Kraft, B. M.; Lachicotte, R. J.; Jones, W. D. *J. Am. Chem. Soc.* **2001**, *123*, 10973.

(38) Alelyunas, Y. W.; Guo, Z.; LaPointe, R. E.; Jordan, R. F. *Organometallics* **1993**, *12*, 544.

(39) Shultz, L. H.; Tempel, D. J.; Brookhart, M. *J. Am. Chem. Soc.* **2001**, *123*, 11539.

Chapter 7

Analysis of Polymer Microstructure

7.1. Introduction.

Through detailed NMR analysis, polymer microstructure can be determined with a good degree of precision to ascertain the percentage of stereo- and regioerrors. Also, if termination events occur to a significant degree, the end groups can be determined so long as the molecular weight of the polymer is not large enough that the small end group signals get swamped out. In this respect, investigating low molecular weight oligomers proves advantageous through the homogeneity of the mixture and the ease with which characterization is performed on lower molecular weight materials. In addition, oligomerization experiments can provide evidence toward mechanistic details that aid in further understanding of the system that cannot be delineated from high molecular weight polymers.[1-4]

7.2. Detailed Analysis of PH.

While PH does not itself have much commercial interest, it is quite useful for academic pursuits due to the easy to handle monomer and the simplicity of polymer characterization. Several reports have presented ^{13}C NMR microstructures of PH with regard to regio- and stereochemistry.[5,6] Other published work has discussed results from the oligomerization of 1-hexene up to molecular weights of pentamers.[7,8] The polymerization systems used to prepare these polymers, however, were not living. It would not then be much more difficult to inspect the polymer end groups because of the variety present from reinitiation of a polymer chain after an elimination process. Also,

most end groups are not visible due to the their insignificant contribution compared to the main chain resonances.

With these deficiencies, oligomerization of 1-hexene with a living catalyst system would provide greater information since all polymer chains are well-defined and virtually identical. At low molecular weights, the end group resonances should be more apparent, for the short chain will not contain long runs of identical insertion events. The saturated polymers should all appear as methyl terminated at both ends since no terminations events have occurred. Also from this, the enantiofacial selectivity for initiation (or first insertion into the Zr-Me bond) should be attainable.

First, Figure 53 shows the ^{1}H NMR spectrum for an oligomeric PH prepared from **22a** at –10 °C. The material has a molecular weight of 1800 and a narrow PDI of 1.06.

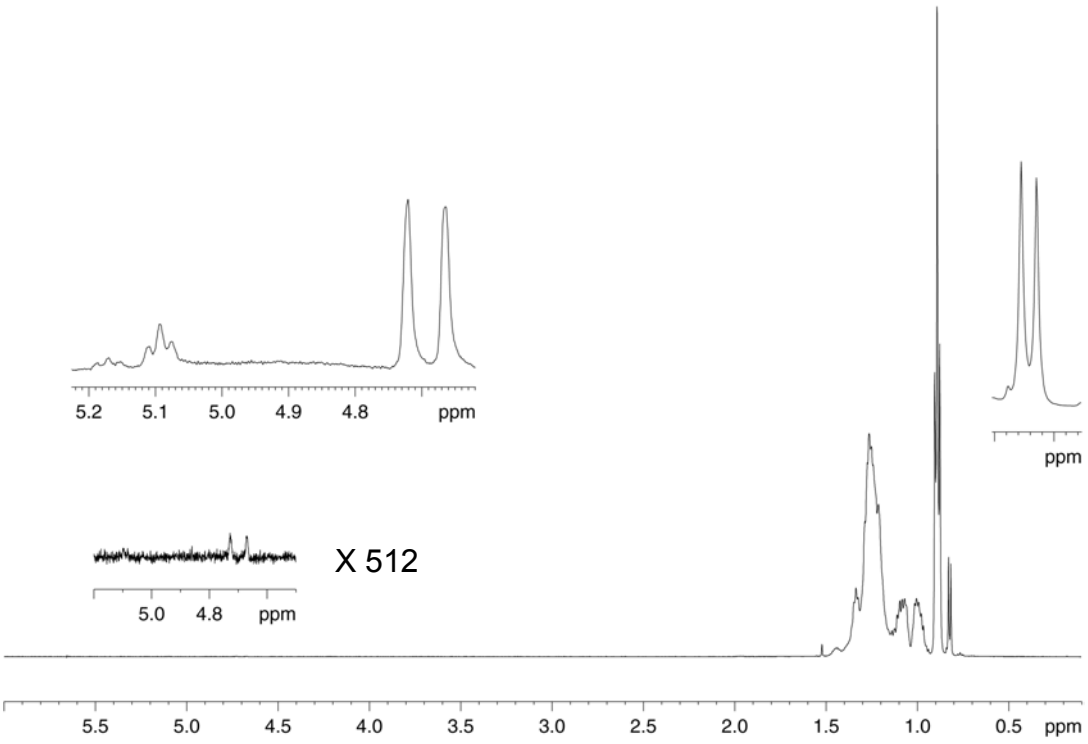

Figure 53. ^{1}H NMR spectrum (400 MHz, $CDCl_3$, RT) of oligomeric PH prepared from **22a** at –10 °C.

With a calculated DP of only 15, the methyl end group is apparent as a doublet at δ 0.83 ppm. No other information can be gleaned from the saturated portion of the spectrum. Looking further downfield, high magnification is necessary to see the very small signals indicating that elimination reactions are active. An optimized acquisition on this region enhances these signals, and aside from the broad singlets for β-hydride elimination, triplets assigned to elimination after 1,3-isomerizations (presumably following the same pathway as chain-end epimerization to get the Zr center onto C3 of the last inserted monomer unit) are also visible.

For the same PH oligomer, the ^{13}C NMR spectrum is shown in Figure 54. Aside from the peaks assignable to the main chain carbon units, many smaller resonances appear which are presumed to be end groups; that is, terminal insertion units. Starting with ^{13}C-**22a**, a separate oligomerization experiment was performed to ascertain which signals represented the terminal CH_3 end caps and the relative ratio of the two diastereomeric products from the first insertion. Integration of the two large resonances at δ 19.93 and 20.37 within an nOe-suppressed ^{13}C {^1H} NMR spectrum provided a 90 : 10 ratio for the enantiofacial selectivity of insertion into the Zr-Me bond. Selectivity for the first insertion of monomer for other systems has not been nearly as successful. Zambelli reported, for a heterogeneous Ziegler-Natta system, that the first insertion of styrene was highly regiospecific, though the initiation featured an enantioselectivity of only 2 : 1.[9] Erker and coworkers discovered that a mere 60 : 40 mixture for initiation with propylene was induced with a chiral metallocene.[10] As mentioned previously, insertions into M-H and M-Et (or M-polymer) bonds occur with high but opposite enantioselectivity with the *rac*-EBTHI ligand set, whereas insertion into Zr-Me has no face selectivity.[11-13]

After successfully pinpointing the terminal CH_3 groups, the identities of the remaining signals still did not immediately come to light. Asakura assigned resonances in the ^{13}C NMR for isotactic PH along with the relevant stereoerrors,[5] and this analysis was first employed to assign the additional resonances. His microstructural analysis did not match with the observed resonances seen for C1, C2, or C4. Also, the fact that these signals steadily diminished with molecular weight of PH would have necessitated that misinsertions would have to be occurring early during polymerization, when monomer concentration was highest, but would cease as the chain lengthened. While not common for Ziegler-Natta systems,[14] Rieger has observed a reduction in isotacticity

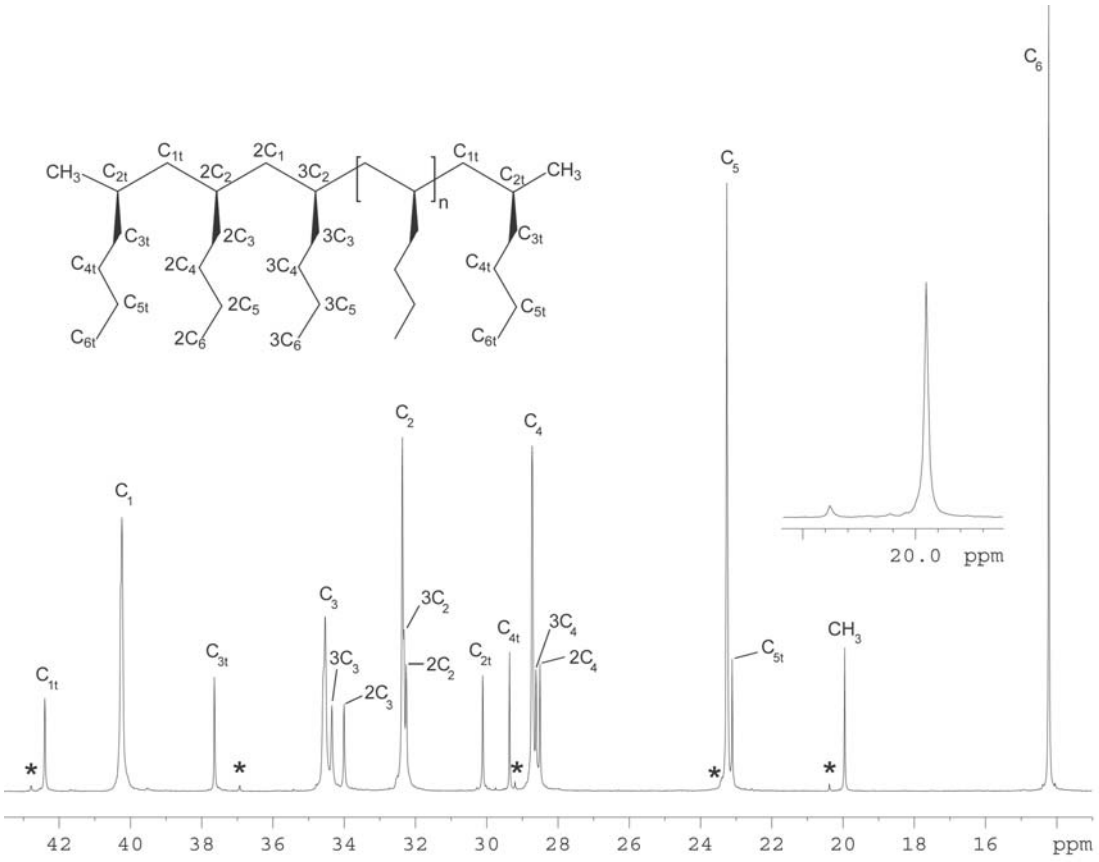

Figure 54. ^{13}C NMR spectrum (400 MHz, $CDCl_3$, RT) of a PH oligomer from **22a**. The asterisk (*) denotes the product of opposite enantiofacial selectivity for the first insertion.

at higher propylene concentration for a C_1-symmetric metallocene.[15] Performing polymerizations with **22a** at monomer concentrations of 1.14 and 0.092 M provided PH with superimposable ^{13}C NMR spectra, suggesting that polymer microstructure was not dependent on monomer concentration.

This then lead to the assumption that the signals were indeed terminal insertion events, since they are likely to be experiencing different environments compared to the units buried in the center of the chain. To aid in further identification, a 2D ^{1}H-^{13}C HSQC-TOCSY experiment was performed on the PH oligomer. From this, it was possible to trace carbon-carbon connectivity from a point in the spectrum where a resonance had been identified, which turned out to be the methyl end group. Starting from the signal at 19.93 ppm, a strong correlation peak is present with the five other resonances at 42.40, 30.11, 37.62, 29.33, and 23.07 ppm (Table 9). These correspond to the signals for the first and last inserted monomer unit, since a symmetry plane exists in isotactic PH. A ^{13}C DEPT NMR experiment agrees with these assessments.

Carbon	Terminal Unit (ppm)	2nd Unit (ppm)	3rd Unit (ppm)	Misinsertion Unit (ppm)
C_1	42.40	n.o.	n.o.	42.78
C_2	30.11	(32.27)	(32.31)	29.18
C_3	37.62	34.00	(34.34)	36.91
C_4	29.33	28.50	(28.59)	n.o.
C_5	23.07	n.o.	n.o.	23.33
C_6	n.o.	n.o.	n.o.	n.o.

Table 9. ^{13}C NMR chemical shifts for end groups present in low molecular weight PH. Numbers in parentheses represent signals present within the 1D spectrum, but without sufficient resolution to show correlation in the 2D HSQC-TOCSY experiment. (n.o. = not observable).

Importantly, it is possible to see further into the chain, for the additional signals are due to the second and third insertions. While sufficient resolution was not achieved distinguish the very small chemical shift differences between the main chain and some of the end group resonances, designating them as subsequent insertion units is not a stretch. The error in the first insertion imparts slight chemical shift differences to the carbon atoms of this unit which can also be identified from this spectrum by discovery of correlation peaks between the minor terminal CH_3 resonance for opposite face insertion.

This is an illustration of how precarious it can be to assign microstructure to low molecular weight materials based on one ^{13}C NMR spectrum. In oligomers from **22a**, the C3 end units could easily be mistaken for stereoerrors. With metallocenes undergoing several eliminations / reinitiations, the build-up of additional resonances in NMR spectrum can easily lead to misassignments.

Polymers obtained with **29d** feature a loss of stereocontrol, and this is also mimicked in the corresponding oligomers. As shown in Figure 55, the ^{13}C NMR spectrum contains many more signals as compared to the stereoregular material from **22a**. Inspection of the CH_3 end group resonance shows more than the two signals that should arise from the options available for enantiofacial selectivity of the first insertion. The other signals do not, however, correspond to 2,1-insertions. The numerous resonances make sense in terms of long range reporting of microstructure. Just as the C3 resonance of the polymer is sensitive to adjacent asymmetric centers, so to is the methyl group. Therefore, the methyl end group senses the nonstereoregular insertions and displays the variety of ensuing insertion patterns.

A common practice in α-olefin polymerization with metallocenes is the use of excess precatalyst or cocatalyst, in particular those based on Al, to scavenge impurities from the reaction vessel during polymerization. This then raises the question on whether these additional materials may affect polymer microstructure, or if they are

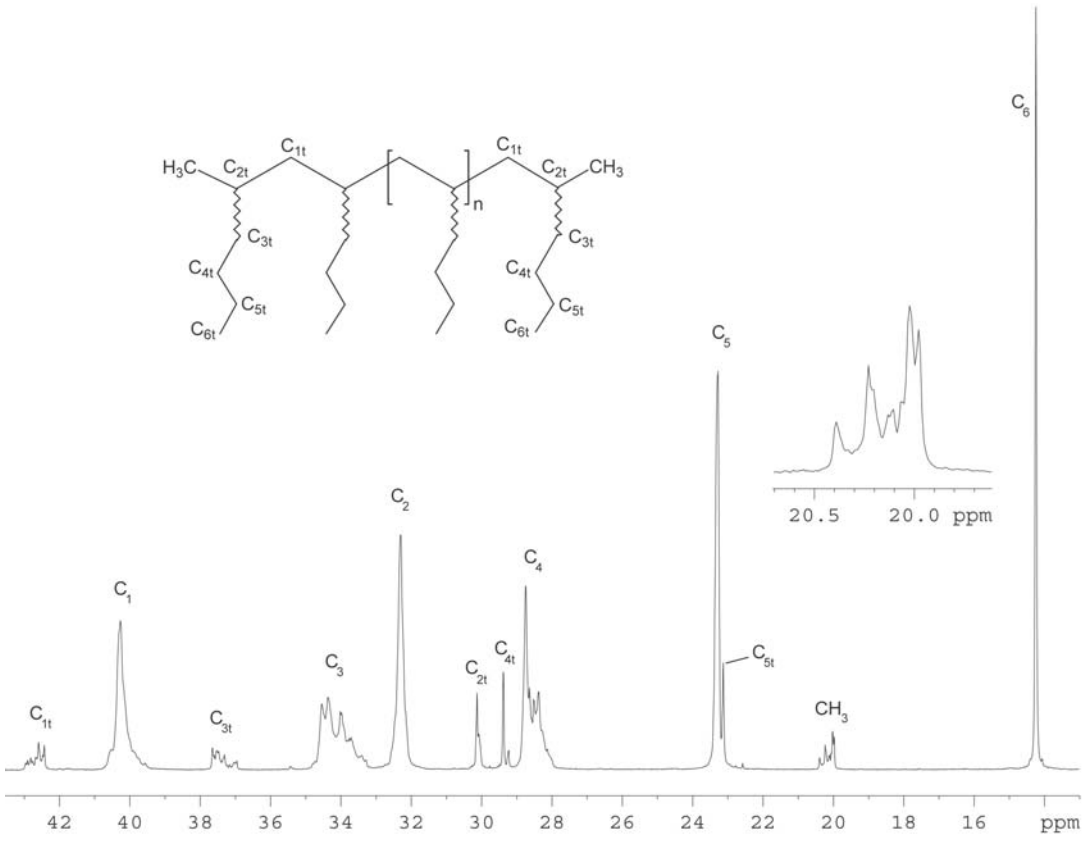

Figure 55. ^{13}C NMR spectrum (400 MHz, $CDCl_3$, RT) of PH oligomers prepared from **15d**.

merely innocent bystanders. In the first experiment, a 10 % stoichiometric excess of $[Ph_3C][B(C_6F_5)_4]$ was used in an oligomerization with **6a**. The resultant low molecular weight PH (M_n = 1760 and PDI = 1.04) yielded a material with ^1H and ^{13}C NMR spectra essentially superimposable with that prepared from 1 : 1 stoichiometry. Thus, excess cocatalyst does not appear to impact the first insertion or further insertions.

An oligomerization employing 10 % excess **6a**, however, negatively affected each step of monomer insertion, including initiation. As can be seen in Figure 56, the once sharp end group resonances in Figure 54 are now riddled with smaller partners about the base of each. The material still maintains a high degree of isotactic nature,

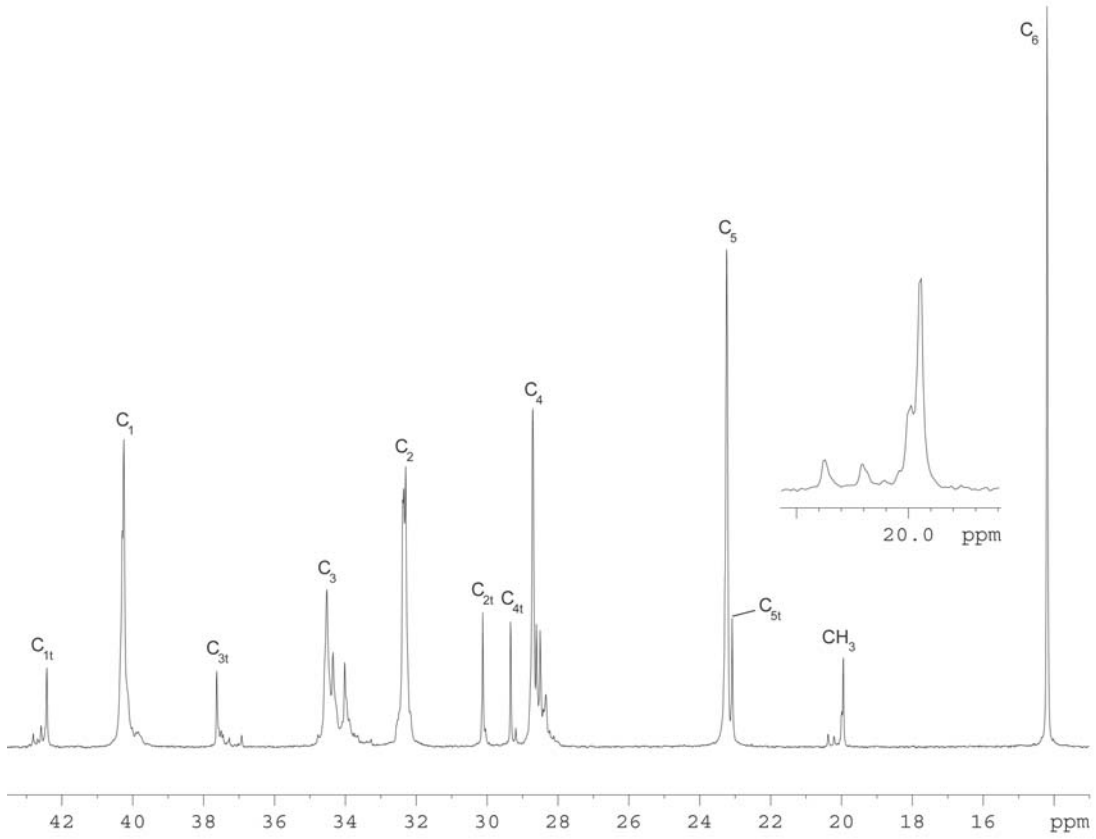

Figure 56. ^{13}C NMR spectrum (400 MHz, $CDCl_3$, RT) of oligomeric PH prepared with 10 mol % excess **6a**.

certainly better so than the material derived from **22d**. Our group has discussed other results in this regard in terms of a degenerative transfer mechanism.[16] While this will not be discussed in greater detail, the premise behind degenerative transfer involves dimeric monocationic species, as discussed earlier in Chapter 4, formed from a neutral and a cationic complex through an methyl bridge. Via this bridge, the methyl group can be exchanged between the two species, reversing their roles. However, the neutral species will undergo a certain amount of amidinate ring flipping which, upon facile methyl group exchange, will result in an opposite face selectivity for olefin, resulting in less stereoregular monomer insertion.

With knowledge that excess neutral species can affect polymer microstructure, this raised an interesting conceptual dilemma. If activation of the precatalyst by the cocatalyst, whether it be a borate or MAO, is not faster than both initiation and propagation, then initial catalytically active centers that have undergone several insertions would be in solution with unactivated neutral species, and this should influence the stereochemistry of those insertions. Only upon full activation by the cocatalyst would all centers commence stereospecific polymerization with **6a**. While it is difficult to quantitate the concentration of catalytically active species in a polymerization system, Landis has shown that unlike living polymerizations, the concentration of propagating species steadily increases in a logarithmic manner with **17** / $B(C_6F_5)_3$.[17] Further, he has shown that in an NMR scale experiment, approximately 50 % of the methyl initiator remains after addition of 100 eq of 1-hexene and that this remains even after further addition of ethylene or propylene.[18]

To test this with **6a** and $[Ph_3C][B(C_6F_5)_4]$, two oligomerization experiments were performed in which, for the first, the cation was generated in the presence of 1-hexene, and second, the cation was generated and allowed to sit without monomer for 15

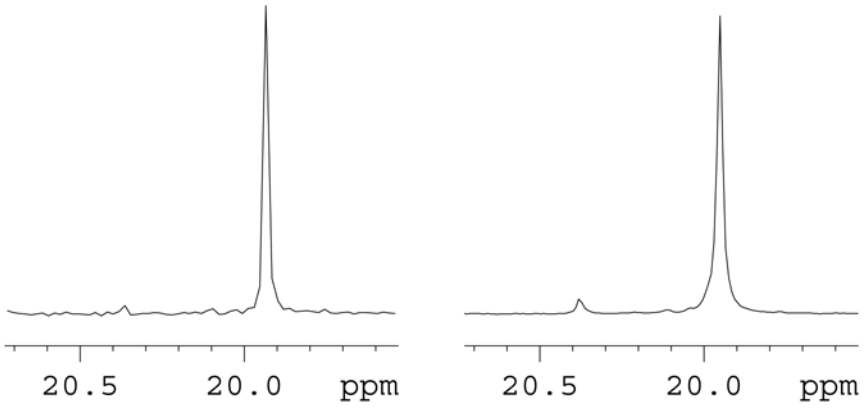

Figure 57. Methyl end group regions of two oligomeric PH samples illustrating the rapidity of activation of Cp*ZA's.

minutes before 1-hexene was added. If activation was not the fastest process, then inspection of the CH_3 end groups should show a mixture of resonances from multiple different stereochemical arrangements of the first few insertions. In this region, the only two signals evident in the ^{13}C NMR spectra for the two experiments were those seen in Figure 57, and in the same integrated ratio, providing evidence that activation of the precatalyst is quite rapid. The remainder of each spectra are equally identical.

One staple of living polymerization systems is the ability to prepare end-functionalized, or telechelic, materials in quantitative yield upon the addition of appropriate reagents to polymerization solutions. Though not with a living system, Marks has used $PhSiH_3$ in polymerizations with Ti CGC's to produce silyl-capped polymers.[19] Chung and Hessen have described methods for preparation of borane[20] and thiophene[21] end capped polymers, respectively. For this work, adding I_2 to a living PH oligomer prepared from **22a** induces homolytic bond cleavage of I_2, quenching the polymerization and generating a telechelic oligomer capped with a primary iodide. The ^{13}C NMR spectrum for this material is shown in Figure 58. Immediately apparent are the larger number of signals, but of greatest import is that at 17.46 ppm. This is the CH_2I group, and unlike the methyl end group which displayed two signals from a selectivity of ~ 90 %, this group is represented by a single resonance. Facial selectivity for main chain insertion must, then, occur with near perfect fidelity as compared to that of initiation. The last inserted monomer units near the CH_2I group are labeled in Figure 58 and assigned in Table 10.

7.3. Detailed Analysis of PB.

As with PH, oligomeric PB can be prepared from an appropriately low ratio of monomer to initiator. For one such oligomer (M_n = 2550, PDI = 1.01) prepared from **22a**, only a very small amount of evidence for elimination is present when the

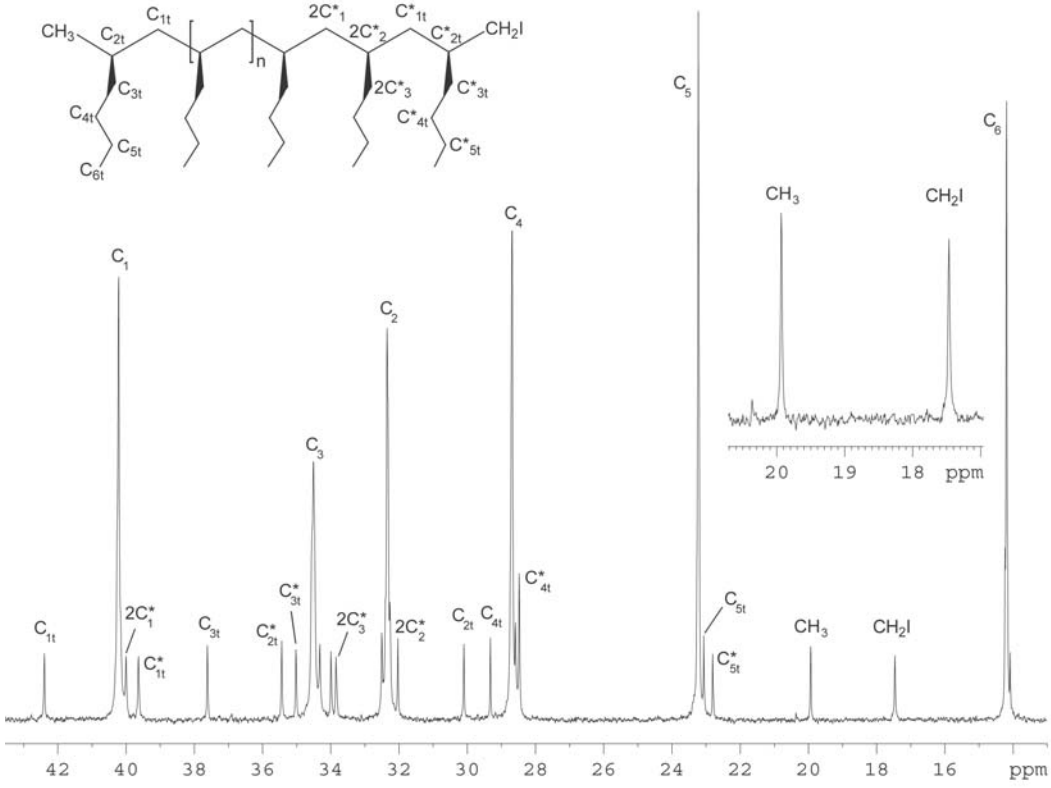

Figure 58. ^{13}C NMR spectrum (400 MHz, $CDCl_3$, RT) of a telechelic oligomer of PH prepared from **22a**.

Carbon Label	Chemical Shift (ppm)		
CH_2I	17.46	C^*_{4t}	28.50
C^*_{1t}	39.65	C^*_{5t}	22.82
C^*_{2t}	35.05	$2C^*_1$	40.10
C^*_{3t}	35.50	$2C^*_2$	32.01
		$2C^*_3$	33.78

Table 10. Chemical shifts and assignments of terminal insertions in I_2 quenched PH.

reaction is performed for two hours at –10 °C. Unlike PH, the methyl end groups of the polymer cannot be seen in the ^1H NMR presumably due to its coincidental chemical shift with the main CH_3 resonance of C_4.

Oligomers were prepared at different temperatures to test the effects on polymer microstructure. The results are listed in Table 11. While very little information can be weened from the aliphatic portion of the ^{1}H NMR, inspection of the unsaturated region where elimination products occur was enlightening.[22] Direct β-hydride elimination from

Run	Condition	M_n	PDI	**A**	**B**	**C**	**D**	**E**
1	-10 °C (75)	2550	1.01	--	--	--	--	--
2	RT (75)	2800	1.02	100	3.2	20.6	2.2	1.8
3	-10 °C (75), then RT (15)	2770	1.01	100	4.1	23.7	1.3	2.4
4	-10 °C (3 days)	2630	1.01	100	38.3	59.5	--	18

Table 11. PB oligomerization experiments with **22a**. Numbers in parentheses are reaction times in minutes.

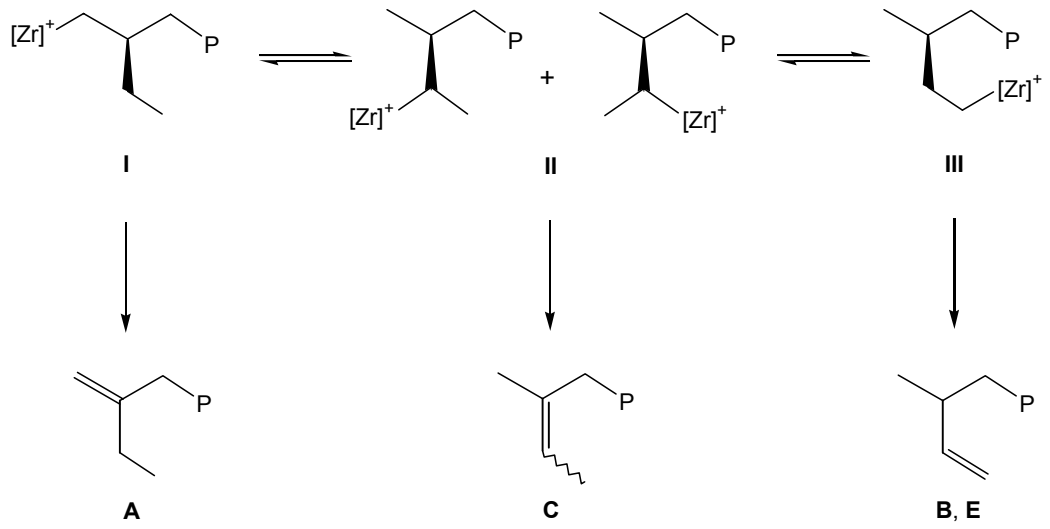

Scheme 43. Mechanisms describing the formation of unsaturated end groups in PB.

the product of a 1,2-insertion yields the vinylidene end group, **A**, as represented in Scheme 43. The two geminal hydrogens are inequivalent, with one cis to an ethyl group and the other cis to the polymer chain. Similar to chain epimerization, the Zr center can

chain walk to the methylene of the pendant ethyl group. Elimination from the methine carbon atom will provide either the (E)- or (Z)-trisubstituted alkene, **C**. The Zr center can further release down the chain to provide, as from 1,2-insertion, a methylene carbon bound to the metal. A vinyl end group will result from an ensuing termination, represented through **B** and **E**. Finally, the very small amounts of **D** may be due to cis-alkenes present upon elimination from a 2,1-insertion product. None, or no significant, amount of internal trisubstituted double bonds are apparent (Scheme 44). These would result from Zr isomerization to the methylene or methine of the last inserted monomer, followed by β-hydride elimination. If this were the case, the vinyl hydrogen should appear as a doublet in the ^{1}H NMR spectrum, yet only quartets are observed as expected from **C**.

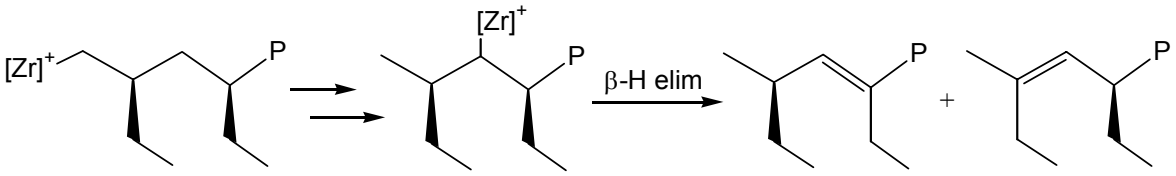

Scheme 44. Production of internal trisubstituted alkenes.

With both E and Z isomers being present, nonstereoselective isomerization must occur from **III** to **II** allowing formation of both isomers of the latter. Taken together, these facts point to facile chain-walking that is limited to the last monomer unit which drastically contrasts this same process within late transition metal complexes.[23] Also, narrow polydispersity oligomers are obtained suggesting that this process is not competitive with propagation, such that any isomerizations occur only after all monomer has been consumed.

From Table 11, the relative ratio of terminated products is comparable between runs 2 and 3. The smaller values relative to **A** in runs 2 and 3 versus 4 may be due to the longer reaction time at the higher temperature. In this case, it is plausible that greater decomposition occurs to form **25** at the higher reaction temperature, from which no further isomerization of the terminated polymer chain could occur. However, maintaining the living polymer at –10 °C for extremely long periods of time, as in run 4, bestowed longevity to the isomerization process, allowing much larger amounts of the vinyl terminated product.

While ^{1}H NMR proves to be a useful tool for examining elimination products in PB, the saturated portion of the spectrum is conversely not instructive. Greater information comes from the ^{13}C NMR of these materials. The ^{13}C NMR spectrum for the waxy PB from run 1 containing saturated end groups is shown in Figure 59. As with oligomeric PH, the CH_3 end groups have a resonance around δ 20 ppm with a similar diastereomeric ratio of 9 : 1 observed for the first insertion. Compared to a 1-butene tetramer prepared by Kaminsky with a chiral C_2-symmetric metallocene, **22a** is more selective, with the former only displaying selectivities of about 2 : 1 for the first insertion and 5 : 1 for the second insertion.[24] As opposed to PH, the last three terminal monomer units can be more easily identified through a 2D ^{13}C-^{1}H HSQC-TOCSY experiment, and the chemical shifts for the respective carbon atoms are as represented in Scheme 45. No signals could be seen in the double bond region of the ^{13}C NMR spectrum for this material.

As with PH, preparation of PB from a C_s-symmetric amidinate precatalyst produced a material with a greater mixture of resonances in the ^{13}C NMR spectrum. This is shown in Figure 60 for an oligomeric PB prepared from **22d** with an M_n value of 2700 and a PDI of 1.01. The CH_3 end group region contains a multitude of resonances,

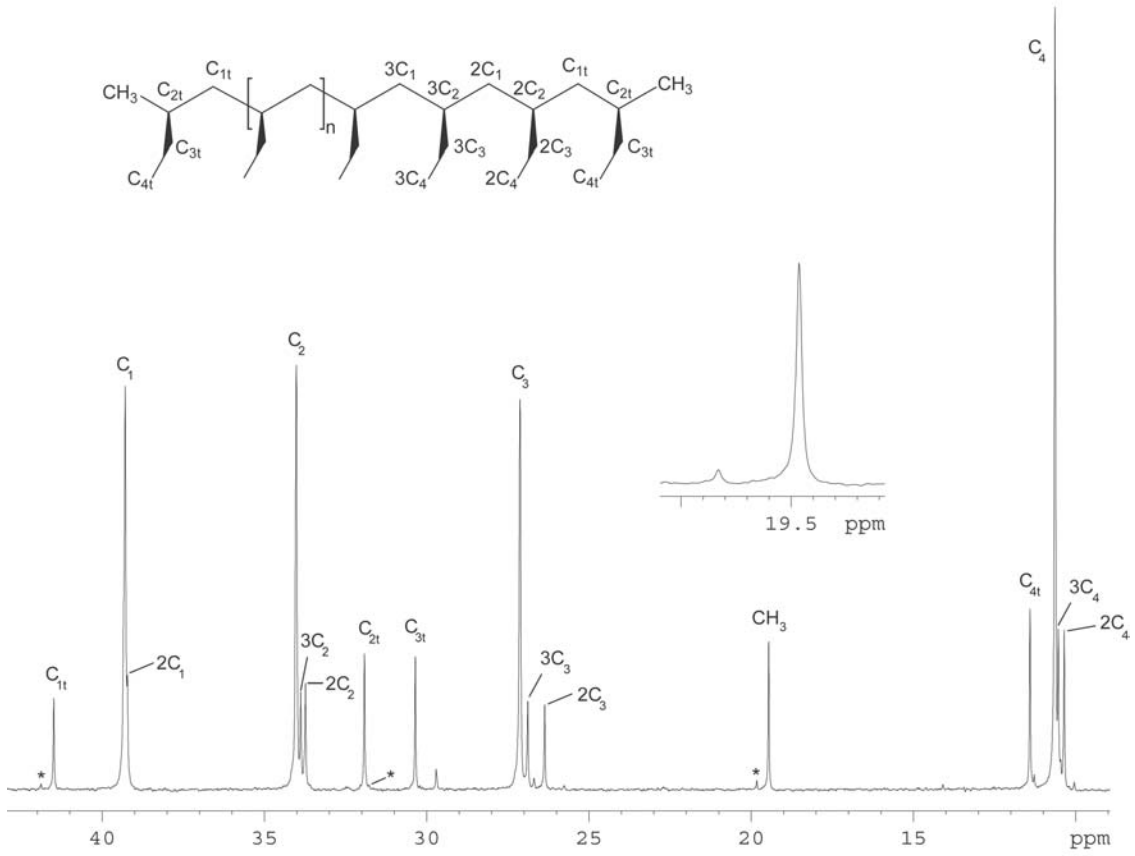

Figure 59. ^{13}C NMR spectrum (400 MHz, $CDCl_3$, RT) of oligomers of PB from precatalyst **6a**.

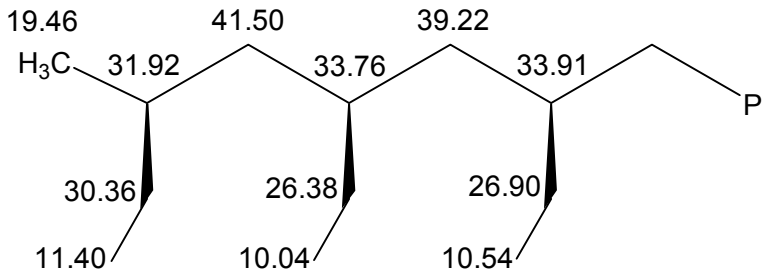

Scheme 45. Schematic representation of ^{13}C NMR chemical shifts of terminal insertion units in low molecular weight isotactic PB.

resonances, indicative of the many varieties of subsequent insertions that impart small chemical shift differences in this signal. This is equally seen upon inspection of the resonances for the last inserted monomer unit.

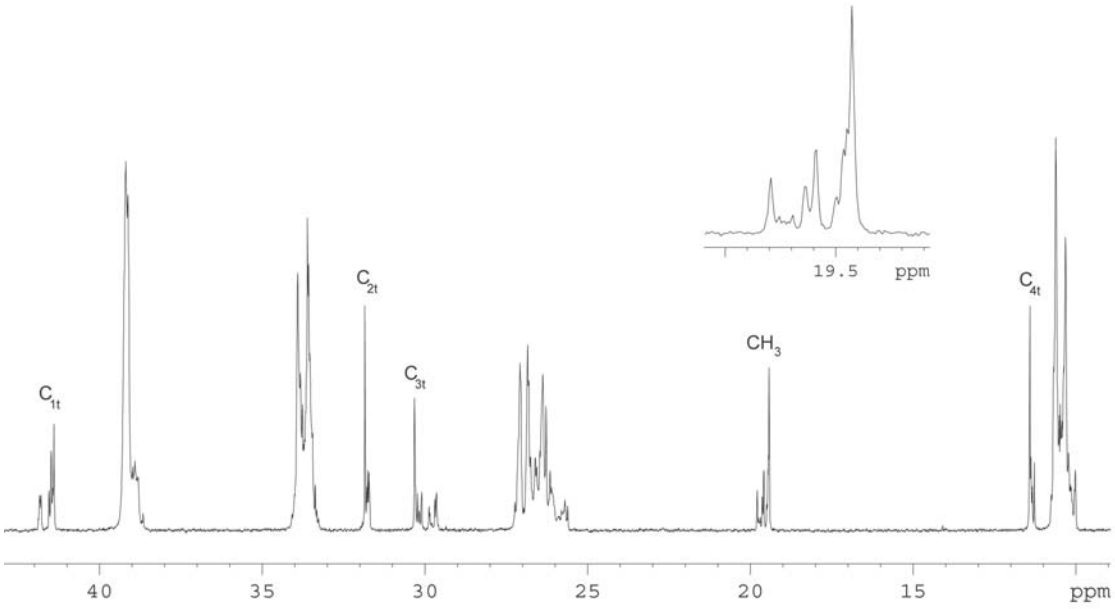

Figure 60. ^{13}C NMR spectrum (400 MHz, $CDCl_3$, RT) of PB oligomers from initiator **22d**.

Unlike 1-butene polymerizations with *rac*-$SiMe_2$(EBTHI)$ZrCl_2$ and MAO, a terminal CH_3 appears to be the only end group present from oligomerizations with **22a** at –10 °C at short reaction times.[22] Presented in Figure 61 is an oligomer from run 4, in which the polymerization was quenched after 72 hours at –10 °C. From the ^1H NMR spectrum of this oligomer, a significant amount of elimination had occurred with three main types of alkene species being formed: vinyl, trisubstituted, and vinylidene. From the ^{13}C NMR spectra, these species could be located as listed in Table 12. More difficult to assign, however, are signals present in the single bond region.

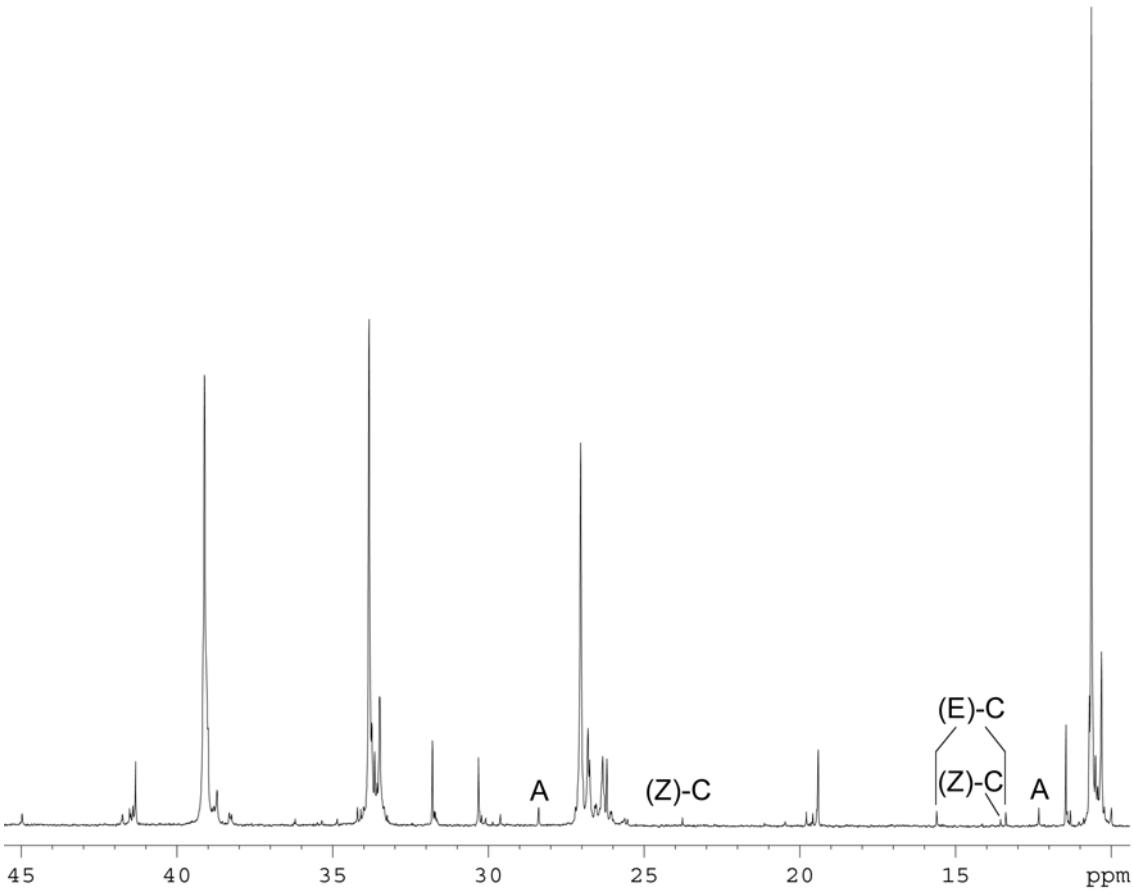

Figure 61. Partial ^{13}C NMR spectrum (400 MHz, $CDCl_3$, RT) of a PB oligomer prepared from **22a** and quenched after 72 hours at –10 °C.

Alkene	C(1) (ppm)	C(2) (ppm)
Vinylidene (**A**)	109.1	150.5
(Z)-trisubstituted (**C**)	119.1	134.0
(E)-trisubstituted (**C**)	119.5	134.7
Vinyl (**B** + **E**)	112.0	145.2

Table 12. ^{13}C NMR chemical shifts of alkene products from PB oligomerization.

Outside the double bond region, it is possible to find resonances representing the major unsaturated products. The assignments are based on a previous report on

PB end groups.[22] Signals from the vinyl end group are difficult to find due to insufficient signal intensity. Not all signals present could be definitively assigned based on this paper, since oligomers from **22a** chain walk only within the last monomer unit, as opposed to the metallocene used which produces internal alkene units. On the other hand, it is possible to determine that no accumulation of 2,1-insertions occurs either within the main chain or at the polymer chain end at –10 °C.

For RT oligomerizations, 2,1-insertions appear to be present. Although quite infrequent, the presence of 1,2-disubstituted alkenes (**D**) seen in the ^{1}H NMR most likely arises from a regioirregular insertion followed by β-hydride elimination (Scheme 46). The elimination, though only shown for one, may actually occur from either of the β-methylene carbons. These signals are absent at lower polymerization temperatures. Being so minor (less than 3 % of the intensity of the vinylidene end group, **A**), resonances in the ^{13}C NMR spectrum are not visible.

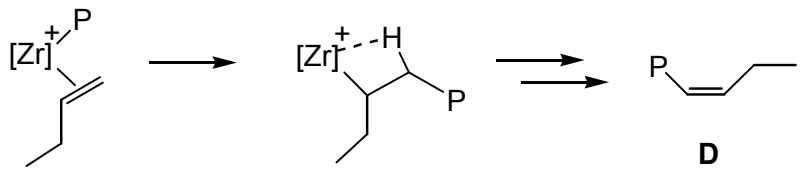

Scheme 46. Production of 1,2-disubstituted alkenes, **D**, after a 2,1-misinsertion.

7.4. Conclusions.

Low molecular weight oligomers of PH and PB are easily prepared from **22a**. Upon closer inspection, what first appear to be stereoerrors actually turn out to be resonances for the terminal, penultimate, and pen-penultimate monomer insertions. Initiation shows an enantiofacial selectivity of 9 : 1 for the first insertion of either 1-hexene or 1-butene into the Zr-CH_3 bond. At –10 °C, the only end group that appears at

short reaction times is the terminal CH_3. However, quenching after several days at low temperature, or warming to RT, displayed a larger degree of unsaturated end groups. Three main alkenes were evident in the ^1H and ^{13}C NMR spectra: vinylidene (**A**), (E)- and (Z)-trisubstituted (**C**), and vinyl (**B** + **E**). It appears that each resonance grows in at an equal rate, meaning that the isomerization, which is relegated to the last inserted monomer unit, is quite facile between the many possible alkenes.

Telechelic polymers have also been prepared upon addition if I_2 to the living oligomer system at –10 °C. Assessing the signal for the primary iodide formed shows a single peak, indicative of main chain monomer insertion that is perfectly stereospecific. Contrary to the excellent regio- and stereoselectivity present at low temperature, oligomers of PB prepared at RT with **22a** show a small amount of evidence for 2,1-insertions.

7.5. References.

(1) Eshuls, J. J. W.; Tan, Y. Y.; Meetsma, A.; Teuben, J. H. *Organometallics* **1992**, *11*, 362.

(2) Rossi, A.; Zhang, J.; Odian, G. *Macromolecules* **1996**, *29*, 2331.

(3) Carvill, A.; Zetta, L.; Zannoni, G.; Sacchi, M. C. *Macromolecules* **1998**, *31*, 3783.

(4) Janiak, C.; Lange, K. C. H.; Marquardt, P.; Kruger, R. P.; Hanselmann, R. *Macromol. Chem. Phys.* **2002**, *203*, 129.

(5) Asakura, T.; Demura, M.; Nishiyama, Y. *Macromolecules* **1991**, *24*, 2334.

(6) Babu, G. N.; NewMark, R. A.; Chien, J. C. W. *Macromolecules* **1994**, *27*, 3383.

(7) Liu, H. Q.; Deffieux, A.; Sigwalt, P. *Makromol. Chem.* **1991**, *192*, 2111.

(8) van der Linden, A. J.; Schaverien, C. J.; Meijboom, N.; Ganter, C.; Orpen, A. G. *J. Am. Chem. Soc.* **1995**, *117*, 3008.

(9) Ammendola, P.; Tancredi, T.; Zambelli, A. *Macromolecules* **1986**, *19*, 307.

(10) Dahlmann, M.; Erker, G.; Nissinen, M.; Frohlich, R. *J. Am. Chem. Soc.* **1999**, *121*, 2820.

(11) Waymouth, R. M.; Pino, P. *J. Am. Chem. Soc.* **1990**, *112*, 4911.

(12) Longo, P.; Grassi, A.; Pellecchia, C.; Zambelli, A. *Macromolecules* **1987**, *20*, 1015.

(13) Sacchi, M. C.; Barsties, E.; Tritto, I.; Locatelli, P.; Brintzinger, H. H.; Stehling, U. *Macromolecules* **1997**, *30*, 3955.

(14) Resconi, L.; Cavallo, L.; Fait, A.; Piemontesi, F. *Chem. Rev.* **2000**, *100*, 1253.

(15) Rieger, B.; Jany, G.; Fawzi, R.; Steinman, M. *Organometallics* **1994**, *13*, 647.

(16) Zhang, Y. H.; Keaton, R. J.; Sita, L. R. *J. Am. Chem. Soc.* **2003**, *125*, 9062.

(17) Liu, Z.; Somsook, E.; White, C. B.; Rosaaen, K. A.; Landis, C. R. *J. Am. Chem. Soc.* **2001**, *123*, 11193.

(18) Landis, C. R.; Rosaaen, K. A.; Sillars, D. R. *J. Am. Chem. Soc.* **2003**, *125*, 1710.

(19) Koo, K. M.; Marks, T. J. *J. Am. Chem. Soc.* **1998**, *120*, 4019.

(20) Chung, T. C.; Xu, G.; Lu, Y.; Hu, Y. *Macromolecules* **2001**, *34*, 8040.

(21) Ringelberg, S. N.; Meetsma, A.; Hessen, B.; Teuben, J. H. *J. Am. Chem. Soc.* **1999**, *121*, 6082.

(22) Rossi, A.; Odian, G.; Zhang, J. *Macromolecules* **1995**, *28*, 1739.

(23) Ittel, S. D.; Johnson, L. K.; Brookhart, M. *Chem. Rev.* **2000**, *100*, 1169.

(24) Kaminsky, W.; Ahlers, A.; Moller-Lindenhof, N. *Angew. Chem. Int. Ed. Engl.* **1989**, *28*, 1216.

Chapter 8

Conclusions

8.1. Mechanism of Polymerization.

As mentioned, the neutral Cp*ZA precatalyst **6a** is configurationally unstable with respect to amidinate ring flipping. Configurational instability has been seen before with non-ansa-bridged metallocenes to produce elastomeric PP. Waymouth has reported a class of unconstrained metallocenes, shown in Scheme 47, which display rapid rotation about the centroid of the 2-(phenyl)indenyl ligands.[1,2] Indeed, the racemization between the *rac* and *meso* forms of this "oscillating catalyst" is so facile that it cannot be frozen out even at –100 °C.[3] In the *rac* mode, isospecific polymerization is proposed due to the C_2-symmetry relationship of the two coordination sites. Upon rotation of either substituted Cp ligand, monomer binding with either face has equal energy, and this will produce an atactic chain. This design yields isotactic-atactic stereoblock polyolefins, which have slightly crystalline, elastomeric properties for PP. The ansa-bridged

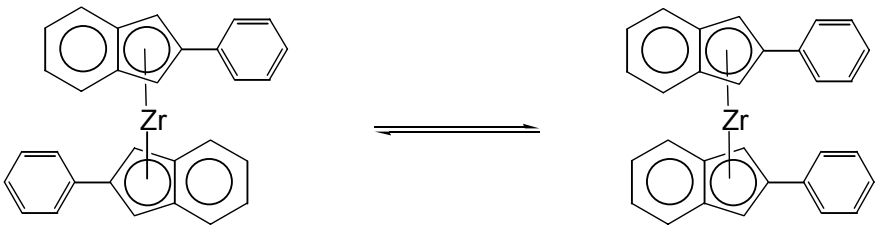

racemic, isotactic meso, atactic

Scheme 47. Interchange between racemic and meso forms for synthesis of isotactic-atactic stereoblock polyolefins via an "oscillating catalyst".

analogue of this metallocene was prepared, and just as seen with $EBIZrCl_2$,[4] the meso and racemic isomers produced atactic and isotactic PP, respectively, consistent with ligand isomerization in solution.[5]

After activation of **6a** via a borate salt to generate cationic **22a**, configurational stability is heightened due to a shortening of the Zr-N bond lengths. This is also substantiated from the lack of stereoblock microstructure, which would result from amidinate ring flipping. It is necessary to understand how an isotactic polymer can be produced from such an asymmetric species. C_1-symmetric metallocenes are capable of polymerizing α-olefins into a whole range of varying microstructures.[6] Starting from the syndiospecific, C_s-symmetric precatalyst shown in Scheme 48, adding a continually larger alkyl substituent to the 3-position of the Cp ring steadily increases the amount of *mmmm* pentads, transforming the catalyst from syndiospecific to isospecific.[7,8]

The mechanism by which this transformation occurs can be explained through steric interactions.[9] The unsubstituted derivative has sites A and B which are enantiotopic and are related by a mirror plane. The sites will bind monomer with opposite face selectivities, producing syndiotactic polymer. For the methyl substituted derivative with the polymer chain located in the open environment of site A, this dictates to site B a preference for *si* monomer in order to place the R group of the monomer anti

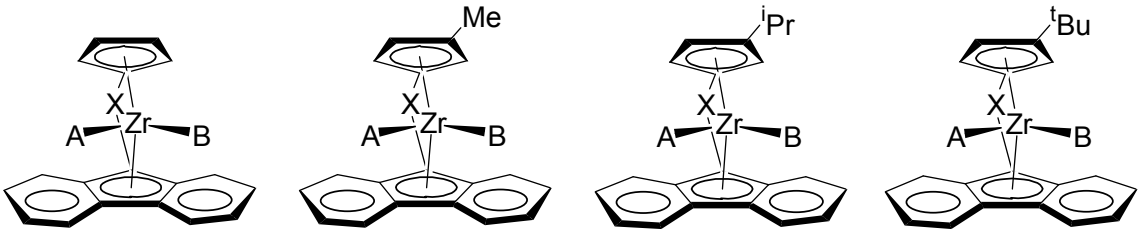

Scheme 48. Cp ring substitution transforms a formerly C_s-symmetric syndiospecific precatalyst into a C_1-symmetric isospecific precatalyst.

to the growing polymer. With the polymer chain occupying site B, no preference is given for the orientation of the polymer chain, and the monomer will bind equally well with both faces, producing the hemiisotactic microstructure in which every other insertion is isotactic, while those in between are atactic.

For the ^{t}Bu derivatized analogue, site B is simply too sterically hindered to allow for the polymer chain to occupy this position. Morokuma and coworkers calculated an energy increase of 12.2 kcal / mol for propylene insertion in the case where the polymer chain is in site B versus site A.[10] Thus it will reside in site A where steric repulsions are less, directing monomer coordination with a *si* facial preference (Scheme 49). Upon chain migratory insertion with the ^{t}Bu derivative, having rate constant k_p, nonbonding steric repulsions will force the polymer chain back to its former position in the open sector. This reestablishment of the growing chain in the same coordination site after each insertion is known as chain back-skip, also referred to as site isomerization (k_{iso}).[11,12] As such, monomer coordination occurs on the same side with the same facial preference, resulting in an isotactic propagation mechanism through one site. It has been argued, however, that this effect is not necessary, since calculational studies by

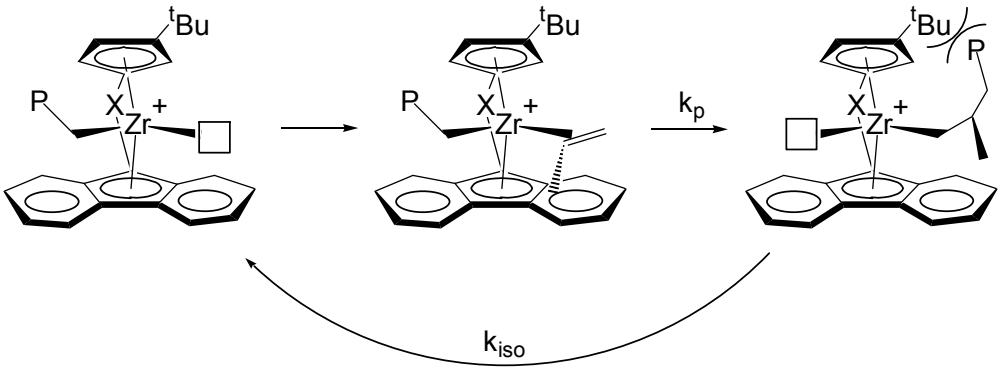

Scheme 49. Isotactic propagation from a C_1-symmetric metallocene through one site mechanism by means of the polymer chain back-skip isomerization.

Fink predict that the coordination of the same face of the monomer to either site has a minimal energy difference in the insertion transition state (ΔE = 0.53 kcal / mol).[8]

Similar site isomerization after insertion was proposed for the nonsubstituted derivative, a syndiospecific catalyst which was found to produce a lower percentage of *rrrr* pentads at low monomer concentrations.[2] Raising the concentration of propylene increased the polymer stereoregularity, decreasing the concentration of the *rrmr* pentad. This behavior at low monomer concentration was explained as a chain back skip after monomer insertion which would result in two consecutive monomer insertions coming from the same site, producing the *m* dyad.[13]

This site isomerization mechanism has direct bearing on the mode of monomer insertion with **22a** (Scheme 50). Whether for insertion into the Zr-CH_3 of **22a** or into a living polymer chain derived from **22a**, monomer binding is proposed to occur on the

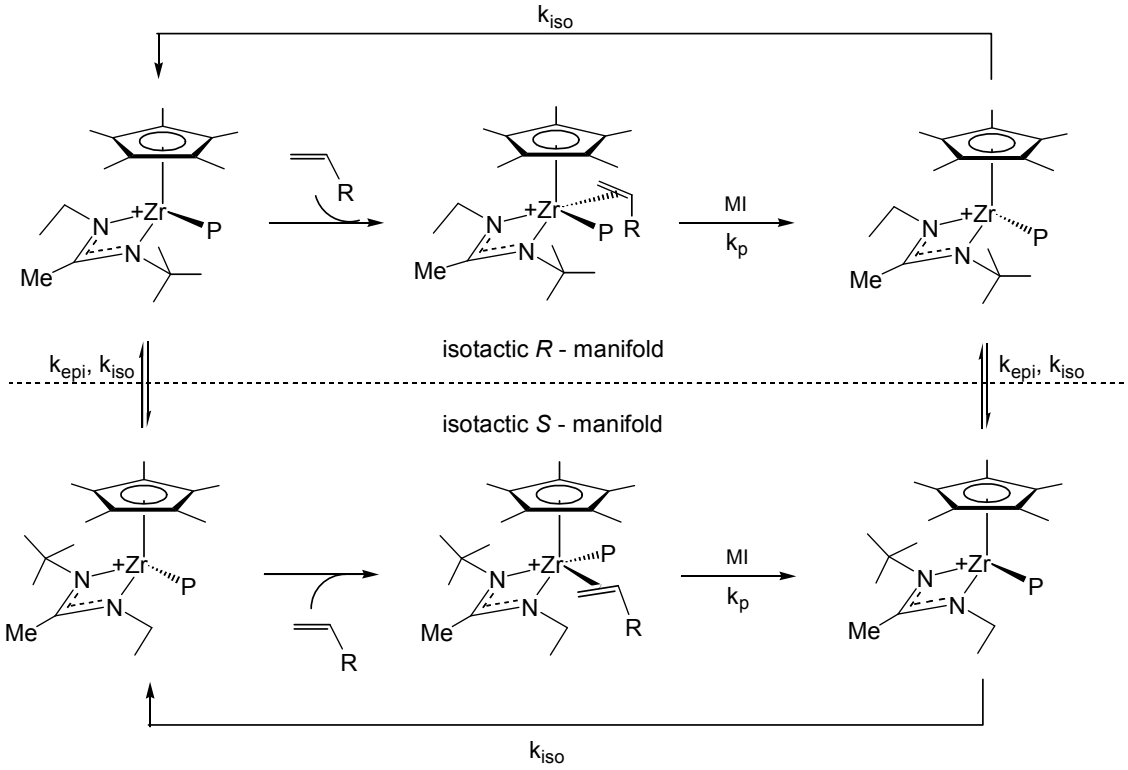

Scheme 50. Mechanism for stereospecific control with initiator **22a**.

side of the metal closest to the ethyl portion of the amidinate as suggested from cyclopentene insertion. Migratory insertion then puts the polymer chain near the ethyl group. However, it is possible that steric congestion cannot allow for monomer coordination to the site of unsaturation on the metal between the polymer chain and the ^{t}Bu group of the amidinate. Thus, chain back skip must occur to put the polymer chain back near the ^{t}Bu side before another unit of monomer can coordinate to lengthen the chain. This mechanism, then, is a mimic of the single-site mechanism proposed above.

To explain the isotactic microstructure and living polymerization behavior that are observed with this initiator, several stipulations must first be met. First, site isomerization (k_{iso}) must be much faster than propagation (k_p) in order to obtain isotactic polymer, otherwise a greater number of stereoerrors would be observed, and atactic behavior would be expected when the two are near equality. With syndiotactic polymer not being observed from C_s-symmetric Cp*ZA's, k_p and k_{iso} must be closer in magnitude for this set of initiators. For polymerization with C_1-symmetric **22a**, both of these processes must be faster than amidinate ring flipping, for this would produce isotactic stereoblock materials. For the living behavior and narrow polydispersity polymers to be realized, initiation (k_i) must be faster the k_p, which in turn must be much faster than termination. Although evidence for termination was evident at longer reaction times, it appears to be sufficiently slow at the short times employed for polymerizations ($\leq$ 2 hrs).

8.2. Ongoing and Future Investigations.

Related to the oligomers of PB, disseminating the rates of formation of each different type of unsaturated end group is currently underway. This will give information about the ability of Cp*ZA's to chain-walk through the alkyl chain of the last inserted monomer unit. Also, current investigations by Matthew Harney appear to suggest that chain walking also occurs during 1-dodecene polymerization. After cleavage with I_2, ^{1}H NMR

spectra do not show a multitude of signals for the various alkyl iodides that would be expected as the [Zr^+] walks along the chain.

Understanding precisely how the living polymer decomposes in solution is of utmost importance. With halide abstraction from the polymerization solvent appearing as the ultimate destination for decomposition, in what manner the Zr center accommodates this process, or in what chemical state the Zr center exists as, will have to be studied in order to circumvent this termination pathway. While structure **24** may play a role along this track, it is likely specific for polymerizations employing [$PhNHMe_2$][$B(C_6F_5)_4$], since it appears that **24** likely results from deprotonation of a bridging methyl group by $PhNMe_2$. Also, the dichloro bridged dimer **25** is formed in polymerizations with [Ph_3C][$B(C_6F_5)_4$], suggesting that $PhNMe_2$ is not required for its formation.

Also related to this, using simple alkyl groups bound to Zr, in order to imitate polymer chains, is not a viable method of studying active processes in, or stabilities of, polymerization solutions. In the studies with **43**, all of the derivatives discussed herein were more stable than a living polymer derived from **22a** and 1-^{13}C-1-decene. In preliminary work by Matthew Harney, **43e** decomposes with a $t_{1/2}$ value of 20.0 hrs at 0 °C, while the living polymer has a half life of only 2.6 hrs (Scheme 51). A more elaborate alkyl group, being (2-ethyl)butyl, bound to Zr ($t_{1/2}$ = 10.3 hrs) was still not sufficient to mimic the living polymer chain.

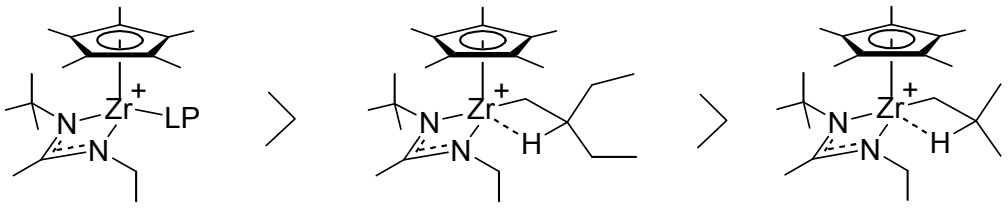

Scheme 51. Relation of Zr bound alkyl groups to their rates of decomposition at 0 °C.

With the dinuclear dimeric dications observed in the simplest system, that being the methyl cation, **22a**, it raises the question of whether these species exist during polymerization when larger alkyl groups are bound to the metal. Evidence against dimers in solution comes from the molecular structures determined for **23** and **43e**. For **23**, a ^{t}Bu substituent instead of a CH_3 on the amidinate provided sufficient steric hindrance to inhibit dimerization. In the case of **43e**, it is feasible that the agostic interaction could have served as the bridge within a dimeric structure, but that is not seen. Instead, the agostically ligated molecule appears as a mononuclear cation, stabilized not through dimerization, but through an intramolecular β-hydrogen agostic interaction. Although no evidence exists for agostic interactions in solutions of Cp*ZA living polymers, these illustrations suggest that dimerization can be sufficiently inhibited through slight manipulations in the sterics about the metal.

A higher facial selectivity for initiation is also a development that needs to be pursued. Although the selectivity is 9 : 1 for **22a**, subsequent insertions are stereospecific. To accomplish this, it may be necessary to enlarge the ligand environment, though it has been shown that increasing the amidinate size has detrimental affects on polymerization. Therefore, the Cp group may be extended to the indenyl or fluorenyl ligands whose rapid rotation may enhance the orientation of the approaching olefin. This also may aid in the removal of stereodefects found in the main chain of PP samples.

8.3. References.

(1) Coates, G. W.; Waymouth, R. M. *Science* **1995**, *267*, 217.

(2) Herfert, N.; Fink, G. *Makromol. Chem., Macromol. Symp.* **1993**, *66*, 157.

(3) Hauptman, E.; Waymouth, R. M.; Ziller, J. W. *J. Am. Chem. Soc.* **1995**, *117*, 11586.

(4) Ewen, J. *J. Am. Chem. Soc.* **1984**, *106*, 6355.

(5) Petoff, J. L. M.; Agoston, T.; lal, T. K.; Waymouth, R. M. *J. Am. Chem. Soc.* **1998**, *120*, 11316.

(6) Resconi, L.; Cavallo, L.; Fait, A.; Piemontesi, F. *Chem. Rev.* **2000**, *100*, 1253.

(7) Kleinschmidt, R.; Reffke, M.; Fink, G. *Macromol. Rapid Commun.* **1999**, *20*, 284.

(8) Angermund, K.; Fink, G.; Jensen, V. R.; Kleinschmidt, R. *Macromol. Rapid Commun.* **2000**, *21*, 91.

(9) Ewen, J. A. *J. Mol. Catal. A: Chem.* **1998**, *128*, 103.

(10) Yoshida, T.; Koga, N.; Morokuma, K. *Organometallics* **1996**, *15*, 766.

(11) Guerra, G.; Cavallo, L.; Moscardi, G.; Vacatello, M.; Corradini, P. *Macromolecules* **1996**, *29*, 4834.

(12) Thomas, E. J.; Chien, J. C. W.; Rausch, M. D. *Macromolecules* **2000**, *33*, 1546.

(13) Farina, M.; Terragni, A. *Makromol. Chem., Rapid Commun.* **1993**, *14*, 791.

Appendix A: Experimental

All synthetic manipulations were conducted in either a Vacuum Atmospheres glovebox or using standard Schlenk line techniques under an inert nitrogen atmosphere. Dry, oxygen-free solvents were utilized throughout: ether (Et_2O), tetrahydrofuran (THF), and pentane were distilled from sodium / benzophenone (with a few milliliters of tetraglyme added to the pot in the case of pentane) and collected under vacuum. Toluene was distilled from Na/K alloy and collected under vacuum. Methylene chloride and chlorobenzene (PhCl) were distilled from CaH_2 and collected under vacuum. Benzene and decalin were distilled from $LiAlH_4$. C_6D_6, C_7D_8, and all α-olefins were stirred overnight over Na/K alloy (1:1), and each was vacuum distilled following three freeze-pump thaw cycles. CD_2Cl_2 and C_6D_5Cl were stirred overnight over CaH_2 and each was vacuum distilled following three freeze-pump thaw cycles. Titrations were performed using salicylaldehyde phenylhydrazone as previously described.[1] Cp^*ZrCl_3 and $CpZrCl_3$ were purchased from Strem and used as received. Lithium amidinates were prepared from literature procedures.[2,3] $EBIZrCl_2$ was purchased from Boulder Scientific Co. and used as received. $EBIZrMe_2$ was prepared from a literature procedure.[4]

NMR spectra were recorded at ambient temperature, unless otherwise noted, using a 400 or 500 MHz Bruker FT-NMR instrument. Elemental analyses were performed by Midwest Microlabs. Single crystal X-ray analysis experiments were performed using a Bruker SMART1000 CCD. GPC data was obtained at 40 °C in THF (HPLC grade) using a Waters 510 HPLC Pump (1.1 ml/min flow rate) and a Waters 410 Differential Refractometer in conjunction with four columns: Styragel HR1, HR3, HR4, and a Shodex K-806M. Calibration curves were established using seven PS standards

ranging from M_n = 1700 to 565000. Polymer samples contained 1.5-2.0 mg of polymer dissolved per ml of THF, and injection volumes were 25 μL. GC data was collected using a Shimadzu GC-9A with N_2 as the carrier gas. Undecane was used as the internal standard for calibration. Volume of injections was 1.0 μL.

Synthesis of Cp*ZrMe$_3$ (5): (η^5-C_5Me_5)$ZrCl_3$ (2.50 g, 7.50 mmol) in 150 mL of Et_2O was cooled to –25 °C and 22.5 mmol of MeLi in 50mL of Et_2O was added via cannula. The mixture was stirred for 1 h at –25 °C and quenched with excess TMSCl. The solvent was removed *in vacuo* to yield the crude product as a white-yellow solid (1.86 g, 91% crude yield). ^{1}H NMR (400 MHz, 298 K, C_6D_6): δ (ppm) 1.77 (s, 15H), 0.26 (s, 6H).

Synthesis of Cp*ZrMe$_2$[R^{1}NC(Me)NR^2], (6): To a –30 °C ether (200 mL) solution of Cp*$ZrCl_3$ (2.50 g, 7.50 mmol), MeLi (24.7mmol) in 20 mL of ether was added via cannula. This mixture was stirred for 90 min and quenched with excess TMSCl. To this was added, via cannula, a RT ether (30 mL) solution of 7.50 mmol of the carbodiimide. After 2 hr, the solution was slowly warmed to RT, and stirred for 1 hr. The volatiles were removed *in vacuo* and the residue was extracted with pentane. After concentrating and cooling the pentane solution to –30 °C, the product was obtained as white crystals. Yields: 65-95%.

Cp*ZrMe$_2$[^{t}BuNC(Me)NEt] (6a): ^{1}H NMR (400 MHz, C_6D_6, 295 K): δ (ppm) 2.86 (q, ^{3}J=7.2 Hz, 2H), 2.02 (s, 15H), 1.68 (s, 3H), 1.16 (s, 9H), 0.90 (t, ^{3}J=7.2 Hz, 3H), 0.25 (s, 6H). Elemental Analysis for $C_{20}H_{38}N_2Zr$: Calc'd %C 60.39, %H 9.63, %N 7.04; Found %C 60.54, %H 9.61, %N 7.03.

$Cp^*ZrMe_2[^tBuNC(Me)NCy]$ (6b): ^{1}H NMR (400 MHz, C_6D_6, 295 K): δ (ppm) 2.93 (tt, ^{3}J=11.6 Hz, ^{3}J=3.6 Hz, 1H), 2.05 (s, 15H), 1.83 (s, 3H), 1.69 (m, 4H), 1.52 (m, 4H), 1.19 (s, 12H), 1.09 (m, 2H), 0.36 (s, 6H). Elemental Analysis for $C_{24}H_{44}N_2Zr$: Calc'd %C 63.80, %H 9.81, %N 6.20; Found %C 63.81, %H 9.93, %N 6.21.

$Cp^*ZrMe_2[^tBuNC(Me)N(2,6\text{-}iPr_2Ph)]$ (6c): ^{1}H NMR (400 MHz, C_6D_6, 295 K): δ (ppm) 7.12 (m, 3H), 3.27 (septet, ^{3}J=8.0 Hz, 2H), 1.97 (s, 15H), 1.67 (s, 3H), 1.35 (d, ^{3}J=8.0 Hz, 6H), 1.21 (s, 9H), 1.16 (d, ^{3}J=8.0 Hz, 6H), 0.21 (s, 6H). Elemental Analysis for $C_{30}H_{50}N_2Zr$: Calc'd %C 67.99, %H 9.51, %N 5.29; Found %C 67.70, %H 9.60, %N 5.26.

Cp^*ZrMe_2[CyNC(Me)NCy] (6d): ^{1}H NMR (400 MHz, C_6D_6, 295 K): δ (ppm) 2.95 (tt, ^{2}J=11.5 Hz, ^{3}J=3.6 Hz, 2H), 2.04 (s, 15H), 1.73 (m, 8H), 1.68 (s, 3H), 1.48 (m, 6H), 1.11 (m, 6H), 0.34 (s, 6H). Elemental Analysis for $C_{26}H_{46}N_2Zr$: Calc'd %C 65.35, %H 9.70, %N 5.86; Found %C 64.97, %H 9.67, %N 6.02.

$Cp^*ZrMe_2[^iPrNC(Me)N^iPr]$ (6e): ^{1}H NMR (400 MHz, C_6D_6, 295 K): δ (ppm) 3.32 (septet, 2H), 2.02 (s, 15H), 1.59 (s, 3H), 1.06 (d, 12H), 0.30 (s, 6H). Elemental Analysis for $C_{20}H_{38}N_2Zr$: Calc'd %C 60.39, %H 9.63, %N 7.047; Found %C 60.03, %H 9.51, %N 7.29.

Synthesis of $Cp^*ZrCl_2[R^1NC(H)NR^2]$ (7): To a –30 °C ether (20 mL) solution of Cp^*ZrCl_3 (1.0 g, 3.0 mmol), was slowly added a RT ether solution (20 mL) of the lithium formamidinate, $Li[R^1NC(H)NR^2]$ (0.43 g, 3.0 mmol] (formed from **14** and ^{n}BuLi in ether at –40 °C). After stirring overnight at RT, the solvent was removed *in vacuo*, the yellow

solid dissolved in toluene, filtered, and concentrated. Recrystallization at –30 °C produced yellow crystals. Yields: 0.70-0.85 g (62-74%).

Cp*ZrCl$_2$[^{t}BuNC(H)NEt] (7a): ^{1}H NMR (400 MHz, C_6D_6, 293K): δ (ppm) 7.98 (s, 1H), 3.06 (q, ^{3}J=7.2 Hz, 2H), 2.03 (s, 15H), 1.12 (s, 9H), 0.96 (d, ^{3}J=7.2 Hz, 3H). Elemental analysis for $C_{17}H_{30}Cl_2N_2Zr$: Calc'd %C 48.09, %H 7.12, %N 6.60; Found %C 48.19, %H 7.02, %N 6.36.

Cp*ZrCl$_2$[^{i}PrNC(H)N^{i}Pr] (7b): ^{1}H NMR (400 MHz, C_6D_6, 293 K): δ (ppm) 8.14 (s, 1H), 3.46 (septet, ^{3}J=6.8 Hz, 2H), 2.01 (s, 15H), 1.00 (d, ^{3}J=6.8 Hz, 12H). ^{13}C NMR (100 MHz, C_6D_6, 293K): δ (ppm) 159.9, 125.4, 50.9, 24.2, 12.4. Elemental analysis for $C_{17}H_{30}Cl_2N_2Zr$: Calc'd %C 48.09, %H 7.12, %N 6.60; Found %C 48.35, %H 7.17, %N 6.23.

Synthesis of Cp*ZrCl$_2$[R^{1}NC(R^2)NR^3] (8-10): To a –30 °C ether (60 mL) solution of Cp*ZrCl$_3$ (3.00 g, 9.0 mmol), 1.33 g (9.0 mmol) of the lithium amidinate, Li[R^{1}NC(R^2)NR^3], in 20 mL of ether was slowly added. After stirring overnight at RT, the solvent was removed *in vacuo*, the yellow solid dissolved in toluene, filtered, and concentrated. Recrystallization at –30 °C produced yellow crystals. Yields: 3.2-3.7 (82-95%).

Cp*ZrCl$_2$[^{t}BuNC(Me)NEt] (8a): ^{1}H NMR (400 MHz, C_6D_6, 295 K): δ (ppm) 3.06 (q, ^{3}J=7.2 Hz, 2H), 2.06 (s, 15H), 1/49 (s, 3H), 1.23 (s, 9H), 0.94 (t, ^{3}J=7.2 Hz, 3H). Elemental Analysis for $C_{18}H_{32}Cl_2N_2Zr$: Calc'd %C 49.28, %H 7.37, %N 6.39; Found %C 49.57, %H 7.18, %N 6.09.

$Cp^*ZrCl_2[^iPrNC(Me)N^iPr]$ (8b): ^1H NMR (400 MHz, C_6D_6, 295 K): δ (ppm) 3.49 (septet, ^3J=6.8 Hz, 2H), 2.04 (s, 15H), 1.50 (2, 3H), 1.14 (d, ^3J=6.8 Hz, 12H). ^{13}C NMR (100 MHz, 298 K, C_6D_6): δ (ppm) 174.3, 125.1, 49.2, 23.6, 15.1, 12.7. Elemental Analysis for $C_{18}H_{32}Cl_2N_2Zr$: Calc'd %C 49.28, %H 7.37, %N 6.39; Found %C 49.26, %H 7.35, %N 6.24.

$Cp^*ZrCl_2[CyNC(Me)NCy]$ (8c): ^1H NMR (400 MHz, C_6D_6, 295 K): δ (ppm) 3.10 (m, 2H), 2.07 (s, 15H), 1.80 – 1.14 (m, 20H), 1.59 (s, 3H). Elemental Analysis for $C_{24}H_{40}Cl_2N_2Zr$: Calc'd %C 55.58, %H 7.77, %N 5.38; Found %C 54.17, %H 7.70, %N 5.33.

$Cp^*ZrCl_2[^tBuNC(^tBu)NEt]$ (9): ^1H NMR (400 MHz, C_6D_6, 295 K): δ (ppm) 3.39 (q, ^3J=7.0 Hz, 2H), 2.04 (s, 15H), 1.37 (s, 9H), 1.20 (s, 9H), 1.09 (t, ^3J=7.0 Hz, 3H). Elemental Analysis for $C_{18}H_{32}Cl_2N_2Zr$: Calc'd %C 51.04, %H 7.76, %N 5.55; Found %C 51.23, %H 7.77, %N 5.43.

$Cp^*ZrCl_2[^tBuNC(Ph)NEt]$ (10): ^1H NMR (400 MHz, C_6D_6, 295 K): δ (ppm) 6.94-6.87 (m, 5H), 2.915 (q, ^3J=7.0 Hz, 2H), 2.13 (s, 15H), 1.15 (s, 9H), 0.85 (t, ^3J=7.0 Hz, 3H). Elemental Analysis for $C_{23}H_{34}Cl_2N_2Zr$: Calc'd %C 55.17, %H 6.79, %N 5.60; Found %C 55.01, %H 7.01, %N 5.49.

Synthesis of $Cp^*ZrMe_2[R^1NC(H)NR^2]$ (11): To a –78 °C ether (10 mL) solution of **7** (0.30 g, 0.71 mmol), was slowly added MeLi (14.3 mmol) in 1 mL of ether. After 30 minutes, the mixture was slowly warmed to RT for 1 hr. The reaction was quenched with TMSCl and the volatiles were removed *in vacuo*. The yellow solid was dissolved in

pentane, filtered, and concentrated. Recrystallization at –30 °C produced off-white crystals. Yields: 0.13-0.19 g (48-70%).

$Cp^*ZrMe_2[^tBu\,NC(H)NEt]$ (11a): ^{1}H NMR (400 MHz, C_6D_6, 293 K): δ (ppm) 8.25 (s, 1H), 2.91 (q, ^{3}J=7.2 Hz, 2H), 1.99 (s, 15H), 1.07 (s, 9H), 0.94 (t, ^{3}J=67.2 Hz, 3H), 0.26 (s, 6H). ^{13}C NMR (100 MHz, C_6D_6, 293K): δ (ppm) 165.2, 120.5, 46.1, 32.1, 23.0, 18.7, 14.9, 12.3.

$Cp^*ZrMe_2[^iPrNC(H)N^iPr]$ (11b): ^{1}H NMR (400 MHz, C_6D_6, 293 K): δ (ppm) 8.31 (s, 1H), 3.17 (septet, ^{3}J=6.8 Hz, 2H), 1.98 (s, 15H), 1.01 (d, ^{3}J=6.8 Hz, 12H), 0.24 (s, 6H). ^{13}C NMR (100 MHz, C_6D_6, 293K): δ (ppm) 161.9, 96.8, 49.0, 43.9, 23.1, 9.9.

$Cp^*ZrMe_2[^tBuNC(^tBu)NEt]$ (12): ^{1}H NMR (400 MHz, C_6D_6, 295 K): δ (ppm) 3.18 (q, ^{3}J=7.0 Hz, 2H), 1.99 (s, 15H), 1.35 (s, 9H), 1.25 (s, 9H), 1.05 (t, ^{3}J=7.0 Hz, 3H), 0.08 (s, 6H). ^{13}C NMR (100MHz, C_6D_6, 293 K): δ (ppm) 180.1, 119.3, 55.8, 43.7, 40.7, 40.5, 34.4, 31.4, 19.0, 12.0.

$Cp^*ZrMe_2[^tBuNC(Ph)NEt]$ (13): ^{1}H NMR (400 MHz, C_6D_6, 295 K): δ (ppm) 7.12-7.00 (m, 5H), 2.68 (q, ^{3}J=7.0 Hz, 2H), 2.07 (s, 15H), 1.06 (s, 9H), 0.81 (t, ^{3}J=7.0 Hz, 3H), 0.38 (s, 6H). Elemental Analysis for $C_{25}H_{40}N_2Zr$: Calc'd %C 65.29, %H 8.79, %N 6.09; Found %C 65.20, %H 8.62, %N 6.14.

Synthesis of $R^1NC(H)N(SiEt_3)(R^2)$ (14): To a mixture of 10.1 g (80.0 mmol) of carbodiimide, R^1NCNR^2, and 11.1 g (95.4 mmol) of triethylsilane was added 0.24 g (1.35 mmol, 1.6 mol%) of $PdCl_2$ and the Schlenk tube was sealed under N_2. The mixture was

heated at 150 °C overnight. After cooling to RT, vacuum distillation (85 °C at 4mm Hg for **14a** and 90 °C at 7mm Hg for **14b**) provided the target compounds. Yields: 11.6-15.5 g (61-81%).

^{t}BuNC(H)N(SiEt$_3$)(Et) (14a): ^{1}H NMR (400 MHz, C_6D_6, 293K): δ (ppm) 7.57 (s, 1H), 3.26 (q, ^{3}J=6.8 Hz, 2H), 1.28 (s, 9H), 1.18 (t, ^{3}J=6.8 Hz, 3H), 0.90 (t, ^{3}J=7.6 Hz, 9H), 0.59 (q, ^{3}J=7.6 Hz, 6H).

^{i}PrNC(H)N(SiEt$_3$)(^{i}Pr) (14b): ^{1}H NMR (400 MHz, $CDCl_3$, 293K): δ (ppm) 7.53 (s, 1H), 3.52 (septet, ^{3}J=6.8 Hz, 1H), 3.11 (septet, ^{3}J=6.8 Hz, 1H), 1.26 (d, ^{3}J=6.8 Hz, 6H), 1.05 (d, ^{3}J=6.8 Hz, 6H), 0.92 (t, ^{3}J=7.6 Hz, 9H), 0.71 (q, ^{3}J=7.6 Hz, 6H).

Synthesis of R^{1}NC(H)N(H)(R^2) (20): To 11.6 g (47.8 mmol) of freshly distilled R^{1}NC(H)N(SiEt$_3$)(R^2) was added excess methanol. For **20a**, vacuum distillation (42 °C, 4 mm Hg) provided 5.0 g (81%) of colorless liquid. For **20b**, the solution was recrystallized at –25 °C to provide 5.7 g (93%) of tan crystals.

^{t}BuNC(H)N(H)(Et) (20a): ^{1}H NMR (400 MHz, $CDCl_3$, 293K): δ (ppm) 7.40 (s, 1H), 3.16 (bq, 2H), 1.18 (s, 9H), 1.10 (bt, 3H).

^{i}PrNC(H)N(H)(^{i}Pr) (20b): ^{1}H NMR (400 MHz, $CDCl_3$, 293K): δ (ppm) 7.34 (s, 1H), 3.42 (septet, ^{3}J=6.4 Hz, 2H), 3.09 (bs, 1H), 1.12 (d, ^{3}J=6.4 Hz, 12H). ^{13}C NMR (100 MHz, $CDCl_3$, 293K): δ (ppm) 150.2, 24.9, 7.2, 6.8.

Synthesis of $CpZrMe_2[R^1NC(Me)NR^2]$ (15): This procedure is typical for the preparation of all **15a-d**. To a –65 °C ether (50 mL) solution of $CpZrCl_3$ (0.50 g, 1.9 mmol), 5.7 mmol of MeLi in 25 mL of ether was added via cannula. The mixture was stirred for 1 hr at –65 °C and quenched with TMSCl. To this was added, via cannula, a 25 mL ether solution of 1.5 mmol of carbodiimide. The mixture was slowly warmed to –20 °C over 90 min, then removed from the cold bath and stirred at RT for 30 min. The volatiles were removed *in vacuo* and the residue was extracted with pentane. After concentrating and cooling the pentane solution to –30 °C, the product was obtained as a white crystalline solid. Yields: 55-90%.

$CpZrMe_2[^tBuNC(Me)NEt]$ (15a): ^{1}H NMR (400 MHz, C_6D_6, 295 K): δ (ppm) 6.24 (s, 5H), 2.91 (q, ^{3}J=7.2 Hz, 2H), 1.54 (s, 3H), 1.09 (s, 9H), 0.77 (t, ^{3}J=7.2 Hz, 3H), 0.42 (s, 6H).

$CpZrMe_2[^tBuNC(Me)NCy]$ (15b): ^{1}H NMR (400 MHz, C_6D_6, 295 K): δ (ppm) 6.30 (s, 5H), 2.79 (tt, ^{3}J=11.4 Hz, ^{3}J=4.8 Hz 1H), 1.68 (s, 3H), 1.63 (m, 2H), 1.48 (m, 5H), 1.11 (m, 3H), 1.08 (s, 9H), 0.53 (s, 6H). Elemental Analysis for $C_{19}H_{34}N_2Zr$: Calc'd %C 59.78, %H 8.98, %N 7.34; Found %C 59.59, %H 9.02, %N 7.28.

$CpZrMe_2[^iPrNC(Me)N^iPr]$ (15c): ^{1}H NMR (400 MHz, C_6D_6, 295 K): δ (ppm) 6.26 (s, 5H), 3.18 (septet, ^{3}J=6.4 Hz, 2H), 1.39 (s, 3H), 0.97 (d, ^{3}J=6.4 Hz, 12H), 0.51 (s, 6H). Elemental Analysis for $C_{15}H_{28}N_2Zr$: Calc'd %C 54.99, %H 8.61, %N 8.55; Found %C 54.66, %H 8.52, %N 8.61.

$CpZrMe_2[CyNC(Me)NCy]$ (15d): ^{1}H NMR (400 MHz, C_6D_6, 295 K): δ (ppm) 6.30 (s, 5H), 2.85 (tt, ^{2}J=11.5 Hz, ^{3}J=2.6 Hz, 2H), 1.66 (m, 4H), 1.53 (m, 6H), 1.51 (s, 3H), 1.20 (m, 10H), 0.54 (s, 6H). Elemental Analysis for $C_{21}H_{36}N_2Zr$: Calc'd %C 61.86, %H 8.90, %N 6.87; Found %C 61.56, %H 9.96, %N 6.77.

$[^iPrNC(Me)N^iPr]_2ZrMe_2$ (16): ^{1}H NMR (400 MHz, C_6D_6, 295 K): δ (ppm) 3.42 (septet, ^{3}J=7.2 Hz, 4H), 1.54 (s, 6H), 1.23 (d, ^{3}J=7.2 Hz, 24H), 0.81 (s, 6H).

Cp_2ZrMe_2 (17)[5]: ^{1}H NMR (400 MHz, C_6D_6, 295 K): δ (ppm) 5.71 (s, 10H), -0.13 (s, 6H).

***rac*-$EBIZrMe_2$ (18)[4]:** ^{1}H NMR (400 MHz, C_6D_6, 295 K): δ (ppm) 7.32 (d, ^{3}J = 8.8 Hz, 2H), 7.08 (m, 4H), 6.90 (d, ^{3}J = 7.2 Hz, 2H), 6.42 (d, ^{3}J = 3.2 Hz, 2H), 5.65 (d, ^{3}J = 3.2 Hz, 2H), 2.80 (m, 2H), 2.67 (m, 2H).

$CpZrMe[^tBuNC(Me)NEt]_2$ (19a): ^{1}H NMR (400 MHz, C_6D_6, 295 K): δ (ppm) 6.22 (s, 5H), 1.61 (s, 3H), 1.53 (s, 3H), 1.37 (s, 9H), 1.17 (s, 9H), 1.03 (t, ^{3}J= 7.2 Hz, 3H), 0.86 (t, ^{3}J= 7.2 Hz, 3H), 0.29 (s, 3H).

$CpZrMe[^iPrNC(Me)N^iPr]_2$ (19b): ^{1}H NMR (500 MHz, C_7D_8, 295 K): δ (ppm) 6.29 (s, 5H), 3.50 (b, 4H), 1.54 (bs, 6H), 1.11 (b, 24H), 0.22 (s, 3H).

$CpZrCl_2[^tBuNC(Me)NEt]$ (21): ^{1}H NMR (400 MHz, C_6D_6, 293 K): δ (ppm) 6.33 (s, 5H), 3.00 (q, ^{3}J=6.8 Hz, 2H), 1.27 (s, 3H), 1.17 (s, 9H), 0.89 (t, ^{3}J=6.8 Hz, 3H).

Synthesis of Cp*Zr(R)(Cl)[R^1NC(Me)NR^3]: The following is representative for **33a-h**, **34**, **35** unless otherwise noted: To a –78 °C mixture of **8a** or **8b** (500 mg, 1.14 mmol) was added an ether solution of 1.14 mmol of EtMgCl, ^{n}PrMgCl, ^{n}BuMgCl, ^{i}BuMgCl, ^{t}BuLi, and $LiCH_2C(CH_3)_3$, respectively. After slowly warming the mixture to RT, the reaction was quenched with 0.5 ml TMSCl, the volatiles were removed *in vacuo*, and the resulting yellow solid was taken up in pentane and filtered. The mother liquor was concentrated and recrystallized at –30 °C to afford yellow crystals with an isolated yield of 80-95%.

Cp*Zr(Et)(Cl)[^{t}BuNC(Me)NEt] (33a): After EtMgCl addition, mixture was stirred for 1 hr at –78 °C. ^{1}H NMR (400 MHz, C_6D_6, 295 K): δ (ppm) 2.75 (dq, ^{2}J=14.0 Hz, ^{3}J=7.2 Hz, 1H), 2.58 (dq, ^{2}J=14.0 Hz, ^{3}J=7.2 Hz, 1H), 2.01 (s, 15H), 1.66 (s, 3H), 1.56 (t, ^{3}J=7.6 Hz, 3H), 1.33 (s, 3H), 0.78 (t, ^{3}J=7.2 Hz, 3H), 0.66 (dq, ^{2}J=13.2 Hz, ^{3}J=7.6 Hz, 1H), 0.13 (dq, ^{2}J=13.2 Hz, ^{3}J=7.6 Hz, 1H). Elemental analysis for $C_{20}H_3ClN_2Zr$: Calc'd %C 55.57, %H 8.65, %N 6.48; Found %C 55.64, %H 8.59, %N 6.23.

Cp*Zr(^{n}Pr)(Cl)[^{t}BuNC(Me)NEt] (33b): ^{1}H NMR (400 MHz, C_6D_6, 295 K): δ (ppm) 2.79 (dq, ^{2}J=14.0 Hz, ^{3}J=7.0 Hz, 1H), 2.62 (dq, ^{2}J=14.4 Hz, ^{3}J=7.2 Hz, 1H), 2.13 (m, 1H), 2.01 (s, 15H), 1.67 (s, 3H), 1.54 (m, 1H), 1.33 (s, 9H), 1.22 (t, ^{3}J=7.0 Hz, 3H), 0.80 (t, ^{3}J=7.2 Hz, 3H), 0.59 (ddd, ^{2}J=13.6 Hz, ^{2}J=10.8 Hz, ^{3}J=4.4 Hz, 1H), 0.27 (ddd, ^{2}J=12.8 Hz, ^{2}J=11.2 Hz, ^{3}J=5.6 Hz). Elemental analysis for $C_{21}H_{39}ClN_2Zr$: Calc'd %C 56.52, %H 8.81, %N 6.28; Found %C 56.50, %H 8.73, %N 6.21.

Cp*Zr(^{i}Pr)(Cl)[^{t}BuNC(Me)NEt] (33c): ^{1}H NMR (400 MHz, C_6D_6, 295 K): δ (ppm) 2.60 (dq, ^{2}J=14.0 Hz,^{3}J=7.2 Hz, 1H), 2.55 (dq, ^{2}J=14.0 Hz,^{3}J=7.2 Hz, 1H), 1.99 (s, 15H), 1.62

(d, ^{3}J=7.2 Hz, 3H), 1.57 (s, 9H), 1.41 (d, ^{3}J=7.2 Hz, 3H), 1.26 (s, 9H), 0.74 (t, ^{3}J=7.2 Hz, 3H), -0.20 (septet, ^{3}J=7.2 Hz, 1H). Elemental analysis for $C_{21}H_{39}ClN_2Zr$: Calc'd %C 56.52, %H 8.81, %N 6.28; Found %C 56.48, %H 8.77, %N 6.20.

Cp*Zr(^{n}Bu)(Cl)[^{t}BuNC(Me)NEt] (33d): ^{1}H NMR (400 MHz, C_6D_6, 293K): δ (ppm) 2.80 (dq, ^{2}J=14.0 Hz, ^{3}J=7.2 Hz, 1H), 2.61 (dq, ^{2}J=14.0 Hz, ^{3}J=7.2 Hz, 1H), 2.02 (s, 15H), 2.09 (m, 1H), 1.70 (s, 3H), 1.58 (m, 1H), 1.50 (m, 2H), 1.33 (s, 9H), 1.06 (t, ^{3}J=7.2 Hz, 3H), 0.81 (t, ^{3}J=7.2 Hz, 3H), 0.56 (ddd, ^{2}J=13.2 Hz, ^{2}J=10.4 Hz, ^{3}J=4.2 Hz, 1H), 0.24 (ddd, ^{2}J=12.8 Hz, ^{2}J=11.2 Hz, ^{3}J=5.2 Hz, 1H). Elemental analysis for $C_{22}H_{41}ClN_2Zr$: Calc'd %C 57.41, %H 8.98, %N 6.09; Found %C 57.36 %H 8.90, %N 5.89.

Cp*Zr(^{i}Bu)(Cl)[^{t}BuNC(Me)NEt] (33e): ^{1}H NMR (400 MHz, C_6D_6, 293K): δ (ppm) 2.89 (dq, ^{2}J=14.3 Hz, ^{3}J=7.2 Hz 1H), 2.72 (dq, ^{2}J=14.3 Hz, ^{3}J=7.2 Hz, 1H), 2.24 (nonet, ^{3}J=6.4 Hz, 1H), 2.00 (s, 15H), 1.70 (s, 3H), 1.33 (s, 9H), 1.32 (d, ^{3}J=6.4 Hz, 3H), 1.15 (d, ^{3}J=6.4 Hz, 3H), 0.82 (t, ^{3}J=7.2 Hz, 3H), 0.73 (dd, ^{2}J=13.6 Hz, ^{3}J=6.4 Hz), -0.03 (dd, ^{2}J=13.6 Hz, ^{3}J=6.4 Hz). Elemental analysis for $C_{22}H_{41}ClN_2Zr$: Calc'd %C 57.41, %H 8.98, %N 6.09; Found %C 57.21 %H 8.80, %N 5.91.

Cp*Zr(^{s}Bu)(Cl)[^{t}BuNC(Me)NEt] (33f): ^{1}H NMR (400 MHz, C_6D_6, 293K): δ (ppm) δ 2.61 (m, 1H), 2.53 (m, 1H), 2.05 (s, 15H), 1.85 (m, 1H), 1.67 (s, 3H), 1.63 (d, 3H), 1.62 (m, 1H), 1.32 (s, 9H), 1.11 (t, 3H), 0.82 (t, 3H), -0.49 (m, 1H). Anal Calcd for $ZrN_2ClC_{22}H_{41}$: %C 57.41, %H 8.98, %N 6.09; Found %C 57.24, %H 8.85, %N 6.11.

Cp*Zr(^{t}Bu)(Cl)[^{t}BuNC(Me)NEt] (33g): After addition of ^{t}BuLi, mixture was stirred for 90 minutes at –78 °C before quenching. ^{1}H NMR (400 MHz, C_6D_6, 293K): δ (ppm) 2.95 (dq,

^{2}J=14.4 Hz, ^{3}J=7.0 Hz, 1H), 2.72 (dq, ^{2}J=14.4 Hz, ^{3}J=7.0 Hz, 1H), 2.04 (s, 15H), 1.65 (s, 3H), 1.38 (s, 9H), 1.33 (s, 9H), 0.78 (t, ^{3}J=7.0 Hz, 3H). Elemental analysis for $C_{22}H_{41}ClN_2Zr$: Calc'd %C 57.41, %H 8.98, %N 6.09; Found %C 57.21, %H 8.88, %N 6.05.

Cp*Zr(neopentyl)(Cl)[^{t}BuNC(Me)NEt] (33h): ^{1}H NMR (400 MHz, C_6D_6, 293K): δ (ppm) 2.87 (dq, ^{2}J=14.2 Hz, ^{3}J=7.2 Hz, 1H), 2.83 (dq, ^{2}J=14.2 Hz, ^{3}J=7.2 Hz, 1H), 1.98, (s, 9H), 1.67 (s, 3H), 1.31 (s, 9H), 0.98 (d, ^{2}J=14.0 Hz, 1H), 0.84 (t, ^{3}J=7.2 Hz, 3H), -0.17 (d, ^{2}J = 14.0 Hz). Elemental analysis for $C_{23}H_{43}ClN_2Zr$: Calc'd %C 58.24, %H 9.14, %N 5.91; Found %C 58.16, %H 9.01, %N 5.79.

Cp*Zr(^{t}Bu)(Cl)[CyNC(Me)NCy] (34): ^{1}H NMR (400 MHz, C_6D_6, 293K): δ (ppm) 3.16 (m, 2H), 2.06 (s, 15H), 1.83 (m, 4H), 1.59 (m, 6H), 1.38 (m, 4H), 1.25 (m, 6H), 1.67 (s, 3H).

Cp*Zr(neopentyl)(Cl)[^{i}PrNC(Me)N^{i}Pr] (35): ^{1}H NMR (400 MHz, C_6D_6, 293K): δ (ppm) 3.40 (septet, ^{3}J = 6.4 Hz, 2H), 2.00 (s, 15H), 1.54 (s, 3H), 1.40 (s, 9H), 1.34 (d, ^{3}J = 6.4 Hz, 3H), 1.28 (d, ^{3}J = 6.4 Hz, 3H), 1.11 (d, ^{2}J = 14.0 Hz, 1H), 1.09 (d, ^{3}J = 6.4Hz, 3H), 1.07 (d, ^{3}J = 6.4Hz, 3H), -0.09 (d, ^{2}J = 14.0 Hz, 1H). Elemental analysis for $C_{23}H_{43}ClN_2Zr$: Calc'd %C 58.24, %H 9.14, %N 5.91; Found %C 58.06, %H 8.93, %N 5.78.

Synthesis of Cp*Zr(R)(Me)[R^{1}NC(Me)NR^3]: The following is representative for **36a-e**, **h** or **37** unless otherwise noted: To a –78 °C mixture of **33** or **35** (250 mg, 1.14 mmol) in 10 mL of ether was added an ether solution of MeLi (1.14 mmol) in 1 mL of ether. After slowly warming the mixture to RT, the reaction was quenched with 0.5 ml TMSCl, the

volatiles were removed *in vacuo* and the yellow solid was taken up in pentane and filtered. The mother liquor was concentrated and the product was recrystallized at –30 °C.

Cp*Zr(Et)(Me)[^{t}BuNC(Me)NEt] (36a): ^{1}H NMR (400 MHz, C_6D_6, 293K): δ (ppm) 2.87 (dq, ^{2}J=13.6 Hz, ^{3}J=6.8 Hz, 2H), 2.70 (bm, 1H), 1.99 (s, 15H), 1.73 (s, 3H), 1.64 (bt, ^{3}J=13.6 Hz, 3H), 1.18 (s, 9H), 1.18 (m, 1H), 0.87 (t, ^{3}J=7.2 Hz, 3H), 0.33 (dq, ^{2}J=13.2 Hz, ^{3}J=7.2 Hz, 1H), 0.10 (s, 3H).

Cp*Zr(^{n}Pr)(Me)[^{t}BuNC(Me)NEt] (36b): ^{1}H NMR (400 MHz, C_6D_6, 293K): δ (ppm) 2.90 (dq, ^{2}J=14.0 Hz, ^{3}J=7.2 Hz, 1H), 2.70 (b, 1H), 1.99 (s, 15H), 1.98 (m, 2H), 1.74 (s, 3H), 1.23 (t, ^{3}J=7.0 Hz, 3H), 1.18 (s, 9H), 0.88 (t, ^{3}J=6.8 Hz, 3H), 0.88 (m, 1H), 0.27 (m, 1H), 0.14 (s, 3H). Elemental Analysis for $C_{22}H_{42}N_2Zr$: Calc'd %C 62.06, %H 9.94, %N 6.58; Found %C 62.00, %H 9.85, %N 6.39.

Cp*Zr(^{i}Pr)(Me)[^{t}BuNC(Me)NEt] (36c): ^{1}H NMR (400 MHz, C_6D_6, 293K): δ (ppm) 2.77 (dq, ^{2}J=14.0 Hz, ^{3}J=7.0 Hz, 1H), 2.67 (dq, ^{2}J=14.0 Hz, ^{3}J=7.0 Hz, 1H), 2.02 (s, 15H), 1.69 (s, 3H), 1.57 (d, ^{3}J=7.2 Hz, 3H), 1.54 (d, ^{3}J=7.2 Hz, 3H), 1.19 (s, 9H), 0.86 (t, ^{3}J=7.0 Hz, 3H), 0.07 (s, 3H), -0.50 (septet, ^{3}=7.2 Hz, 1H).

Cp*Zr(^{n}Bu)(Me)[^{t}BuNC(Me)NEt] (36d): ^{1}H NMR (400 MHz, C_6D_6, 293K): δ (ppm) 2.91 (dq, 1H), 2.74 (bm, 1H), 2.01 (m, 2H), 2.00 (s, 15H), 1.75 (bs, 3H), 1.53 (bq, 2H), 1.19 (s, 9H), 1.19 (m, 1H), 1.09 (t, 3H), 0.89 (bt, 3H), 0.27 (b, 1H), 0.13 (bs, 3H).

Cp*Zr(^{i}Bu)(Me)[^{t}BuNC(Me)NEt] (36e): ^{1}H NMR (400 MHz, C_6D_6, 293K): δ (ppm) 2.97 (dq, ^{2}J=14.4 Hz, ^{3}J=7.2Hz, 1H), 2.75 (dq, ^{2}J=14.4 Hz, ^{3}J=7.2Hz, 1H), 2.20 (bm, 1H), 1.98 (s, 15H), 1.80 (s, 3H), 1.27 (d, ^{3}J=6.4 Hz, 3H), 1.23 (d, ^{3}J=6.4 Hz, 3H), 1.19 (s, 9H), 0.85 (t, ^{3}J=7.2 Hz, 3H), 0.41 (dd, ^{2}J=13.2 Hz, ^{3}J=6.4 Hz, 1H), 0.23 (s, 3H), -0.26 (dd, ^{2}J=13.2 Hz, ^{3}J=6.4 Hz, 1H).

Cp*Zr(neopentyl)(Me)[^{t}BuNC(Me)NEt] (36h): ^{1}H NMR (400 MHz, C_7D_8, 293K): δ (ppm) 2.96 (dq, ^{2}J=14.0 Hz, ^{3}J=7.2 Hz, 1H), 2.82 (dq, ^{2}J=14.0 Hz, ^{3}J=7.2 Hz, 1H), 1.96 (s, 9H), 1.79 (s, 3H), 1.27 (s, 9H), 1.19 (s, 9H) 0.90 (t, ^{3}J=7.2 Hz, 3H), 0.77 (d, ^{2}J=14.0 Hz, 1H), -0.54 (d, ^{2}J=14.0 Hz, 1H).

Cp*Zr(neopentyl)(Me)[^{i}PrNC(Me)N^{i}Pr] (37): ^{1}H NMR (400 MHz, C_7D_8, 293K): δ (ppm) 3.37 (septet, ^{3}J=7.0 Hz, 2H), 1.97 (s, 15H), 1.65 (s, 3H), 1.34 (s, 9H), 1.13 (bm, 12H), 1.02 (d, ^{2}J=14.0 Hz, 1H), 0.41 (s, 3H), -0.31 (d, ^{2}J=14.0 Hz, 1H). Elemental Analysis for $C_{24}H_{43}N_2Zr$: Calc'd %C 63.48, %H 9.55, %N 6.17; Found %C 63.56, %H 9.85, %N 6.09.

Cp*Zr(^{i}Bu)$_2$[^{t}BuNC(Me)NEt] (38a): ^{1}H NMR (400 MHz, C_6D_6, 293K): δ (ppm) 2.89 (q, ^{3}J=7.2 Hz, 2H), 2.35 (septet, ^{3}J=6.4 Hz, 2H), 1.98 (s, 15H), 1.72 (s, 3H), 1.31 (d, ^{3}J=6.8 Hz, 6H), 1.25 (d, ^{3}J=6.8 Hz, 6H), 1.22 (s, 9H), 0.91 (t, ^{3}J=7.2 Hz, 3H), 0.74 (b, 2H), 0.27 (dd, ^{2}J=13.2 Hz, ^{3}J=6.4 Hz, 2H). Elemental Analysis for $C_{26}H_{50}N_2Zr$: Calc'd %C 64.80, %H 10.46, %N 5.81; Found %C 64.55, %H 10.02, %N 5.48.

Cp*Zr(^{i}Bu)$_2$[^{i}PrNC(Me)N^{i}Pr] (38b): ^{1}H NMR (400 MHz, C_6D_6, 293K): δ (ppm) 3.40 (septet, ^{3}J = 6.8 Hz, 2H), 2.41 (septet, ^{3}J = 6.8 Hz, 2H), 1.99 (s, 15H), 1.65 (s, 3H), 1.31

(d, ^3J = 6.8 Hz, 6H), 1.26 (d, ^3J = 6.8 Hz, 6H), 1.12 (d, ^3J = 6.8 Hz, 12H), 0.84 (dd, 2H), 0.29 (dd, 2H).

Cp*Zr(^{n}Bu)$_2$[^{t}BuNC(Me)NEt] (39a): ^{1}H NMR (400 MHz, C_6D_6, 293K): δ (ppm) 2.97 (q, ^3J = 6.8 Hz, 2H), 1.99 (s, 15H), 1.74 (m, 4H), 1.50 (m, 8H), 1.19 (s, 9H) 1.10 (t, ^3J = 7.2 Hz, 6H), 0.90 (t, ^3J = 6.8 Hz, 3H).

Cp*Zr(^{n}Bu)$_2$[CyNC(Me)NCy] (39b): ^{1}H NMR (400 MHz, C_6D_6, 293K): δ (ppm) 2.97 (m, 2H), 2.02 (s, 15H), 1.94 (m, 4H), 1.74 (m, 8H), 1.70 (s, 3H), 1.55 (m, 4H), 1.50 (m, 6H), 1.16 (m, 6H), 1.13 (t, 6H), 0.49 (m, 4H).

Cp*Zr(C_4H_6)[CyNC(Me)NCy] (40): ^{1}H NMR (400 MHz, C_6D_6, 293K): δ (ppm) 6.18 (m, 2H), 2.94 (m, 2H), 2.07 (s, 15H), 1.87 (m, 4H), 1.86 (t, ^3J = 19 Hz, 2H), 1.58 (m, 6H), 1.46 (m, 4H), 1.43 (m, 6H), 1.42 (s, 3H), 0.43 (t, ^3J = 19 Hz, 2H).

Cp*Zr(TMM)[^{t}BuNC(Me)NEt] (40a): ^{1}H NMR (400 MHz, C_6D_6, 293K): δ (ppm) 2.90 (dq, ^2J = 10.4 Hz, ^3J = 6.8 Hz, 1H), 2.69 (dq, ^3J = 10.4 Hz, ^3J = 6.8 Hz, 1H), 2.60 (b, 6H), 1.93 (s, 15H), 1.61 (s, 3H), 0.97 (s, 9H), 0.92 (t, ^3J = 6.8 Hz, 3H).

Cp*Zr(TMM)[^{i}PrNC(Me)N^{i}Pr] (40b): ^{1}H NMR (400 MHz, C_6D_6, 293K): δ (ppm) 3.40 (septet, ^3J = 6.4 Hz, 2H), 2.64 (b, 6H), 1.97 (s, 15H), 1.56 (s, 3H), 0.86 (d, ^3J = 6.4 Hz, 6H), 0.82 (^3J = 6.4 Hz, 6H).

[Cp*Zr[^{t}BuNC(Me)NEt]]$_2$(μ-H)(μ-C_4H_5) (40a): ^{1}H NMR (400 MHz, C_6D_6, 293K): δ (ppm) 7.20 (s, 2H), 3.48 (dq, ^2J = 11.2 Hz, ^3J = 7.2 Hz, 2H), 3.13 (dq, ^2J = 11.2 Hz, ^3J = 7.2 Hz,

2H), 2.42 (s, 1H), 2.03 (s, 15H), 1.98 (s, 6H), 1.76 (s, 3H), 1.35 (bs, 18H), 1.78 (t, ^3J = 7.2 Hz). Elemental Analysis for $C_{40}H_{70}N_4Zr_2$: Calc'd %C 60.86, %H 8.94, %N 7.10; Found %C 60.67, %H 8.77, %N 7.00.

Preparation of Cations: The following procedure is a representative example for the whole series of **22** and **43**: A 15 mg sample of **6**, **11**, **12**, **15**, **36a-e**, **h** or **37** and 31 mg of $[PhNHMe_2][B(C_6F_5)_4]$ were dissolved in 0.8 ml of C_6D_5Cl at –10 °C in an NMR tube and transported to the NMR spectrometer at -10 °C.

$[Cp^*Zr(Me)[^tBuNC(Me)NEt]]^+[B(C_6F_5)_4]^-$ (22a): ^{1}H NMR (500 MHz, C_6D_5Cl, 263K): δ (ppm) 3.05 (m, 2H), 2.01 (s, 3H), 1.87 (s, 15H), 1.04 (s, 9H), 0.89 (t, ^{3}J=7.0 Hz, 3H), 0.52 (s, 3H).

$[Cp^*Zr(Me)[^iPrNC(Me)N^iPr]]^+[B(C_6F_5)_4]^-$ (22e): ^{1}H NMR (500 MHz, C_6D_5Cl, 263K): δ (ppm) 3.40 (septet, ^{3}J = 7.0 Hz, 2H), 2.00 (s, 3H), 1.88 (s, 15H), 0.96 (d, ^{3}J = 7.0 Hz, 6H), 0.88 (d, ^{3}J = 7.0 Hz, 6H), 0.57 (s, 3H).

$[Cp^*Zr(Me)[^tBuNC(^tBu)NEt]]^+[B(C_6F_5)_4]^-$ (26): ^{1}H NMR (500 MHz, C_6D_5Cl, 263K): δ (ppm) 3.54 (dq, ^{2}J=14.0 Hz, ^{3}J=7.2 Hz, 1H), 3.21 (dq, ^{2}J=14.0 Hz, ^{3}J=7.2 Hz, 1H), 1.90 (s, 9H), 1.21 (s, 9H), 1.19 (s, 9H), 0.82 (bt, ^{3}J = 7.2 Hz), 0.54 (bs, 3H).

$[Cp^*Zr(Me)[^tBuNC(H)NEt]]^+[B(C_6F_5)_4]^-$ (27a): ^{1}H NMR (500 MHz, C_6D_5Cl, 263K): δ (ppm) 8.76 (s, 1H), 3.31 (bm, 1H), 3.20 (bm, 1H), 2.05 (s, 15H), 1.21 (s, 9H), 1.10 (t, ^{3}J = 7.2 Hz, 3H), 0.62 (s, 3H).

[Cp*Zr(Me)[^{i}PrNC(H)N^{i}Pr]]$^{+}$[B(C_6F_5)$_4$]$^{-}$ (27b): ^{1}H NMR (500 MHz, C_6D_5Cl, 263K): δ ppm) 8.76 (s, 1H), 3.46 (septet, ^{3}J = 6.4 Hz, 2H), 1.89 (s, 15H), 1.00 (bm, 12H), 0.46 (s, 3H).

[CpZr(Me)[^{t}BuNC(Me)NEt]]$^{+}$[B(C_6F_5)$_4$]$^{-}$•Et_2O (28a•Et_2O) : ^{1}H NMR (500 MHz, C_6D_5Cl, 243K): δ (ppm) 6.36 (s, 5H), 3.59 (bq), 3.10 (q, ^{3}J = 6.9 Hz, 2H), 1.95 (s, 3H), 1.38 (bt), 1.21 (s, 9H), 0.99 (t, ^{3}J = 6.9 Hz, 3H), 0.61 (s, 3H).

[CpZr(Me)[^{i}PrNC(Me)N^{i}Pr]]$^{+}$[B(C_6F_5)$_4$]$^{-}$ (28c) : ^{1}H NMR (500 MHz, C_6D_5Cl, 243K): δ (ppm) 6.36 (s, 5H), 3.48 (septet, ^{3}J = 6.5 Hz), 1.95 (s, 3H), 1.04 (d, ^{3}J = 6.5 Hz, 2H), 0.74 (s, 3H).

[CpZr(Me)[CyNC(Me)NCy]]$^{+}$[B(C_6F_5)$_4$]$^{-}$ (28d) : ^{1}H NMR (500 MHz, C_6D_5Cl, 243K): δ (ppm) 6.31 (s, 5H), 3.09 (bm), 1.90 (s, 3H), 1.52 (bm,), 1.14 (m, 10H), 1.02 (m, 10H), 0.63 (s, 3H).

[CpZr(Cl)[^{t}BuNC(Me)NEt]]$^{+}$[B(C_6F_5)$_4$]$^{-}$•Et_2O (29•Et_2O) : ^{1}H NMR (500 MHz, C_6D_5Cl, 243K): δ (ppm) 6.31 (s, 5H), 3.59 (bq), 3.13 (q, ^{3}J = 7.4 Hz, 2H), 1.92 (s, 3H), 1.38 (bt), 1.18 (s, 9H), 1.12 (t, ^{3}J = 6.9 Hz, 3H).

{[CpZr(Cl)[^{t}BuNC(Me)NEt]]$^{+}$[B(C_6F_5)$_4$]$^{-}$}$_2$ (29) : ^{1}H NMR (500 MHz, C_6D_5Cl, 243K): δ (ppm) 6.55 (s, 5H), 3.13 (bq, 2H), 1.99 (s, 3H), 1.23 (s, 9H), 1.07 (t, ^{3}J = 7.0 Hz, 3H). ^{13}C NMR (500 MHz, C_6D_5Cl, 243K): δ (ppm) 148.5, 115.13, 54.4, 41.6, 30.7, 15.4, 14.2.

[Cp*Zr(Et)[^{t}BuNC(Me)NEt]]$^+$[B(C$_6$F$_5$)$_4$]$^-$ (43a): ^{1}H NMR (500 MHz, C_6D_5Cl, 263K): δ (ppm) 3.15 (q, ^{3}J = 7.0 Hz, 2H), 2.13 (s, 3H), 1.94 (s, 15H), 1.60 (dt, ^{2}J = 15.0 Hz, ^{3}J = 7.5 Hz, 1H), 1.19 (dt, 1H), 1.13 (s, 9H), 0.95 (t, ^{3}J = 7.0 Hz, 3H), 0.63 (t, ^{3}J = 7.5 Hz, 3H).

[Cp*Zr(^{n}Pr)[^{t}BuNC(Me)NEt]]$^+$[B(C$_6$F$_5$)$_4$]$^-$ (43b): ^{1}H NMR (500 MHz, C_6D_5Cl, 263K): δ (ppm) 2.99 (dq, ^{2}J = 14.0 Hz, ^{3}J = 7.0 Hz, 1H), 2.98 (dq, ^{2}J = 14.0 Hz, ^{3}J = 7.0 Hz, 1H), 2.00 (s, 3H), 1.80 (s, 15H), 1.66 (m, 1H), 1.04 (bt, 3H), 1.00 (s, 9H), 0.93 (m, 2H), 0.97 (t, ^{3}J = 7.0 Hz, 3H), -0.32 (bm, 1H).

[Cp*Zr(^{i}Pr)[^{t}BuNC(Me)NEt]]$^+$[B(C$_6$F$_5$)$_4$]$^-$ (43c): ^{1}H NMR (500 MHz, C_6D_5Cl, 263K): δ (ppm) 3.07 (dq, ^{2}J = 14.0 Hz, ^{3}J = 7.0 Hz, 1H), 2.98 (dq, ^{2}J = 14.0 Hz, ^{3}J = 7.0 Hz, 1H), 1.95 (s, 3H), 1.74 (s, 15H), 1.73 (m, 1H), 0.99 (s, 9H), 0.83 (t, ^{3}J = 7.0 Hz, 3H), 0.78 (d, ^{3}J = 7.5 Hz, 3H), 0.29 (d, ^{3}J = 7.5 Hz, 3H).

[Cp*Zr(^{n}Bu)[^{t}BuNC(Me)NEt]]$^+$[B(C$_6$F$_5$)$_4$]$^-$ (43d): ^{1}H NMR (500 MHz, C_6D_5Cl, 263K): δ (ppm) 3.04 (dq, , ^{2}J = 14.0 Hz, ^{3}J = 7.0 Hz, 1H), 3.01 (dq, ^{2}J = 14.0 Hz, ^{3}J = 7.0 Hz, 1H), 2.01 (s, 3H), 1.72 (s, 15H), 1.60 (dt, 1H), 1.43 (m, 1H), 1.36 (m, 1H), 1.00 (s, 9H), 0.99 (m, 1H), 0.94 (t, 3H), 0.90 (m, 1H), 0.85 (t, 3H), -0.12 (bm, 1H).

[Cp*Zr(iBu)[^{t}BuNC(Me)NEt]]$^+$[B(C$_6$F$_5$)$_4$]$^-$ (43e): ^{1}H NMR (500 MHz, C_6D_5Cl, 263K): δ (ppm) 3.04 (dq, ^{2}J = 13.2 Hz, ^{3}J = 6.8 Hz, 1H), 3.01 (dq, ^{2}J = 13.2 Hz, ^{3}J = 6.8 Hz, 1H), 1.96 (s, 3H), 1.84 (s, 15H), 1.57 (dd, ^{2}J = 12.2 Hz, ^{3}J= 3.7 Hz, 1H), 1.12 (d, ^{3}J = 5.5 Hz, 3H), 0.98 (s, 9H), 0.95 (d, ^{3}J = 6.8 Hz, 3H), 0.88 (t, ^{3}J = 6.8 Hz, 3H), 0.73 (dd, ^{2}J = 12.2 Hz, ^{3}J = 7.2 Hz, 1H), -0.27 (m, 1H).

[Cp*Zr(neopentyl)[^{t}BuNC(Me)NEt]]$^{+}$[B(C_6F_5)$_4$]$^{-}$ (43h): ^{1}H NMR (500 MHz, C_6D_5Cl, 263K): δ (ppm) 3.18 (dq, ^{2}J=13.8 Hz, ^{3}J=7.0 Hz, 1H), 3.15 (dq, ^{2}J=13.8 Hz, ^{3}J = 7.0 Hz, 1H), 2.18 (s, 3H), 1.94 (d, ^{2}J = 15.0 Hz, 1H), 1.84 (s, 15H), 1.08 (s, 9H), 0.96 (t, ^{3}J = 7.0 Hz, 3H), 0.90 (s, 9H), 0.46 (d, ^{2}J = 15.0 Hz, 1H).

[Cp*Zr(neopentyl)[^{i}PrNC(Me)N^{i}Pr]]$^{+}$[B(C_6F_5)$_4$]$^{-}$ (44): ^{1}H NMR (500 MHz, C_6D_5Cl, 263K): δ (ppm) 3.42 (septet, ^{3}J = 6.2 Hz, 1H), 3.40 (dq, 1H), 2.05 (s, 3H), 1.88 (s, 15H), 1.16 (s, 2H), 0.96 (d, ^{3}J = 6.2 Hz, 6H), 0.92 (d, ^{3}J = 6.2 Hz, 6H), 0.86 (s, 9H).

Cp*ZrMe[^{t}BuNC(H)NEt]$^{+}$[B(C_6F_5)$_4$]$^{-}$ (27a): ^{1}H NMR (400 MHz, C_6D_5Cl, 263 K): δ (ppm) 8.76 (s, 1H), 3.32 (bm, 1H), 3.20 (bm, 1H), 2.05 (s, 15H), 1.21 (s, 9H), 1.11 (t, ^{3}J=7.0 Hz, 3H), 0.62 (s, 3H).

Cp*ZrMe[^{i}PrNC(H)N^{i}Pr]$^{+}$[B(C_6F_5)$_4$]$^{-}$ (27b): ^{1}H NMR (400 MHz, C_6D_5Cl, 263 K): δ (ppm) 8.76 (s, 1H), 3.46 (septet, ^{3}J = 8.0 Hz, 2H), 1.90 (s, 15H), 1.01 (bm, 12H), 0.46 (s, 3H).

Preparation of 1-Hexene Oligomers. In a typical polymerization, a –10 °C solution of 0.25 mol of **6a**, **6e**, or **15c** in 2 mL of PhCl was added to a –10 °C solution of 200 mg (0.25mol) of [$PhNHMe_2$][B(C_6F_5)$_4$] in 40 mL of PhCl. After 5 minutes, neat 1-hexene (0.32 g, 3.8 mmol), precooled to –10 °C, was quickly added. The reaction was quenched after 75 min by addition of silica gel. The mixture was then filtered and volatiles removed *in vacuo*. The residue was dissolved in $CHCl_3$ and precipitated from a vigorously stirred solution of 450 mL MeOH and HCl. Collection of the polymer precipitate and further removal of volatiles provided a colorless oil. Yield: 0.26 g (80%).

Preparation of a Triblock Copolymer. In a typical experiment, a –10 °C solution of 10.0 mg (24.5 μmol) of **6a** in 2.0 mL of PhCl was added to a –10 °C solution of 19.6 mg (24.5 μmol) of $[PhNHMe_2][B(C_6F_5)_4]$ in 7.75 mL of PhCl. After 5 minutes, neat 1-hexene (0.158 g, 1.9 mmol), precooled to –10 °C, was quickly added. After 1 hour, vinylcyclohexane (VCH) (208 mg, 1.9 mmol), which was precooled to –10 °C, was quickly injected into the reaction mixture. After another hour, 1-hexene (158 mg, 1.9 mmol), which was precooled to –10 °C, was quickly injected into the reaction mixture. After an aliquot was removed and quenched in silica gel, the reaction was quenched after another hour by addition of MeOH. The mixture was then filtered, stripped of solvent, dissolved in $CHCl_3$ and precipitated from a vigorously stirred solution of 450mL MeOH and HCl. Collection of the polymer precipitate and further removal of volatiles provided a colorless oil. Yield: 0.355 g (68%).

Kinetics of VCH Polymerization. In a general polymerization, a –10 °C solution of 10.4 mg (0.0255 mol) of **15c** in 2.0mL of PhCl was added to a –10 °C solution of 20.4 mg (0.0255 mol) of $[PhNHMe_2][B(C_6F_5)_4]$ and 166 mg of undecane in 7.32mL of PhCl. After 5 minutes, neat VCH (0.5508 g, 5.0mmol), precooled to –10 °C, was quickly added. Aliquots (0.5 mL) of the reaction mixture were removed and quenched in ~30mg of silica gel in 0.5 mL of PhCl cooled to –10 °C. Aliquots were tightly closed with polyethylene capped vials and immediately stored at –10 °C after quenching. The reaction was quenched after 125 minutes by addition of MeOH. Aliquots were then stored at –78 °C. To get GC data, the samples were taken one at a time and thawed,

where a 1.0 μL portion was removed. To obtain GPC data (after GC data was reliably taken), samples were thawed and filtered with addition of 2-3 mL hexane washings of the Kimwipe filter. Solvent removal in vacuo provided small amounts of polymer samples, which were taken up in minimal THF.

Preparation of Isotactic VCH. Typically, a –10 °C solution of 10.4 mg (25.5 μmol) of **15d** in 2.0 mL of PhCl was added to a –10 °C solution of 20.4 mg (25.5 μmol) of $[PhNHMe_2][B(C_6F_5)_4]$ in 6.63 mL of PhCl. After 5 minutes, neat VCH (1.102 g, 10.0 mmol), precooled to –10 °C, was quickly added. The reaction was quenched after two hours by addition of MeOH. The mixture was then stripped of volatiles, dissolved in CCl_4 and precipitated from a vigorously stirred solution of 450 mL MeOH and HCl. Collection of the polymer precipitate and further removal of volatiles provided a white crystalline solid. Yield: 0.80g (77%).

Insertion of cyclopentene. At –10 °C, a 0.6 mL solution of 15 mg (0.038 mmol) of **6a** in d_5-PhCl was added to 39 mg (0.042 mmol) of $[Ph_3C][B(C_6F_5)_4]$. This yellow solution was added to a solution of cyclopentene (5 mg, 0.074 mmol) in 0.2 mL of precooled d_5-PhCl, which was subsequently transferred to an NMR tube and maintained at –10 °C.

Preparation of 1,2-*d_2*-cyclopentene: A solution of 6.01 g (65.2 mmol) of 1,7-heptadiyne in 15 mL of decalin was combined with 0.51 g (5 mol%) of Lindlar's catalyst. After degassing the mixture, the tube was pressurized with D_2. Once complete, the mixture was filtered through Celite and washed with an additional 5 mL of decalin. To this was added 0.5 g (0.06 mmol, 1 mol%) of Grubb's 1st generation catalyst. After stirring overnight, low-boiling volatiles were collected via vacuum distillation following

three freeze-pump-thaw cycles providing 3.5 g (77% yield, 90% D incorporation) of target compound. ^{1}H NMR (400 MHz, $CDCl_3$, 293K): δ (ppm) 2.31 (t, ^{3}J = 7.6 Hz, 4H), 1.83 (pentet, ^{3}J = 7.6 Hz, 2H).

References:

(1) Love, B. E.; Jones, E. G. *J. Org. Chem.* **1999**, *64*, 3755.

(2) Barker, J.; Kilner, M. *Coord. Chem. Rev.* **1994**, *133*, 219.

(3) Edelmann, F. T. *Coord. Chem. Rev.* **1994**, *137*, 403.

(4) Kaminsky, W.; Kulper, K.; Brintzinger, H. H. *Angew. Chem., Int. Ed. Engl.* **1985**, *24*, 507.

(5) Hunter, W. E.; Hrncir, D. C.; Bynum, R. V.; Pentilla, R. A.; Atwood, J. L. *Organometallics* **1983**, *2*, 750.

REFERENCES

(1) Pino, P.; Mulhaupt, R. *Angew. Chem., Int. Ed. Engl.* **1980**, *19*, 857.

(2) Ziegler, K. *Angew. Chem.* **1952**, *64*, 323.

(3) Natta, G.; Pino, P.; Corradini, P.; Danusso, F.; Mazzanti, G.; Moraglio, G. *J. Am. Chem. Soc.* **1955**, *77*, 1708.

(4) Ketley, A. D.; Harvey, M. C. *J. Org. Chem.* **1961**, *26*, 4649.

(5) Samoilov, S. M. *J. Macromol. Sci.; Rev. Macromol. Chem.* **1981**, *C20*, 333.

(6) Doak, K. W. *Encycl. Polym. Sci. Eng.* **1986**, *6*, 386.

(7) Natta, G.; Pino, P.; Mazzanti, G.; Giannini, U. *J. Am. Chem. Soc.* **1957**, *79*, 2975.

(8) Breslow, D. S.; Newburg, N. R. *J. Am. Chem. Soc.* **1959**, *81*, 81.

(9) Brintzinger, H. H.; Fischer, D.; Mulhaupt, R.; Rieger, B.; Waymouth, R. M. *Angew. Chem., Int. Ed. Engl.* **1995**, *34*, 1143.

(10) Eisch, J. J.; Piotrowski, A. M.; Brownstein, S. K.; Gabe, E. J.; Lee, F. L. *J. Am. Chem. Soc.* **1985**, *107*, 7219.

(11) Cossee, P. *J. Catal.* **1964**, *3*, 80.

(12) Arlman, E. J. *J. Catal.* **1964**, *3*, 89.

(13) Arlman, E. J.; Cossee, P. *J. Catal.* **1964**, *3*, 99.

(14) Resconi, L.; Cavallo, L.; Fait, A.; Piemontesi, F. *Chem. Rev.* **2000**, *100*, 1253.

(15) Reichert, K. H.; Meyer, K. R. *Makromol. Chem.* **1973**, *169*, 163.

(16) Andreson, A.; Cordes, H. G.; Herwig, H.; Kaminsky, W.; Merk, A.; Mottweiler, R.; Pein, J.; Sinn, H.; Vollmer, H. J. *Angew. Chem., Int. Ed. Engl.* **1976**, *15*, 630.

(17) Sinn, H.; Kaminsky, W.; Vollmer, H. J.; Woldt, R. *Angew. Chem., Int. Ed. Engl.* **1980**, *19*, 390.

(18) Herwig, J.; Kaminsky, W. *Polym. Bull.* **1983**, *1983*.

(19) Kaminsky, W.; Miri, M.; Sinn, H.; Woldt, R. *Makromol. Chem. Rapid Commun.* **1983**, *4*, 417.

(20) Khrushch, N. E.; Dyachkovskii, F. S.; Marin, V. P.; Bravaya, N. M. *Kinetics and Catalysis* **1997**, *38*, 350.

(21) Gassman, P. G.; Callstrom, M. R. *J. Am. Chem. Soc.* **1987**, *109*, 7875.

(22) Sishta, C.; Hathorn, R. M.; Marks, T. J. *J. Am. Chem. Soc.* **1992**, *114*, 1112.

(23) Harlan, C. J.; Mason, M. R.; Barron, A. R. *J. Am. Chem. Soc.* **1994**, *13*, 2957.

(24) Yang, X. M.; Stern, C. L.; Marks, T. J. *Organometallics* **1991**, *10*, 840.

(25) Yang, X. M.; Stern, C. L.; Marks, T. J. *J. Am. Chem. Soc.* **1991**, *113*, 3623.

(26) Natta, G.; Corradini, P.; Bassi, I. W. *J. Am. Chem. Soc.* **1958**, *80*, 755.

(27) Yang, X. M.; Stern, C. L.; Marks, T. J. *J. Am. Chem. Soc.* **1994**, *116*, 10015.

(28) Siedle, A. R.; Newmark, R. A. *J. Organomet. Chem.* **1995**, *497*, 119.

(29) Chien, J. C. W.; Tsai, W.-M.; Rausch, M. D. *J. Am. Chem. Soc.* **1991**, *113*, 8570.

(30) Hlatky, G. G.; Eckman, R. R.; Turner, H. W. *Organometallics* **1992**, *11*, 1413.

(31) Scollard, J. D.; McConville, D. H.; Rettig, S. J. *Organometallics* **1997**, *16*, 1810.

(32) Thorn, M. G.; Vilardo, J. S.; Fanwick, P. E.; Rothwell, I. P. *Chem. Commun.* **1998**, 2427.

(33) Piers, W. E.; Chivers, T. *Chem. Soc. Rev.* **1997**, *26*, 345.

(34) Chen, E. Y. X.; Marks, T. J. *Chem. Rev.* **2000**, *100*, 1391.

(35) Woo, T. K.; Fan, L.; Ziegler, T. *Organometallics* **1994**, *13*, 2252.

(36) Ittel, S. D.; Johnson, L. K.; Brookhart, M. *Chem. Rev.* **2000**, *100*, 1169.

(37) Wu, Z.; Jordan, R. F.; Petersen, J. L. *J. Am. Chem. Soc.* **1995**, *117*, 5867.

(38) Casey, C. P.; Hallenbeck, S. L.; Wright, L. M.; Landis, C. R. *J. Am. Chem. Soc.* **1997**, *119*, 9680.

(39) Carpentier, J.-F.; Wu, Z.; Lee, C. W.; Stromberg, S.; Christopher, J. N.; Jordan, R. F. *J. Am. Chem. Soc.* **2000**, *122*, 7750.

(40) Stoebenau III, E. J.; Jordan, R. F. *J. Am. Chem. Soc.* **2003**, *125*, 3222.

(41) Casey, C. P.; Lee, T. Y.; Tunge, J. A.; Carpenetti, D. W. *J. Am. Chem. Soc.* **2001**, *123*, 10762.

(42) Casey, C. P.; Klein, J. F.; Fagan, M. A. *J. Am. Chem. Soc.* **2000**, *122*, 4320.

(43) Corradini, P.; Guerra, G. *Prog. Polym. Sci.* **1991**, *16*, 239.

(44) Yoshida, T.; Koga, N.; Morokuma, K. *Organometallics* **1996**, *15*, 766.

(45) Longo, P.; Grassi, A.; Pellecchia, C.; Zambelli, A. *Macromolecules* **1987**, *20*, 1015.

(46) Sacchi, M. C.; Barsties, E.; Tritto, I.; Locatelli, P.; Brintzinger, H. H.; Stehling, U. *Macromolecules* **1997**, *30*, 3955.

(47) Ewen, J. A. *J. Am. Chem. Soc.* **1984**, *106*, 6355.

(48) Resconi, L.; Abis, L.; Franciscono, G. *Macromolecules* **1992**, *25*, 6814.

(49) Hagihara, H.; Shiono, T.; Ikeda, T. *Macromol. Chem. Phys.* **1998**, *199*, 2439.

(50) Wild, F. R. W. P.; Zsolnai, L.; Huttner, G.; Brintzinger, H. H. *J. Organomet. Chem.* **1982**, *232*, 233.

(51) Kaminsky, W.; Kulper, K.; Brintzinger, H. H. *Angew. Chem., Int. Ed. Engl.* **1985**, *24*, 507.

(52) Ewen, J. A.; Haspeslach, L.; Atwood, J. L.; Zhang, H. *J. Am. Chem. Soc.* **1987**, *109*, 6544.

(53) Ewen, J. A. *J. Mol. Catal. A: Chem.* **1998**, *128*, 103.

(54) Resconi, L.; Camurati, I.; Sudmeijer, O. *Top. Catal.* **1999**, *7*, 145.

(55) Waymouth, R. M.; Pino, P. *J. Am. Chem. Soc.* **1990**, *112*, 4911.

(56) Kashiwa, N.; Yoshitake, J. *Polym. Bull.* **1984**, *11*, 479.

(57) Cavallo, L.; Guerra, G.; Corradini, P. *J. Am. Chem. Soc.* **1998**, *120*, 2428.

(58) Resconi, L.; Piemontesi, F.; Camurati, I.; Balboni, D.; Sironi, A.; Moret, M.; Rychlicki, H.; Zeigler, R. *Organometallics* **1996**, *15*, 5046.

(59) Schneider, M. J.; Mulhaupt, R. *Makromol. Chem. Phys.* **1997**, *198*, 1121.

(60) Resconi, L.; Piemontesi, F.; Franciscono, G.; Abis, L.; Fiorani, T. *J. Am. Chem. Soc.* **1992**, *114*, 1025.

(61) Hajela, S.; Bercaw, J. E. *Organometallics* **1994**, *13*, 1147.

(62) Guo, Z.; Swenson, D.; Jordan, R. F. *Organometallics* **1994**, *13*, 1424.

(63) Sini, G.; Macgregor, S. A.; Eisenstein, O.; Teuben, J. H. *Organometallics* **1994**, *13*, 1049.

(64) Chien, J. C. W.; Razavi, A. *J. Polym. Sci., A: Polym. Chem.* **1988**, *26*, 2369.

(65) Resconi, L.; Bossi, S.; Abis, L. *Macromolecules* **1990**, *23*, 4489.

(66) Gell, K. I.; Schwartz, J. *J. Am. Chem. Soc.* **1978**, *100*, 3246.

(67) McAlister, D. R.; Erwin, D. K.; Bercaw, J. E. *J. Am. Chem. Soc.* **1978**, *100*, 5966.

(68) Sperry, C. K.; Bazan, G. C.; Cotter, W. D. *J. Am. Chem. Soc.* **1999**, *121*, 1513.

(69) Tsutsui, T.; Kashiwa, N.; Mizuno, A. *Makromol. Chem. Rapid Commun.* **1990**, *11*, 565.

(70) Jungling, S.; Mulhaupt, R.; Stehling, U.; Brintzinger, H. H.; Fisher, D.; Langhauser, F. *J. Polym. Sci., A: Polym. Chem.* **1995**, *33*, 1305.

(71) Resconi, L.; Fait, A.; Piemontesi, F.; Colonnesi, M.; Rychlicki, H.; Zeigler, R. *Macromolecules* **1995**, *28*, 6667.

(72) Leclerc, M. K.; Brintzinger, H. H. *J. Am. Chem. Soc.* **1995**, *117*, 1651.

(73) Leclerc, M. K.; Brintzinger, H. H. *J. Am. Chem. Soc.* **1996**, *118*, 9024.

(74) Yoder, J. C.; Bercaw, J. E. *J. Am. Chem. Soc.* **2002**, *124*, 2548.

(75) Resconi, L. *J. Molec. Catal. A: Chem.* **1999**, *146*, 167.

(76) Lohrenz, J. C. W.; Buhl, M.; Weber, M.; Thiel, W. *J. Organomet. Chem.* **1999**, *592*, 11.

(77) Chung, T. C. *Macromolecules* **1988**, *21*, 865.

(78) Kesti, M. R.; Coates, G. W.; Waymouth, R. *J. Am. Chem. Soc.* **1992**, *114*, 9679.

(79) Wilen, C. E.; Luttikhedde, H.; Hjertberg, T.; Nasman, J. H. *Macromolecules* **1996**, *28*, 8569.

(80) Johnson, L. K.; Killian, C. M.; Brookhart, M. *J. Am. Chem. Soc.* **1995**, *117*, 6414.

(81) Killian, C. M.; Tempel, D. J.; Johnson, L. K.; Brookhart, M. *J. Am. Chem. Soc.* **1996**, *118*, 11664.

(82) Gates, D. P.; Svejda, S. K.; Onate, E.; Killian, C. M.; Johnson, L. K.; White, P. S.; Brookhart, M. *Macromolecules* **2000**, *33*, 2320.

(83) Svejda, S. A.; Johnson, L. K.; Brookhart, M. *J. Am. Chem. Soc.* **1999**, *121*, 10634.

(84) Shultz, L. H.; Tempel, D. J.; Brookhart, M. *J. Am. Chem. Soc.* **2001**, *123*, 11539.

(85) Komon, Z. J. A.; Diamond, G. M.; Leclerc, M. K.; Murphy, V.; Okazaki, M.; Bazan, G. C. *J. Am. Chem. Soc.* **2002**, *124*, 15280.

(86) Szwarc, M. *Nature* **1956**, *178*, 1168.

(87) Szwarc, M.; Levy, M.; Milkovich, R. *J. Am. Chem. Soc.* **1956**, *78*, 2656.

(88) Quirk, R. P.; Lee, B. *Polym. Int.* **1992**, *27*, 359.

(89) Doi, Y.; Suzuki, S.; Soga, K. *Macromolecules* **1986**, *19*, 2896.

(90) Scollard, J. D.; McConville, D. H. *J. Am. Chem. Soc.* **1996**, *118*, 10008.

(91) Gottfried, A. C.; Brookhart, M. *Macromolecules* **2001**, *34*, 1140.

(92) Matyjaszewski, K. *J. Phys. Org. Chem.* **1995**, *8*, 197.

(93) Baumann, R.; Davis, W. M.; Schrock, R. R. *J. Am. Chem. Soc.* **1997**, *119*, 3830.

(94) Liang, L. C.; Schrock, R. R.; Davis, W. M.; McConville, D. H. *J. Am. Chem. Soc.* **1999**, *121*, 5797.

(95) Mehrkhodavandi, P.; Bonitatebus, P. J.; Schrock, R. R. *J. Am. Chem. Soc.* **2000**, *122*, 7841.

(96) Mehrkhodavandi, P.; Schrock, R. R. *J. Am. Chem. Soc.* **2001**, *123*, 10746.

(97) Schrock, R. R.; Bonitatebus, P. J.; Schrodi, Y. *Organometallics* **2001**, *20*, 1056.

(98) Hagihara, H.; Shiono, T.; Ikeda, T. *Macromolecules* **1998**, *31*, 3184.

(99) Fukui, Y.; Murata, M.; Soga, K. *Macromol. Rapid Commun.* **1999**, *20*, 637.

(100) Tshuva, E. Y.; Goldberg, I.; Kol, M.; Weitman, H.; Goldschmidt, Z. *Chem. Commun.* **2000**, 379.

(101) Tshuva, E. Y.; Goldberg, I.; Kol, M. *J. Am. Chem. Soc.* **2000**, *122*, 10706.

(102) Matsui, S.; Tohi, Y.; Mitani, M.; Saito, J.; Makio, H.; Tanaka, H.; Nitabaru, M.; Nakano, T.; Fujita, T. *Chem. Lett.* **1999**, 1065.

(103) Tian, J.; Coates, G. W. *Angew. Chem., Int. Ed. Engl.* **2000**, *112*, 3772.

(104) Tian, J.; Hustad, P. D.; Coates, G. W. *J. Am. Chem. Soc.* **2001**, *123*, 5134.

(105) Hustad, P. D.; Tian, J.; Coates, G. W. *J. Am. Chem. Soc.* **2002**, *124*, 3614.

(106) Coates, G. W.; Hustad, P. D.; Reinartz, S. *Angew. Chem., Int. Ed. Engl.* **2002**, *41*, 2237.

(107) Angermund, K.; Fink, G.; Jensen, V. R.; Kleinschmidt, R. *Chemical Reviews* **2000**, *100*, 1457.

108) Chen, E. Y. X.; Marks, T. J. *Chemical Reviews* **2000**, *100*, 1391.

(109) Rappe, A. T.; Skiff, W. M.; Casewit, C. J. *Chemical Reviews* **2000**, *100*, 1435.

(110) Resconi, L.; Cavallo, L.; Fait, A.; Piemontesi, F. *Chemical Reviews* **2000**, *100*, 1253.

(111) Alt, H. G.; Koppl, A. *Chemical Reviews* **2000**, *100*, 1205.

(112) Coates, G. W. *Chemical Reviews* **2000**, *100*, 1223.

(113) McKnight, A. L.; Waymouth, R. M. *Chemical Reviews* **1998**, *98*, 2587.

(114) Ittel, S. D.; Johnson, L. K.; Brookhart, M. *Chemical Reviews* **2000**, *100*, 1169.

(115) Britovsek, G. J. P.; Gibson, V. C.; Wass, D. F. *Angew. Chem., Int. Ed. Engl.* **1999**, *38*, 428.

(116) Gibson, V. C.; Spitzmesser, S. K. *Chemical Reviews* **2003**, *103*, 283.

(117) Barker, J.; Kilner, M. *Coordination Chemistry Reviews* **1994**, *133*, 219.

(118) Edelmann, F. T. *Coordination Chemistry Reviews* **1994**, *137*, 403.

(119) Gomez, R.; Duchateau, R.; Chernega, A. N.; Meetsma, A.; Edelmann, F. T.; Teuben, J. H.; Green, M. L. H. *J. Chem. Soc., Dalton Trans.* **1995**, 217.

(120) Gomez, R.; Duchateau, R.; Chernega, A. N.; Teuben, J. H.; Edelmann, F. T.; Green, M. L. H. *Journal of Organometallic Chemistry* **1995**, *491*, 153.

(121) Gomez, R.; Green, M. L. H.; Haggitt, J. L. *J. Chem. Soc., Chem. Commun.* **1994**, 2607.

(122) Chernega, A. N.; Gomez, R.; Green, M. L. H. *J. Chem. Soc., Chem. Commun.* **1993**, 1415.

(123) Duchateau, R.; van Wee, C. T.; Meetsma, A.; van Duijnen, P. T.; Teuben, J. H. *Organometallics* **1996**, *15*, 2279.

(124) Littke, A.; Sleiman, N.; Bensimon, C.; Richeson, D. S.; Yap, G. P. A.; Brown, S. J. *Organometallics* **1998**.

(125) Edelmann, F. T. *Journal of Organometallic Chemistry* **1992**, *426*, 295.

(126) Richter, J.; Edelmann, F. T.; Noltemeyer, M.; Schmidt, H. G.; Shmulinson, M.; Eisen, M. S. *Journal of Molecular Catalysis A: Chemical* **1998**, *130*, 149.

(127) Drew, M. G. B.; Wilkins, J. D. *J. Chem. Soc., Dalton Trans.* **1974**, 1579.

(128) Gambarotta, S.; Strologo, S.; Floriani, C.; Chiesi-Villa, A.; Guastini, C. *Inorg. Chem.* **1985**, *24*, 654.

(129) Gambarotta, S.; Strologo, S.; Floriani, C.; Chiesi-Villa, A.; Guastini, C. *Journal of the American Chemical Society* **1985**, *107*, 6278.

(130) Coles, M. P.; Swenson, D. C.; Jordan, R. F. *Organometallics* **1997**, *16*, 5183.

(131) Coles, M. P.; Swenson, D. C.; Jordan, R. F.; Young Jr., V. G. *Organometallics* **1998**, *17*, 4042.

(132) Sita, L. R.; Babcock, J. R. **1998**, *17*, 5228.

(133) Koterwas, L. A.; Fettinger, J. C.; Sita, L. R. **1999**, *18*, 4183.

(134) Babcock, J. R.; Incarvito, C.; Rheingold, A. L.; Fettinger, J. C.; Sita, L. R. **1999**, *18*, 5729.

(135) Wolczanski, P. T.; Bercaw, J. E. *Organometallics* **1982**, *1*, 793.

(136) Jayaratne, K. C.; Sita, L. R. *Journal of the American Chemical Society* **2000**, *122*, 958.

(137) Babcock, J. R.; Sita, L. R. **1998**, *120*, 5585.

(138) Ojima, A.; Inaba, S. I. *Journal of Organometallic Chemistry* **1977**, *140*, 97.

(139) Maier, S.; Hiller, W.; Strahle, J.; Ergezinger, C.; Dehnicke, K. *Naturforsch.* **1988**, *43b*, 1628.

(140) Fenske, D.; Baum, G.; Zinn, A.; Dehnicke, K. *Naturforsch.* **1990**, *45b*, 1273.

(141) Brunner, H.; Agrifoglio, G. *Journal of Organometallic Chemistry* **1980**, *202*, C43.

(142) Brunner, H.; Lukassek, J.; Agrifoglio, G. *Journal of Organometallic Chemistry* **1980**, *195*, 63.

(143) Wedler, M.; Knosel, F.; Edelmann, F. T.; Behrens, U. *Chem. Ber.* **1992**, *125*, 1313.

(144) Stewart, P. J.; Blake, A. J.; Mountford, P. *Organometallics* **1998**, *17*, 3271.

(145) Keaton, R. J.; Jayaratne, K. C.; Henningsen, D. A.; Koterwas, L. A.; Sita, L. R. *Journal of the American Chemical Society* **2001**, *123*, 6197.

(146) Sotoodeh, M.; Leichtweis, I.; Roesky, H. W.; Noltemeyer, M.; Schmidt, H. G. *Chem. Ber.* **1993**, *126*, 913.

(147) Hunter, W. E.; Hrncir, D. C.; Bynum, R. V.; Pentilla, R. A.; Atwood, J. L. *Organometallics* **1983**, *2*, 750.

(148) Averbuj, C.; Tish, E.; Eisen, M. S. *J. Am. Chem. Soc.* **1998**, *120*, 8640.

(149) Flores, J. C.; Chien, J. C. W.; Rausch, M. D. *Organometallics* **1995**, *14*, 1827.

(150) Walther, D.; Fischer, R.; Gorls, H.; Koch, J.; Schweder, B. *J. Organomet. Chem.* **1996**, *508*, 13.

(151) Herskovics-Korine, D.; Eisen, M. S. *J. Organomet. Chem.* **1995**, *503*, 307.

(152) Richter, J.; Edelmann, F. T.; Noltemeyer, M.; Schmidt, H.-S.; Shmulinson, M.; Eisen, M. S. *J. Molec. Catal. A: Chem.* **1998**, *130*, 149.

(153) Volkis, V.; Shmulinson, M.; Averbuj, C.; Lisovskii, A.; Edelmann, F. T.; Eisen, M. S. *Organometallics* **1998**, *17*, 3155.

(154) Volkis, V.; Nelkenbaum, E.; Lisovskii, A.; Hasson, G.; Semiat, R.; Kapon, M.; Botoshansky, M.; Eishen, Y.; Eisen, M. S. *J. Am. Chem. Soc.* **2003**, *125*, 2179.

(155) Lancaster, S. J.; Robinson, O. B.; Bochmann, M.; Coles, S. J.; Hursthouse, M. B. *Organometallics* **1995**, *14*, 2456.

(156) Eisen, M. S.; Marks, T. J. *Organometallics* **1992**, *11*, 3939.

(157) Averbuj, C.; Eisen, M. S. *J. Am. Chem. Soc.* **1999**, *121*, 8755.

(158) Chernega, A. N.; Gomez, R.; Green, M. L. H. *J. Chem. Soc., Chem. Commun.* **1993**, 1415.

(159) Gomez, R.; Green, M. L. H.; Haggitt, J. L. *J. Chem. Soc., Chem. Commun.* **1994**, 2607.

(160) Gomez, R.; Duchateau, R.; Chernega, A. N.; Teuben, J. H.; Edelmann, F. T.; Green, M. L. H. *J. Organomet. Chem.* **1995**, *491*, 153.

(161) Ferraris, D.; Cox, C.; Anand, R.; Lectka, T. *J. Am. Chem. Soc.* **1997**, *119*, 4319.

(162) Kraft, B. M.; Lachicotte, R. J.; Jones, W. D. *J. Am. Chem. Soc.* **2001**, *123*, 10973.

(163) Jayaratne, K. C.; Sita, L. R. *J. Am. Chem. Soc.* **2000**, *122*, 958.

(164) Kissounko, D. A.; Fettinger, J. C.; Sita, L. R. *Inorg. Chim. Acta* **2002**, *00*, 1.

(165) Schrock, R. R.; Bonitatebus, P. J.; Schrodi, Y. *Organometallics* **2001**, *20*, 1056.

(166) Yang, X. M.; Stern, C. L.; Marks, T. J. *J. Am. Chem. Soc.* **1994**, *116*, 10015.

(167) Littke, A.; Sleiman, N.; Bensimon, C.; Richeson, D. S.; Yap, G. P. A.; Brown, S. J. *Organometallics* **1998**, *17*, 446.

(168) Mehrkhodavandi, P.; Bonitatebus, P. J.; Schrock, R. R. *J. Am. Chem. Soc.* **2000**, *122*, 7841.

(169) Hagihara, H.; Shiono, T.; Ikeda, T. *Macromolecules* **1998**, *31*, 3184.

(170) Ewen, J. A. *J. Mol. Catal. A: Chem.* **1998**, *128*, 103.

(171) Mehrkhodavandi, P.; Schrock, R. R. *J. Am. Chem. Soc.* **2001**, *123*, 10746.

(172) Asakura, T.; Demura, M.; Nishiyama, Y. *Macromolecules* **1991**, *24*, 2334.

(173) Babu, G. N.; NewMark, R. A.; Chien, J. C. W. *Macromolecules* **1994**, *27*.

(174) Marvel, C. S.; Stille, J. K. *J. Am. Chem. Soc.* **1958**, *80*, 1740.

(175) Resconi, L.; Waymouth, R. M. *J. Am. Chem. Soc.* **1990**, *112*, 4953.

(176) Coates, G. W.; Waymouth, R. M. *J. Am. Chem. Soc.* **1991**, *113*, 6270.

(177) Coates, G. W.; Waymouth, R. M. *J. Am. Chem. Soc.* **1993**, *115*, 91.

(178) Coates, G. W.; Waymouth, R. M. *J. Mol. Catal.* **1992**, *76*, 189.

(179) Jayaratne, K. C.; Keaton, R. J.; Henningsen, D. A.; Sita, L. R. *J. Am. Chem. Soc.* **2000**, *122*, 10490.

(180) Matyjaszewski, K. *J. Phys. Org. Chem.* **1995**, *8*, 197.

(181) Keaton, R. J.; Jayaratne, K. C.; Henningsen, D. A.; Koterwas, L. A.; Sita, L. R. *J. Am. Chem. Soc.* **2001**, *123*, 6197.

(182) Quirk, R. P.; Lee, B. *Polym. Int.* **1992**, *27*, 359.

(183) Soga, K.; Nakatani, H.; Shiono, T. *Macromolecules* **1989**, *22*, 1499.

(184) Endo, K.; Otsu, T. *J. Polym. Sci. A: Polym. Chem.* **1992**, *30*, 679.

(185) Ammendola, P.; Tancredi, T.; Zambelli, A. *Macromolecules* **1986**, *19*, 307.

(186) Zambelli, A.; Ammendola, P.; Sivak, A. J. *J. Am. Chem. Soc.* **1984**, *17*, 461.

(187) Mani, R.; Burns, C. M. *Polymer* **1993**, *34*, 1941.

(188) Marques, M.; Yu, Z.; Rausch, M. D.; Chien, J. C. W. *J. Polym. Sci. A: Polym. Chem.* **1995**, *33*, 2787.

(189) Longo, P.; Grassi, A.; Grisi, F.; Milione, S. *Marcomol. Rapid Comm.* **1998**, *19*, 229.

(190) Horton, A. D.; de With, J.; van der Linden, A. J.; van de Weg, H. *Organometallics* **1996**, *15*, 2672.

(191) Baumann, R.; Davis, W. M.; Schrock, R. R. *J. Am. Chem. Soc.* **1997**, *119*, 3830.

(192) Resconi, L.; Abis, L.; Franciscono, G. *Macromolecules* **1992**, *25*, 6814.

(193) Hagihara, H.; Shiono, T.; Ikeda, T. *Macromol. Chem. Phys.* **1998**, *199*, 2439.

(194) Bates, F. S. *Science* **1991**, *251*, 898.

(195) Keaton, R. J.; Jayaratne, K. C.; Henningsen, D. A.; Koterwas, L. A.; Sita, L. R. *J. Am. Chem. Soc.* **2001**, *123*, 6197.

(196) Ferraris, G.; Corno, C.; Priola, P.; Cesca, S. *Macromolecules* **1977**, *10*, 188.

(197) Coates, G. W.; Hustad, P. D.; Reinartz, S. *Angew. Chem., Int. Ed.* **2002**, *41*, 2237.

(198) Eisch, J. J.; Piotrowski, A. M.; Brownstein, S. K.; Gabe, E. J.; Lee, F. L. *J. Am. Chem. Soc.* **1985**, *107*, 7219.

(199) Gassman, P. G.; Callstrom, M. R. *J. Am. Chem. Soc.* **1987**, *109*, 7875.

(200) Natta, G.; Pino, P.; Mazzanti, G.; Giannani, U. *J. Am. Chem. Soc.* **1957**, *79*, 2975.

(201) Jordan, R. F.; Bajgur, C. S.; Willett, R.; Scott, B. *J. Am. Chem. Soc.* **1986**, *108*, 7410.

(202) Yang, X. M.; Stern, C. L.; Marks, T. J. *Organometallics* **1991**, *10*, 840.

(203) Yang, X. M.; Stern, C. L.; Marks, T. J. *J. Am. Chem. Soc.* **1991**, *113*, 3623.

(204) Yang, X. M.; Stern, C. L.; Marks, T. J. *J. Am. Chem. Soc.* **1994**, *116*, 10015.

(205) Keaton, R. J.; Jayaratne, K. C.; Fettinger, J. C.; Sita, L. R. *J. Am. Chem. Soc.* **2000**, *122*, 12909.

(206) Hunter, W. E.; Hcnzir, D. C.; Bynum, R. V.; Penttila, R. A.; Atwood, J. L. *Organometallics* **1983**, *2*, 750.

(207) Jordan, R. F.; Bradley, P. K.; Baenziger, N. C.; LaPointe, R. E. *J. Am. Chem. Soc.* **1990**, *112*, 1289.

(208) Jones, S. B.; Peterson, J. L. *Inorg. Chem.* **1981**, *20*, 2889.

(209) Grubbs, R. H.; Coates, G. W. *Acc. Chem. Res.* **1996**, *29*, 85.

(210) Jordan, R. F.; Bradley, P. K.; Baenziger, N. C.; LaPointe, R. E. *J. Am. Chem. Soc.* **1990**, *112*, 1289.

(211) Lancaster, S. J.; Robinson, O. B.; Bochmann, M.; Coles, S. J.; Hursthouse, M. B. *Organometallics* **1995**, *14*, 2456.

(212) Bochmann, M.; Lancaster, S. J. *J. Organomet. Chem.* **1992**, *434*, C1.

(213) Chen, Y. X.; Stern, C. L.; Yang, S. T.; Marks, T. J. *J. Am. Chem. Soc.* **1996**, *118*, 12451.

(214) Bochmann, M.; Lancaster, S. J. *Angew. Chem., Int. Ed. Engl.* **1994**, *33*, 1634.

(215) Mehrkhodavandi, P.; Bonitatebus, P. J.; Schrock, R. R. *J. Am. Chem. Soc.* **2000**, *122*, 7841.

(216) Fischer, D.; Mulhaupt, R. *J. Organomet. Chem* **1991**, *417*, C7.

(217) Beck, S.; Geyer, A.; Brintzinger, H. H. *Chem. Commun.* **1999**, 2477.

(218) Beck, S.; Lieber, S.; Schaper, F.; Geyer, A.; Brintzinger, H. H. *J. Am. Chem. Soc.* **2001**, *123*, 1483.

(219) Bochmann, M.; Cuenca, T.; Hardy, D. T. *J. Organomet. Chem.* **1994**, *484*, C10.

(220) Vollmerhaus, R.; Rahim, M.; Tomaszewski, R.; Xin, S. X.; Taylor, N. J.; Collins, S. *Organometallics* **2000**, *19*, 2161.

(221) Gomez, R.; Green, M. L. H.; Haggitt, J. L. *J. Chem. Soc., Chem. Commun.* **1994**, 2607.

(222) Kissounko, D. A.; Fettinger, J. C.; Sita, L. R. *Inorg. Chim. Acta* **2003**, *345*, 121.

(223) Chen, Y. X.; Marks, T. J. *Organometallics* **1997**, *16*, 3649.

(224) Schrock, R. R.; Bonitatebus, P. J.; Schrodi, Y. *Organometallics* **2001**, *20*, 1056.

(225) Alt, H. G.; Koppl, A. *Chem. Rev.* **2000**, *100*, 1205.

(226) Resconi, L.; Cavallo, L.; Fait, A.; Piemontesi, F. *Chem. Rev.* **2000**, *100*, 1253.

(228) Buchwald, S. L.; Watson, B. T.; Huffman, J. C. *J. Am. Chem. Soc.* **1987**, *109*, 2544.

(229) Negishi, E.; Nguyen, T.; Maye, J. P.; Choueiri, D.; Suzuki, N.; Takahashi, T. *Chem. Lett.* **1992**, 2367.

(230) Negishi, E.; Swanson, D. R.; Takahashi, T. *Chem. Let.* **1987**, 623.

(231) Negishi, E.; Cedarbaum, F. E.; Takahashi, T. *Tetrahedron Lett.* **1986**, *27*, 2829.

(232) Jayaratne, K. C.; Sita, L. R. *J. Am. Chem. Soc.* **2000**, *122*, 958.

(233) Keaton, R. J.; Koterwas, L. A.; Fettinger, J. C.; Sita, L. R. *J. Am. Chem. Soc.* **2002**, *124*, 5932.

(234) Zhang, Y. H.; Keaton, R. J.; Sita, L. R. *J. Am. Chem. Soc.* **2003**, *125*, 8746.

(235) Buchwald, S. L.; Kreutzer, K. A.; Fisher, R. A. *J. Am. Chem. Soc.* **1990**, *112*, 4600.

(236) Swanson, D. R.; Negishi, E. *Organometallics* **1991**, *10*, 825.

(237) Haaland, A.; Scherer, W.; Ruud, K.; McGrady, G. S.; Downs, A. J.; Swang, O. *J. Am. Chem. Soc.* **1998**, *120*, 3762.

(238) Scherer, W.; Priermeier, T.; Haaland, A.; Downs, A. J.; Boese, R.; Blaser, D. *Organometallics* **1998**, *17*, 4406.

(239) Hart, D. W.; Schwartz, J. *J. Am. Chem. Soc.* **1974**, *96*, 8115.

(240) Chirik, P. J.; Day, M. W.; Labinger, J. A.; Bercaw, J. E. *J. Am. Chem. Soc.* **1999**, *121*, 10308.

(241) Fernandez, F. J.; GomezSal, P.; Manzanero, A.; Royo, P.; Jacobsen, H.; Berke, H. *Organometallics* **1997**, *16*, 1553.

(242) Zhang, Y. H.; Keaton, R. J.; Sita, L. R. *J. Am. Chem. Soc.* **2003**, *125*, 9062.

(243) Gomez, R.; Duchateau, R.; Chernega, A. N.; Teuben, J. H.; Edelmann, F. T.; Green, M. L. H. *J. Organomet. Chem.* **1995**, *491*, 153.

(244) Gomez, R.; Duchateau, R.; Chernega, A. N.; Meetsma, A.; Edelmann, F. T.; Teuben, J. H.; Green, M. L. H. *J. Chem. Soc., Dalton Trans.* **1995**, 217.

(245) Littke, A.; Sleiman, N.; Bensimon, C.; Richeson, D. S.; Yap, G. P. A.; Brown, S. J. *Organometallics* **1998**, *17*, 446.

(246) Nishihara, Y.; Ishida, T.; Huo, S.; Takahashi, T. *J. Organomet. Chem.* **1997**, *547*, 209.

(247) Planalp, R. P.; Andersen, R. A.; Zalkin, A. *Organometallics* **1983**, *2*, 16.

(248) Buchwald, S. L.; Lum, R. T.; Fisher, R. A.; Davis, W. M. *J. Am. Chem. Soc.* **1989**, *111*, 9113.

(249) Paolucci, G.; Pojana, G.; Zanon, J.; Lucchini, V.; Avtomonov, E. *Organometallics* **1997**, *16*, 5312.

(250) Wendt, O. F.; Bercaw, J. E. *Organometallics* **2001**, *20*, 3891.

(251) Schrock, R. R.; Baumann, R.; Reid, S. M.; Goodman, J. T.; Stumpf, R.; Davis, W. M. *Organometallics* **1999**, *18*, 3649.

(252) Negishi, E.; Takahashi, T. *Acc. Chem. Res.* **1994**, *27*, 124.

(253) Negishi, E.; Holmes, S. J.; Tour, J. M.; Miller, J. A.; Cedarbaum, F. E.; Swanson, D. R.; Takahashi, T. *J. Am. Chem. Soc.* **1989**, *111*, 3336.

(254) Baumann, R.; Stumpf, R.; Davis, W. M.; Liang, L. C.; Schrock, R. R. *J. Am. Chem. Soc.* **1999**, *121*, 7822.

(255) Amor, F.; Spaniol, T. P.; Okuda, J. *Organometallics* **1997**, *16*, 4765.

(256) Mehrkhodavandi, P.; Bonitatebus, P. J.; Schrock, R. R. *J. Am. Chem. Soc.* **2000**, *122*, 7841.

(257) Dioumaev, V. K.; Harrod, J. F. *Organometallics* **1997**, *16*, 1452.

(258) Rodriguez, G.; Bazan, G. C. *J. Am. Chem. Soc.* **1997**, *119*, 343.

(259) Keaton, R. J.; Sita, L. R. *Organometallics* **2002**, *21*, 4315.

(260) Chen, E. Y. X.; Marks, T. J. *Chem. Rev.* **2000**, *100*, 1391.

(261) Pool, J. A.; Bradley, C. A.; Chirik, P. J. *Organometallics* **2002**, *21*, 1271.

(262) Kraft, B. M.; Lachicotte, R. J.; Jones, W. D. *J. Am. Chem. Soc.* **2001**, *123*, 10973.

(263) Alelyunas, Y. W.; Guo, Z.; LaPointe, R. E.; Jordan, R. F. *Organometallics* **1993**, *12*, 544.

(264) Shultz, L. H.; Tempel, D. J.; Brookhart, M. *J. Am. Chem. Soc.* **2001**, *123*, 11539.

(265) Eshuls, J. J. W.; Tan, Y. Y.; Meetsma, A.; Teuben, J. H. *Organometallics* **1992**, *11*, 362.

(266) Rossi, A.; Zhang, J.; Odian, G. *Macromolecules* **1996**, *29*, 2331.

(267) Carvill, A.; Zetta, L.; Zannoni, G.; Sacchi, M. C. *Macromolecules* **1998**, *31*, 3783.

(268) Janiak, C.; Lange, K. C. H.; Marquardt, P.; Kruger, R. P.; Hanselmann, R. *Macromol. Chem. Phys.* **2002**, *203*, 129.

(269) Asakura, T.; Demura, M.; Nishiyama, Y. *Macromolecules* **1991**, *24*, 2334.

(270) Babu, G. N.; NewMark, R. A.; Chien, J. C. W. *Macromolecules* **1994**, *27*, 3383.

(271) Liu, H. Q.; Deffieux, A.; Sigwalt, P. *Makromol. Chem.* **1991**, *192*, 2111.

(272) van der Linden, A. J.; Schaverien, C. J.; Meijboom, N.; Ganter, C.; Orpen, A. G. *J. Am. Chem. Soc.* **1995**, *117*, 3008.

(273) Ammendola, P.; Tancredi, T.; Zambelli, A. *Macromolecules* **1986**, *19*, 307.

(274) Dahlmann, M.; Erker, G.; Nissinen, M.; Frohlich, R. *J. Am. Chem. Soc.* **1999**, *121*, 2820.

(275) Waymouth, R. M.; Pino, P. *J. Am. Chem. Soc.* **1990**, *112*, 4911.

(276) Longo, P.; Grassi, A.; Pellecchia, C.; Zambelli, A. *Macromolecules* **1987**, *20*, 1015.

(277) Sacchi, M. C.; Barsties, E.; Tritto, I.; Locatelli, P.; Brintzinger, H. H.; Stehling, U. *Macromolecules* **1997**, *30*, 3955.

(278) Resconi, L.; Cavallo, L.; Fait, A.; Piemontesi, F. *Chem. Rev.* **2000**, *100*, 1253.

(279) Rieger, B.; Jany, G.; Fawzi, R.; Steinman, M. *Organometallics* **1994**, *13*, 647.

(280) Zhang, Y. H.; Keaton, R. J.; Sita, L. R. *J. Am. Chem. Soc.* **2003**, *125*, 9062.

(281) Liu, Z.; Somsook, E.; White, C. B.; Rosaaen, K. A.; Landis, C. R. *J. Am. Chem. Soc.* **2001**, *123*, 11193.

(282) Landis, C. R.; Rosaaen, K. A.; Sillars, D. R. *J. Am. Chem. Soc.* **2003**, *125*, 1710.

(283) Koo, K. M.; Marks, T. J. *J. Am. Chem. Soc.* **1998**, *120*, 4019.

(284) Chung, T. C.; Xu, G.; Lu, Y.; Hu, Y. *Macromolecules* **2001**, *34*, 8040.

(285) Ringelberg, S. N.; Meetsma, A.; Hessen, B.; Teuben, J. H. *J. Am. Chem. Soc.* **1999**, *121*, 6082.

(286) Rossi, A.; Odian, G.; Zhang, J. *Macromolecules* **1995**, *28*, 1739.

(287) Ittel, S. D.; Johnson, L. K.; Brookhart, M. *Chem. Rev.* **2000**, *100*, 1169.

(288) Kaminsky, W.; Ahlers, A.; Moller-Lindenhof, N. *Angew. Chem. Int. Ed. Engl.* **1989**, *28*, 1216.

(289) Coates, G. W.; Waymouth, R. M. *Science* **1995**, *267*, 217.

(290) Herfert, N.; Fink, G. *Makromol. Chem., Macromol. Symp.* **1993**, *66*, 157.

(291) Hauptman, E.; Waymouth, R. M.; Ziller, J. W. *J. Am. Chem. Soc.* **1995**, *117*, 11586.

(292) Ewen, J. *J. Am. Chem. Soc.* **1984**, *106*, 6355.

(293) Petoff, J. L. M.; Agoston, T.; Ial, T. K.; Waymouth, R. M. *J. Am. Chem. Soc.* **1998**, *120*, 11316.

(294) Resconi, L.; Cavallo, L.; Fait, A.; Piemontesi, F. *Chem. Rev.* **2000**, *100*, 1253.

(295) Kleinschmidt, R.; Reffke, M.; Fink, G. *Macromol. Rapid Commun.* **1999**, *20*, 284.

(296) Angermund, K.; Fink, G.; Jensen, V. R.; Kleinschmidt, R. *Macromol. Rapid Commun.* **2000**, *21*, 91.

(297) Ewen, J. A. *J. Mol. Catal. A: Chem.* **1998**, *128*, 103.

(298) Yoshida, T.; Koga, N.; Morokuma, K. *Organometallics* **1996**, *15*, 766.

(299) Guerra, G.; Cavallo, L.; Moscardi, G.; Vacatello, M.; Corradini, P. *Macromolecules* **1996**, *29*, 4834.

(300) Thomas, E. J.; Chien, J. C. W.; Rausch, M. D. *Macromolecules* **2000**, *33*, 1546.

(301) Farina, M.; Terragni, A. *Makromol. Chem., Rapid Commun.* **1993**, *14*, 791.

(302) Love, B. E.; Jones, E. G. *J. Org. Chem.* **1999**, *64*, 3755.

(303) Barker, J.; Kilner, M. *Coord. Chem. Rev.* **1994**, *133*, 219.

(304) Edelmann, F. T. *Coord. Chem. Rev.* **1994**, *137*, 403.

(305) Kaminsky, W.; Kulper, K.; Brintzinger, H. H. *Angew. Chem., Int. Ed. Engl.* **1985**, *24*, 507.

(306) Hunter, W. E.; Hrncir, D. C.; Bynum, R. V.; Pentilla, R. A.; Atwood, J. L. *Organometallics* **1983**, *2*, 750.